

**A Third Order Analysis of a Low
Temperature Differential
Ringbom–Stirling Engine**

Andrew Peter Robson

A thesis submitted in partial fulfilment of the
requirements of Napier University for the degree of
Doctor of Philosophy

April 2007

Declaration

I hereby declare that the work presented in this thesis has been solely carried out by myself at Napier University, Edinburgh. In the case of exceptions to the above declaration due acknowledgement is made. This thesis has not been submitted for any other degree.

Andrew Peter Robson (Candidate)

Date 20 April 2007

Abstract

The analysis of the Stirling engine has long been hampered by a lack of understanding of the complex relationship between the mechanical dynamics, thermodynamics and fluid dynamics operating within the engine.

This thesis outlines the research into Low Temperature Differential Stirling Engines (LTDSE) at Napier University. These engines typically operate at temperatures between 273K and 373K. The pressure profile within the engine varies about atmospheric pressure. As such they are naturally able to exploit heat sources such as process waste heat, solar passive collectors and geothermal hot springs. So far the majority of investigations have been in the field of high temperature engines, with a temperature differential counted in the thousands of Kelvin.

This work presents a third order analysis of the low temperature differential Ringbom – Stirling engine (LTDRSE). This is achieved by identifying the key elements of the engine. The laws of conservation and the ideal gas law are applied to each of these elements. From this a series of equations is written down, describing each element in turn. Simplifying assumptions are used to set boundary and limiting conditions. The equations are encoded to form the prediction program presented in the work. A test engine has been designed and manufactured, which, when equipped with a data logging system designed specifically for the engine, produces data sets for comparison purposes.

It was found that the prediction program indicated many of the unique operating characteristics of the LTDRSE that were confirmed by the data for the test engine. These showed a good correlation between the piston and displacer phase relationship, the discontinuous motion of the displacer and the pressure profiles. Accuracy of the prediction program data was found to be within 30% of the values for test engine data.

Contents

Declaration	i
Abstract	ii
Contents	iii
List of Figures	vii
List of Tables	ix
Acknowledgement	x
Nomenclature	xi
1 Introduction and Historical Background	1
1.1 A definition of the Stirling engine	2
1.2 Stirling engine types	3
1.2.1 Drive Methods	5
1.2.2 Engine configurations advantages and disadvantages	6
1.3 The Ringbom Variant.....	7
1.4 The Low Temperature Differential Stirling Engine (LTDSE)	7
1.5 The Low Temperature Differential Ringbom – Stirling Engine.....	8
1.6 Analysis of the Stirling engine	8
1.7 The relevance of this work.....	9
1.8 Advantages of the Stirling engine	12
1.9 A Brief History	13
1.10 An outline of this work	15
2 Literature review	17
2.1 The advent of the Stirling engine	18
2.2 The classic Stirling cycle	18
2.3 Previous analysis	21
2.3.1 The isothermal analysis.....	21
2.3.2 Limitations of the isothermal analysis.....	26
2.3.3 The isothermal problem is four fold:	27
2.4 Introduction to the theoretical analysis	28
2.5 Modern analysis	31
2.6 Operation of the Ringbom – Stirling engine.....	32
2.6.1 The Ringbom cycle using a gamma configuration.....	33
2.7 The Free Piston Stirling Engine (FPSE)	35

2.7.1	Multi element multi degree of freedom system.....	40
2.7.2	Two degree of freedom damped spring mass system.....	41
2.7.3	Vibrating systems and the limit cycle.....	45
2.7.4	Advantages of the FPSE Stirling engine	47
2.7.5	Disadvantages of the FPSE	48
2.7.6	Modes of operation.....	48
2.7.7	Self starting FPSE.....	50
2.7.8	Discontinuous motion of the displacer.....	53
2.7.9	The free displacer Ringbom - Stirling engine	54
2.7.10	The Regenerator	54
2.8	Final remarks.....	57
3	Research Aims	58
3.1	Research Questions	58
3.2	Focus of Study	58
4	Experimental work	60
4.1	Methodology.....	61
4.2	The unmodified Senft Ringbom LTDSE.....	61
4.3	The modified Senft Ringbom LTDSE.....	63
4.4	Instrument package.....	66
4.4.1	Temperature.....	66
4.4.1.1	Resistance temperature detector (RTD)	67
4.4.1.2	Thermocouples	67
4.4.1.3	Hardware filters	68
4.4.1.4	Software filters	69
4.4.1.5	Numerical techniques.....	69
4.4.1.6	Software smoothing	70
4.4.1.7	Infrared thermometry.....	70
4.4.1.8	Integrated circuits.....	71
4.4.2	Sensor and filter choice for temperature readings.....	71
4.4.3	Location of temperature sensors	72
4.4.4	Pressure.....	73
4.4.5	Location.....	76
4.4.5.1	Photographic interpretation	76
4.4.5.2	Slotted optical switch (optical integrated circuit).....	78

4.4.5.3	Procedure for displacer position.....	79
4.4.5.4	Procedure for piston location.....	82
4.4.6	Data acquisition.....	82
4.4.7	Calibration of sensors.....	83
4.4.7.1	Resistance Temperature Detectors.....	83
4.4.7.2	Thermocouples	84
4.4.7.3	Pressure.....	84
4.4.7.4	Location	84
4.4.8	Experimental technique.....	84
4.4.8.1	Experimental error.....	86
4.5	Experimental results	86
4.5.1	Qualitative observations and trends	86
4.5.1.1	Starting procedure.....	86
4.5.1.2	Rocking phenomena	87
4.5.1.3	The first engine	88
4.5.1.4	The second engine.....	89
4.5.1.5	Displacer motion	90
4.6	Quantitative results.....	91
4.7	Qualitative results.....	100
5	Theoretical Analysis and Numerical Techniques.....	103
5.1	The Ringbom Stirling engine and third order analysis	103
5.2	Analysis of the expansion space	104
5.3	Analysis of the compression space	108
5.4	Analysis of the displacer.....	112
5.5	Analysis of the piston / flywheel assembly.....	115
5.5.1	Piston	118
5.5.2	The flywheel	119
5.6	Analysis of the regenerator.....	124
5.6.1	Simple regenerator.....	124
5.6.2	Multi cell regenerator.....	127
5.7	Summary of governing equations.....	130
5.8	Numerical techniques	132
5.8.1	Flywheel location.....	133
5.8.2	Piston location.....	135

5.8.3	Displacer location	136
5.8.4	Compression space temperature	137
5.8.5	Mass flow for compression space	139
5.8.6	Expansion space temperature.....	139
5.8.7	Mass flow for expansion space	140
5.8.8	Compression space pressure.....	140
5.8.9	Compression space mass	141
5.8.10	Expansion space pressure	141
5.8.11	Expansion space mass	141
5.8.12	Regenerator	141
5.9	Preparation of data for the program	145
5.9.1	Order of calculations	146
5.10	Testing the program	148
5.10.1	Parameters of the model	149
5.10.2	Inertia of the flywheel	151
5.10.3	Spring constant	152
5.10.4	Flow leakage constants.....	152
5.10.5	Flywheel loss parameters.....	155
5.10.6	Heat transfer parameter for internal surfaces.....	156
5.10.6.1	Heat transfer from hot reservoir	156
5.10.6.2	Porosity of regenerator matrix.....	160
5.10.6.3	Structure of regenerator cells.....	161
5.10.6.4	Heat transfer within the regenerator matrix.....	161
5.10.6.5	Parameters for engine.....	166
5.11	Theoretical results	168
5.11.1	Quantitative results.....	168
5.11.2	Qualitative analysis	174
6	Discussion	180
6.1	Comparison of the data sets.....	181
7	Conclusions and further work	184
7.1	Further work	186
	References	187
	Papers Published.....	195
	Appendix A Engineering Drawings	1

Appendix B	Engine Simulation Program.....	1
Appendix C	Conference Paper Durham (12 th ISEC).....	1
Appendix D	Pressure Sensor Data.....	1

List of Figures

Figure 1.1	Alpha Stirling Engine.....	4
Figure 1.2	Beta Stirling Engine	4
Figure 1.3	Gamma Stirling Engine.....	5
Figure 1.4	Free Piston Stirling Engine.....	6
Figure 2.1	Stage 1 Isothermal expansion.....	19
Figure 2.2	Stage 2 Isochoric displacement	19
Figure 2.3	Stage 3 Isothermal compression.....	19
Figure 2.4	Stage 4 Isochoric displacement	20
Figure 2.5	Temperature profile across the ideal regenerator.....	22
Figure 2.6	P-v and T-S diagrams and the ideal Stirling cycle	24
Figure 2.7	P-V diagram of ideal Stirling cycle.....	29
Figure 2.8	Ringbom compression stroke	33
Figure 2.9	Ringbom first transfer stroke.....	34
Figure 2.10	Ringbom expansion stroke	34
Figure 2.11	Ringbom second transfer Stroke	35
Figure 2.12	Simple damped mass system (1 dof).....	36
Figure 2.13	Graph of displacement velocity and acceleration.....	38
Figure 2.14	The FPSE as a multi degree of freedom system.....	41
Figure 2.15	Two degree of freedom spring damped mass system.....	42
Figure 2.16	Vectors for a) acceleration, velocity and displacement and b) forces.....	44
Figure 2.17	Diagram suggesting different stable and quasi-stable operating states.....	46
Figure 2.18	Phase relationship of displacer and piston overdriven mode	49
Figure 2.19	Phase relationship of displacer and piston at the overdriven limit.....	50
Figure 2.20	P-V diagram for the self starting FPSE	52
Figure 2.21	Results to indicate discontinuous motion of displacer	53
Figure 4.1	Exploded assembly of the first test engine - enlargement in appendix A	62

Figure 4.2	Exploded assembly of second engine - enlargement in appendix A.....	65
Figure 4.3	Dimensioned section of second engine	66
Figure 4.4	Balanced L-C low pass filter.....	69
Figure 4.5	Thermal image of the first engine	70
Figure 4.6	RTD placement for first engine.....	72
Figure 4.7	Second test engine showing the location of drillings and tappings.....	73
Figure 4.8	First engine pressure tapping layout.....	74
Figure 4.9	Pressure transducer circuit.....	75
Figure 4.10	Example of photograph from photo-analysis	77
Figure 4.11	Photo analysis of displacer location	77
Figure 4.12	Optical switch circuit.....	78
Figure 4.13	Flywheel with slots.....	79
Figure 4.14	Displacer and bottom dead centre marks	81
Figure 4.15	Test apparatus in laboratory, engine without insulating jacket.	85
Figure 4.16	Run time 0 to 2 seconds	92
Figure 4.17	Run time 5 to 7 seconds	93
Figure 4.18	Run time 12 to 14 seconds	93
Figure 4.19	Run time 21 to 23 seconds	94
Figure 4.20	Run time 119 to 121 seconds	94
Figure 4.21	Piston and Displacer referred to P_e (0 to 0.6s).....	95
Figure 4.22	Differential pressure referred to P_e (0 to 0.6s).....	96
Figure 4.23	Piston and Displacer location referred to P_e (3.4 to 4s).....	96
Figure 4.24	Differential Pressure referred to P_e (3.4 to 4s).....	97
Figure 4.25	Piston and Displacer referred to P_e (12.4 to 13s).....	97
Figure 4.26	Differential Pressure referred to P_e (12.4 to 13s).....	98
Figure 4.27	Piston and Displacer Location referred to P_e (21.6 to 22.2s).....	98
Figure 4.28	Differential Pressure referred to P_e (21.6 to 22.2s).....	99
Figure 4.29	Piston and Displacer Location referred to P_e (120 to 120.6s).....	99
Figure 4.30	Differential Pressure referred to P_e (120 to 120.6s).....	100
Figure 5.1	Schematic of Ringbom Stirling engine	103
Figure 5.2	Forces acting upon the displacer	112
Figure 5.3	Detail section of stub springs and displacer	113
Figure 5.4	Piston and flywheel assembly	115
Figure 5.5	Piston forces	118

Figure 5.6	Piston-flywheel dynamics	119
Figure 5.7	Simple one cell regenerator	125
Figure 5.9	Regenerator of N cells	128
Figure 5.10	Graph of change in angular velocity with respect to time.....	156
Figure 5.11	Displacer motion	157
Figure 5.12	Displacer within the displacer chamber	157
Figure 5.13	Displacer inside the displacer chamber showing annular gap.....	161
Figure 5.14	Equivalent annular gap shown as two plates.....	163
Figure 5.15	Piston and relative expansion pressure 12 to 14 seconds.....	169
Figure 5.16	Differential and relative expansion pressures, 12 to 14 seconds.....	170
Figure 5.17	Piston and Displace position with reference to differential pressure	170
Figure 5.18	Piston and relative expansion pressure 21 to 23 seconds.....	171
Figure 5.19	Differential and relative expansion pressures, 21 to 23 seconds.....	171
Figure 5.20	Piston and Displace position with reference to differential pressure	172
Figure 5.21	Piston and relative expansion pressure 118 to 120 seconds.....	172
Figure 5.22	Differential and relative expansion pressures, 118 to 120 seconds.....	173
Figure 5.23	Piston and Displace position with reference to differential pressure	173

List of Tables

Table 1.1	Mileposts in Stirling engine development	13
Table 4.1	Temperature change for periods of run time.	92
Table 5.1	Physical characteristics of the test engine	150
Table 5.2	Experimental data for mass flow constant.....	154
Table 5.3	Intermediate values	154
Table 5.4	Mass flow constants.....	154
Table 5.5	Physical constants used for the engine	166
Table 5.6	Geometry and constants calculated by the prediction program.....	166
Table 5.7	Verification runs	174
Table 5.8	Run description.....	175

Acknowledgement

I would like to give special thanks to Professor Jorge Kubie and Doctor Thomas Grassie. Patient when required, firm in keeping to deadlines, steadfast in their commitment to this work, always willing to discuss when issues became confused.

Thanks are also extended to Mr Ian MacLeod for input during the design phase, Ronnie Tait for the manufacture of parts for both engines, Bill Campbell for computer support, and Dr Malcolm Renton and James Gordon for their help with data logging.

I would like to give quiet thank you to Dr Neil Hay, whose door has always been open when frustration clouded judgement and provided an oasis of calm.

My very special thanks go to my family, to my parents whose never ending support and encouragement has brought me this far.

And lastly but most importantly, especially for my wife Marianne, who has lived with me through this, edited my punctuation and syntax, providing countless cups of coffee and biscuits, and sharing this journey with me.

*Do not believe in anything simply because you have heard it.
Do not believe in traditions because they have been handed down for many generations.
Do not believe anything because it is spoken and rumoured by many.
Do not believe in anything because it is written in your religious books.
Do not believe in anything merely on the authority of your teachers and elders.
Rely not on the teacher or person, but on the teaching.
Rely not on the words of the teaching, but on the spirit of the words.
Rely not on theory, but on experience*

The Buddha.

Nomenclature

Label	Description	Unit	Variable
α	Angle formed by piston axis and con-rod at joint	<i>radian</i>	alpha
α_1	Second angle formed by piston axis and con-rod at joint	<i>radian</i>	alpha1
Δt	Delta t, time step	<i>s</i>	delta
$t + \Delta t$	First time step	<i>s</i>	delta1
$t + 2\Delta t$	Second time step	<i>s</i>	delta2
ε	Regenerator surface porosity, volumetric porosity	-	epsilon
γ	Angle formed between con-rod and crank arm	<i>radian</i>	gamma
γ_1	Second angle formed between con-rod and crank arm	<i>radian</i>	gamma1
ω	Angular velocity	<i>rad/s</i>	omega
π	Pi, numerical constant	-	pi
ρ_C	Density of cold plate material	<i>kg/m³</i>	rhoC
ρ_H	Density of hot plate material	<i>kg/m³</i>	rhoH
ρ_{RW}	Density of regenerator wire	<i>kg/m³</i>	rhoRW
θ	Flywheel angle for first time step	<i>radian</i>	theta
θ_1	Flywheel angle for $t = \Delta t$ time step	<i>radian</i>	theta1
θ_2	Flywheel angle for $t = 2\Delta t$ time step	<i>radian</i>	theta2
A	Area (general prefix)	<i>m²</i>	a
A_C	Area of cold plate	<i>m²</i>	ac
A_D	Area of displacer	<i>m²</i>	ad
A_{DC}	Area of displacer chamber	<i>m²</i>	adc
A_{DE}	Area of displacer effective	<i>m²</i>	ade
A_{DR}	Area of displacer rod end	<i>m²</i>	adr
A_{FR}	Free flow area of regenerator	<i>m²</i>	afr
A_H	Area of hot plate	<i>m²</i>	ah
A_P	Area of piston	<i>m²</i>	ap
A_R	Area of regenerator front	<i>m²</i>	ar

A_{RE}	Effective front area of regenerator	m^2	are
C_{Cell}	Length of one side of regenerator cell	m	cell
C_C	Specific heat capacity of cold plate material	$kJ/(kg \cdot K)$	cc
C_H	Specific heat capacity of hot plate material	$kJ/(kg \cdot K)$	ch
C_m	Specific heat capacity of matrix material	$kJ/(kg \cdot K)$	cm
C_P	Specific heat at constant pressure of working fluid	$kJ/(kg \cdot K)$	cp
C_v	Specific heat at constant volume of working fluid	$kJ/(kg \cdot K)$	cv
D_C	Diameter of cold plate	m	dc
D_D	Diameter of displacer	m	dd
D_{DC}	Diameter of displacer chamber	m	ddc
D_{DR}	Diameter of displacer rod	m	ddr
D_H	Diameter of hot plate	m	dh
D_P	Diameter of piston	m	dp
D_R	Diameter of regenerator	m	dr
D_{RW}	Diameter of regenerator wire	m	drw
E_C	Energy in cold plate per degree K	kJ	ec
E_E	Energy in expansion space – total, specific	$kJ, kJ/kg$	ee
E_H	Energy in hot plate per degree K	kJ	eh
E_K	Energy in compression space – total, specific	$kJ, kJ/kg$	ek
F_A	Force operator for the displacer stub springs	N	fa
g	Acceleration due to gravity	m/s^2	g
H, h	Enthalpy – total, specific	$kJ, kJ/kg$	h
h_C	Height of cold place	m	hc
h_D	Height of displacer	m	hd
h_{DC}	Height of displacer chamber	m	hdc
h_H	Height of hot plate	m	hh
h_P	Height of piston	m	hp
h_{SE}	Height of expansion space spring	m	hse

h_{SK}	Height of compression space spring	m	hsk
I_F	Moment of mass for flywheel	$kg\ m^2$	lfw
K_{DF}	Combined loss constant for flywheel (also power out)	Js/rad	kdf
K_{HC}	Constant for heat transfer to cold plate	W/K	khc
K_{HH}	Constant for heat transfer from hot plate	W/K	khh
K_{HRM}	Heat transfer constant for matrix material and working fluid	W/K	khrm
K_{MD}	Constant for mass flow past displacer	$kg/s\ Pa$	kmd
K_{MP}	Constant for mass flow past piston	$kg/s\ Pa$	kmp
K_{MR}	Constant for mass flow through the regenerator	$kg/s\ Pa$	kmr
K_{SE}	Spring rate for expansion space stub spring	N/m	kse
K_{SK}	Spring rate for compression space stub spring	N/m	ksk
ℓ	Length of connecting rod	m	l
m_C	Mass of cold plate	kg	mc
m_D	Mass of the displacer	kg	md
m_{DA}	Mass of displacer assembly	kg	mda
m_{DR}	Mass of displacer rod	kg	mdr
m_E	Mass of working fluid in expansion space	kg	me
m_{E1}	Mass of working fluid in expansion space previous time-step	kg	me1
m_{E2}	Mass of working fluid in expansion space calculation time-step	kg	me2
m_H	Mass of hot plate	kg	mh
m_K	Mass of working fluid in compression space	kg	mk
m_{K1}	Mass of working fluid in compression space previous time-step	kg	mk1
m_{K2}	Mass of working fluid in compression space current time-step	kg	mk2
m_M	Mass of matrix material	kg	mm
m_{MC}	Mass of matrix material in cell	kg	mmc
m_P	Mass of the piston	kg	mp
m_R	Mass of working fluid in regenerator	kg	mr
m_{RC}	Mass of working fluid in regenerator cell	kg	mrc

\dot{m}_{MD}	Mass flow to/from atmosphere via displacer rod gap	kg/s	mddot
\dot{m}_{MP}	Mass flow to/from atmosphere via piston gap	kg/s	mpdot
\dot{m}	Mass flow rate	kg/s	mdot
\dot{m}_A	Mass flow via piston and displacer rod gaps	kg/s	madot
\dot{m}_R	Mass flow rate through the regenerator	kg/s	mrdot
N_R	Number of regenerators in displacer	-	nr
P_A	Pressure of atmosphere	Pa	pa
P_E	Pressure in expansion space	Pa	pe
$P_{E,1}$	Pressure in expansion space previous time-step	Pa	pe1
$P_{E,2}$	Pressure in expansion space current time-step	Pa	pe2
P_K	Pressure in compression space	Pa	pk
$P_{K,1}$	Pressure in compression space previous time-step	Pa	pk1
$P_{K,2}$	Pressure in compression space current time-step	Pa	pk2
Q, q	Heat transfer – total, specific	$kJ, kJ/kg$	q
r	Radius for crank arm length	m	r
R_a	Gas constant for air	$kJ/kg \cdot K$	ra
S	Entropy	kJ/K	s
T_A	Temperature of surroundings (ambient)	K	ta
T_C	Temperature of cold plate	K	tc
T_E	Temperature in expansion space	K	te
$T_{E,1}$	Temperature in expansion space previous time-step	K	te1
$T_{E,2}$	Temperature in expansion space current time-step	K	te2
T_H	Temperature of hot plate	K	th
T_K	Temperature in compression space	K	tk
$T_{K,1}$	Temperature in compression space previous time-step	K	tk1
$T_{K,2}$	Temperature in compression space current time-step	K	tk2
$T_{M,any}$	Regenerator matrix material temperature for 'any' cell	K	tma
T_{max}	Temperature maximum for cycle	K	tmax

T_{\min}	Temperature minimum for cycle	K	tmin
$T_{R,any}$	Working fluid temperature in regenerator cell 'any'	K	tra
T_{RE}	Temperature of working fluid from regenerator to exp. space	K	tre
T_{RK}	Temperature of working fluid from regenerator to comp. space	K	trk
U	Internal energy	kJ	u
V_C	Volume of cold plate	m^3	vc
V_{Cell}	Volume of one cell	m^3	vcell
V_D	Volume of displacer	m^3	vd
V_{DC}	Volume of displacer chamber	m^3	vdc
V_H	Volume of hot plate	m^3	vh
V_{PC}	Volume of piston cylinder	m^3	vpc
W	Work done	kJ	w
$x_{D,0}$	Location of displacer	m	xd
$x_{D,1}$	Location of displacer previous time-step	m	xd1
$x_{D,2}$	Location of displacer current time-step	m	xd2
$x_{P,0}$	Location of piston	m	xp
$x_{P,1}$	Location of piston previous time-step	m	xp1
$x_{P,2}$	Location of piston current time-step	m	xp2
x_T	Total length of crank arm and con rod with parallel axes	m	xt

1 Introduction and Historical Background

One of the earliest records of an operating closed cycle heat engine is attributed to Philo of Byzantium in the second century B.C. [Sier 1999]. This is a description of the operation of temple doors by the heating and cooling (therefore expansion and contraction) of air enclosed in an offering altar.

During the following two thousand years the heat engine has developed into the ubiquitous internal combustion engine. The poor relation in this development has been the external combustion engine. This disparity is now being addressed with favourable applications as diverse as solar power [Bonnet 2003], [Bin Li 2005], combined heat and power [Tomas 2005], and also from potential third world applications [Mendoza 2003] to power for space exploration [Lanney 2002]. The following chapter aims to give a background as to how the external combustion engine, in the form of that proposed and built by the Reverend Robert Stirling, has developed.

In 1816 the Reverend Robert Stirling, aided by his brother James, patented

‘Improvements for Diminishing the Consumption of Fuel, and in particular an Engine capable of being Applied to the Moving of Machinery on a Principle Entirely New.’

[UK Patent Number 4081 of 1816]

The patent introduced two inventions, the hot air engine and the thermal regenerator (or economiser). Being the first to file for patent, the subsequently identified cycle became known as the Stirling cycle. Throughout his life, Stirling continued to improve the design of the closed cycle regenerative heat engine with external combustion.

The Stirling engine has gone through several periods of investigation since its invention, notably by the early mechanists of the European industrial revolution [Sier 1999], Phillips of Eindhoven (electrical manufacture) in the nineteen-forties

[Hargreaves 1991], General motors and the Ford motor company in the nineteen-seventies, Kokums of Sweden [Walker et al 1994] and at the turn of the twenty first century British Gas [Microgen Energy Ltd 2003] and Power Gen [EON UK 2005] in the UK.

As with many scientific inventions there is an abstract argument that Stirling was not the first to produce a working hot air engine. Further it could be argued that Sir George Cayley had built a hot air engine as early as 1807, so has more right to be thought of as the father of hot air engines (although the Cayley engine of 1807 operated on an open cycle with internal combustion [Walker 1980], [Sier 1999], [Finkelstein and Organ 2001]).

1.1 A definition of the Stirling engine

In this thesis the Stirling engine will be classified as a closed cycle regenerative heat engine. This would be a true description of the engine described in the patent of 1816 by Robert Stirling. This statement will benefit from some clarification.

An engine utilising a closed cycle is one where the working fluid is retained within the engine and so undergoes successive process cycles. In the case of this work, the working fluid is air.

The regenerator is a specialised heat exchanger constructed of many wire mesh screens laid one on top of another. When hot working fluid is passed through the cooler screens heat from the flow is transferred and stored, raising the temperature of the matrix. If the flow is reversed with colder fluid being passed through a hotter matrix, then heat is given up to the fluid from the matrix. Thus the regenerator abides by the laws of thermodynamics, where processes occur in the direction of decreasing quality of energy. Although the regenerator is not an essential part of a heat engine, this retention of a proportion of available energy improves the thermal efficiency.

The term heat engine comes from the fact that the engine operates because of a temperature differential between the hot end heat exchanger and the cold end heat exchanger.

A simple physical description of the Stirling engine could be an engine with three heat exchangers (Hot end, Cold end and Regenerator), a power piston and a displacer (maybe connected through some form of crank / lost motion mechanism) housed within a casing.

Since the patent in 1816 to the work of the Phillips laboratories in the 1940's, many engines that do not fall into this classification have been labelled as Stirling engines, which caused some confusion over what is and is not a Stirling engine. This situation was clarified by Meijer, head of the Stirling Research at Phillips laboratories who

'coined the generic title 'Stirling engines' to embrace all types of closed cycle regenerative gas engines regardless of the identity of the working fluid'

[Walker et al 1994]

With this in mind, one may safely say that Stirling is indeed the father of the closed cycle regenerative heat engine, and his place in history is correct.

1.2 Stirling engine types

The layout of all Stirling Engines has been categorised into three distinct types following the work of Kirkley [Kirkley 1962], as alpha, beta and gamma as described below.

Alpha (α). An alpha engine, shown in figure 1.1 consists of two opposed pistons separated by a heater, regenerator and cooler, all arranged in series with no displacer.

Beta (β). The beta type layout, shown in figure 1.2 is discerned by having a displacer, which occupies the same cylinder as the piston with the displacer rod piercing the piston. This is considered as the classic configuration, as the original patent shows an engine operating with this arrangement.

Gamma (γ). The gamma layout as shown in figure 1.3 is distinguished by the power piston and the displacer occupying separate cylinders. This removes the need to seal the path of the displacer rod through the piston, but tends to increase the dead space within the engine.

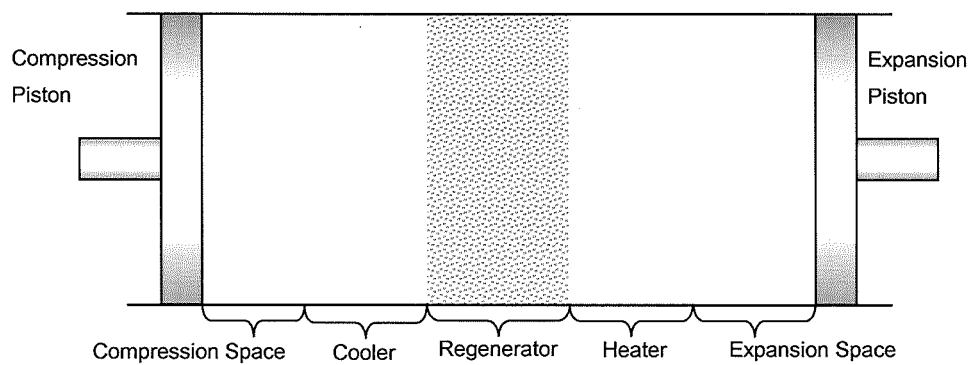


Figure 1.1 Alpha Stirling Engine

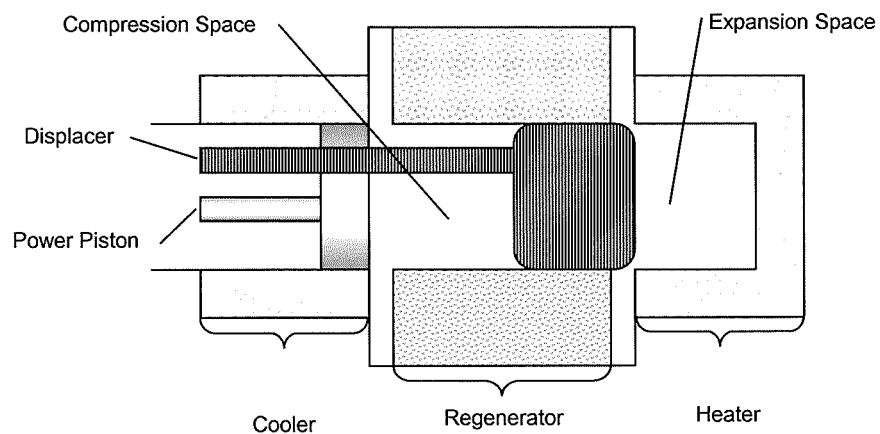


Figure 1.2 Beta Stirling Engine

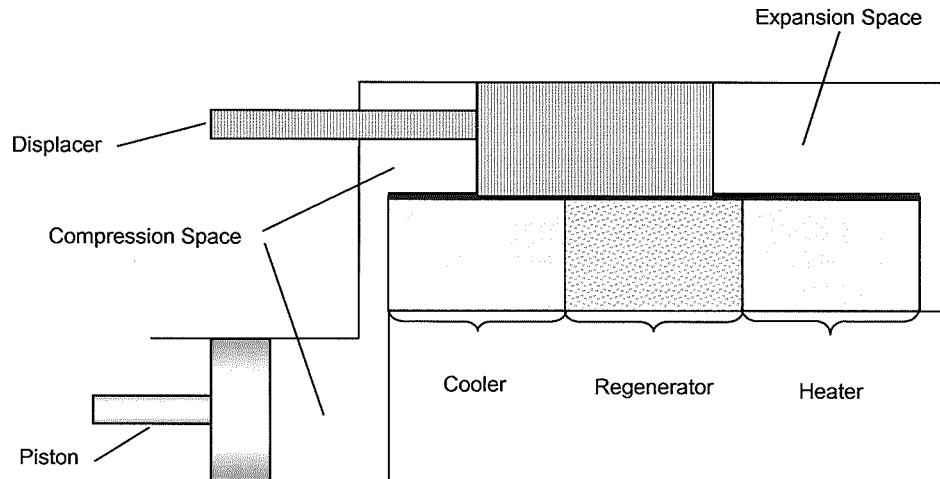


Figure 1.3 Gamma Stirling Engine

Each configuration favours a different type of analysis; most of the available analytical literature has been undertaken upon the α configuration, this is due, in the main part to the ease with which the alpha layout can be adapted to a double action upon the piston making it more desirable to design engineers as a prime mover.

1.2.1 Drive Methods

The drive for Stirling engines can be split into two types, kinematic and free piston.

- Kinematic. Utilises mechanical elements such as cranks, con-rods and flywheels where thermodynamic work is translated into shaft power. Engine performance is calculated from set parameters and dv/dt .
- Free piston. Variations in working fluid pressure and the use of spring elements produce and maintain the motion and phase relationship of the pistons and displacer. Engine performance is an amalgam of thermodynamic and kinematic phase relationships.

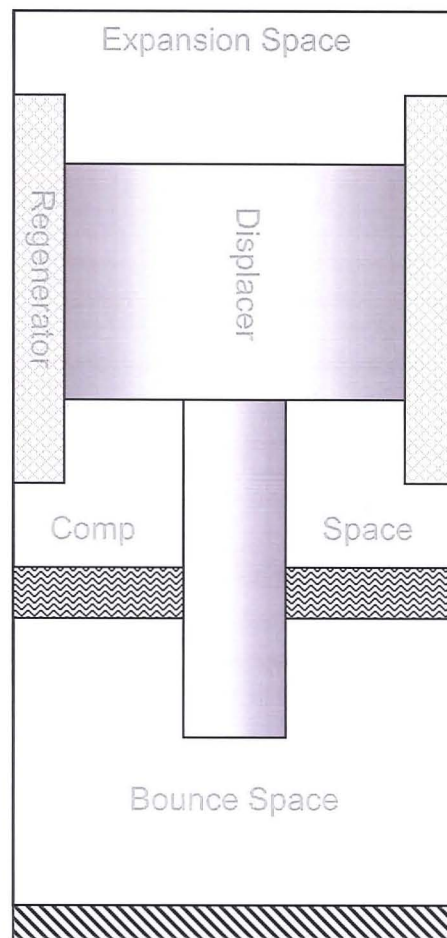


Figure 1.4 Free Piston Stirling Engine

1.2.2 Engine configurations advantages and disadvantages

Alpha configurations have mainly been used for automotive engines where compact, multi cylinder, double acting layouts provide high specific power output. These machines require extensive and difficult (expensive) to achieve sealing solutions, as well as either sinusoidal crank shafts (inherent loss), or cam-follower actuators to achieve a (more) suitable piston phase relationship. The design often becomes 'overcomplicated' with high wear of timing components. The space occupied by the heater, regenerator and cooler is dead space, reducing the specific power output.

Beta configuration is the classic layout for the Stirling engine, being the one which the Rev. Stirling used in his patent of 1816. The piston and displacer being in the same cylinder means that at different parts of the cycle the swept volumes of the compression and expansion space can overlap, reducing dead space. Free piston designs have tended to be based on the beta layout and benefit from an absence of a physical linkage between the components. An added benefit is the ability to be hermetically sealed, have a simple design with minimal moving parts (two), hence having reliable operation and long working life(also can be self starting).

The gamma configuration has separate cylinders for the piston and displacer with an inherent increase in dead space and an attendant lowering in specific power.

1.3 The Ringbom Variant

In 1905 Ossian Ringbom published a monograph detailing his observations on reducing the mechanical complexity of the Stirling engine. The breakthrough which Ringbom made was to use the pressure differential between the inside of the engine and the atmosphere to cause the displacer to move. In Ringbom's United States of America patent of 1907 the illustration shows that the upward movement of the displacer is actuated by the pressure differential, and the return stroke of the displacer by gravity and a snifter port.

1.4 The Low Temperature Differential Stirling Engine (LTDSE)

Previous to the early nineteen eighties investigations had concentrated on the high temperature variant of the engine requiring highly engineered and, by inference, high cost solutions. In 1983 Kolin [Senft 2000c] introduced the Low Temperature Differential Stirling Engine (LTDSE) at the Inter University Centre, Dubrovnik, during a short course on Stirling engines, followed six months later by Senft. Over the next ten years Kolin and Senft set themselves the target of finding the lowest possible temperature difference at which a Stirling engine would operate. Senft demonstrated an Ultra Low Temperature Differential Stirling Engine at the 5th

International Stirling Engine Conference, Dubrovnik, 1991, which achieved sustained motion with one half a Kelvin temperature difference [Senft 2000c], [Walker et al 1994]. The ultra low temperature work of Kolin and Senft has not addressed the question of whether any useful work can be extracted from the LTDSE. Kolin did investigate the energy production potential, but his work appears to have been more theoretical in nature than practical [Kolin 2000]. Some work has been undertaken in Japan and Germany to investigate LTDSEs in the 100W to 1kW range [National Maritime Research Institute, Japan 1995 to present], [Bonnet 2003], [Kolin 1986]

1.5 The Low Temperature Differential Ringbom – Stirling Engine

During the work carried out by Senft on LTDSE's he applied the principal of the Ringbom variant to the low temperature engine. Senft modified the Ringbom design by removing the snifter port. This modification allows for greater engine running speeds as both displacer strokes are now initiated under the action of the pressure differentials.

1.6 Analysis of the Stirling engine

The first analysis which produced closed form solutions was developed by Gustav Schmidt in 1871 [Schmidt 1871], [Reader and Hooper 1983]; [Urieli and Berchowitz 1984]. This was based upon an assumption that the processes were ideal, often referred to as an isothermal analysis. Schmidt encountered the problem of oversimplification of the complex interactions of cycles of operation and these assumptions flaw this analysis, resulting in over optimistic predictions of output power. This said, the Schmidt analysis stands as the first credible attempt to formulate a mathematical equation to describe the Stirling cycle.

Much effort has been applied to improving the Schmidt analysis, Kolin [Walker 1980] produced a graphical representation, Berchowitz [Urieli and Berchowitz 1984] reduced the classic Schmidt analysis [Reader and Hooper 1983] to a simple

equation multiplied by a complex 'Schmidt number' and Organ applied further simplifying criteria for non sinusoidal motion. Beale analysed several engines and formed an equation that is scaled by an empirically derived 'Beal number' [Walker 1980], [Reader and Hooper 1983], [Urieli and Berchowitz 1984], [Walker et al 1994]. The usefulness of the modified Schmidt equation and Beal equation is that they may be used for 'back of the envelope' calculations.

The complexity of analysis methods has increased as an understanding of the engine operation has developed. The most rigorous analysis available is the third order or nodal analysis which is used in this work

1.7 The relevance of this work

This work is to investigate the possibility of optimising the design of the Low Temperature Differential Stirling Engine so that it can produce power from low quality heat sources such as the output from solar hot water panels or waste heat from power generation.

With the possibility of an energy shortfall for the United Kingdom in the next ten to fifteen years, alternatives to the traditional generating plant need to be explored [IEA 2001], [IEA 2006], [BP 2002], [BP 2006], [BBC 2003]. This technology may help improve the efficiency of energy usage, or give the opportunity to incorporate Micro Combined Heat and Power (MCHP) into the local electricity distribution network.

The global demand, and by inference supply of primary energy, is continually increasing. Evidence of this phenomenon is available from agencies involved in gathering energy usage data. Examples to illustrate energy trends for this paper are taken from the International Energy Agency (IEA), Key World Energy Statistics [IEA 2001], [IEA 2006] and from British Petroleum (BP) Statistical review [BP 2002], [BP 2006]. A more focused view of energy usage in the United Kingdom (UK) may be found in The Digest of United Kingdom Energy Statistics (DUKES) [DTI DUKES 2006] or Energy Trends from the UK Statistics Office. With the

majority of world primary energy supply derived from fossil fuel there are major implications for resource depletion and greenhouse gas propagation.

Between 1973 and 2001 world primary energy supply increased by 4 billion tonnes of oil equivalent (btoe), from 6 btoe to 10 btoe. The IEA projects that this trend will increase, and by 2030 world primary energy supply will reach 16.3 btoe.

It is suggested by the IEA that the geographic use of energy will change, with the traditional high-energy users such as the Organisation of Economic Cooperation and Development (OECD) countries taking a lower percentage of world energy supply. Countries with emerging economies and increased industrialisation such as Africa, Asia, China, Latin America and the Middle East are expected to become the main energy users. What is apparent is that all countries are increasing their energy dependence year on year.

Fossil fuels such as oil, coal, gas, oil sands and oil shale account for 75% of the world primary energy supply for 2001. This is set to rise to 83% by 2030. In context in 2001, 75% of 10 btoe came from fossil fuel, in 2030 it is expected that 83% of 16.3 btoe will come from fossil fuel. This rise in both percentage and amount in btoe has significant implications upon greenhouse gas (ghg) emissions. (many of the future major green house gas contributors are not signatories to the Kyoto Protocol).

The time required for the formation of fossil fuels precludes the natural replacement of reserves. Extraction far outstrips the replacement process. As such, fossil fuels should be considered as a finite resource. Any technology that reduces the rate of extraction and usage must be considered beneficial.

Methods of predicting the quantity of reserves fall short. Geographic interpretation has proven unreliable, and test drilling costly. The logistics curve method overlays a curve, which describes the extraction of a finite resource over time. This relies upon an accurate estimation of the resource size [Cassedy and Grossman 1998]. This shows that there are many differing estimates as to the size of the world fossil fuel reserve.

Current predicted worldwide reserve to production ratios estimate that at present and predicted rates of extraction/ the supply of primary energy will consume the oil reserve in 50 years, the natural gas reserve in 75 years and the coal reserve in 200 years [BP 2002], [BP 2004], [BP 2006]. Improvements in exploration and extraction techniques will lengthen the life of the reserve.

To reduce the rate of exhaustion, the way in which fossil fuel derived energy is used must be improved, either by a move away from fossil fuels or by improving the efficiency of processes using fossil fuel. There are many technologies being investigated as to suitability for this purpose, including the classical wind, wave and tidal approaches, and the less mature technologies of photo voltaics, fuel cells, also carbon neutral fuels such as ethanol and hydrogen.

When combined with a conventional heating boiler the Stirling engine also joins this group of technologies. The Sankey diagram of a micro combined heat and power plant (MCHP) indicates that the main loss of energy is keeping the flue gases hot enough to avoid harmful condensation forming.

The introduction of a 'disruptive technology' such as Low Temperature Differential Stirling Engines (LTDSE) working in the kW range, capable of utilising process waste heat or solar hot water as the motive energy source. may be one of many options used to improve energy efficiency.

The opportunity for the Stirling engine in the 21st century may be in domestic combined heat and power or micro combined heat and power (MCHP). The objective is to integrate a small Stirling engine into a domestic gas boiler, which will generate electricity whenever the boiler is operating. Several companies are readying themselves for production, notably in the UK, British Gas with its MicroGen unit developed in conjunction with Sunpower USA [Microgen Energy Ltd 2003]; and Power Gen is developing a unit with Whisper Tech from New Zealand [Cogeneration and On-Site Power Production 2003] [12th International Stirling Engine Conference, Durham Keynote speech by Don Clacus]. These MCHP units produce around 1 kW of electricity.

By just replacing one or two central heating boilers with MCHP units no advantage to society would be gained. Where the technology becomes 'disruptive' is when several thousand units are all operating at the same time. A disruptive technology is one that has the potential to substantially disrupt an established industry, both economically and technologically.

The boiler churn (replacement) market is in the order of 850 000 units per year in the UK [EST 2001]. With a similar take up of the new technology as there was for condensing boilers (10%), within 5 years a capacity of 1 GW (electric) will be installed, and within 10 years there could be a capacity of 5 GW (electric) installed. With the market place 'pump primed' then take-up will happen in a shorter timescale. All these investigations have concentrated on the high temperature variant of the engine, requiring highly engineered and by inference, high cost solutions.

On a global scale this technology may provide a low cost low technology solution for stand alone small-scale power. Potential applications range from providing water pumping, power for medicinal refrigeration, and communications to simple lighting. The only limiting factor being a requirement of suitable solar radiation intensity, low quality hot water from process plant or geothermal hot water. It is felt that an opportunity has been identified for a low – tech, inexpensive engine that could be built and maintained by the 'village handyman' who does not need to know how it works, just that it does.

The author sees a design such as a Ringbom – Stirling engine [Senft 1993], [Senft 2000] that may be reduced to two moving parts and a housing incorporating a linear motion induction generator or linear pump as having the mechanical simplicity called for by this application.

1.8 Advantages of the Stirling engine

The Stirling engine offers several advantages over conventional internal combustion engines, having:

- Multi fuel / heat source capacity
- Possible high thermal efficiency
- Self starting capability (for some designs)
- Option of using several working fluids
- Minimal lubrication requirements
- Long operating life (Harwell engine ran for over eight years, only requiring refuelling)
- Virtually silent operation, as no explosive detonation of fuel
- Burners (if used) may be set to the optimum for economy and emissions
- No requirement for valves
- Few moving parts within the engine

1.9 A Brief History

The table below gives a brief outline of events with the Stirling engine history, for a more comprehensive treatise upon the historic aspect the reader is directed to Sier [Sier 1999]

Table 1.1 Mileposts in Stirling engine development

Date	Event
1807	Sir George Cayley experiments with his first hot air engine
1816	Rev. Robert Stirling patents his first engine
1824	Sadi Carnot describes a fully reversible thermodynamic cycle and an impossible engine
1849	James Prescott Joule establishes the 'mechanical equivalent of heat' refuting 'caloric'
1850	Rudolf Gottlieb (Clausius) speculates on heat as a property of a particle of matter
1851	Lord Kelvin publishes 'On the Dynamical Theory of Heat'
1853	James Robert Napier and William McQuorne Rankine patent an air engine with extended heat transfer surfaces (Patent 1416 of 1853)
1854	William McQuorne Rankine provides one of the first explanations of the

	Stirling cycle	
1871	Gustav Schmidt produces the “Classical” Stirling engine analysis with closed form solutions	
1878	<p>Slaby Produces the first classifications for Stirling Engines</p> <p>Open Cycle, where a fresh charge of working fluid is mixed with the products of combustion (internal combustion), such as Cayley’s engine</p> <p>Open Cycle, where a fresh charge of working fluid is heated externally but without mixing with combustion products, such as Ericsson’s engines</p> <p>Closed Cycle, the charge of working fluid is retained within the engine and repeatedly used, such as the Stirling engine</p>	
1905	Ossian Ringbom publishes his monograph on reducing the mechanical complexity of the Stirling engine and UK patent 10,675	
1907	Ossian Ringbom Patents an engine incorporating the improvements from 1905 in the United States of America patent number 856,102	
1927	Helmuth Hausen produces his first study of periodic flow heat exchangers, to be distilled into his heat transfer book of 1957	
1937	Phillips of Eindhoven begins an analysis of the Stirling engine	
1950	Phillips of Eindhoven end their work for radio generators with the advent of the silicone transistor. Phillips continues development of larger automotive and marine engines up to 1979. This later work was carried out in collaboration with the Ford motor company, the US navy, United Stirling of Sweden (Kokums) and NASA	
1953	Rhombic drive by Meijer of Phillips enables better balancing of rotating components thus allowing higher working pressures (higher power output)	
1960	Finklestein presents his first analysis using adiabatic working spaces and ideal heat transfer	
1962	Kirkley identifies that Stirling engines may be categorised into three types and suggests a naming strategy as Alpha Beta and Gamma configurations. This is expanded upon below in section 1.2	
1962	General Motors (USA)	<ul style="list-style-type: none"> a. Outboard motor / automotive engine b. Solar heated generator for space exploration c. Ground Power Unit for US military

1964	Beale 'invents' the free piston Stirling engine
1968	General motors nears completion of automotive engine and torpedo engine work
1968	Free Piston / Displacer investigations by Beal et al and by Harwell (UK)
1969	General Motors terminates all Stirling work in response to fears of litigation over school bus brake issues (unconnected with Stirling work)
1974	MAN / MWM concentrate on underwater power plant. Later work is taken over by the German Government and declared state secret.
1974	Bradley demonstrates a low temperature differential Stirling engine (probably the first)
1975	NASA takes over the running of the DoE Stirling engine automotive programs
1980	Japanese Government begins funding of four research projects
1980	First run of Kolin's Ltdse
1983	First demonstration of Kolin's Ltdse
1991	NASA works on space power demonstration engines
2000	NASA continues work at the Glen Research Centre
2004	In recent years disclosure of work in progress tends to be sketchy, with tantalising glimpses of current state of the art given at conferences. Unfortunately security, both national and commercial, means that full disclosure is not a possibility.

Notable successes for hot air engines of this time were the Ericsson water pump (open cycle external combustion engine) and later the Ky-Ko (generic) fan.

1.10 An outline of this work

In this work a full differential analysis is developed. The validity of this analysis is shown by comparison with a test engine.

To this end, the author has created (and will present) a generic set of equations describing the operation of a LTDSE Ringbom type engine. Developing a

FORTTRAN program of a virtual engine (the parameters of which may be changed), the results of which, when compared to a physical engine will test the equations

Chapter two forms the literature review; this presents the development of the analysis from trivial to third order. Chapter three describes the aims of the work. Chapter four covers the experimental aspect of the work which includes design of the engine, development of the instrument and monitoring package, and the results gained from the experimental engine. Chapter five uses third order analysis techniques. Equation sets are derived from first principles and developed to a form ready for encoding into a computer program. The results from the analysis are then presented. Chapter six discusses the results. Chapter seven closes the body of the thesis with conclusions and gives recommendations for future work.

2 Literature review

The field of Stirling engine research is the province of academics and research engineers undertaking specific investigations. The outcome of many of these investigations is a report. These reports, and the distilled information, are often reported in scientific magazines and presented in subject specific books.

This has resulted in a large body of literature covering the Stirling engine, and the regenerator becoming available, but often in very general terms. The analysis of engine operation remains the province of research theses and commercially sensitive research and development.

This situation causes the formation of small centres of excellence in academic institutions. These institutions, engaged in free research, aim to disseminate the work they are engaged in, and to discuss techniques and approaches for analysis. The antithesis is drawn from the commercial development of Stirling engine technology, where disclosure of techniques may give a competitor an advantage.

Today, several companies are on the brink of large-scale commercialisation of Stirling Engine (and family derivative) technology. British Gas alone has invested over £40M [Conversation with David Bryce, 30th Oct 2002] into its MicroGen project. PowerGen working with Whisper Tech of New Zealand are also just about to release their micro combined heat and power unit [12th International Stirling Engine Conference 2005].

The main outlets for contemporary information are engineering journals and the proceedings form conferences such as the International Stirling Engine Conference (ISEC) and European Stirling Engine Forum. With such a small community, publicising research being carried out is often by word of mouth at conferences. This means it is not always easy to discover who is working on what and at which locations.

2.1 The advent of the Stirling engine

To understand the reason for the Stirling engine invention, one would need to look at the social and economic drivers for the period. Water power was on the wane therefore a new motive power was required, a prime mover which was not restricted by geography or seasonal variations in weather. Steam was at the beginning of its development and the main rival to hot air engines. This development pushed the boundaries of contemporary metallurgy. For steam, a greater specific power meant increasing steam pressures, making boiler explosions an everyday hazard rather than an unusual occurrence. These explosions, if not immediately fatal, would at least be harmful to anybody in the vicinity. The economic driver was based upon how much work could be extracted from the engine per bushel of coal.

The hot air engine appeared to solve many of these issues. The inclusion of the regenerator helps to improve the economy of the engine. By retaining heat within the engine, less coal would be required for an equivalent amount of work. Using air as the working medium meant that explosions were less likely to cause injury or death to those nearby. Eventually steam came out as the medium of choice. For many years, the Stirling engine may have been considered as being a solution in search of an application.

It may be true that attempts to produce a working hot air engine existed before Stirling [Hargreaves 1991][Sier 1999]. What sets Sterling above these earlier forays is the fact that he was the first to patent a working engine.

2.2 The classic Stirling cycle

It is worth considering how the classic Stirling cycle is described, using the Alpha configuration as an example [Reader and Hooper 1983], [Walker et al 1994].



Figure 2.1 Stage 1 Isothermal expansion

At state 1, shown in figure 2.1, all the working fluid is in the expansion space. The compression piston is held in place at inner dead centre by the action of the flywheel and eccentric (lost motion) linkage. The working fluid is at T_{max} , P_{max} and V_{min} . The heating of the working fluid causes the high pressure, which pushes the expansion piston out, performing work upon the flywheel. The volume increases and pressure decreases as the expansion process continues. T_{max} is maintained as a constant by additional heat from the hot end heat exchanger.

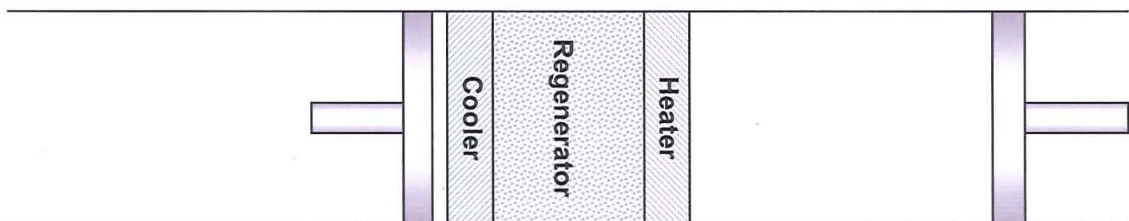


Figure 2.2 Stage 2 Isochoric displacement

At state 2, shown in figure 2.2, the expansion piston is at its outer dead centre. The expansion piston and compression pistons begin an inward and outward movement (respectively) under control of the flywheel and crank linkages. The working fluid is transferred at constant volume from the hot end into the cold end via the regenerator. As the fluid passes through the regenerator it gives up some of its thermal energy to each matrix layer, thus enters at T_{max} and leaves at T_{min} .

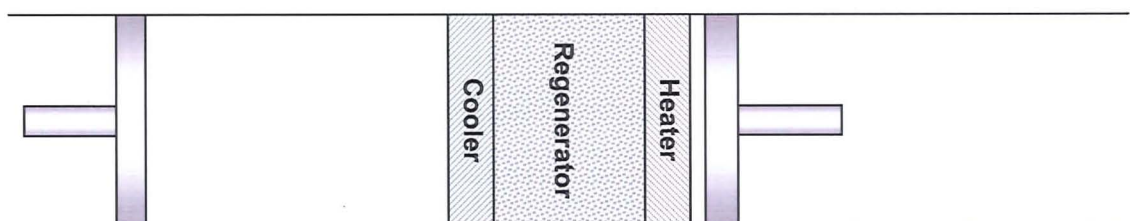


Figure 2.3 Stage 3 Isothermal compression

At stage 3, shown in figure 2.3, the compression piston is at its outer dead centre and the compression piston is at its inner dead centre, all the working fluid is in the compression space at T_{min} , P_{min} and V_{max} .

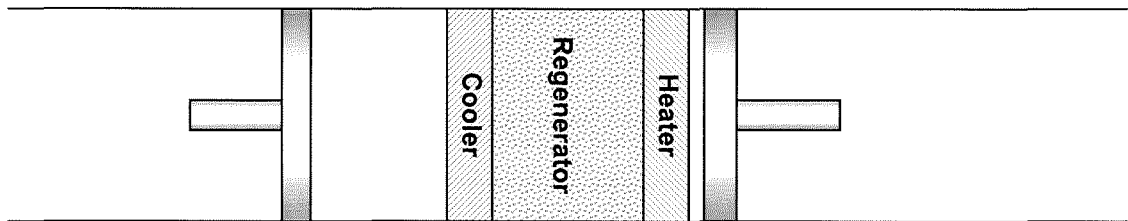


Figure 2.4 Stage 4 Isochoric displacement

At stage 4, shown in figure 2.4, the compression piston is pushed inwards by the action of the flywheel, whilst the expansion piston is held in place by a lost motion linkage. In most applications the motion of the displacer and piston is usually sinusoidal.

The above phase relationship between the pistons of the alpha configuration is similar to that of the phase relationship between the piston and displacer in beta and gamma configuration Stirling engines.

Much has been written about the original engine of Robert Stirling, notably by Organ [Organ 2000b]. In his work Organ has analysed the original Stirling engine in depth, as well as more contemporary engines. The analysis of the Stirling cycle notably begins with Schmidt, in his analysis of 1871 [Schmidt 1871], although it should be put in context.

The general operation of the Stirling engine can be described as:

- Heat is applied to the hot end of the engine; this may be from any thermal generation. For example, combustion of hydrocarbons, heat from radio isotopes or solar concentrators
- The working fluid expands doing work on the piston
- The working fluid is moved from the expansion space to the compression space by means of the displacer
- During this displacement heat is given up by the fluid to the regenerator

- The working fluid is then cooled and compressed
- Heat is removed from the engine via the cold plate
- The working fluid is then moved from compression space to the expansion space, by means of the displacer
- During this displacement heat is given up by the regenerator to the working fluid
- The working fluid is once again expanded in expansion space by the addition of heat from the hot end

2.3 Previous analysis

2.3.1 The isothermal analysis

The classic or textbook isothermal analysis as given by Walker (Walker 1980, 1994) and Reader and Hooper (Reader and Hooper 1983) may be summed up as follows

For the isothermal analysis several assumptions are made

- The working fluid is an ideal gas and can be described by the ideal gas law
- The system is closed so the mass of the working fluid remains constant
- There is no pressure drop throughout the system (no pumping loss)
- Working fluid in the expansion space is all at T_{max}
- Working fluid in the compression space is all at T_{min}
- Continuous motion of the piston and displacer
- (Schmidt uses sinusoidal to give closed form)
- Isothermal working spaces, heat exchangers and regenerator
- There is no dead space; all the fluid is available to do work
- No parasitic losses such as friction
- Steady state flow and thermodynamic conditions apply (not pulsed)
- No aerodynamic effects around the displacer or through the regenerator
- No heat is lost to the surroundings

The ideal isothermal model assumes the following temperature profile (figure 2.5)

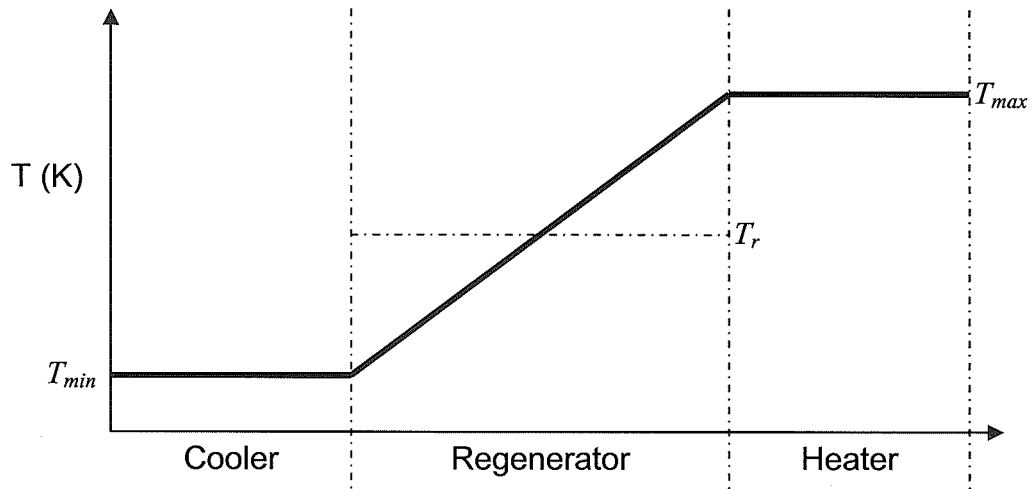


Figure 2.5 Temperature profile across the ideal regenerator

Where

T_{min} is the cooler space internal temperature

T_{max} is the heater space internal temperature

T_r is the regenerator average temperature defined as

$$\tau_{iso} = \text{Temperature ratio} = T_{min} / T_{max}$$

$$r = \text{volume ratio} = V_{max} / V_{min}$$

$$T_r = \frac{T_{max} - T_{min}}{\ln\left(\frac{T_{max}}{T_{min}}\right)}$$

Equation 2.1

The ideal gas law is given as

$$PV = mRT$$

Equation 2.2

Since the system is closed, mass is conserved, at any instantaneous point in the cycle the mass balance can be described as

$$m_{system} = m_{expansion} + m_{regenerator} + m_{compression}$$

By transposing the ideal gas law, mass conservation can be rewritten as

$$m_{\text{system}} = \left(\frac{PV}{RT}\right)_{\text{Expansion}} + \left(\frac{PV}{RT}\right)_{\text{Re generator}} + \left(\frac{PV}{RT}\right)_{\text{Compression}} \quad \text{Equation 2.3}$$

Rewriting for constants P and R

$$m_{\text{system}} = P \left(\frac{V_e}{T_e} + \frac{V_r}{T_r} + \frac{V_c}{T_c} \right) \frac{1}{R} \quad \text{Equation 2.4}$$

Putting T_r in the form of equation 2.4 gives

$$m_{\text{system}} = P \left(\frac{V_e}{T_e} + \left(\frac{V_r}{1} \cdot \frac{\ln\left(\frac{T_{\max}}{T_{\min}}\right)}{T_{\max} - T_{\min}} \right) + \frac{V_c}{T_c} \right) \frac{1}{R} \quad \text{Equation 2.5}$$

For the isothermal analysis $T_{\max} = T_e$ and $T_{\min} = T_c$

So, equation 2.5 can be rewritten as

$$m_{\text{system}} = P \left(\frac{V_e}{T_e} + \left(\frac{V_r}{1} \cdot \frac{\ln\left(\frac{T_e}{T_c}\right)}{T_e - T_c} \right) + \frac{V_c}{T_c} \right) \frac{1}{R} \quad \text{Equation 2.6}$$

Solving for pressure

$$P = mR / \left(\frac{V_e}{T_e} + \left(\frac{V_r \ln T_e / T_c}{T_e - T_c} \right) + \frac{V_c}{T_c} \right) \quad \text{Equation 2.7}$$

Work balance within the engine due to volume change

$$W = W_e + W_c$$

Over a complete cycle, assuming that the piston and displacer movement is sinusoidal.

$$W = \oint P dV_e + \oint P dV_c \quad \text{Equation 2.8}$$

$$W = \oint P \left(\frac{dV_e}{d\theta} + \frac{dV_c}{d\theta} \right) \quad \text{Equation 2.9}$$

The classic closed form gives results in the following P-V and T-S diagrams, an explanation of which is given below.

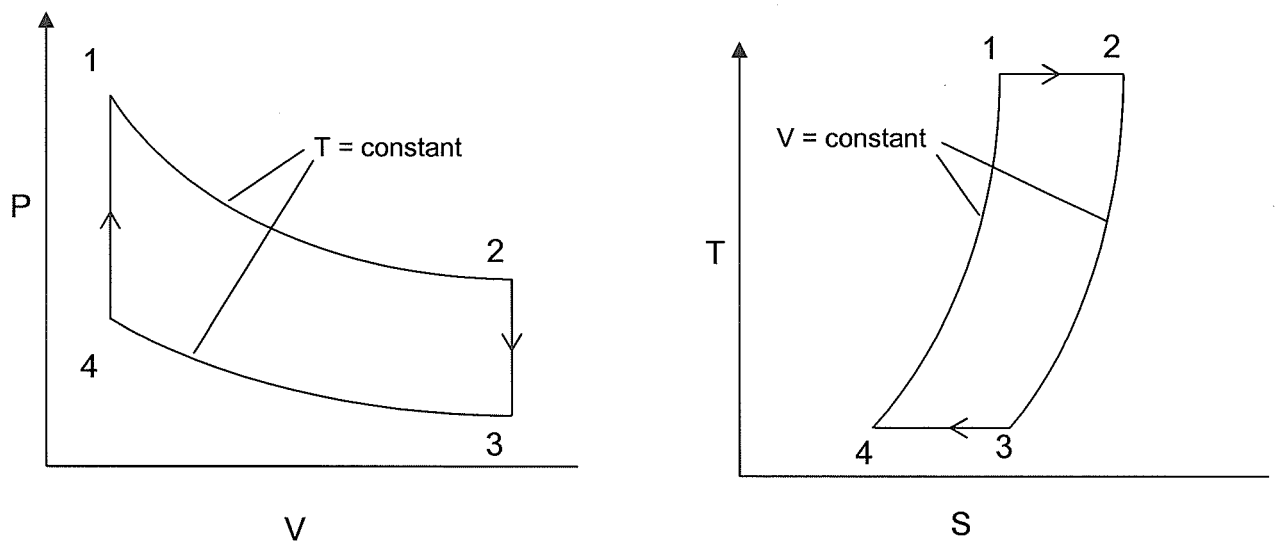


Figure 2.6 P-V and T-S diagrams and the ideal Stirling cycle

For the process paths

1 – 2 Isothermal Expansion

Heat is supplied at T_{max} , work is performed by the working fluid upon the piston, equal in magnitude to the heat supplied.

$$P_2 = P_1 V_1 / V_2 = P_1 (1/r)$$

$$T_1 = T_2 = T_{max}$$

Heat transfer = work done : $Q = W$

$$\text{Heat transfer} = P_1 V_1 \ln r = RT_1 \ln r$$

No change in internal energy U

$$\text{Change in entropy (increase), } (S_2 - S_1) = R \ln r$$

2 – 3 Isochoric regenerative working fluid transfer

Working fluid is transferred from the hot end to the cold end of the engine by action of the displacer. The working fluid passes through the regenerator separating the two ends, energy in the form of heat is given up to the regenerative matrix. Ideal operation has the fluid entering the matrix at T_{max} and leaving the matrix at T_{min} . No work is extracted from the cycle by the displacer operation.

Internal energy and entropy are decreased

$$P_3 = P_2 T_2 / T_3 = P_3 \tau_{iso}$$

$$V_3 = V_2$$

$$\text{Heat transfer } (Q) = C_v(T_3 - T_2)$$

$$\text{Change in entropy} = (S_3 - S_2) = C_v \ln \tau_{iso}$$

3 – 4 Isothermal Compression

Heat is removed from the working fluid and rejected at the minimum cycle temperature. Work is done to the working fluid equal in magnitude to the heat rejected.

No change in internal energy: Decrease in entropy

$$P_4 = P_3 V_3 / V_4 = P_3 r$$

$$T_4 = T_3 = T_{min}$$

$$Q = W = P_3 V_3 \ln(1/r) = RT_3 \ln(1/r)$$

$$\text{Change in entropy } (S_4 - S_3) = R \ln(1/r)$$

4 – 1 Isochoric regenerative transfer of working fluid

Working fluid is transferred from the cold end to the hot end of the engine under the action of the displacer. Heat is transferred from the regenerative matrix to the working fluid raising the temperature of the working fluid from T_{min} to T_{max} .

No work is done, $W = 0$: Internal energy and entropy of the working fluid increase

$$P_1 = P_4 T_1 / T_4 = P_4 / \tau_{iso}$$

$$V_4 = V_1$$

$$\text{Heat transfer } (Q) = C_v(T_1 - T_4)$$

$$P_4 = P_3 V_3 / V_4 = P_3 r$$

$$\text{Change in entropy } (S_1 - S_4) = C_v \ln(1/\tau_{iso})$$

2.3.2 Limitations of the isothermal analysis

The isothermal analysis is based upon an ideal cycle and, as such, various assumptions have been made to aid in simplification.

In process 1 – 2 (isothermal expansion), all the working fluid is believed to be in the expansion space, this neglects dead space such as clearances and the regenerator. The regenerator will have imparted some heat to the working fluid, but no expansion of the working fluid occurs until all the working fluid is in the

expansion space. All the fluid is heated / expanded equally, ignoring any turbulent of thermal conduction effects. The expansion is isothermal, so takes place at one constant temperature, this assumes a perfect heat exchanger.

In process 2 –3 (isochoric displacement), all the working fluid is moved under the action of the displacer from the hot end to the cold end of the engine. This is considered instantaneous, with perfect regeneration as the working fluid is passed through the regenerative matrix. The volume of the working fluid does not change until all the working fluid is in the cold end at temperature T_{min} . The action of the displacer requires no work input to overcome friction or working fluid resistance (pumping loss).

In process 3 – 4 (isothermal compression), all the process work is done on the working fluid, friction effects are neglected. Any thermal gain from the compression of the working fluid is removed by the cold end heat exchanger. Assumption is made of a uniform temperature and pressure distribution throughout the working fluid.

In process 4 – 1 (isochoric displacement), the working fluid is moved under the action of the displacer from the cold end to the hot end of the engine. Once again, a perfect regenerative heat exchanger is assumed and instantaneous mass transfer without pressure anomalies.

From the above cycle one could almost imagine a ‘perpetual motion machine’, as the energy required for expansion and compression is the heat stored in the regenerator being used repetitively, this ignores conversion losses and assumes a perfect regenerator.

2.3.3 The isothermal problem is four fold:

1. Friction and leakage is assumed to be zero.
2. There is a requirement for infinite heat transfer rates, or an infinite time for the process to be completed.

3. It assumes that the dead space (unused volume) reduces the effective mass of working fluid for the process reducing performance.
4. It presumes the discontinuous motion required for the displacer and piston in the ideal cycle.

Gustav Schmidt [Reader and Hooper 1983]; [Urieli and Berchowitz 1984] went on to improve the accuracy of the isothermal analysis, but the basic problem of oversimplification and sweeping assumptions flaws this analysis as over optimistic by 100 to 200 percent (as suggested by both the references in this paragraph).

2.4 Introduction to the theoretical analysis

Previously, the theoretical analysis of the Stirling cycle has been categorised in four classes or orders. These range from the 'zeroeth' order analysis to the third order analysis, [Martini, 1983].

In the literature, different authors give alternative definitions, with the next most common being first to fourth order. Where there is consistency throughout the literature is that there are four types of analyses available, increasing in rigour.

In this work the definitions given by Martini [1983] will be used, these are outlined below.

The zeroeth order or 'trivial' analysis is reproduced in thermodynamic text books, and is outlined below. This proposes that the engine power and efficiency may be calculated purely as a function of variations in fluid characteristics; such as temperature, pressure and volume changes. The cycle is assumed to be operating without losses and that the regenerator can be represented as a perfect heat exchanger. As such the cycle is considered an ideal, reversible cycle. The idealised process paths are indicated in figure 5.1. The implications of this analysis are discussed earlier.

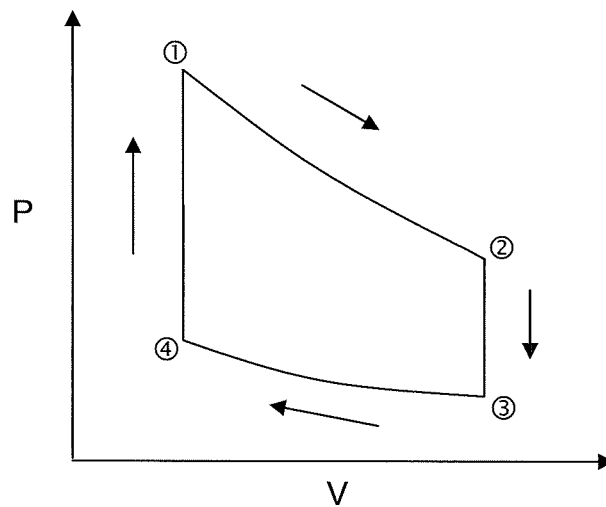


Figure 2.7 P-V diagram of ideal Stirling cycle

Where the indicated process path is described as:

- 1 – 2 Isothermal Expansion
- 2 – 3 Isochoric regenerative fluid transfer (displacement)
- 3 – 4 Isothermal Compression
- 4 – 1 Isochoric regenerative transfer of working fluid (displacement)

Subsequent analyses become progressively more thorough in defining Stirling engine operation.

The first order analysis attempts to relate engine power output and efficiency to the source and sink temperatures (hot plate and cold plate respectively), and engine speed and volumes (usually the swept volume of the power piston). Examples of this type of analysis are Schmidt [Schmidt 1871] and Beale [Beale 1980].

The second order analysis uses an equation to describe the engine which indicates power output and heat input, such as the Schmidt equation. Mechanical losses are then calculated separately (both kinematic and fluid) and subtracted from the output, and thermal losses are calculated separately and added to the input. Thus an approximation of real mechanical output and thermal input may be

made in a straightforward process. The accuracy of prediction is a function of the ability to identify and quantify kinematic and thermal losses throughout the engine. The Martini-Weiss code [Walker et al 1994] is one computer program using second order analysis techniques. The main reason for error in prediction using a second order analysis is the fact that this analysis ignores the complex interactions of the kinematic, thermal and fluid cycles.

The third order analysis considers the engine as comprising discrete nodes or elements. Laws of conservation of mass, momentum and energy are applied to each of the nodes and a gas state equation is applied to the working fluid at each relevant node. This allows the development of a set of differential equations, describing the processes occurring at all the nodes at any given time. Thus all processes are considered to happen simultaneously and to interact with each other. In this thesis the term third order analysis will be used as defined above. To enable coding for computer simulation of engine operation, the differential equations describing the simultaneous processes are manipulated to form discrete terms within the time domain (one dimensional form).

Presently, there are several third order analyses that use numerical methods to return nodal solutions, namely Finklestein [Finklestein 1961], Ureili-Berchowitz code [Ureili-Berchowitz 1984], and the Stirling Numerical Analysis Program code [Chen and Griffin 1983], [Altman 2003]. These analyses concentrate upon sealed engines with positive drive to the displacer. As yet there is no third order analysis of the Ringbom variant of the Stirling engine.

The third order analysis of the Ringbom Stirling engine is significant due to a unique feature of operation within the engine. The Ringbom variant, as discussed in chapter 2 section 5, uses a pressure differential to drive the displacer. The more common method attaches the displacer to the drive shaft or flywheel, with the phase angle between the displacer and piston being set and remaining constant as the engine runs. This translates the sinusoidal motion of the piston to the displacer, unless a discontinuous motion link is utilised [Kolin 1986]. The pressure differential is formed between the atmosphere outside the engine and the working fluid inside the engine. For part of the cycle the internal pressure is greater than

atmospheric, and for part of the cycle the internal pressure falls below atmosphere. This pressure differential acting across the displacer rod provides the motive force for displacer movement.

2.5 Modern analysis

Finkelstein took the Schmidt analysis a stage further by defining two limiting cases for the expansion and compression processes. This analysis takes the two extremes of isothermal and adiabatic processes and tries to quantify the degree to which each type of process affects the cycle, thus introducing a method of non-isothermal analysis.

Walker and Kahn carried this work forward showing that thermal efficiency for the Stirling engine was not just a function of temperature (as in Carnot) but is also a function of swept volume, phase angle and dead space [Walker 1980].

Feurer (Walker 1980) working for MAN / MWM (before the German government classified the work of MAN / MWM as secret), developed an adiabatic cycle analysis corrected for residual losses (accounts for phase difference between temperature changes and pressure changes) and aerodynamic losses.

Finkelstein in Newark N.J. at the 10th IECEC Aug 17 – 22 1975 produced a nodal analysis for the Stirling engine. This analysis uses the conservation equations for mass, momentum and energy resolved for nodes, cells or elements.

This can be used to create a model that indicates all the processes occurring within the engine simultaneously, be it energy flow, fluid flow or displacement of the displacer or piston. The equation sets are discretised into the time domain to form algorithms which can then be calculated with small changes in time. This method has formed the basis of many of the computer programs developed to simulate Stirling engines.

Urieli [Urieli and Berchowitz 1984] further developed the computational approach and uses parts of his analysis as a teaching aid for his lectures. Schock [Walker

1980] has developed a similar approach (and program) as Urieli, producing a commercial code, the Stirling Numerical Analysis Program (SNAP). The SNAP program has been developed over the years as a commercial tool and draws upon the works of Martini, Berchowicz, Senft, Thomas, Urieli and Organ [I.S.E.C. 2003, pp166-172]

The direction of research thus far has been in high temperature applications, the analysis of low temperature engines being limited, with Kolin and Senft contributing mainly to the body of knowledge.

2.6 Operation of the Ringbom – Stirling engine.

Ossian Ringbom showed that the drive and synchronisation mechanism for the Stirling engine could be greatly simplified. In his American patent of 1907 lines seven to 15 states:

'The aim of the present invention is to produce a hot air engine in which the movement of the displacing piston is obtained without the connection of rods or cranks or eccentrics or other mechanical parts of the engine, but solely by the expansion of the heated air and the weight of the piston; and to obtain at the same time a simple regulating device for the velocity.'

(US Patent No. 856,102 of 1907)

The way in which Ringbom simplified his engine was to rely upon gravity for the return stroke of the displacer and the higher pressure difference between internal and external spaces acting upon the displacer rod for the upward stroke, incorporating dashpots at each stroke end to cushion the deceleration. An idea that is both elegant in conception and straightforward to put into operation. Ringbom had a small port in the power piston to allow the minimum cycle pressure to adjust to atmospheric. A modification suggested by Senft [Senft 1993 pg 36] does away with this port, has the atmospheric pressure as the mean cycle pressure which means that not only is the displacer up stroke initiated (and

propelled) by the internal/external pressure difference, but also the return stroke, allowing faster engine operation.

The author feels that the Ringbom – Stirling engine shows great promise for the application of low-tech power supply. If the fly wheel and crank assembly were removed from the power piston and replaced with a gas spring and the piston made of magnetic material the whole device could be constructed from five parts, only two of which are moving, thus creating a free piston Stirling engine. In this unique type of Stirling engine, displacer movement is achieved by pressure differences caused by the piston motion and the thermodynamic cycle.

2.6.1 The Ringbom cycle using a gamma configuration

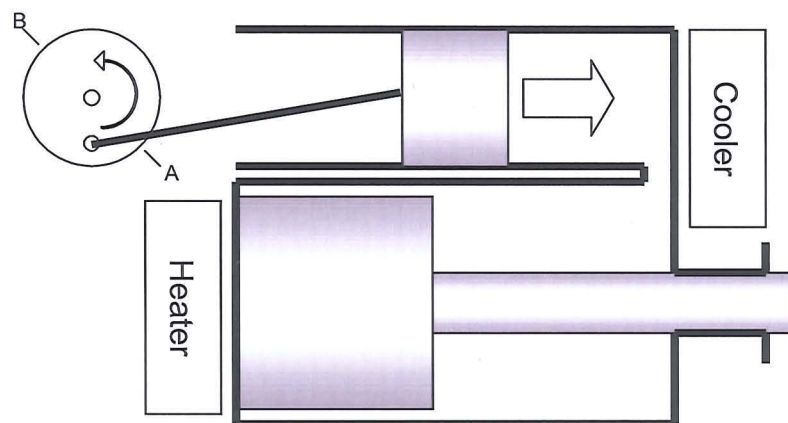


Figure 2.8 Ringbom compression stroke

At the start of the compression stroke as shown in figure 2.8, the displacer is at rest in the hot end and the working fluid is in the cold end, the state is P_{min} , T_{min} , and V_{max} . The pressure of the working fluid is below that of the surrounding atmosphere. This keeps the displacer pushed inwards and pushes the piston inwards (assisted by the flywheel). The volume decreases and the internal pressure rises. The engine geometry is proportioned so that when the crank angle reaches point A indicated on the fly wheel above (just before inner dead centre), internal and external pressures equalise. The momentum of the flywheel/crank/rod/piston assembly causes the piston to move further into the cylinder, causing

the internal pressure to rise above the external pressure. This pressure difference causes the displacer to be pushed outwards into the cold end, forcing the working fluid into the hot end, thus beginning the transfer stroke.

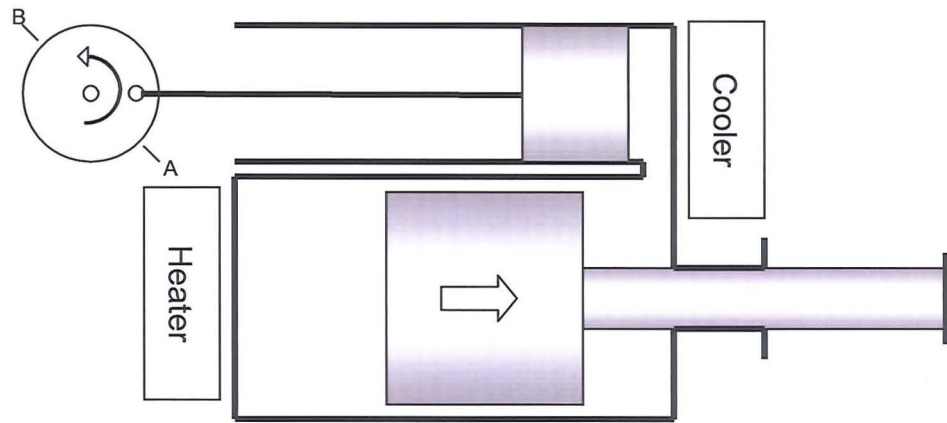


Figure 2.9 Ringbom first transfer stroke

The momentum of the flywheel assembly causes the piston to go through inner dead centre; the displacer continues to move outward by the internal / external pressure difference, as shown in figure 2.9. Working fluid is transferred from the cold end into the hot end, raising the internal pressure (as it is heated), causing the displacer to accelerate into the cold end. Movement of the displacer is arrested by means of a dashpot or cushion. At the completion of the transfer stroke the condition of the engine is V_{min} , P_{max} , and T_{max} .

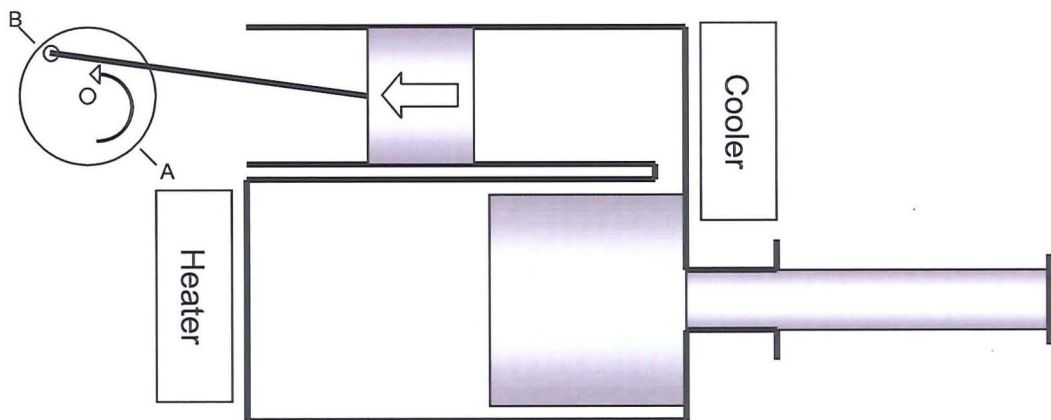


Figure 2.10 Ringbom expansion stroke

As the working fluid is expanding as shown in figure 2.10, internal pressure remains above external pressure until the crank angle reaches the equilibrium point labelled B above. The flywheel assembly causes the piston to continue on its outward journey, reducing the internal pressure below that of the surroundings. This causes the displacer to begin its motion into the hot end.

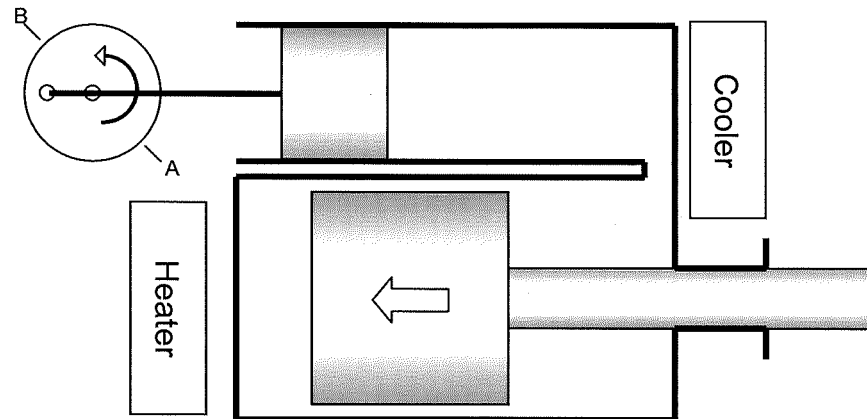


Figure 2.11 Ringbom second transfer Stroke

The working fluid is transferred from the hot end to the cold end, lowering the internal pressure, further accelerating the displacer motion as shown in figure 2.11. The displacer completes its transfer stroke and stops just as the piston reaches outer dead centre...so the cycle continues.

2.7 The Free Piston Stirling Engine (FPSE)

The title of free piston Stirling engine (FPSE) is used as a generic term for any Stirling engine where one of the reciprocating elements that make up the engine is not coupled directly to any other element. [Walker and Senft 1984]. Rather, the motion of the element is imparted from working fluid pressure changes due to thermal effects. Work is delivered from reciprocating motion as opposed to rotational motion.

To expand, the term FPSE covers a multitude of different configurations, from having one free element such as the piston or displacer (sometimes called a

hybrid engine) as found in the Ringbom Stirling engine, to ones where either the piston and displacer are free to move, or where the cylinder casing and displacer are free to move as in the Beale / Sunpower FPSE.

The kinematic cycle for a FPSE is designed as a stable tuned resonant circuit, classic vibration theory will be used to help explain the action of the cycle, beginning with a brief description and notation.

Consider a damped mass system, as shown in figure 2.12, a single coordinate, $x(t)$ can completely define the system. The number of coordinates required to fully define a system specifies the number of degrees of freedom (dof) which a system possesses.

At equilibrium, the mass M is motionless. The upward force (resisting the product of gravity and the magnitude of the mass) is created from torsion in a mechanical spring or by a magnetic spring.

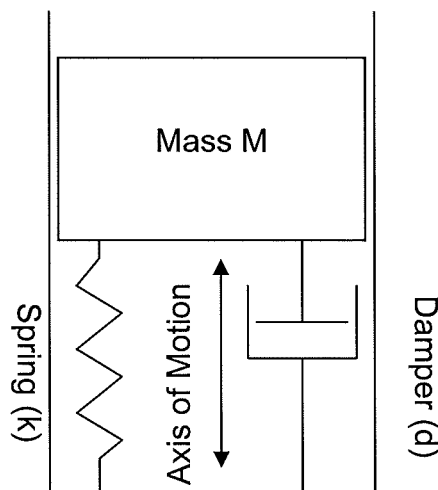


Figure 2.12 Simple damped mass system (1 dof)

If the mass is raised, its potential energy is increased and work is done against the spring and damper. If the mass is then released the mass falls due to the force of gravity and also the restorative force of the spring (equal to the product of the

spring constant k and extension). As the mass reaches the rest position, there is no spring restorative force in action, the mass continues its downward travel due to inertia, and compresses the spring. If there were no damping forces present the spring compression would equal that of the extension and the system would continue to oscillate about the rest position ad infinitum. The presence of damping reduces the amplitude of the oscillation during each half cycle; damping may be in the form of air damping, fluid friction, magnetic damping or gas spring hysteresis and may be intentional or parasitic.

In many of the standard texts and even recently published papers there is a belief that the motion of both the displacer and piston may be (for ease of analysis) described using simple harmonic motion (SHM) (the same texts that dismiss the thermal analysis of the FPSE as identical to that of the isothermal kinematic engine cycle). It is the opinion of the author that the piston may be analysed using SHM, but only as long as the engine is operating in a stable tuned resonant mode. This caveat becomes more important in the description of the displacer movement, especially if the engine is operating at the overdriven limit to improve cycle performance. Stable resonant operation tends to be achieved in a narrow operating band; fluctuations in load can easily push the operation into under-driven or overdriven modes. Mode of operation will be covered later.

In a spring mass system without damping, the acceleration of the mass is proportional to the distance of the mass from the static equilibrium point.

The motion can then be described by using rotating vectors of magnitude X

Instantaneous displacement x

$$x = X \cos \omega t$$

Equation 2.10

Instantaneous velocity \dot{x}

$$\dot{x} = -X\omega \sin \omega t = X\omega \cos(\omega t + \pi/2)$$

Equation 2.11

Instantaneous acceleration \ddot{x}

$$\ddot{x} = -X\omega^2 \cos \omega t = X\omega^2 \cos(\omega t + \pi)$$

Equation 2.12

The amplitude of \dot{x} is ω that of the displacement leading by a phase angle of 90° ($\pi/2$ rad)

The amplitude of \ddot{x} is ω^2 that of the displacement leading by a phase angle of 180° (π rad)

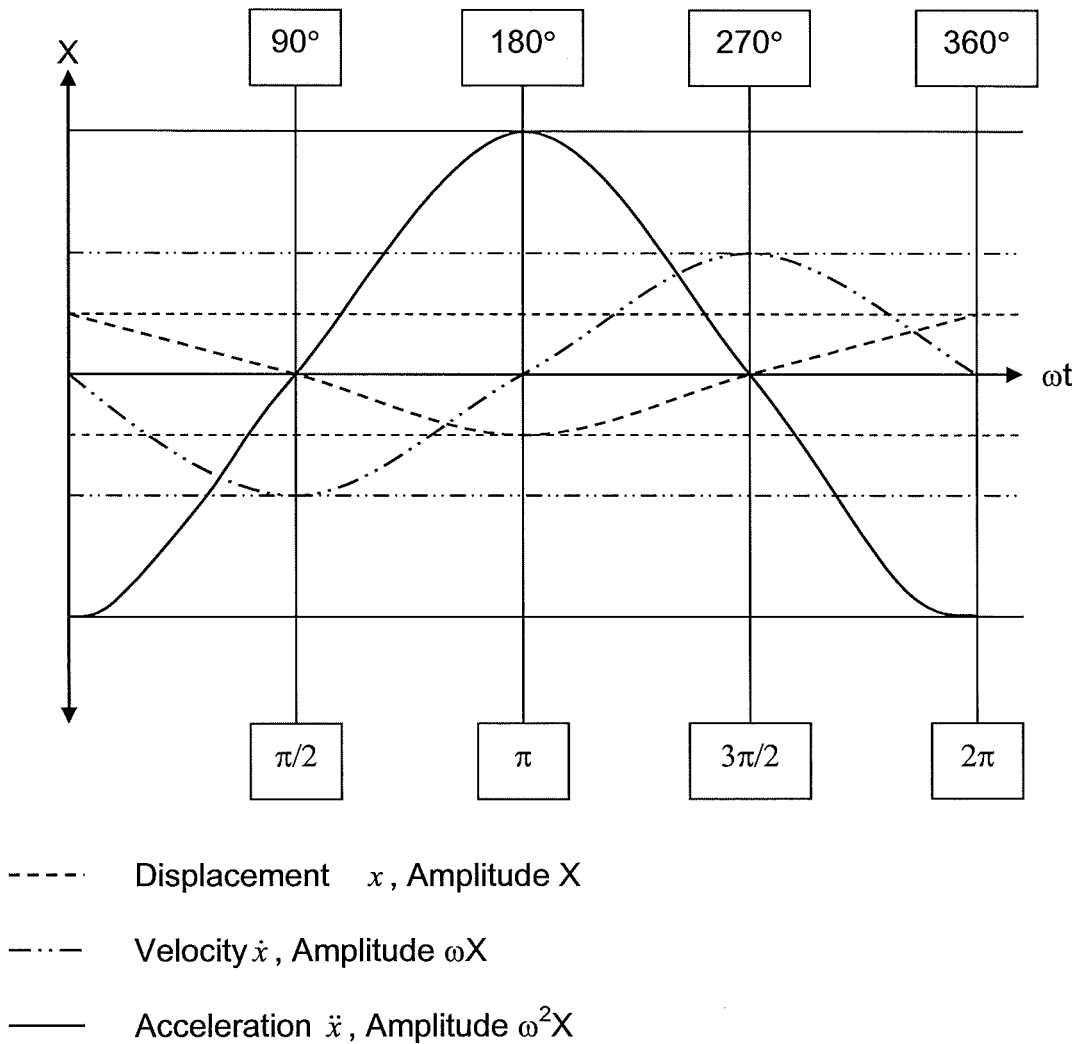


Figure 2.13 Graph of displacement velocity and acceleration

Vibration can be classified in one of two ways:

- Free vibration where the vibration is caused by a single impulse, the amplitude of which dies away in accordance to the damping forces applied, the mass oscillating at its natural frequency (f_n).
- Forced vibration where vibration is caused by a force of uniform period or cycle, often described in the form $F(t) = F \sin \omega t$ or $F(t) = F \cos \omega t$, and settles down to steady state vibration at the frequency of the applied force (F), with the natural frequency effects dissipating through damping.

By reference to standard texts for vibration such as Rao [Rao 1995], it can be shown that when the natural frequency and the applied frequency of a spring-damped system are the same, the system enters resonance, with the amplitude of oscillation increasing towards the resonant point and decreasing either side of the resonance condition. The amplitude of oscillation being solely a function of viscous damping present in the system.

$$\text{Displacement is given by } x = \frac{\mu F}{k} \quad \text{Equation 2.13}$$

Where μ is the amplification factor.

The frequency ratio r is defined as:

$r = \text{frequency of imposed force} / \text{natural frequency}$

$$\Rightarrow \frac{f}{f_n} = \frac{\omega}{\omega_n} \quad \text{Equation 2.14}$$

Viscous damping ρ is defined as:

$$\rho = \frac{C}{C_{crit}} \quad \text{Equation 2.15}$$

Where C is the coefficient of viscous damping

C_{crit} is the coefficient of viscous damping for a critically damped system

For a FPSE with a bounce space, hysteresis damping is considered the main secondary parasitic loss, where the friction between the working fluid molecules converts some of the energy imparted to the gas spring into heat. Coulomb or dry sliding damping imposes a constant resistive force in the annular spaces between the piston and the cylinder wall. Viscous damping will be present due to the movement of working fluid by the displacer. Non-viscous damping (dashpot) will be present due to working fluid movement around the displacer and if dashpots have been used to decelerate the displacer at each end of its travel.

The equation of motion for the spring damped mass system is taken from Newton's second law of motion, $\Sigma F = Ma$, which for a single mass gives:

$$M\ddot{x} + C\dot{x} + kx = 0$$

Equation 2.16

2.7.1 Multi element multi degree of freedom system

The system represented in figure 2.14 is a generalised spring damper mass system for FPSEs consisting of three masses. All the masses are constrained so that they can only move in one ordinate, as such the system may be fully described by the use of three coordinates at any instant in time. The masses are connected by spring forces and damping forces.

The elements have an axis of symmetry about which they may rotate, the degrees of freedom required to describe this motion are ignored, as any change in the angular position has no bearing on the motion of the element in the operational axis. Hence the above system is a damped spring mass system with three degrees of freedom.

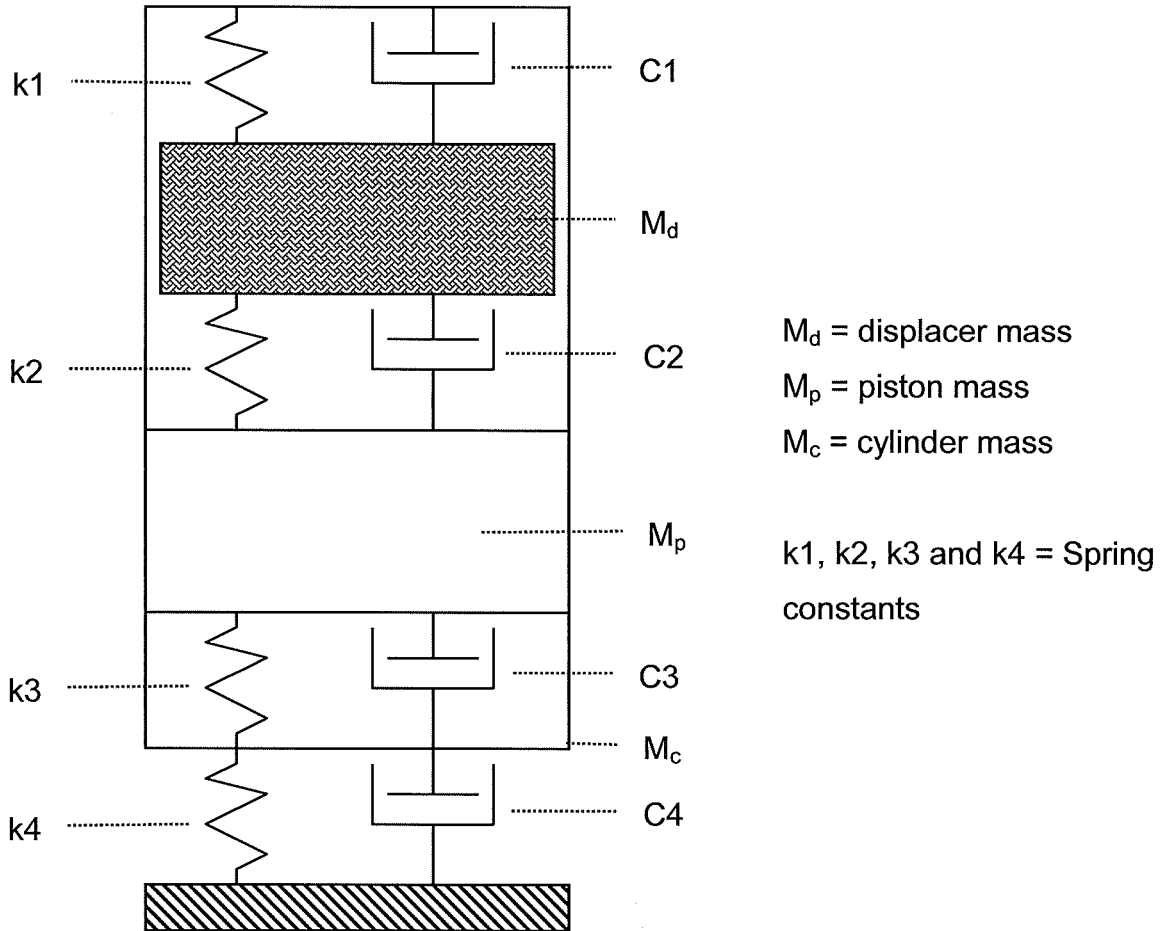


Figure 2.14 The FPSE as a multi degree of freedom system

In real applications the piston may be made so large that it is virtually an immovable object, or the casing may be attached firmly to a large mass, reducing the analysis to a two-degree of freedom spring mass system.

2.7.2 Two degree of freedom damped spring mass system

The system has a light displacer, typically between one-third and one-tenth the mass of the piston. There are two springs k_d and k_p for the displacer and piston respectively, which apply restorative forces to the masses. Restorative in this sense is to return the mass to its equilibrium position. The action of the springs can readily be described by SHM.

The amplitude of the oscillation is a function of the forcing frequency with constant damping, thus as the frequency ratio r approaches 1, the amplitude of oscillation increases.

The working area of the displacer is one quarter that of the piston, thus any pressure acting on each will only have a quarter of the surface to act upon in relation to the piston.

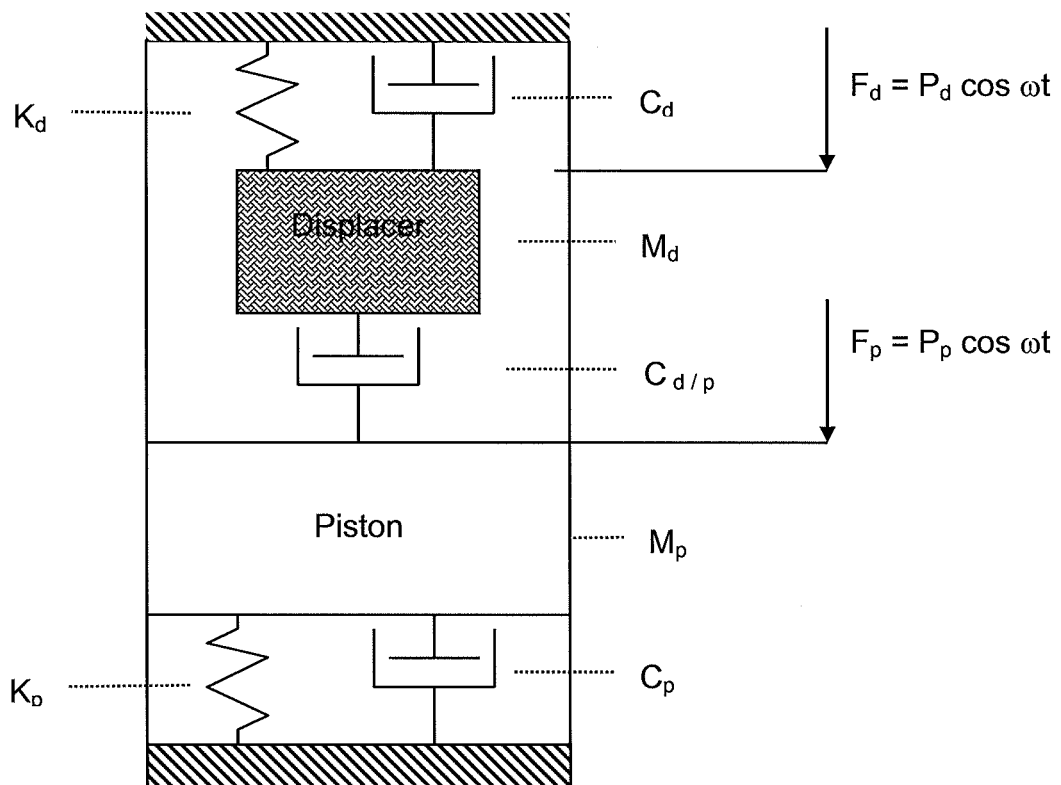


Figure 2.15 Two degree of freedom spring damped mass system

$$\text{Therefore } F_b = \frac{1}{4} F_p \Leftrightarrow F_p = 4F_b$$

By a similar argument, as the spring is provided by the bounce space the spring constant for the two elements may be defined as:

$$k_d = \frac{1}{4} k_p \Leftrightarrow k_p = 4k_d$$

The above consideration assumes SHM for the system elements. In reality the systems are non linear to some degree, in the FPSE analysis during the expansion stroke the displacer accelerates from top dead centre until it contacts with the top of the piston. At this point the piston has gained an extra quarter of surface area for the pressure to act upon.

Simple analysis of FPSEs assumes a linear system where all reciprocating elements may be described by SHM; in most cases it is safe to assume SHM for the piston (or cylinder). It would be erroneous to assume SHM for displacer motion in anything other than stable resonant operation. If the displacer is 'overdriven' then it assumes the motion described in the thermal FPSE and Ringbom operation, the advantage of which is to bring the real cycle closer to the theoretical cycle. This results in an engine with both linear and non-linear motions for different elements. Figure 2.16 indicates the phase relationship of the displacer and piston in the overdriven engine.

In kinematic engines the phase angle of the reciprocating elements may be calculated by the use of trigonometric relationships. The motion of elements in the FPSE is not constrained by linkages, rather controlled by the laws of motion and working fluid pressure effects. It is these pressure effects (created by temperature differences) that govern the mode of operation of the engine, resulting in under-driven, resonant and overdriven modes.

In the under-driven state the reciprocating elements vibrate within the confines of the cylinder due to the energy supplied, but never achieve cyclic operation.

In the stable resonant state of operation the piston (cylinder) and displacer operate with a constant phase angle, the reciprocating elements never contact and their motions can be described using SHM equation sets. Analysis may be undertaken using rotating vectors.

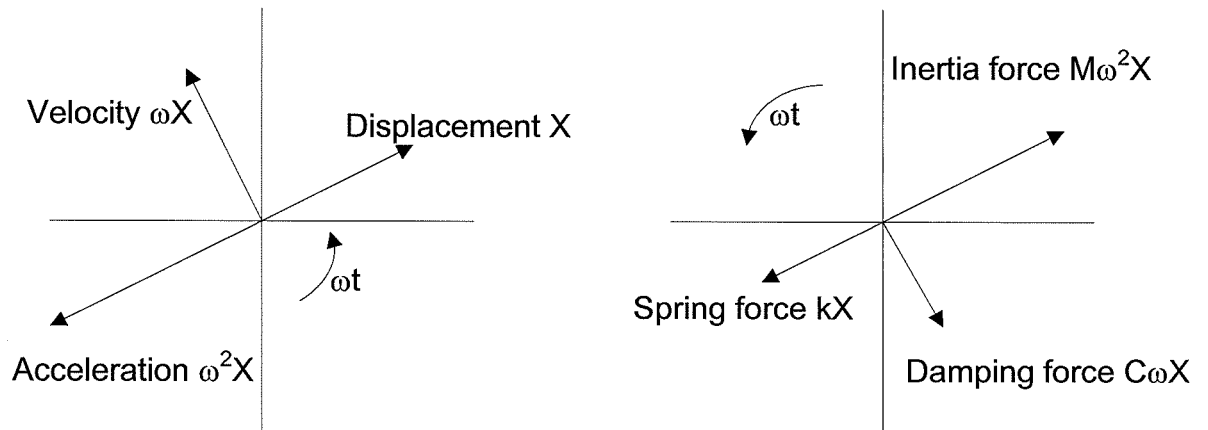


Figure 2.16 Vectors for a) acceleration, velocity and displacement and b) forces.

Inertia force $M\ddot{x}$ always resists the acceleration of the mass and is represented by a vector $M\omega^2X$ in the opposite sense to the acceleration vector.

Damping force $C\dot{x}$ always resists the motion of the mass (due to its velocity) and is represented by a vector $C\omega X$ in the opposite sense to the velocity vector.

Spring force kx always resists the displacement of the mass and is represented by a vector kX in the opposite sense to the displacement vector.

The imposed or excitation force which would be a vector in the opposite sense to the resolved vector may also be placed on the vector diagram, its position given by an angle α leading the displacement, with magnitude F at phase $\cos(\omega t + \alpha)$.

If $\omega_{\text{imposed}} < \omega_{\text{natural}}$ then α is between 0 and $\pi/2$

If $\omega_{\text{imposed}} = \omega_{\text{natural}}$ then $\alpha = \pi/2$

If $\omega_{\text{imposed}} > \omega_{\text{natural}}$ then α is between $\pi/2$ and π

Hence the classic FPSE describing equation may be written as

$$M\ddot{x} + C\dot{x} + kx = F \cos(\omega t + \alpha) \quad \text{Equation 2.17}$$

In the overdriven mode the use of vectors is not appropriate apart from one very specialised case laid out below.

In the overdriven mode the displacer action is discontinuous, with dwell points at top and bottom dead centre. It is interesting to note that as the engine speeds up the dwell period reduces, until a point called the overdriven limit is reached. At this point there is no dwell period, although the transit time for the displacer is still the same. Beyond the overdriven limit the engine operation becomes erratic due to the phase relationship being able to slip or jump cycle; thus an inherent over-speed limiter is built in. At the overdriven limit the phase relationship between the Piston (displacer) and the displacer can be described as quasi-simple harmonic motion.

2.7.3 Vibrating systems and the limit cycle

As discussed earlier the FPSE operates due to a complex interaction of thermofluid and kinematic forces, which create the reciprocating motion of the machine elements. The way in which the present cycle operates is governed by the previous cycle and the next cycle will be governed by the present cycle. This type of feed forward system is often referred to as a limit cycle.

After start up the system will reduce to a stable resonant or overdriven state of operation. A change in the magnitude of the driving force (through temperature change) will tend to move the cycle envelope within a velocity displacement graph as shown in figure 2.17 below.

Hamilton's Principle of minimum energy states covers this settling of the cycle into a stable state. This says that any system will seek the lowest energy state, or will be in its lowest (present) energy state when at equilibrium.

Walker and Senft (1983) take this further and state

'The implication of this is that an FPSE has a preferred stable operating frequency, close to the resonant frequency of the largest dynamic mass'

Beale (1973) suggests that the operating frequency may be calculated as:

$$f_n = C\sqrt{k/M} \quad \text{Equation 2.18}$$

where C is a constant between 0.7 and 1

k is the spring stiffness

M is the mass of the piston.

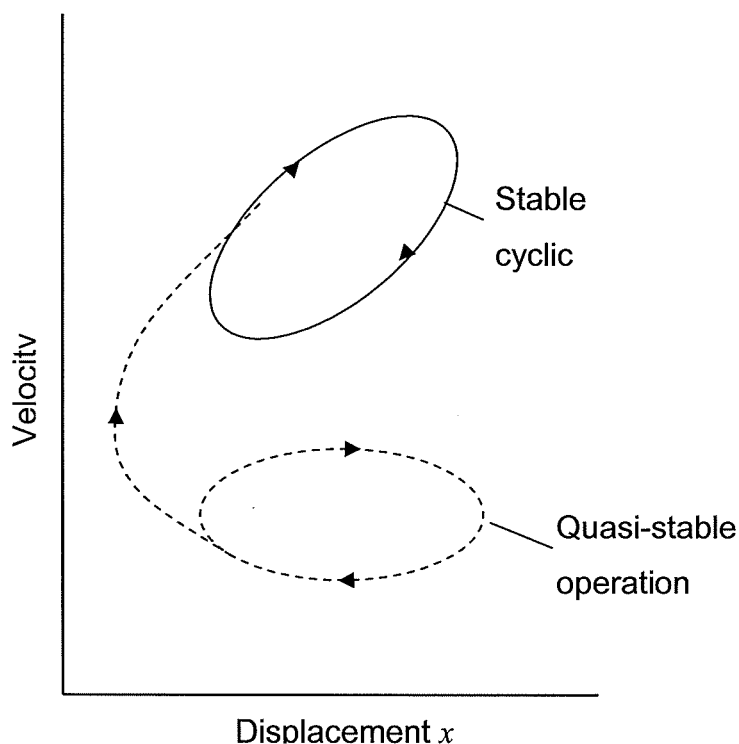


Figure 2.17 Diagram suggesting different stable and quasi-stable operating states

Much of the work on analysis of the FPSE assumes stable resonant operation so that simple harmonic motion may be applied. This allows for linear solutions for the motion of reciprocating elements. The author suggests that stable resonant motion only occurs at resonance and at the overdriven limit, at all other times the cycle is either under-driven, so no complete cycle is achieved or overdriven where the displacer motion is discontinuous.

In stable resonant operation the displacer and piston never contact, in overdriven operation the displacer contacts with the piston; although the displacer is in the order of one tenth of the mass of the piston, it has three times the acceleration, so the momentum of the displacer after contact must be added to that of the piston. After making contact the effective surface area of the displacer rod is added to the area of the piston, increasing the area of action for the applied pressure. Hence not only is the motion of the displacer discontinuous, but also that of the piston.

The author feels that the advantages of operating in the overdriven region make this a desirable option. Hence the methods of analysis for discontinuous motion should be the next logical step. The Ringbom offers other advantages in this free piston free displacer mode discussed below.

2.7.4 Advantages of the FPSE Stirling engine

The FPSE offers many advantages over the more conventional layouts, these being:

- The FPSE is in effect a dynamic resonant circuit. When heat is applied to the engine the temperature rise of the working fluid causes a resulting pressure change, the system then enters a phase of unstable equilibrium, the slightest vibration will cause the engine to start. Consider a mass on top of a column with a pin joint at the base, only the slightest of forces causes the system to go from vertical to horizontal. This 'property' of the FPSE means that it has a self-starting capability.
- The reciprocating elements operate axially with no crank linkage, eliminating side loading of the components and the resulting wear and fouling. This has the advantage of adding longevity to the engine and increasing the time between services. The need for lubrication is also reduced to the level that the working fluid is used as the lubricant.
- The cylinder may be hermetically sealed allowing the use of more exotic or difficult to restrain working fluids, removing the requirement for external seals.

- The engine is self-regulating (to a point). When the resistive force (load) is low then the piston assumes a long stroke. As the load increases, the stroke shortens and the acting force increases. As such, it is very unlikely that an FPSE would stall, there would always be some miniscule vibration left to restart the engine as the load reduces.
- There is a reduction in the number of moving parts down to two in the most reduced of cases.

2.7.5 Disadvantages of the FPSE

As with any system there are also some disadvantages associated with the FPSE, these being:

- Loss of phase angle between the vibrating elements due to imperfect sealing between the bounce space and the working space also termed as piston centring. This may be eradicated by the use of a displacer relief valve or bypass valve to maintain phase relationship.
- The output is in the form of linear motion. This may be considered by some as a disadvantage, but linear motion alternators can be used, or linear pumps may be employed as such this disadvantage may be arguable. If rotary motion is required there are many solutions such as wobble or Scotch yokes or other linear to rotary mechanical converters.

2.7.6 Modes of operation

In kinematic engines, also known as disciplined motion engines, the phase angle of the reciprocating elements may be calculated by the use of trigonometric relationships. The motion of elements in the FPSE is not constrained by linkages, rather controlled by the laws of motion and working fluid pressure effects. These pressure effects (created by temperature differences) govern the mode of operation of the engine, resulting in under-driven, resonant and overdriven-modes. As such the analysis of the FPSE is inherently complicated, with dynamically

indeterminate phases for the reciprocating elements, the solution of which requires iterative methods. The three modes of operation for the FPSE are:

- In the under-driven state, the reciprocating elements vibrate within the confines of the cylinder due to the energy supplied, but never achieve cyclic operation.
- In the stable resonant state of operation the piston and displacer operate with a constant phase angle, the reciprocating elements motions can be described using simple harmonic motion.
- In the overdriven mode the displacer, action is discontinuous, with dwell periods at top and bottom dead centre. It is interesting to note that as the engine speeds up the dwell period reduces, until a point called the overdriven limit is reached. At this point, there is no dwell period, although the transit time for the displacer is still the same. Beyond the overdriven limit the engine operation becomes erratic due to the phase relationship being able to slip or jump cycle, thus an inherent over-speed limiter is built in. At the overdriven limit the phase relationship between the Piston (displacer) and the displacer can be described as quasi-simple harmonic motion.

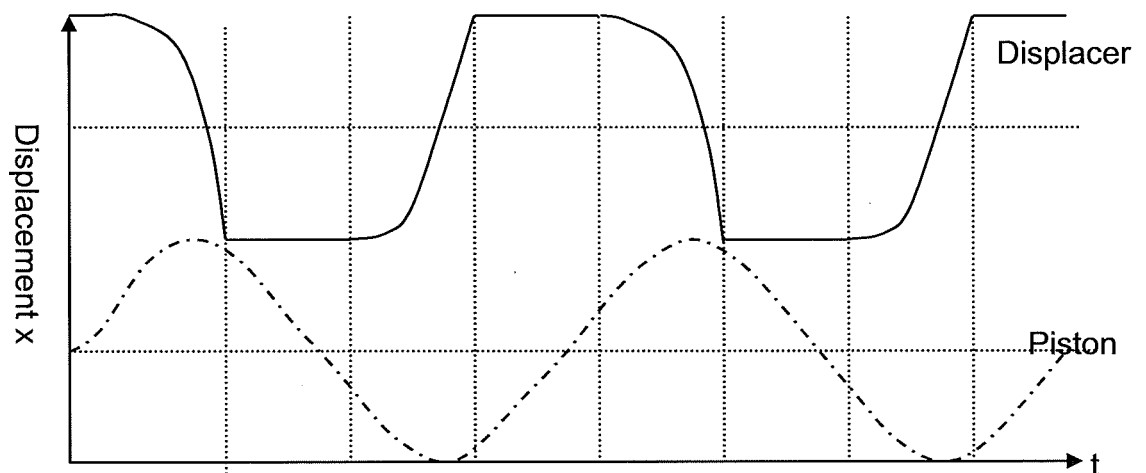


Figure 2.18 Phase relationship of displacer and piston overdriven mode

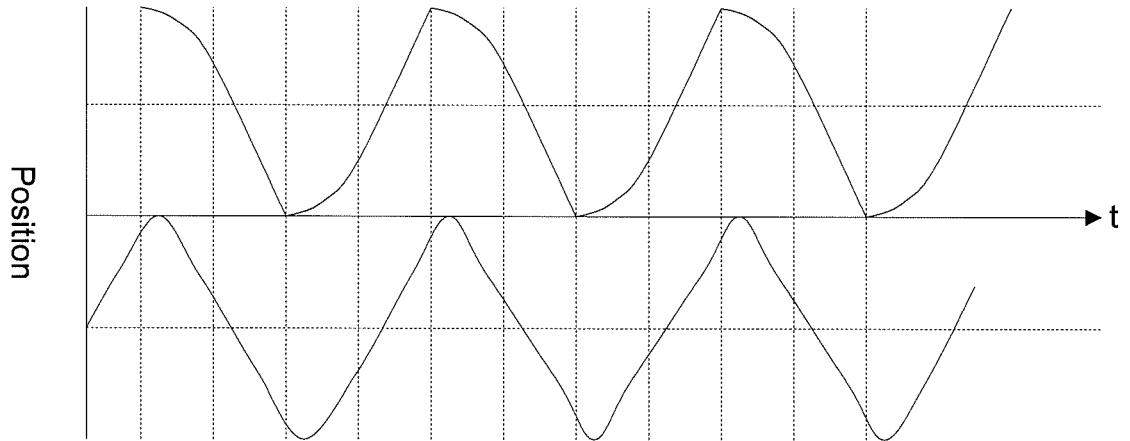


Figure 2.19 Phase relationship of displacer and piston at the overdriven limit

From this the advantage of the FPSE running in overdriven mode may be stated as:

Any FPSE operating in the overdriven mode has the advantage of being able to accept changes in engine speed due to load or operating condition changes, without becoming unstable.

2.7.7 Self starting FPSE

To start up, energy is applied to the hot end and the system enters a state of instability where the slightest vibration will set the system into motion. Taking the system from a point at rest, the self start may be described as follows:

- The system is at rest (no heat applied), the position of the displacer and piston being maintained by either bounce space pressure or mechanical spring.
- The fluid temperature and pressure are in equilibrium, the pressure being that of the bounce space, point S in figure 2.20 below. Internal pressure is made up of the pressure in the expansion/compression space above the piston.
- Energy is applied at the hot end causing the temperature of the hot end to increase, which is in turn transferred to the working fluid. Expansion of the

working fluid increases the pressure, causing the displacer and piston to move downward within the cylinder, point 1 in figure 2.20 below.

- The displacer is designed to be much lighter than the piston (at least 1/3rd the mass). This means that if the pressure acting upon the piston and displacer is the same (as it is in this case), then the displacer will accelerate faster than the piston for any given pressure scenario. Also the piston has greater momentum than the displacer.
- Working fluid in the compression space is transferred into the expansion space via the regenerator. This results in further expansion of the working fluid and a rise in internal pressure. The displacer, having greater acceleration than the piston over the same given time, catches up with the piston and assists the piston on its downward journey.
- As the displacer and piston are in face-to-face contact, all the working fluid must be in the expansion space. The movement of the displacer/piston group downwards causes the internal pressure to decrease, point 3 in figure 2.20.
- Expansion continues, at point 4 in figure 2.20 the internal pressure and the bounce space pressure are equal.
- The inertia of the displacer/piston group causes a continued motion downward into the bounce space. This lowers the internal pressure but increases the bounce space pressure. The pressure difference causes a greater upward force than downward force on the displacer/piston group. The pressure difference increases as the displacer/piston group moves further downward, increasing the net upward force.
- Eventually the upward force overcomes the downward momentum of the displacer and the displacer stops.
- The piston, having greater momentum continues downward, thus the displacer and piston separate, and some of the working fluid is drawn into the now forming compression space. The downward motion continues to cause an increase in pressure difference between the internal space and the bounce space. This pressure increase in the bounce space and decrease in the internal space causes the displacer to begin its upward journey, transferring working fluid from the expansion space into the

compression space (hot to cold). The decrease in fluid temperature causes the pressure in the internal space to drop further, increasing the upward acceleration of the displacer. The displacer moves into the top of the expansion space, pushing all of the working fluid into the compression space. The displacer is held in position due to the higher bounce space pressure.

- The power piston reaches its bottom dead centre and begins an upward movement under the action of the high bounce space pressure, compressing the working fluid.
- As the working fluid is compressed the internal pressure and bounce space pressure equalise, the fluid is further compressed due to the upward movement of the piston through inertia. This reversal in pressure difference causes the displacer rod to begin its downward motion. The piston then goes through top dead centre. As the expansion space is formed and fluid begins to expand, the displacer is accelerated toward the piston, catches it and continues the cycle.

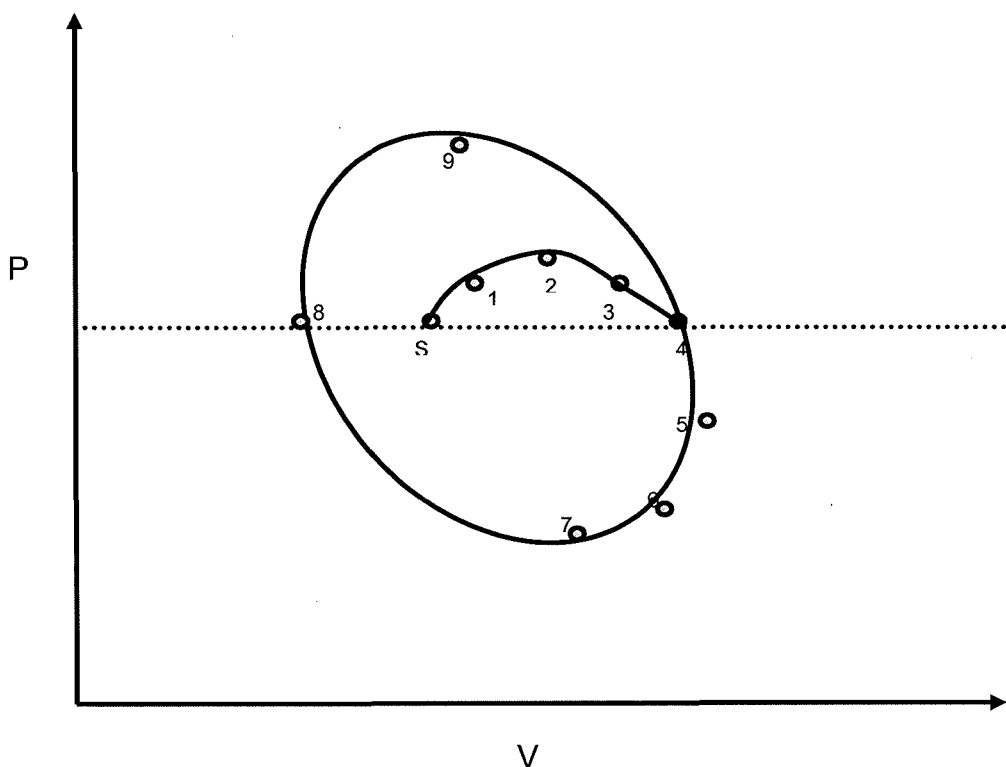


Figure 2.20 P-V diagram for the self starting FPSE

2.7.8 Discontinuous motion of the displacer

As has been expressed above and can be seen in the displacement diagrams for the displacer the motion of the displacer in a FPSE is not sinusoidal or even continuous. This can be shown through a calculation of the pressure gradient within the engine against the external pressure for the Ringbom engine, or of the mass difference of the piston and displacer in a sealed FPSE. The sealed case is expanded below for the engine represented in figure 1.4.

Acceleration ratio for the FPSE

Heat is applied to the expansion end heat exchanger thus raising the expansion space pressure (a.k.a. working space pressure), so the force on the piston is:

$$F_{piston} = (P_{working\ space} - P_{bounce\ space}) (A_{piston} - A_{displacer\ rod}) \dots\dots\dots(1)$$

From Newton's second law of motion

$$F = M a \dots\dots\dots(2)$$

For the piston

$$a_{piston} = F_{piston} / M_{piston} \dots\dots\dots(3)$$

Putting 1 into 3 gives:

$$a_{piston} = (P_w - P_b) (A_p - A_{dr}) / M_p \dots\dots\dots(4)$$

For the displacer

$$F_d = (P_w - P_b) (A_{dr}) \dots\dots\dots(5)$$

$$a_d = (P_w - P_b) (A_{dr}) / M_d \dots\dots\dots(6)$$

Typically the displacer mass is one tenth the mass of the piston, or $M_p / M_d = 10/1$

Typically the effective area of the displacer rod is one quarter that of the piston, or $A_p / A_{dr} = 4/1$

Ratio of accelerations

$$\frac{a_d}{a_p} = \frac{(P_w - P_b)(A_{dr})}{M_d} \times \frac{M_p}{(P_w - P_b)(A_p - A_{dr})} \dots\dots\dots(7)$$

$$\frac{a_d}{a_p} = \frac{M_p}{M_d} \times \frac{A_{dr}}{(A_p - A_{dr})} \dots\dots\dots(8)$$

$$\frac{a_d}{a_p} = \frac{10}{1} \times \frac{1}{(4-1)} \dots\dots\dots(9)$$

$$\therefore \frac{a_d}{a_p} = 3.33\dot{3} \dots\dots\dots(10)$$

Hence the displacer accelerates 3.3 times faster than the piston.

Figure 2.21 Results to indicate discontinuous motion of displacer

Walker and Senft (1984) give the results in figure 2.21 as an indication (proof) of the discontinuous motion of the displacer in a FPSE.

2.7.9 The free displacer Ringbom - Stirling engine

This engine has a free displacer with the power piston attached to a flywheel via a connecting rod as Ringbom intended. The analysis of this type of engine is in some ways more straightforward than the free piston-free displacer engine described above. This is due in the main part to always being able to determine the location of the piston within the cylinder if the phase angle is known.

A second advantage is that the motion is now rotary in nature and a load may be applied by means of a simple brake.

As the test engine is equipped with the flywheel crank assembly, it is felt that for the initial analysis this type of layout should be used; this means that the virtual model created by the computer program would mimic the physical engine.

The nature of the free displacer also means that the cycle efficiency is improved. Kolin [Kolin 1986], suggested that as the displacer actually touches the faces of the source and sink (or heater and cooler) then dead space would be minimised, thus increasing the cycle work envelope. This envelope could be modified further by the action of discontinuous motion, allowing more time for the expansion and compression phases, and due to the nature of the acceleration of the displacer means that the isochoric displacement would happen in a shorter time period, hence staying closer to the process paths.

2.7.10 The Regenerator

The ability to analyse the effects of changing mesh size and spacing will form a part of the optimisation of regenerator efficiency. The regenerator is analysed on the basis of energy balance, where the change of energy within the system is formed from two distinct parts, the flow energy balance and the matrix material energy balance.

The regenerator is constructed by placing several hundred mesh screens one on top of the other. Mesh geometry is defined by the mesh number and wire thickness from which several valuable properties may be derived. Mesh number is defined as the number of holes per inch [ISO 4783-2] from which one cell may be discerned. The following guideline has been modified by the author for a rectangular matrix of uniform mesh.

For a known mesh, taken from catalogue data the aperture 'a' may be found for any given wire diameter 'd', for this we use.

$$a = \left(\frac{25.4 \times 10^{-3}}{\text{Mesh } N^2} \right) - d \quad \text{Equation 2.19}$$

from this surface porosity 'ε' may be calculated using

$$\varepsilon = \frac{a^2}{(a+d)^2} \quad \text{Equation 2.20}$$

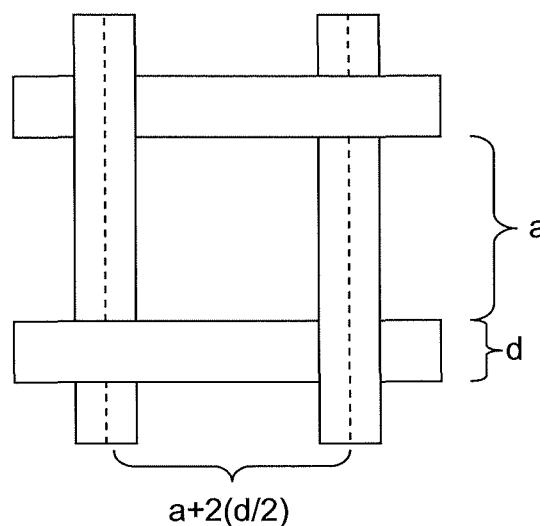


Figure 2.22 Single cell for a mesh screen

For a rectangular matrix of length x , height y

Length of wire in one screen

$$L_s = x \left(\frac{y}{(a+d)} \right) + y \left(\frac{x}{(a+d)} \right) \quad \text{Equation 2.21}$$

Heat transfer area

$$A_{ht} = (\pi d) \left(x \left(\frac{y}{(a+d)} \right) + y \left(\frac{x}{(a+d)} \right) \right) \quad \text{Equation 2.22}$$

Wire volume

$$V_w = \left(\frac{\pi d^2}{4} \right) \left(x \left(\frac{y}{(a+d)} \right) + y \left(\frac{x}{(a+d)} \right) \right) \quad \text{Equation 2.23}$$

Wire mass

$$m_w = \rho \left(\frac{\pi d^2}{4} \right) \left(x \left(\frac{y}{(a+d)} \right) + y \left(\frac{x}{(a+d)} \right) \right) \quad \text{Equation 2.24}$$

Wire thermal capacitance

$$TC_w = C_m \rho \left(\frac{\pi d^2}{4} \right) \left(x \left(\frac{y}{(a+d)} \right) + y \left(\frac{x}{(a+d)} \right) \right) \quad \text{Equation 2.25}$$

This is for one screen for total screen properties multiply the above equations by the number of screens

2.8 Final remarks

As was said at the beginning of this chapter, the body of information available for the researcher in the field of Stirling engines is limited to older texts and conference reports. The author has only found minimal information for low temperature engines, mainly from Senft [Senft 1993], [2000a,b,c] and even less information on Ringbom Stirling engines [Ringbom 1907]; [Senft 1993, 2000b, c]. It is the author's belief that no satisfactory model of the Low Temperature Differential Ringbom Stirling Engine is available. This belief has been reached by searching the available literature and the www.theses.com web site, which lists all theses accepted for higher degrees in Great Britain and Ireland since 1716. European and American searches have also been carried out. This said, one of the main aims of this work is to develop a mathematical model through a generic equation set, thus creating a virtual engine, then validate the virtual engine against an actual engine and use the mathematical model to optimise the engine design.

3 Research Aims

The aim of this research is to derive an equation set which when encoded into a computer program will provide a tool to aid in the optimisation of low temperature differential Ringbom Stirling engines.

To achieve this, the following questions are presented:

3.1 Research Questions

What are the optimum design parameters for a LTDRSE?

By altering one parameter what effect will it have upon:

- The engine power?
- Operation of other engine components?
- Engine efficiency?

3.2 Focus of Study

- Create a generic equation set describing the operation of a simple LTDRSE, complete with stated simplifying assumptions
- Encode the generic equation set into a suitable programming language (FORTRAN PLUS) to create a virtual engine (mathematical model)
- Verification of mathematical model by:
 - Running the virtual engine to gather data sets of expected behaviour, power output and efficiency
 - Running the physical (real) LTDRSE to gather equivalent data sets
 - Comparing results of real and virtual engine
- If the results show divergence then investigate assumptions made to improve (incorporate) the mathematical model

If the results show convergence then alter parameters of both engines and re run tests

- Run the virtual model with different parameters to optimise engine design
- Build physical engine to virtual model dimensions and test accuracy

4 Experimental work

The verification strategy for the simulation program required that a test engine be built. The test engine was used to produce sets of experimental results. These results were used for comparison with the predicted output of the simulation program. Two engines were manufactured for this research.

The first engine was taken from the design by Senft [Senft 2000], which proved useful for early research and observation of engine operation. Unfortunately this design proved problematic when applying the instrument package.

The second experimental engine was designed to overcome the shortcomings of the first. The second design used much greater mass for the hot and cold plates, thus the amount of energy stored or released for any run could be calculated. The new design did away with the cylinder dead space of the original, with the face of the piston at bottom dead centre being set to the top of the compression space. The other modification was the application of stub springs in the expansion and compression spaces. The stub springs act upon the displacer as it approaches the limit of travel in each space. This avoids damage and allows the energy possessed by the displacer due to its motion to be quantified.

In the original design by Ringbom a dashpot arrangement created an 'air spring' to provide deceleration for the displacer. The purpose of the dashpot was to eliminate percussive damage to the displacer or its rod. The Senft LTDRSE did not use a spring for the displacer. The cylindrical shape of the second engine was much easier to insulate.

The simulation program produced data for flywheel angle, piston and displacer location, and expansion space and compression space pressure and temperature. Therefore it was these quantities which the test engine was designed quantify.

4.1 Methodology

The gathering of useful, reproducible data from the experimental engine was undertaken in several phases. Firstly the design for the experimental engine needed to be decided upon and the engine built. Once built, the engine needed to be commissioned and run in. This involved static balancing of the flywheel, breaking unwanted thermal pathways, sealing air leaks and applying an insulating jacket.

Secondly, with a working test engine, an instrumentation package was developed. This included sensors for temperature, pressure and location. The signal from the sensors was conditioned and then collected by a data acquisition system. The system was designed and setup by the author using components and software from National Instruments.

Once the data had been gathered any further manipulation such as signal conditioning and conversion to graphics could be undertaken. With these points fully addressed, experimental data was taken and compared with the predicted data.

4.2 The unmodified Senft Ringbom LTDSE

Plans for this engine are readily available in 'Miniature Ringbom Engines' [Senft 2000]. The displacer chamber walls are made up from three polycarbonate rings, each 10mm high. This allows the displacer chamber volume to be changed by adding or removing rings. The connecting rod attaches to the crank disk by means of a locknut and threaded bar (forming the crank pin). This bar runs in a slot in the crank disk, enabling the swept volume of the power piston to be altered. Initially a crank arm length of 10mm was used, giving a swept volume of 16 cubic centimetres. An exploded assembly drawing is given in figure 4.1.

These plans were used to manufacture the parts for the low temperature differential Ringbom – Stirling engine (LTDRSE) at Napier University Edinburgh. The only parts not manufactured on site were the micro bearings, bolts and pressure fittings. The displacer was made from 10mm thick expanded polystyrene sheet with cut outs for inserting the regenerator. The displacer had springs attached to the top and bottom surfaces, it is these springs which were the first modification upon the Senft design. The application of these springs was to protect the displacer from damage and to quantify the energy transferred by the displacer as it came to rest at the end of each displacement stroke.

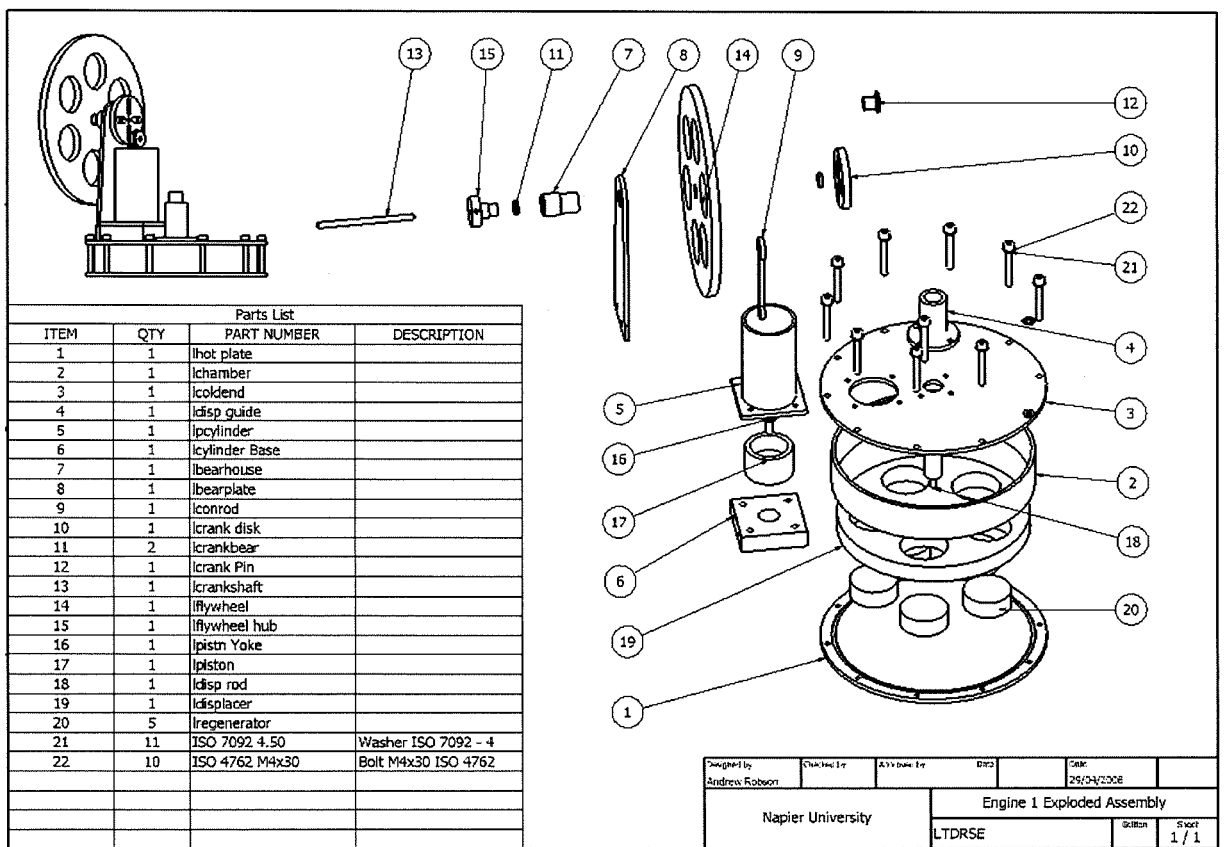


Figure 4.1 Exploded assembly of the first test engine - enlargement in appendix A

The displacer rod was turned from polycarbonate rod, and attached to the displacer by means of a nylon bolt. The displacer rod runs in the brass displacer rod guide, machined for a sliding fit. The piston and piston cylinder were both turned from brass rod. The first piston used was turned from nylon 6,6 rod. This was chosen to reduce weight and to assist in reducing sliding friction between the two surfaces. The dissimilar expansion rate of the materials caused the piston to

seize in the cylinder. The brass piston was not ideal; being heavier it required greater pressure within the engine to lift it; piston mass was investigated during engine development, resulting in the choices of an aluminium piston running in an aluminium liner.

The cylinder was screwed on top of a mounting block, which also held the bearing plate. This block introduced a dead space into the system of approximately 1.6 cubic centimetres. The top and bottom plates were of aluminium to aid in heat transfer from and to the engine. The first regenerator was made of high density foam (lawnmower air filter), as suggested by Senft [Senft 1993, 2000]. This was changed for a more densely woven filter material in an attempt to improve heat capacity and heat transfer. The regenerator material chosen was steel wool. Regenerative meshes of woven sheet using materials such as copper and steel were considered for investigation, but not applied for this work. As can be seen in figure 4.1 the regenerator was embedded in the displacer (as per Kolin's and Senft's designs). It has been noted that the mass of the displacer is raised considerably by doing this. The effect of a static displacer mounted in the annular gap between the displacer side wall and the chamber wall was considered as future work.

This engine had several inherent design problems. These include the mass of the piston, misalignment of the crankshaft axis to the piston axis, and flexing of the bearing plate. Issues over the method to quantify energy entering and leaving the engine and fitting the instrument package were deciding factors in commissioning the second engine.

4.3 The modified Senft Ringbom LTDSE

Several of the parts for the second engine were recycled from the first engine, these being the flywheel, drive shaft, bearing housing and bearings. All other parts were manufactured specifically for the second engine. Modifications made for the second engine, shown in figure 4.2 and appendix A, include the following considerations:

- The connecting rod was made from M4 diameter threaded rod. This allowed the piston face to be aligned with the face of the cold plate for any piston throw, thus eliminating piston cylinder dead space.
- The flywheel had slots cut into the perimeter for an opto-switch to give thirty six, ten degree angular increments for data logging.
- The most straight forward piston location to accurately set was bottom dead centre (by applying a downward force to the piston it settles at bottom dead centre). A second opto-switch was set up to read the edge of a second flange screwed onto the flywheel side. The position of the displacer was found by using a third opto-switch and a scale mounted on the top of the displacer rod. All three optical sensors were adjustable in the x, y, and z planes to aid calibration.
- The piston was manufactured from aluminium to reduce weight. The piston runs in an aluminium liner, sleeved into the cold end block. This was so that matched pairs of pistons and liners of differing diameter can be inserted in the cold block. This allowed an experimental comparison of changing engine geometry with predicted results. This forms a part of future work.
- The displacer rod was manufactured from aluminium. The displacer rod now runs in an aluminium sleeve, which slides into the cold block. With the entire engine cold block components being manufactured from aluminium, it was envisaged that there would be fewer issues with dissimilar material expansion. It is acknowledged that aluminium running against aluminium is not an ideal mechanical situation, but the engine is being run for test purposes only, hence longevity of running parts was not an issue.
- The cold block was tapped for pressure sensors to be attached, and drilled for thermocouples to be mounted. The bearings for the flywheel were mounted in a carrier which is clamped to the wall of the top end. The design of the top end allowed for the modification of the bearings either side of the crank disk to help balance the drive shaft, to be addressed in future work. The chamber was formed from three laminates of 10mm thick acrylic sheet bonded together and then turned to size. The engine bolts locate into threads cut into the chamber wall. Flanges cut into the chamber surfaces fit

into rebates cut into the hot and cold block surfaces. These rebates were designed to accept gaskets to stop air leakages through surface imperfections and interrupt the thermal path from chamber wall to hot and cold blocks. The hot block also had tapings for pressure instruments and drillings for thermocouples.

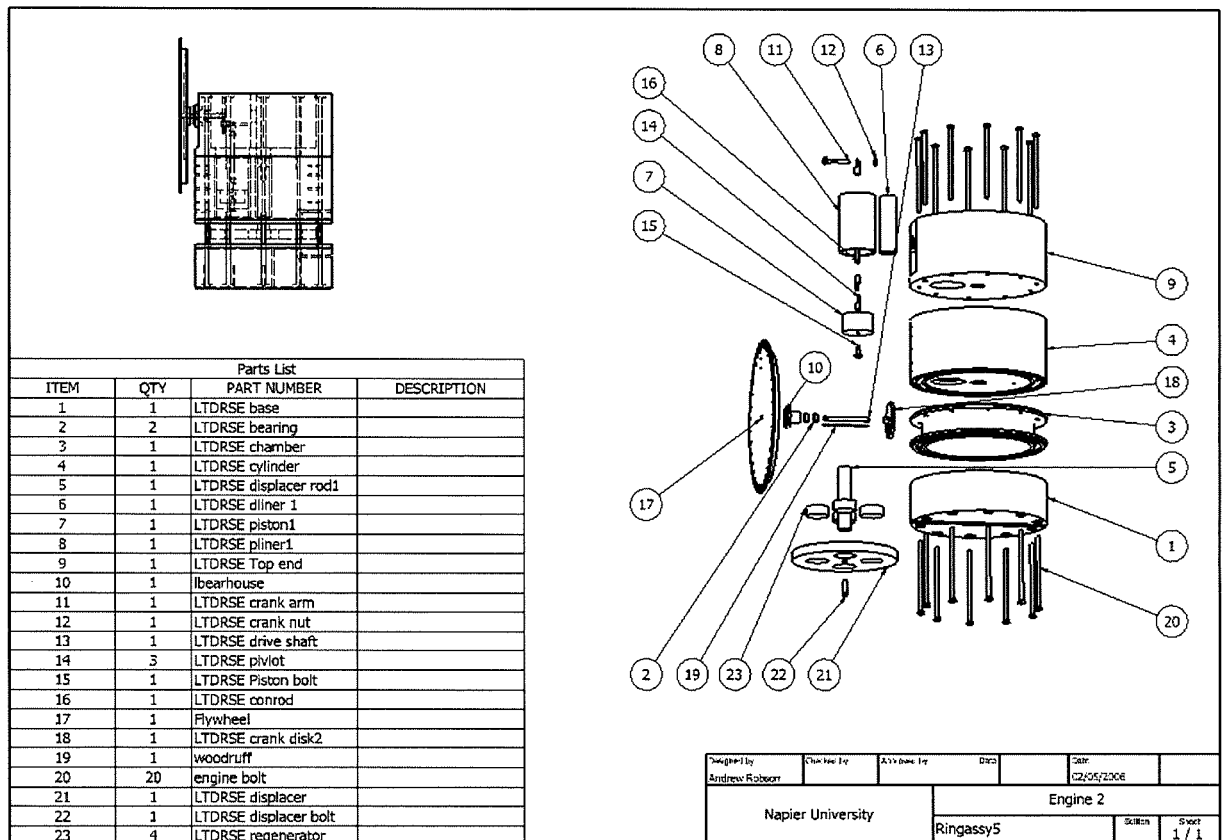


Figure 4.2 Exploded assembly of second engine - enlargement in appendix A

As can be seen from the list of modifications, the experience gained from the first engine has proved useful in design changes for the second experimental engine.

Figure 4.3 shows the key dimensions for the second engine.

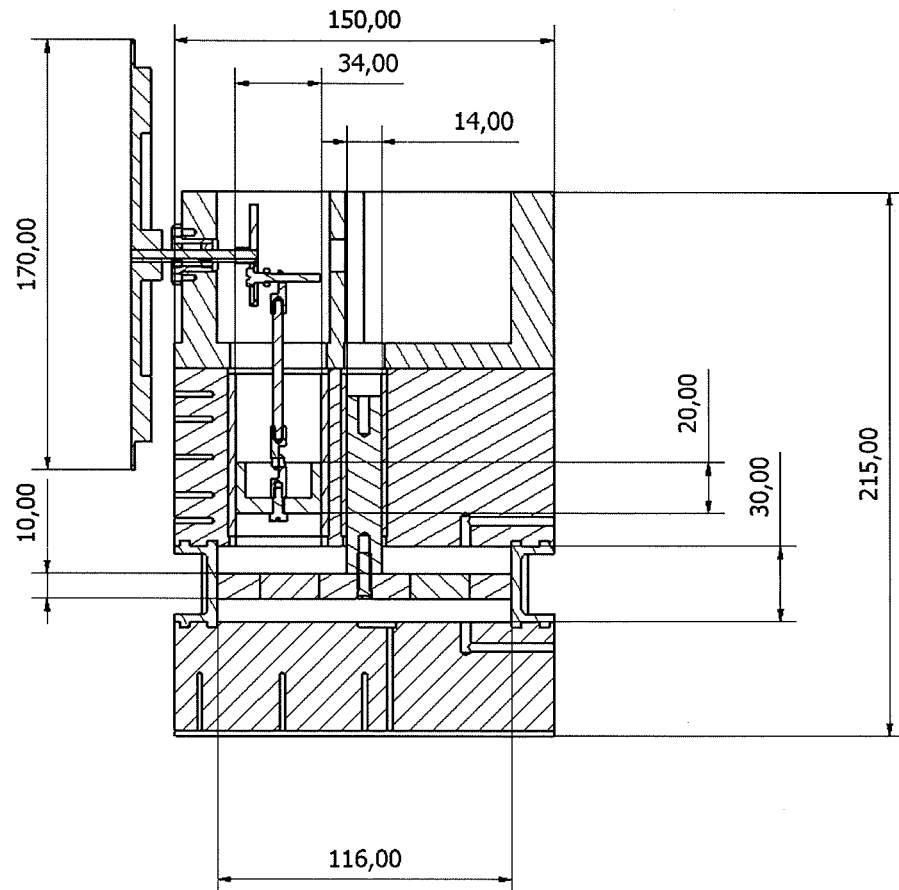


Figure 4.3 Dimensioned section of second engine

4.4 Instrument package

Three types of data were required from the test engine for comparison with the predicted data, these being temperature, pressure and location. The package was designed specifically for the test engine.

4.4.1 Temperature

Several sensors for measuring the temperatures across the engine were considered, these being:

- Resistance temperature detectors (RTD's)
- Thermocouples

- Infra-red thermometry (video)
- Integrated circuits with inbuilt thermal elements

Each type of sensor has been investigated for appropriateness in measuring temperature within the engine.

4.4.1.1 Resistance temperature detector (RTD)

The RTD investigated was the PT100 device, pad mounted and bonded to the reading surface using high thermal conductivity epoxy. Connecting wires are electrically isolated from the surface and each other by a sandwich of insulating tape. The change in resistance of the RTD is a function of temperature. The change is not linear in character, but the non linearity function is known and detailed in BS EN 60584-2:1993. The change in resistance is converted into a 4 – 20 mA signal. This signal is then converted into a 0 – 5 V signal which is fed into a data acquisition system.

The system produces a smooth output with minimal noise over the signal. The system exhibited slow response times (in the order of 1 – 2 seconds from step change), this was due in the main to the thermal pathway traversing the surface bond and the mounting pad. Calibration of a system of several RTDs proved problematic with the original circuit board design, due to interference of current by neighbouring circuits. The system had an uncertainty of ± 2.5 degrees Celsius per reading.

4.4.1.2 Thermocouples

It has been observed and documented that when two dissimilar metals are bonded together to form a junction, an electrical potential difference is created. As the temperature of this junction is changed, so does the potential difference. Thermocouples are divided into types, with each type constructed of known

materials. The electrical characteristics of each type of dissimilar material junction are well documented, and the linearising equations available as part of British Standards. The measuring junction is formed as a bead, and for this work a spark discharge method of fusion is used to form the bead junction. Materials used are nickel constan to form a K type thermocouple.

The bead is in direct contact with the surface giving faster response times in comparison to an RTD. The response time is a function of bead size, where the smaller the bead the lower the `thermal inertia` of the junction and the faster the response. For small beads the response for a step change can be as low as 20 milli-seconds. The change in potential difference with junction temperature is non linear. The polynomials required to linearise the change in potential difference are well known and documented in BS EN 60751. The data acquisition system used automatically applied linearising signal conditioning to the junction signal. Calibration of the thermocouples used cold junction compensation. The reading junction and secondary junctions were calibrated using ice / water baths. Theoretical uncertainty at 100 degrees Celsius is ± 2.11035 degrees Celsius. The data acquisition system will detect changes of 0.61035 degrees Celsius.

The thermocouples have a cable run of one meter and are un-amplified. As such the issue of induced noise is a problem. Strategies to control induced noise are:

- Hardware filters
- Software filters
- Numerical techniques
- Software smoothing

4.4.1.3 Hardware filters

Hardware low pass filters could be applied to the transmission lines, using either inductor – capacitor (L-C) or resistance – capacitor (R-C) designs. These circuits are designed to attenuate signal noise beyond a pre-defined frequency. Typically for a balanced L-C circuit the inductor and capacitor values are high when

attenuating from low frequencies. For the circuit given in figure 4.4 the values are calculated for attenuation beyond 25 Hz, and are found to be:

Inductance = 0.159 Henrys per leg

Capacitance = 2.547 farad

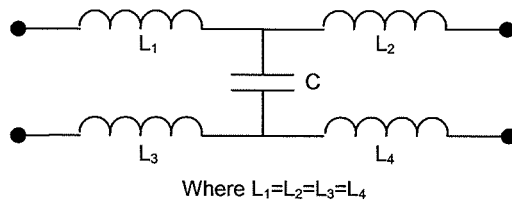


Figure 4.4 Balanced L-C low pass filter

Inherent in the use of a hardware filter is an attenuation of the wanted frequency, and signal phase shift.

4.4.1.4 Software filters

The application of a software low pass filter produces a rising waveform for each scan, starting at the origin and ending at the temperature of the thermocouple. With a scan rate of one kilo hertz the data soon becomes hard to interpret. Any data which are contained within the rise time of the filter are lost.

4.4.1.5 Numerical techniques

The main noise appears to be from the 50Hz mains. By sampling at an integer number of the noise frequency (say 500Hz) for one second half the points will be above the true signal level and half the points will be below the true signal level. Therefore the noise may be averaged out of the signal. This has a drawback, of only being able to remove a truly sinusoidal noise which is symmetrical about the

true signal level and which is divisible as an integer of the sampling frequency. Any other noise will not be removed from the signal.

4.4.1.6 Software smoothing

The smoothing filter produces a smoothed waveform, where each thermocouple can be identified individually and calibrated. Transient noise is also reduced.

4.4.1.7 Infrared thermometry

A thermal camera has been used to monitor the engine as it warms up and runs. The inherent drawback of the thermal camera is scan rate (refresh rate of the ccd) and that it can only produce surface temperature plots. To 'see' inside the engine, a thermally transparent lens would need to be manufactured and fitted. This type of device is not appropriate to read gas temperatures directly, but requires a 'skin' or surface to read from. The polished surfaces of the engine also confused the thermal image.

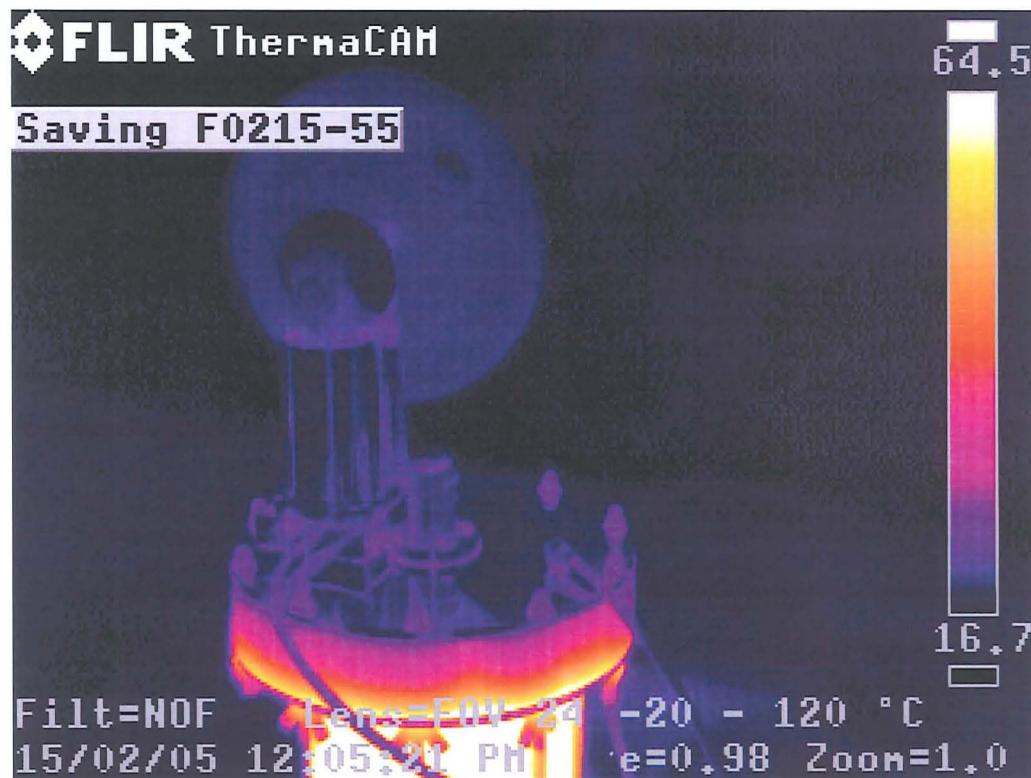


Figure 4.5 Thermal image of the first engine

4.4.1.8 Integrated circuits

Integrated circuits with inbuilt temperature sensors have high refresh rates, but with a large silicone wafer enclosing the sensor, the response times are slow. The physical size of the silicon wafers also cause issues with mounting, and interfere with the operation of the engine.

4.4.2 Sensor and filter choice for temperature readings

Initially the stable and predictable operation of the RTD was considered as the most desirable solution. The required signal conditioning circuits are manufactured at Napier University. During calibration it is found that the circuits have excellent noise rejection capabilities, but the response to thermal changes is slow, in the order of one to two seconds. To speed up the response time would require separating the platinum wire resistance element from the pad and cover; this action was considered but rejected. The manufacture of bare RTDs was also considered, but rejected on the grounds that the calibration and set up of such a device is, in essence, a research project in itself.

For an internal sensor attempting to read the gas flow temperature, the response time is critical. For an engine running at 2 revolutions per second, there will be four displacement operations per second. To try to approximate the temperature profile of the gas flow, many data points are required. It is considered that a thermocouple with a small bead size will react quickly to any change in temperature. With a response time of 0.2 of a second this is still too slow to gain any meaningful data in a single scan. It can be argued that if the simulation program were to be comprehensive enough then, by confirming the validity of the results that can be gathered, by inference the projected gas temperature is probably correct.

The temperature sensor chosen for the engine is a thermocouple, using software smoothing.

4.4.3 Location of temperature sensors

The first engine used Resistance Temperature Detectors rather than thermocouples. Initially eight RTDs were employed as shown in figure 4.6, with signal wires being fed out through a tapping in the bearing plate mounting block.

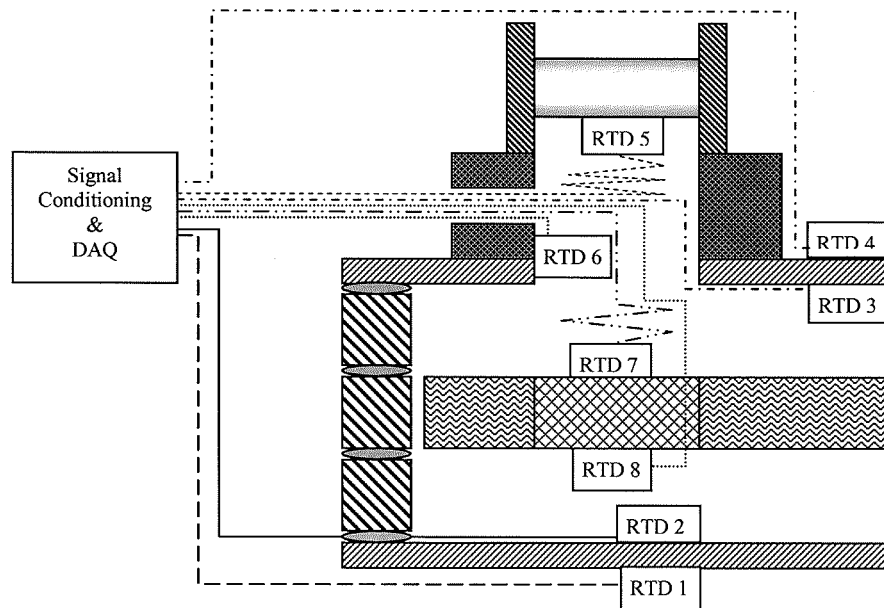


Figure 4.6 RTD placement for first engine

The temperature sensors were changed for thermocouples for the second engine, as these are easier to calibrate and operate than the RTD sensors.

In the second engine each of the blocks has drillings for thermocouples to be placed exactly in a known location, as indicated in figure 4.7. For the hot block, thermocouples are set both radially and axially. This is to read the temperature profile throughout the block. The data from these locations also give an indication of the heat flow through the hot plate during operation of the engine. The cold block has two sets of five drillings which position thermocouples close to the cylinder wall and into to main thermal mass. The locations are chosen to show the temperature profile in the cold block. The numbered locations for the thermocouples are also given in figure 4.7.

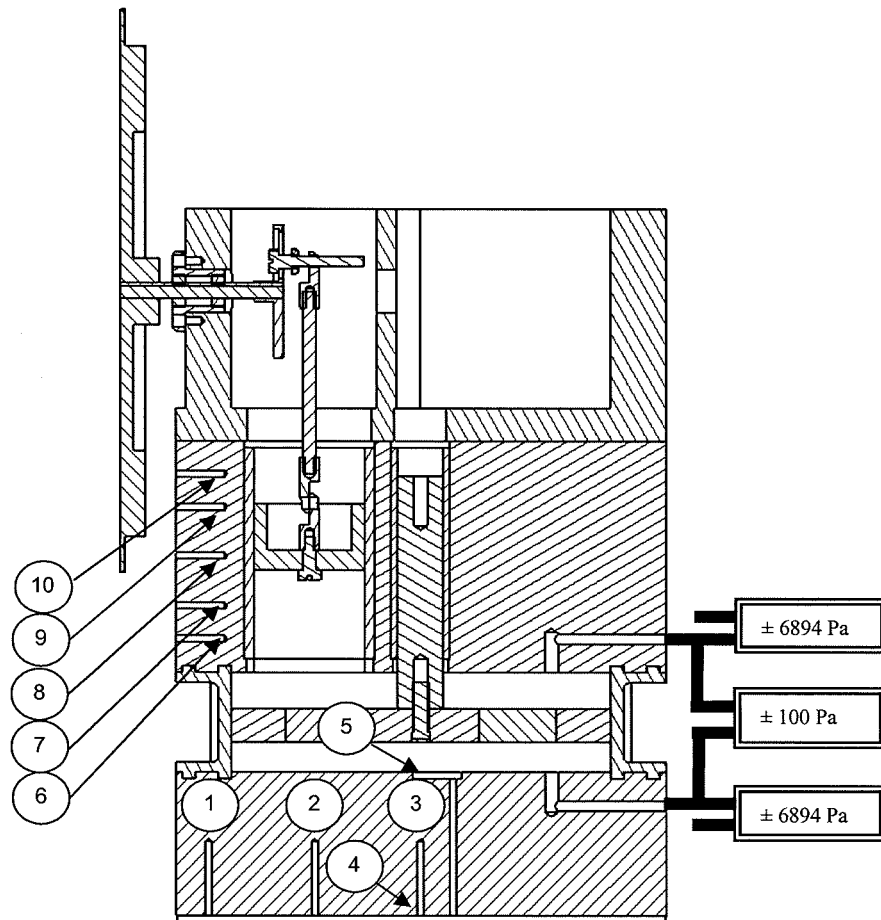


Figure 4.7 Second test engine showing the location of drillings and tapings

4.4.4 Pressure

The first engine has tapings for pressure sensors in the source and sink, arranged as shown in figure 4.8.

Where

Pressure sensor 1 (PS1) has a range of ± 6894 Pa (1 psi)

Pressure sensor 2 (PS2) has a range of ± 100 Pa

Pressure sensor 3 (PS3) has a range of ± 6894 Pa (1psi)

Each of the transducers has an output voltage range of 4 volts, sitting at $3.5V \pm 2.0V$

- PS1 measures the pressure differential between the compression space and atmosphere during the cycle. The refresh rate of the device is given as 200 hertz (Hz), although it appears to function quite adequately at 1 kHz sampling rate. This is p_K of the program.
- PS2 measures the pressure differential across the displacer, the driving pressure for fluid flow through the regenerator. This is the $p_E - p_K$ term of the program.
- PS3 measures the pressure differential between the expansion space and the atmosphere during the cycle. This device has a refresh rate of 200 Hz, and like PS1, appears to work at 1 kHz. This is p_e of the program.

With the pressure tapings piercing the hot and cold plates vertically as shown in figure 4.8, it was difficult to uniformly heat or cool the plates. This led to the modification shown in figure 4.7.

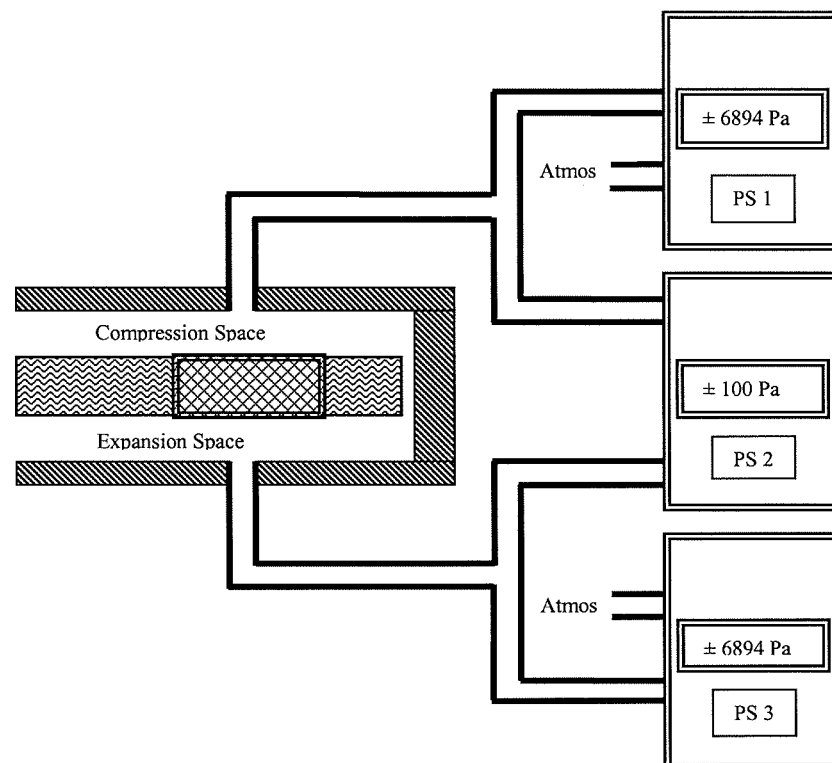


Figure 4.8 First engine pressure tapping layout

The pressure transducers used to measure the differential pressure between the engine spaces and the atmosphere required only two decoupling capacitors to

complete the sensing circuit for data logging. The circuit is given below in figure 4.9. In the second engine pressure tapings are routed through the hot and cold blocks so that the exit is now horizontal and does not interfere with the heat transfer surfaces. The large mass of the hot and cold blocks allows heat flow to be quantified.

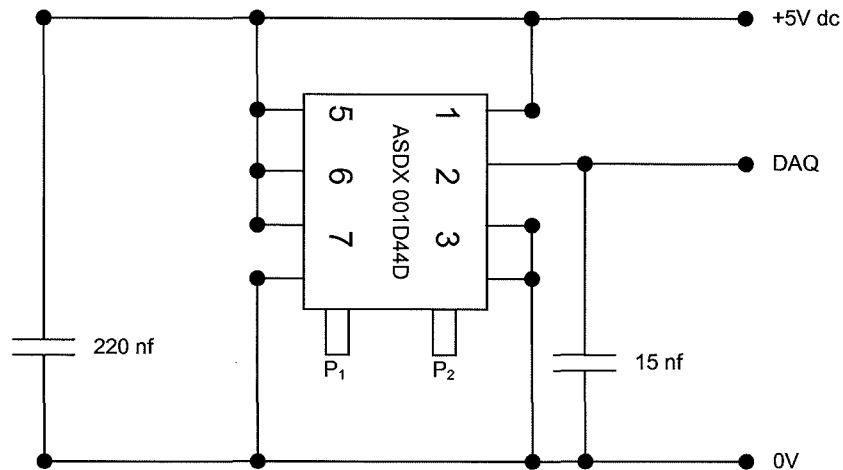


Figure 4.9 Pressure transducer circuit

The uncertainty for the ASDX series of transducers is given as $\pm 2\%$ of full scale of 4V (Data sheet in Appendix D). Hence there is an uncertainty of $\pm 0.08\text{V}$ per reading as detailed in the following paragraph.

The larger range transducers have a stated range of $\pm 6894\text{Pa}$ (1psi), the output of which covers a deflection of 4 volts. The zero pressure differential is set and calibrated to 3 volts output. From this it can be seen that half range (be it positive or negative) is 2V. A transducer multiplication factor may be found from this by finding the 1 volt value for the pressure range, here 1 volt = 3447Pa. Therefore for any voltage output from the transducer a multiplication factor of 3447 may be used to convert voltage to pressure. The reading uncertainty given above, becomes $\pm(0.08 \times 3447)$, which gives an uncertainty of $\pm 275\text{Pa}$ per reading.

The pressure sensor for the internal pressure differences had all the conditioning circuitry already installed, so just required connections to power, and output to the

data acquisition system. The uncertainty for this transducer was calculated in a similar way to that outlined above, giving an uncertainty of 3.8Pa per reading.

4.4.5 Location

To compare the virtual engine, with the real engine the location of the piston and displacer must be known at any point in the cycle. Several methods were considered to find the locations, these being:

- Photographic interpretation
- Slotted optical switches
- Reflective optical switches

4.4.5.1 Photographic interpretation

The flywheel and displacer rod were fitted with graded scales, with known datum marks, as shown in figure 4.10. Whilst the engine was running several hundred photographs were taken. The angle of the flywheel and displacer height were taken from each photograph and plotted against each other.

Although this produced a representation of displacer and piston relationship, the trace can not indicate engine component velocity or acceleration. Another drawback was, that as the engine speed changes, so does the motion of the displacer (from observation). This change in motion appeared as an error rather than a phenomenon during the photo analysis.

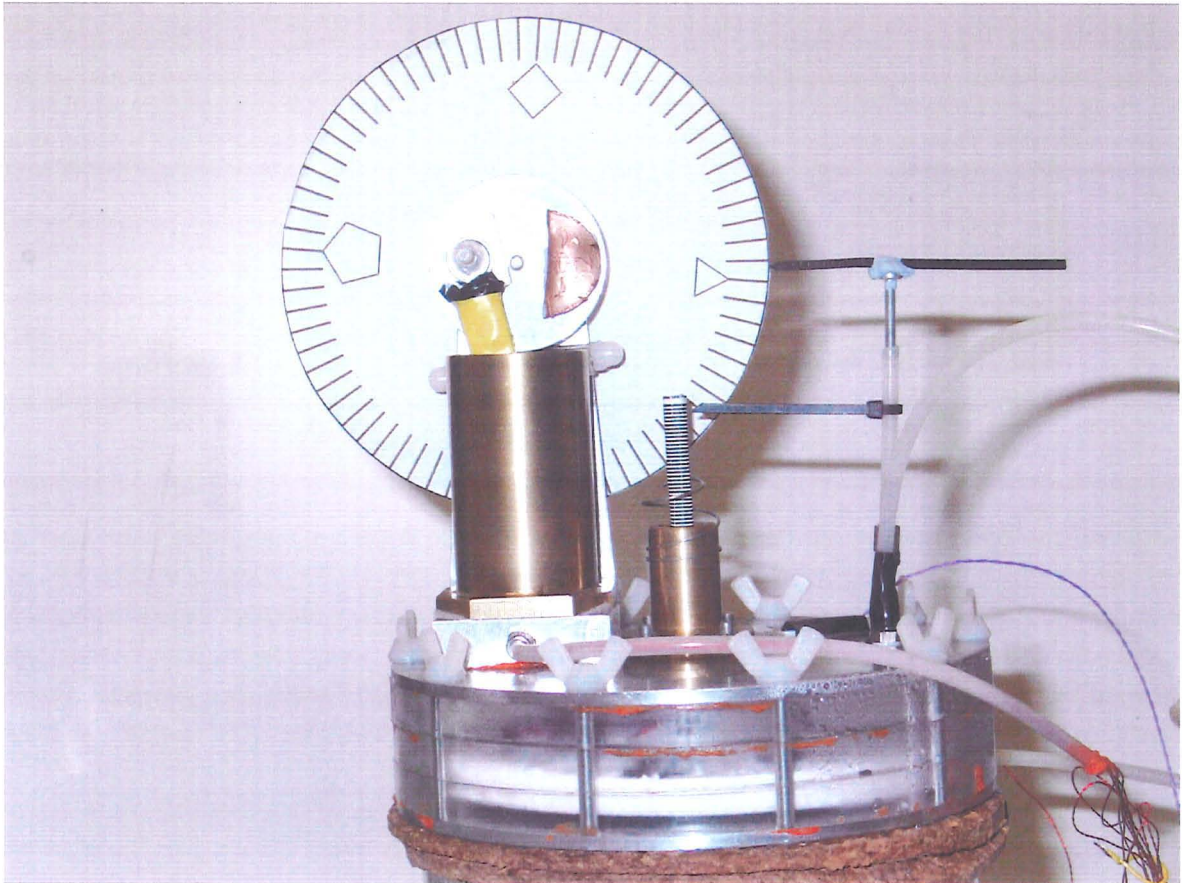


Figure 4.10 Example of photograph from photo-analysis

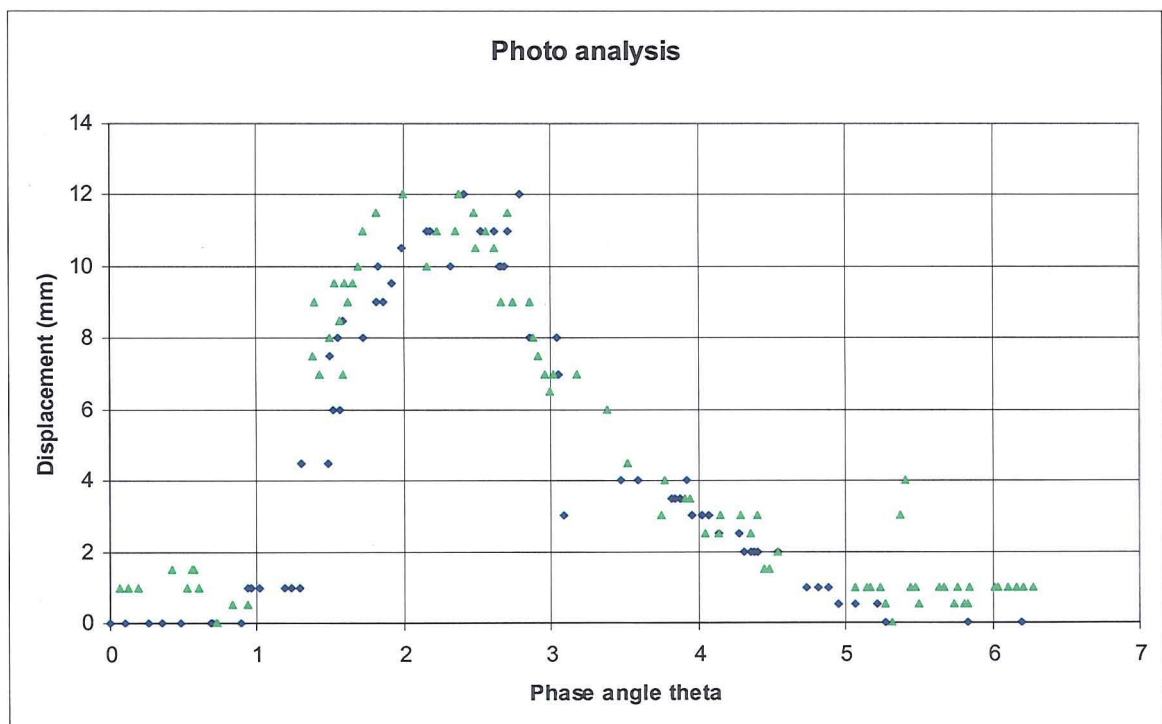


Figure 4.11 Photo analysis of displacer location

A plot of the displacer position against flywheel angle is shown in figure 4.11, piston location could be added to the figure, but would not add to the value of the graph. It has been observed that at the overdriven limit, not only can cycles be jumped by the displacer, but the length of the displacement stroke is reduced. The scatter of data points on the plot is indicative of this.

4.4.5.2 Slotted optical switch (optical integrated circuit)

A slotted optical switch consists of an infra red diode and optical transistor. The energy emitted by the diode energises the base of the transistor, switching it on. The voltage across the emitter collector pathway can then be seen. The circuit for the optical switch is given in figure 4.12.

The rise time of the optical switch used was typically 50 nanoseconds, with a propagation delay of 3 micro seconds. An array of 36 slots was machined into the perimeter of the flywheel. Each slot had a nominal height of $7.75\text{mm} \pm 0.02\text{mm}$, and a width of $1.44\text{mm} \pm 0.02\text{mm}$. The optical integrated circuit (optical i.c.) package was mounted so that the beam is parallel to the axis of the flywheel at a distance of $80\text{mm} \pm 1\text{mm}$ from the centre of rotation. Each slot had a 10° (0.1745 radians) separation from leading edge to leading edge.

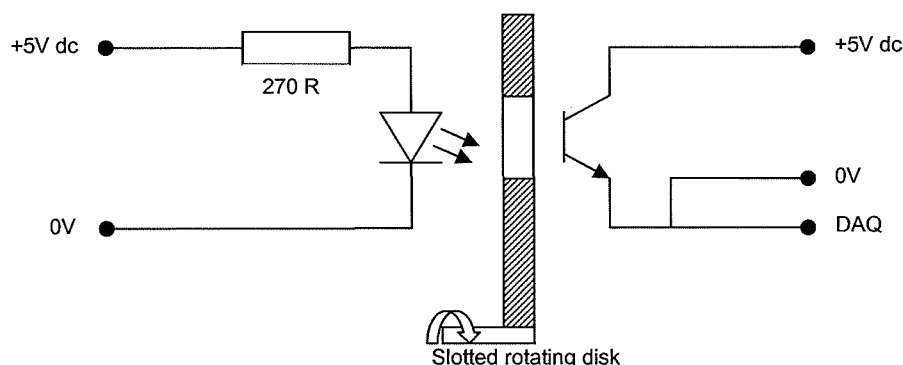


Figure 4.12 Optical switch circuit

A second optical switch was fitted to read a second flange mounted to read the piston bottom dead centre position.

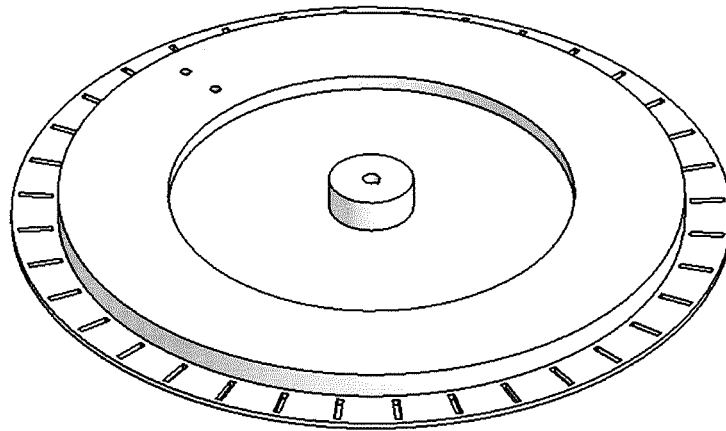


Figure 4.13 Flywheel with slots

The uncertainty for this type of sensor and the flywheel slots was calculated using the following reasoning. The test engine runs at speeds between one and three revolutions per second. At three revolutions per second the engine was near the overdriven limit and cannot run any faster. Thus using a limit speed of three Hz was not unrealistic. The time the optical path was interrupted is called the space, and the time the optical path was clear is called as the mark. The mark begins with the leading edge of the slot and ends with the trailing edge of the slot, and was read by the DAQ as output high (+5V). The angle subtending the slot width was $0.018 \text{ radians} \pm 252\text{E-}6 \text{ radians}$. The optical switch had a response time in the order of 3 micro seconds, data logging was at a rate of 1milisecond; therefore any error in response time would not be seen by the data logger.

4.4.5.3 Procedure for displacer position

There is no end of stroke mark for the displacer optical track; this was not an oversight, but more of a response to the observed behaviour of the displacer. This behaviour includes a reduction of displacer stroke as the cycle approaches the overdriven limit. The second engine has been operated below the overdriven limit

so a reduction in displacer stroke would not become problematic to the data recording system.

The following argument was put forward as one way to determine the location of the displacer during the cycle.

With the piston at bdc the internal pressure is at a maximum, this became evident from an inspection of the graph of the bdc mark and space lines and space pressures. This pressure was the mechanism by which the displacer moves to, and dwells in the top of the displacer chamber.

The working fluid was expanding, performing work upon the piston and forcing it upwards. As this happened the pressure in the engine dropped and the displacer began its downward journey, assisted by gravity.

With this process complete, the piston was now moving downwards due to the energy stored in the flywheel. The pressure change within the engine now pushes the displacer up against gravity.

When inspecting the experimental data one can identify a dwell period just after the piston bottom dead centre mark. From this we may surmise that the displacer is at the top dwell. The fall of the displacer shows an acceleration until it reaches the expansion space stub spring and momentarily enters an indeterminate phase. There follows a dwell period and a steady uniform motion. It is put forward that the accelerated motion was the displacer falling under gravity and the pressure change, and the uniform motion was the rise of the displacer against gravity. Thus the different aspects of the cycle were identified.

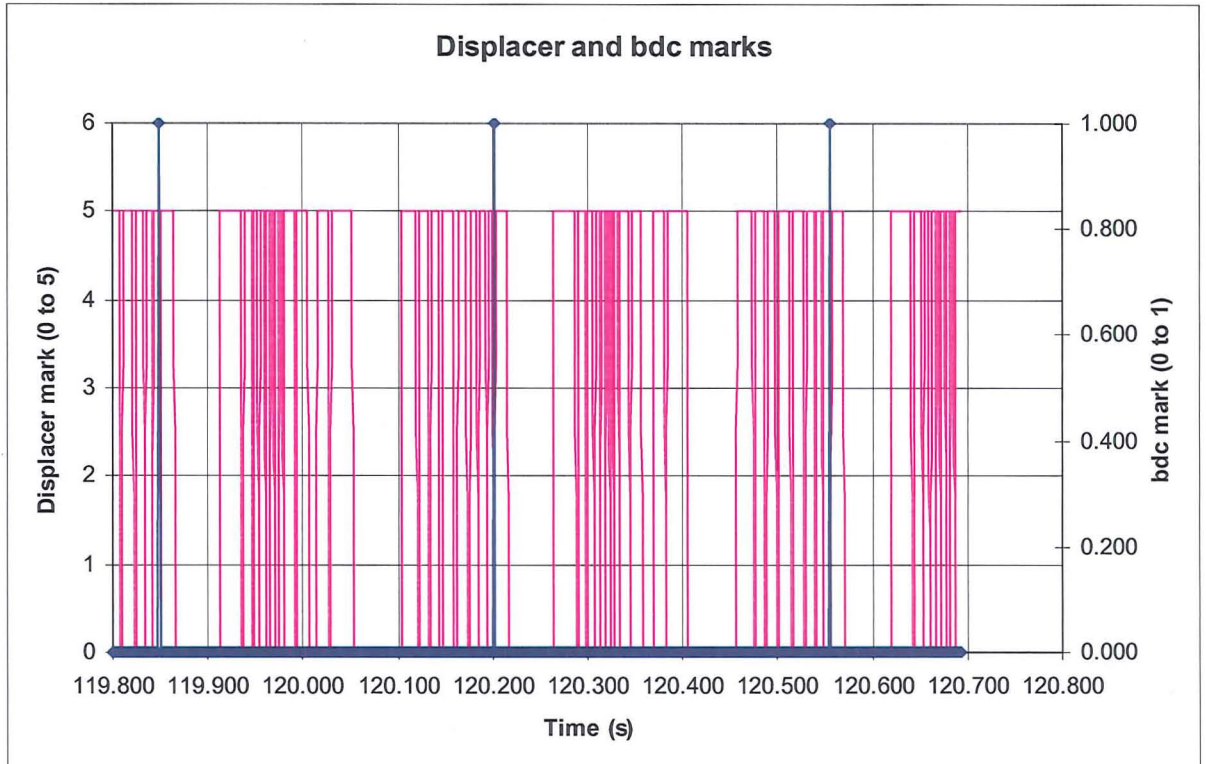


Figure 4.14 Displacer and bottom dead centre marks

For the analysis of displacer location the track is divided into 1mm light and dark stripes. As the displacer moves these graduations were recorded by an optical integrated circuit.

From the operation of the Ringbom Stirling engine given in chapter 2, the reader is reminded that the displacer upper dwell coincides with piston bottom dead centre (bdc). Utilising the piston bdc, mark the upper dwell of the displacer may be ascertained. Figure 4.14 shows the piston bdc mark in relation to the displacer location marks. The piston bdc mark represents the displacer mid point 23mm above the hot plate inner surface. Thus the start location for each cycle was identified.

The rising and falling edges of the track are then identified. A manual method of inserting location is employed. By identifying bdc the 23mm location is found, the next rising edge is allocated the value 22mm, descending on each edge until the 7mm point is reached. The displacer is now in the lower dwell location. The next 23mm point is identified and the points are inserted working backwards to the

7mm point. The two 7mm points are now joined. This method eliminates the indeterminate phase by assuming that the displacer is at rest at the 7mm height.

4.4.5.4 Procedure for piston location

The piston is directly linked to the flywheel by means of a connecting rod. Therefore it can be said that if a sensor is set to some arbitrary mark upon the flywheel and the piston location recorded, for any given change in flywheel angle the piston location can be calculated.

The piston location chosen was bottom dead centre (bdc). This is the easiest point to be identified as, if a rod was used to apply a downward force to the piston, it sits at bdc whilst the sensors were aligned to the flywheel marks. Initially a series of coded slots were employed to indicate bdc and flywheel direction. This approach was found to be unreliable as in some cases the inter slots which form the code were skipped when the engine was running at high speed and the data acquisition system was writing data to file. To overcome this, a second positional sensor was fitted to the flywheel to solely indicate flywheel position at piston bdc. This signal is also used to reset the mark – space counter on the flywheel in case it becomes out of synchronisation due to a data acquisition system write cycle.

4.4.6 Data acquisition

Several methods of data acquisition were considered, ranging from direct data entry to an Excel workbook, (or via a FORTRAN program), utilising a direct link to the PC to proprietary data acquisition and logging systems. The suitability of each solution was decided upon the ease of use, functionality of the hardware and ease with which the system could be set up and availability. The system from Pico Technology was rejected due to lack of logging channels. Direct connection was not advisable due to the amount of signal conditioning required and the risk of damage to the PC components if there was a failure of the isolating circuits. The system which came out top was to use National Instruments data logging cards

and software, both of which were available through Napier University. A separate copy of LabVIEW express was obtained so there were no licensing issues.

Signals from the sensors and transducers were sent to a National Instruments (NI) Data Acquisition (DAQ) card for signal conditioning and data logging. Data logging functions were controlled through the National Instruments 'Laboratory Virtual Instrument Engineering Workbench' (LabVIEW) software. LabVIEW uses a graphical programming language for applications such as data acquisition, signal analysis and instrument / process control. Three types of National Instruments data logging hardware have been investigated for suitability, being:

- Traditional NI DAQ using LabVIEW 6 and AT-MIO-16E-10 card
- USB DAQ using LabVIEW 7 Express and USB 9008 unit
- DAQmx using LabVIEW 7.1 and PCI-6025E card

DAQmx was used due to its superior user interface.

The DAQ system was set to receive signals from three opto-switches reading 0 – 5 V d.c. which gave position data for the flywheel and displacer. There was the input from the three differential pressure transducers, two operating on a 2.5 V d.c. mid point with a ± 2 V deflection representing ± 6894 Pa, and one operating on a 3.5 V d.c. mid point with a ± 2.5 V d.c. deflection representing ± 100 Pa. A further 7 channels were taken by K type thermocouples. The transfer function for the thermocouples is already loaded into the LabVIEW software, so they only require calibrating.

4.4.7 Calibration of sensors

4.4.7.1 Resistance Temperature Detectors

Calibration for the resistance temperature detectors was undertaken by changing the value of one of the resistors in the detector circuit. Further trimming was achieved using the calibration function of the LabVIEW software.

Individual calibration tables for each channel are set up using boiling and freezing water and a reference thermometer.

4.4.7.2 Thermocouples

The DAQmx software interface was used to set up the data acquisition pc card. As part of the setup routine, channels were allocated pre-defined identities such as thermocouples. This gave the opportunity to calibrate each individual channel. In thermocouple setup, the sensing element may be allocated known temperatures, such as boiling water and freezing water with a reference alcohol thermometer and hand held thermocouple. This was performed for each of the thermocouple channels as part of the calibration routine.

4.4.7.3 Pressure

The pressure transducers come pre calibrated and are used with the manufacturers' given error, which is given in Appendix D.

4.4.7.4 Location

The leading edge of the datum slot on the flywheel was set with the piston at bdc. The flange was then set so its leading edge just cut the infra-red beam with the piston at bdc. The displacer location was set to just cut the last darkened area on the occulted strip, with the displacer pushed to its lowest extent.

4.4.8 Experimental technique

The experimental technique and procedure are described below with reference to figure 4.15

- With all the apparatus at ambient temperature the DAQ was run for five seconds. This provides calibration data in case of any calibration / signal drift
- The laboratory hotplate was set to the experiment temperature
- When the hot plate was at the desired temperature (confirmed with hand held thermal probe) the data logger was started and the engine placed upon the hot plate
- Data was gathered until the hot plate and the hot block attain the same temperature (TC's 1 to 5)
- With the hot block at the required temperature, the engine was transferred to its insulating jacket
- The flywheel was turned (initially by hand), or the impetus applied.
- The first two minutes of run data were gathered
- After two minutes, five seconds of run data were collected every 30 seconds until the engine stops
- The gathered data was exported to an Excel workbook for further analysis

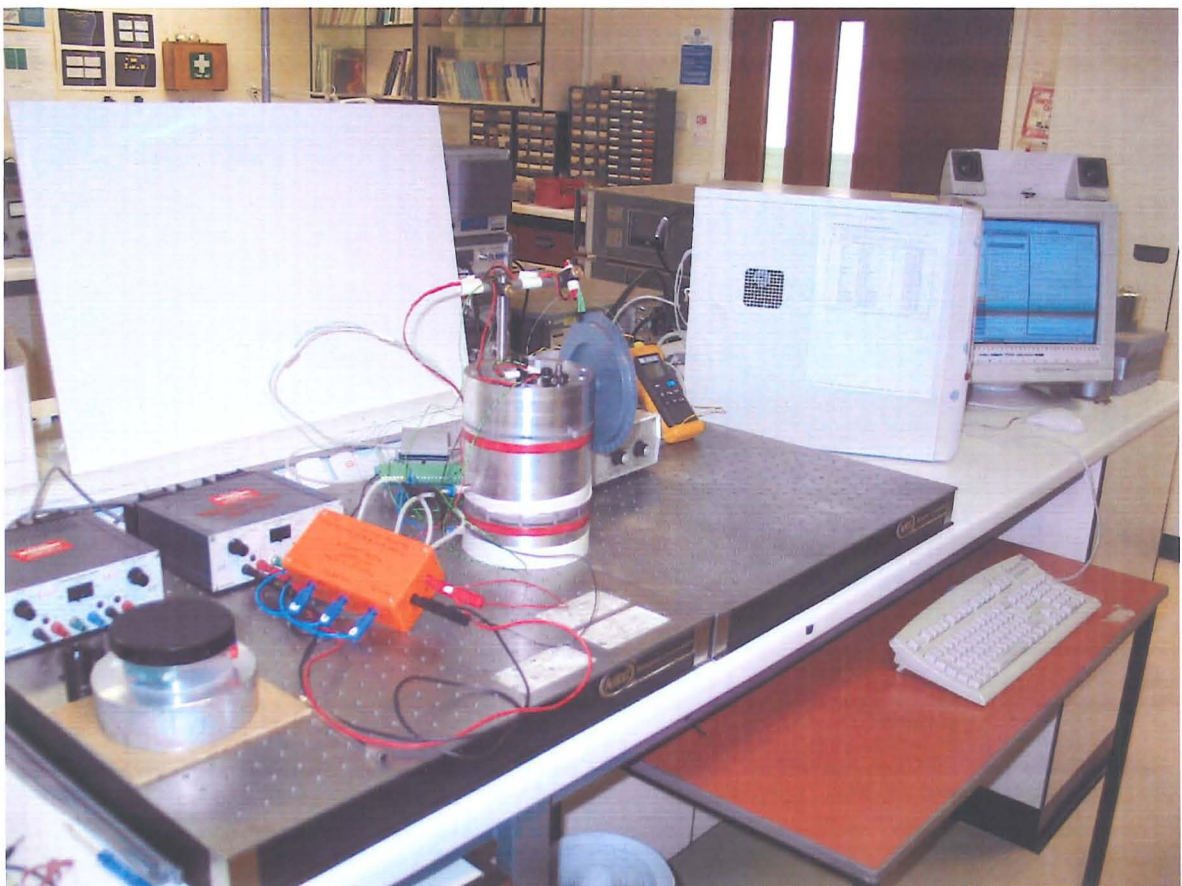


Figure 4.15 Test apparatus in laboratory, engine without insulating jacket.

It should be noted that the load on the engine is provided by friction and, primarily, the windage losses on the flywheel.

4.4.8.1 Experimental error

The error has been given for each type of sensor as each is discussed above.

4.5 Experimental results

4.5.1 Qualitative observations and trends

In this work two Low Temperature Differential Ringbom Stirling Engines have been manufactured at Napier University. The first was manufactured to the design given by Senft [Senft 2000], and the second one was a modified engine, based upon the Senft design. As alluded to above, the first engine has one slight modification to Senft's design, being the inclusion of stub springs in the compression and expansion spaces. The second engine is further modified by increasing the mass of the hot and cold plates, again described above.

4.5.1.1 Starting procedure

Heat was supplied to the hot plate by means of a laboratory electrical heater. As predetermined temperature differentials were reached (between the hot and cold plates) then the flywheel was turned by hand to provide the starting impetus. It was found that as long as the initial turn of the flywheel imparted enough inertia for the flywheel to turn approximately five times then the engine would run with sustained motion (with the caveat that the temperature differential was great enough). By increasing the force of the initial turn the engine would settle down to the same steady state angular velocity after approximately five seconds. This was also indicated by the predictive program. As such the engine is not particularly sensitive to the magnitude of the starting impetus, as long as the impetus is great

enough to initiate the engine cycle. This is considered to be due to engine damping at start-up.

Various flywheel start angles were used, ranging in quarter π radian increments from bottom dead centre (zero radian) to top dead centre (π radian). This was achieved by utilising the optical slots. The piston was held down at bottom dead centre and the alignment of the slots and bdc mark checked. The flywheel was then rotated to the required position by counting slots, thus setting the start angle. The impetus was then applied with the flywheel in the selected start position.

The height of the piston within the cylinder is a function of flywheel angle theta. The amount of working fluid contained within the engine is directly affected by the piston location, which will in turn affect the performance of the engine.

It was observed that the engine was most likely to continue with self sustained motion if the start angle was between $\pi/4$ and $\pi/2$. Below $\pi/4$ the flywheel turns but the engine motion decays to stop with a little rocking. Above $\pi/2$ the piston appears to stall at top dead centre and either 'bounces' in the top end for start angles close to $\pi/2$ or stops in the top dead centre location.

It can be shown that the quantity of fluid retained within the engine is a function of flywheel angle. For any given temperature differential, the pressure of a restrained fluid will increase in relation to the fluid mass. Hence what is being seen for lower flywheel angles is not enough mass to create the pressure required for sustained running. For higher flywheel angles, the quantity of working fluid expands to such a degree that the inertia of the flywheel and piston assembly is lower than that of the resisting pressure, therefore the piston stops.

4.5.1.2 Rocking phenomena

It was observed that as the engine temperature differential increased toward the self sustaining temperature differential, the piston rocked up and down inside the

cylinder without attaining a full cycle. The amplitude of the rocking increased as the operating temperature differential was approached.

4.5.1.3 The first engine

As the engine warmed up the flywheel was turned by hand to impart the start energy. The starting behaviour for differing temperature differentials was found to be as follows:

- For a temperature differential of 20K (20C to 40C) the engine did not sustain motion, the flywheel decelerates to stop
- For a temperature differential of 40K (25C to 65C) the engine did not sustain motion, the flywheel decelerated to stop
- For a temperature differential of 45K (25C to 70C) the engine did not sustain motion, the piston rocks two or three times, decaying from $\pi/4$ symmetrical about bdc
- For a temperature differential of 50K (25C to 75C) the engine did not sustain motion, the piston rocks several times, decaying from above $\pi/4$ symmetrical about bdc
- For a temperature differential of 55K (25C to 80C) the engine did not sustain motion, the piston rocks several times, decaying from around $\pi/2$
- For a temperature differential of 60K (25C to 85C) the engine did not sustain motion, the piston exhibits sustained rocking motion above $\pi/2$
- For a temperature differential of 65K (25C to 90C) the engine did not sustain motion, the piston exhibits sustained rocking motion
- For a temperature differential of 70K (25C to 95C) the engine began to run
- The engine continued to run until the temperature differential reduced to 48K where rocking motion was then observed to decay over several minutes until the flywheel became stationary.

Once the engine began to run the engine speed increased to 280 to 300 rpm where stable operation was observed. The engine appeared to settle to steady state running at the ten second point.

As engine speed increased the dwell time for the displacer reduced, it was also observed that the displacer stroke reduced. This had been observed to the point where the displacer is just vibrating upon the expansion space spring and not raising into the compression space at all, the displacer stroke being no greater than 5mm.

4.5.1.4 The second engine

For the second engine, several parts from the first engine were used, with some design differences being applied, these being:

- A greater mass for the hot and cold plates
- A lighter piston with a tighter tolerance on the fit in its running sleeve
- More accurate alignment of the axis of the piston and drive axle
- Removal of possibility of bearing carrier flexing
- Displacer rod and guide sleeve made from the same material as the top end
- Removal of dead space under the piston

The piston and displacer with their respective guides are manufactured from aluminium; it is acknowledged that this is not the ideal material for sliding surfaces. It is considered that the reduction in the life of the engine is more than offset by the advantage of the identical expansion rates of all the sliding parts. Dissimilar expansion rates were found to be an issue with the first engine.

As the engine warms up the flywheel is turned by hand to impart the start energy. The starting behaviour for differing temperature differentials was found to be as follows:

- For a temperature differential of 20K (20C to 40C) the engine did not sustain motion, with no discernable rocking of the piston
- For a temperature differential of 30K (20C to 50C) the engine did not sustain motion, with slight rocking of the piston
- For a temperature differential of 40K (20C to 60C) the engine did not sustain motion, with decaying rocking of the piston
- For a temperature differential of 50K (20C to 70C) the engine did not sustain motion, with decaying rocking of the piston
- For a temperature differential of 60K (20C to 80C) the engine did not sustain motion, with sustained rocking of the piston
- For a temperature differential of 62K (20C to 82C) the engine begins to run
- The engine continues to run until the temperature differential reduces to 54K

Once the engine begins to run the engine speed increased from 160 to 180 rpm where stable operation is observed. With a greater temperature differential in the region of 80k, the engine speed settles around the 200 to 220 rpm mark.

The second engine does not exhibit the reduced displacer stroke of the first engine.

With both engines sealing the chamber has proved problematic.

4.5.1.5 Displacer motion

The displacer is moved by the internal and external pressure differential acting across the displacer rod of the displacer. The motion of the displacer for the upward (outward) and downward (inward) strokes is not symmetrical. The main supplemental force acting upon the displacer assembly is that of gravity. With the displacer axis orientated to the vertical, the effect of gravity can be seen in the movement. As the internal pressure rises the pressure must be great enough to not only overcome the mass (supply impetus) of the displacer, but to also raise the mass against gravity. The motion is smooth and controlled as indicated by the

uniform mark and space gaps recorded during the displacer outward motion. When the pressure reversal causes downward movement of the displacer, the action of gravity is now assisting and the displacer accelerates until contact with the expansion space stub spring. The upward stroke tends to push the top of the displacer to a point where the compression space spring is fully compressed; even though the motion is slower, there is more pressure pushing the displacer upwards than downwards. This concurs with the description of the net work output for the cycle. With the working fluid expanding, work is done upon the piston and by inference displacer (the work required to raise the displacer); when the working fluid contracts, the displacer 'flops' down onto the expansion space stub spring, hence does not compress the stub spring by more than one or two millimetres.

4.6 Quantitative results

Data for several tens of runs was recorded by the DAQ system, this data was transferred to an Excel workbook and analysed. Initially this data is used to improve the experimental technique and modify the DAQ system. This is invaluable in the quest for clean, accurate, reproducible data. One series of results has been selected as representative for the engine logged data. Within the run data, key points were analysed, indication distinct operational modes these being:

- For 0 to 2 seconds (start-up)
- For 5 to 7 seconds (warming of regenerator)
- For 12 to 14 seconds (stable running, source temperature stabilised)
- For 21 to 23 seconds (stable running, source temperature dropping)
- For 119 to 121 seconds (stable running, source temperature dropping)

For each of the run times analysed the mid second temperature differential is taken, these being:

Nominal temperatures at start up are:

- Source (hot reservoir), $T_H = 100^\circ\text{C}$

- Sink (cold reservoir), $T_C = 20^\circ\text{C}$
- Ambient, $T_A = 20^\circ\text{C}$
- Thermal jacket base = 100°C
- Thermal jacket top = 20°C

Table 4.1 Temperature change for periods of run time.

1st 80°C (1 second)
2nd 80°C (6 seconds)
3rd 73°C (13 seconds)
4th 73°C (22 seconds)
5th 70°C (120 seconds)

For each of these times a series of graphs is generated from the data. These graphs are given in figures 4.16 to 4.30.

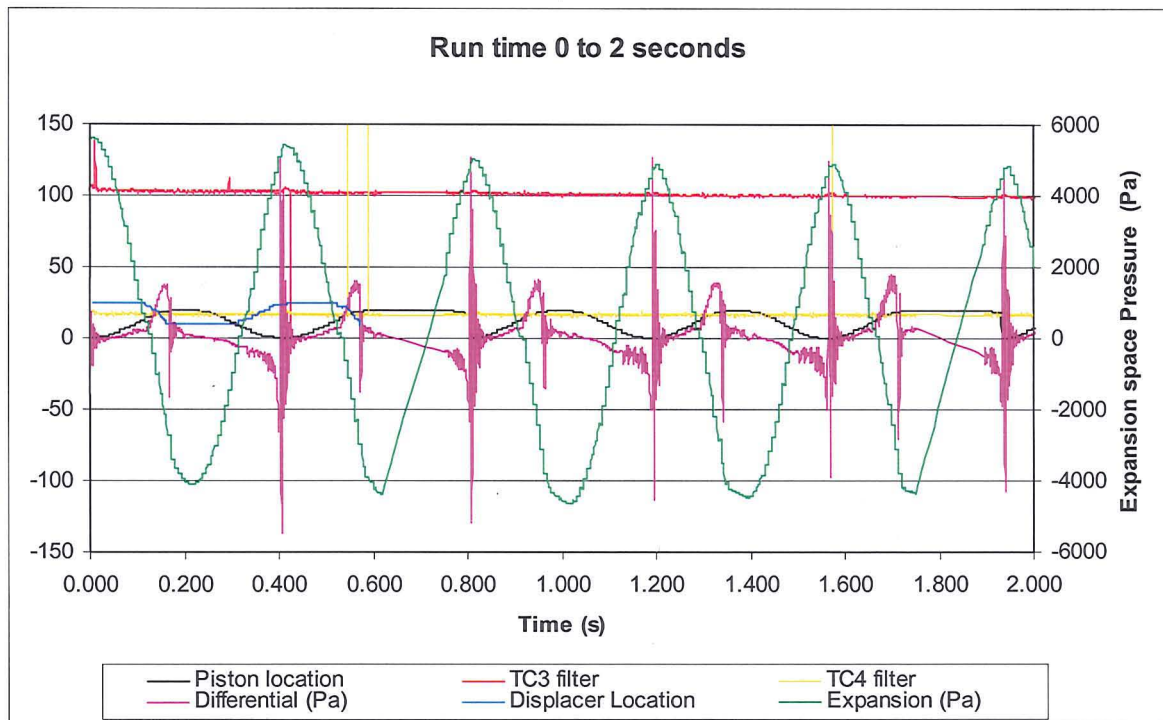


Figure 4.16 Run time 0 to 2 seconds

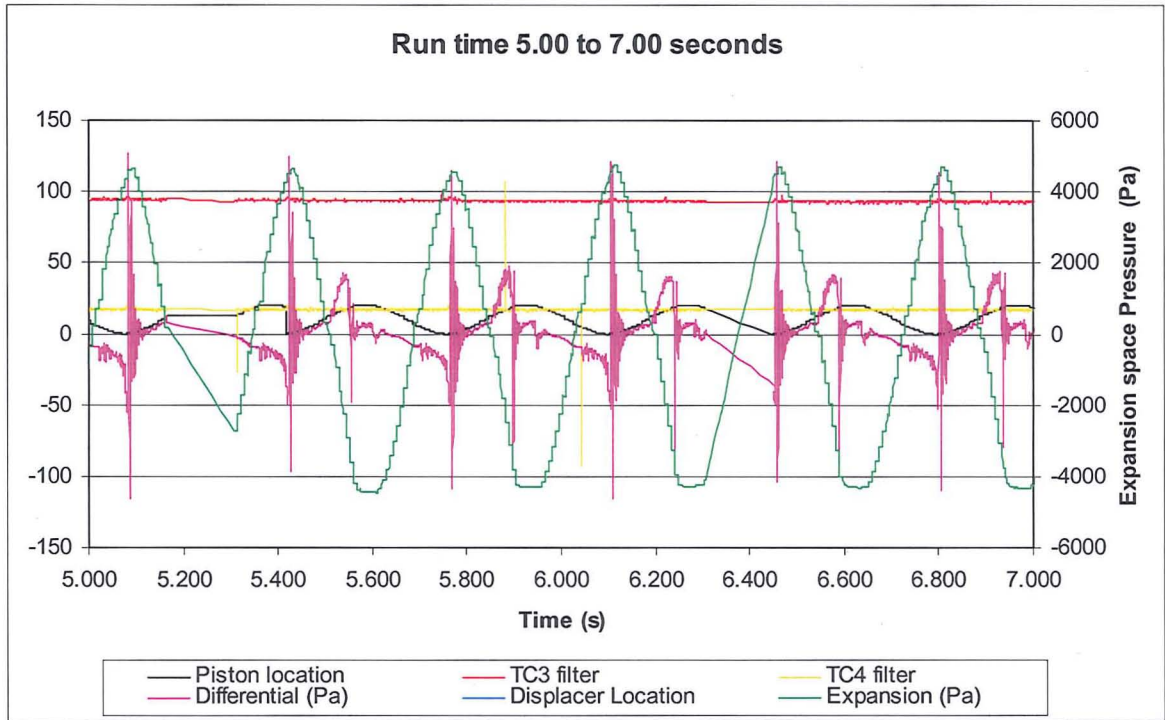


Figure 4.17 Run time 5 to 7 seconds

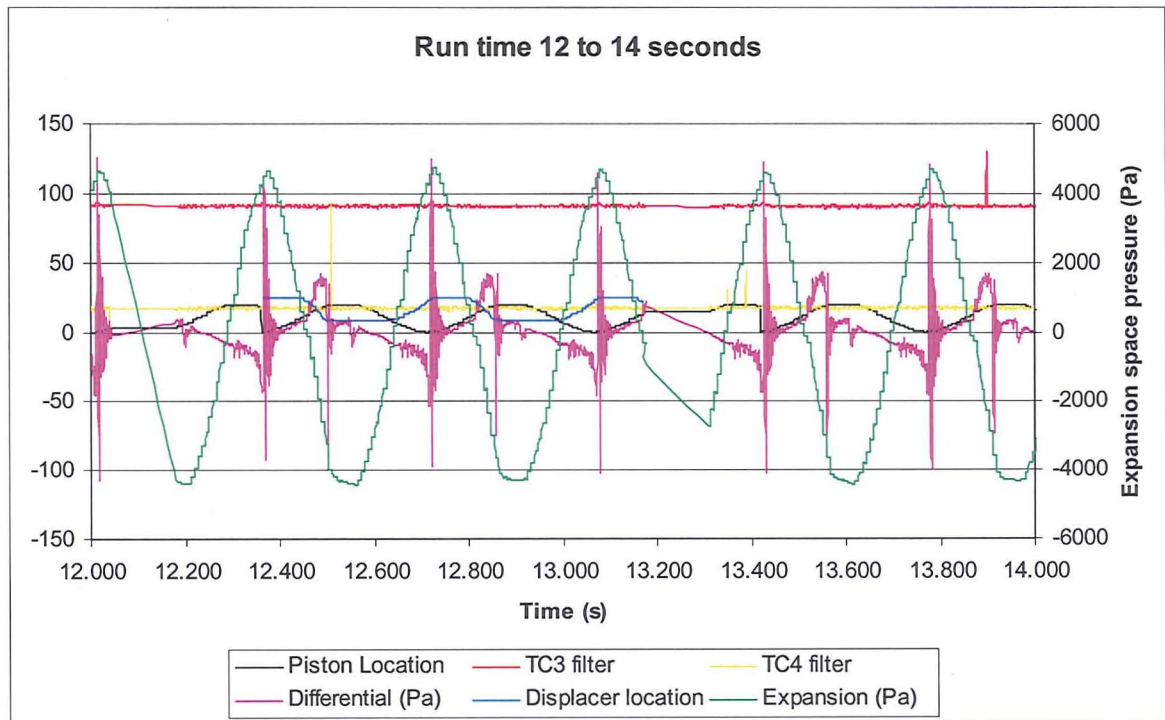


Figure 4.18 Run time 12 to 14 seconds

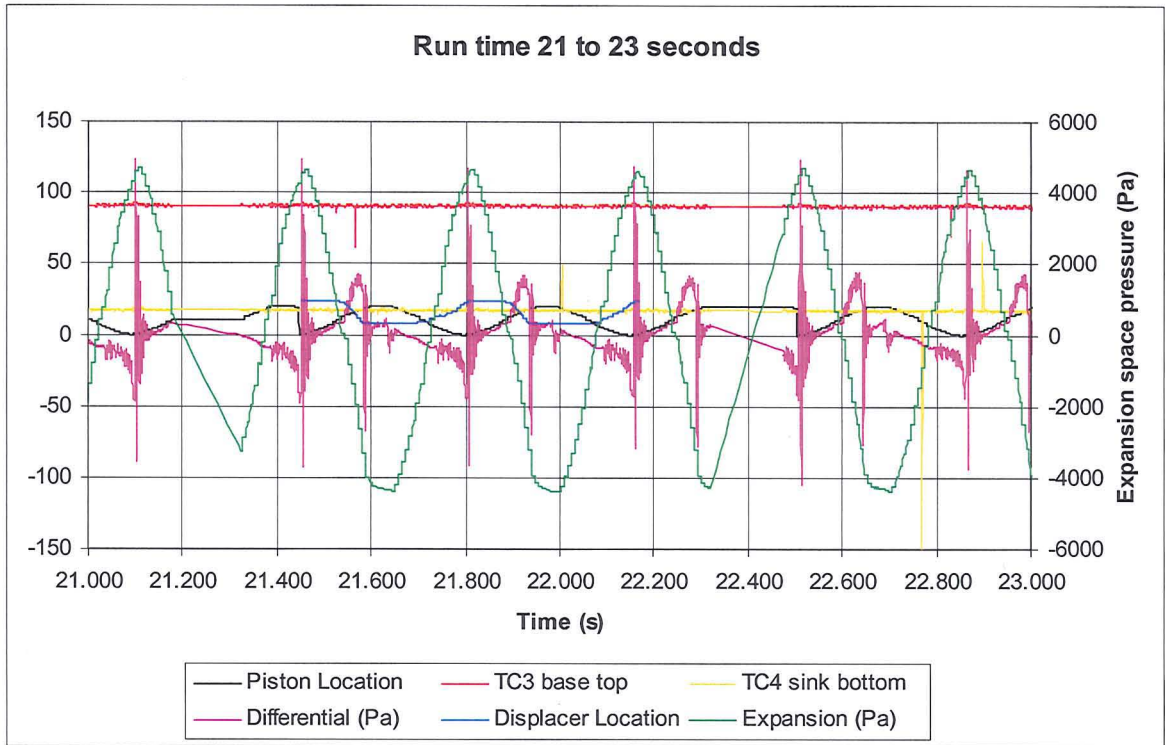


Figure 4.19 Run time 21 to 23 seconds

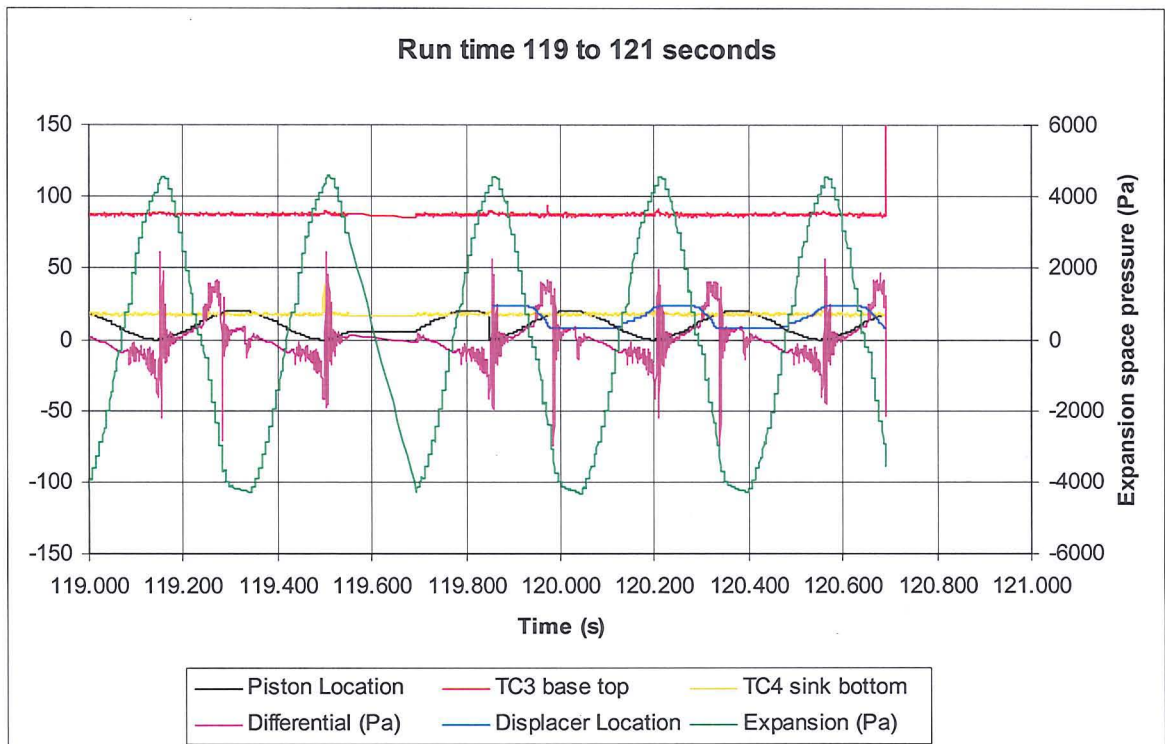


Figure 4.20 Run time 119 to 121 seconds

Each graph has six traces; the left hand axis represents general magnitudes for piston location, source and sink temperatures, pressure differential across the

displacer and displacer location. The right hand axis represents the expansion space pressure.

These graphs have been further analysed to produce the series below. The temperature data is now omitted and two graphs are presented for each time under investigation. One shows the displacer and piston locations in relation to the expansion space pressure and the other shows the differential pressure ($P_e - P_k$) in relation to the expansion space pressure. The expansion space pressure is being used as a reference. This pressure drives the engine and it provides a useful link between the pressure cycle and kinematic cycle.

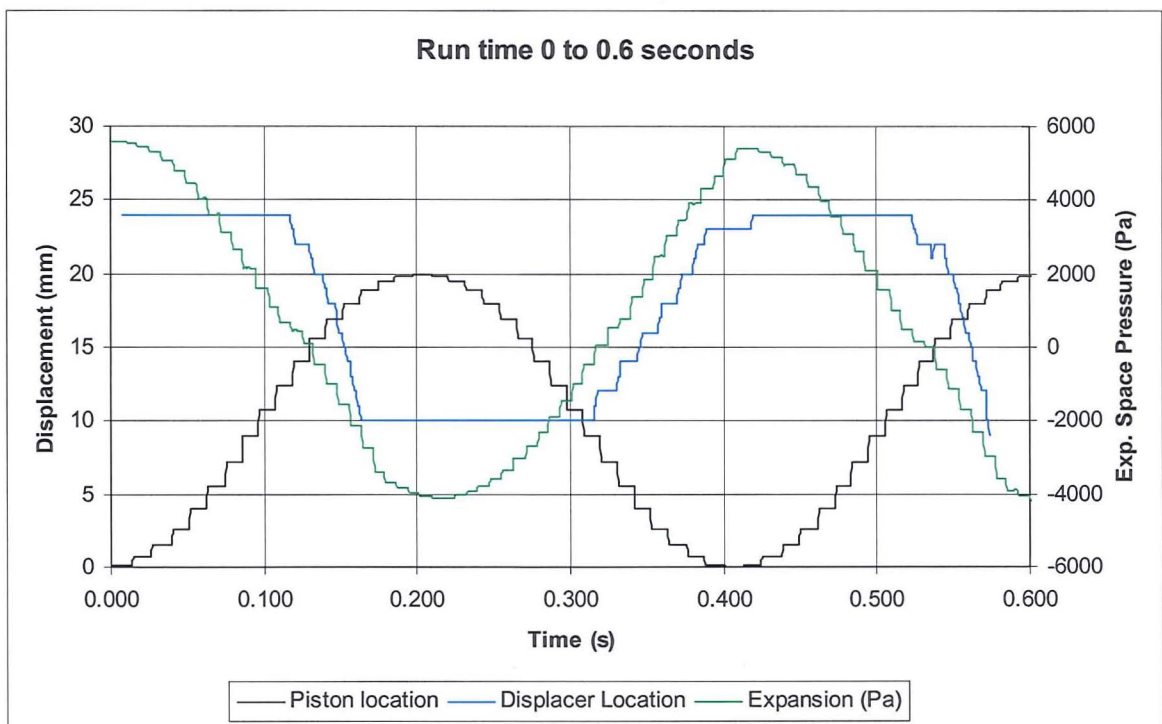


Figure 4.21 Piston and Displacer referred to P_e (0 to 0.6s)

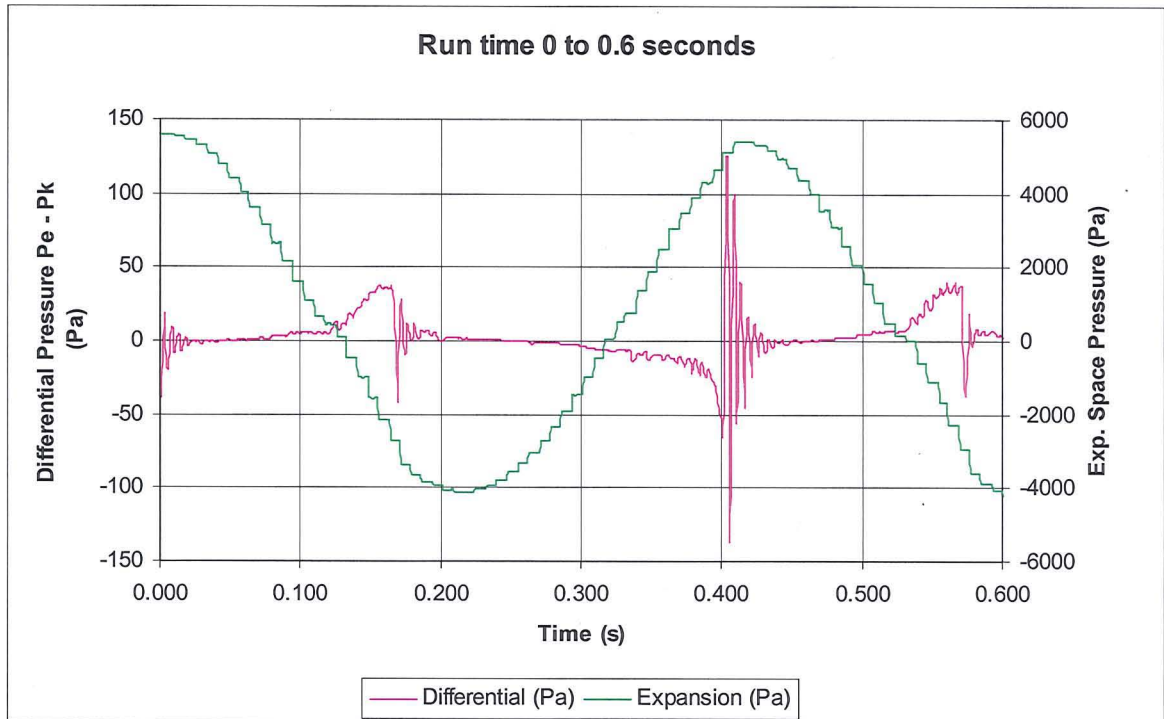


Figure 4.22 Differential pressure referred to P_e (0 to 0.6s)

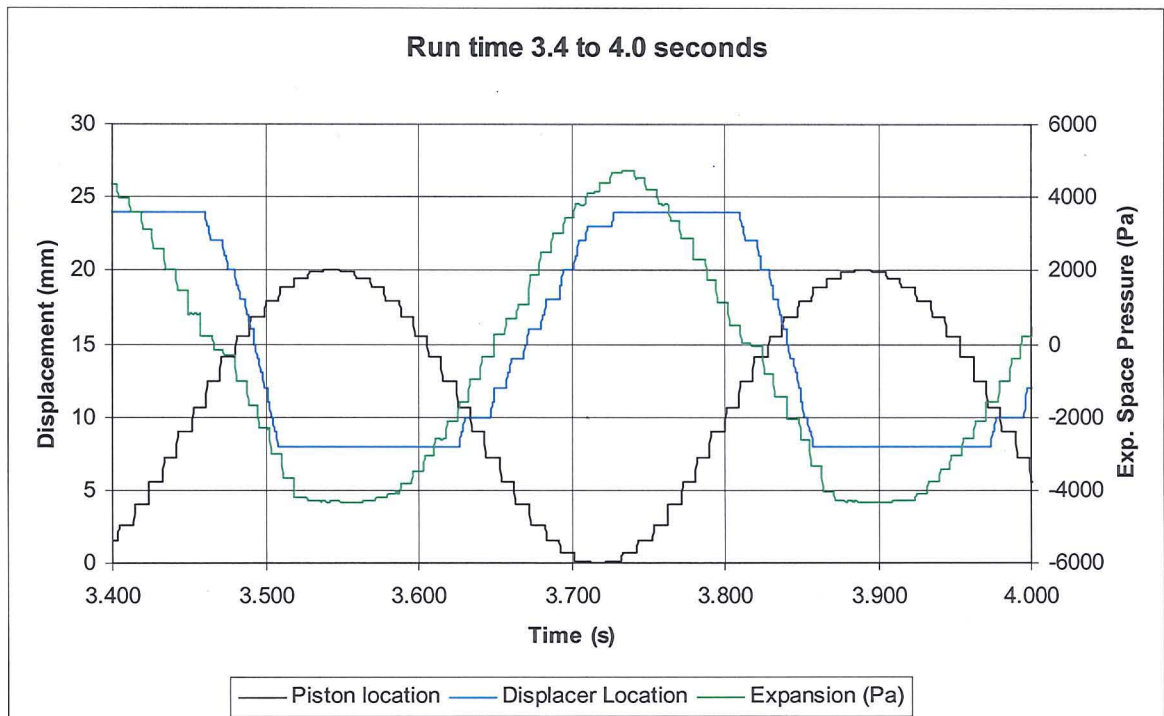


Figure 4.23 Piston and Displacer location referred to P_e (3.4 to 4s)

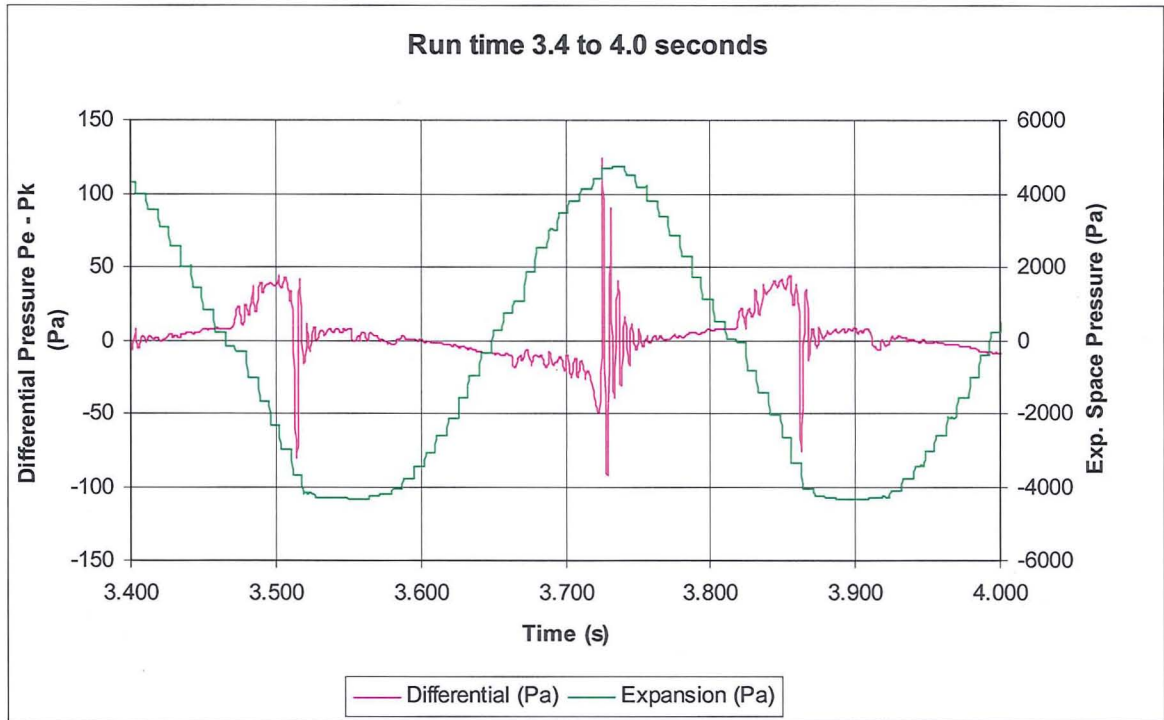


Figure 4.24 Differential Pressure referred to P_e (3.4 to 4s)

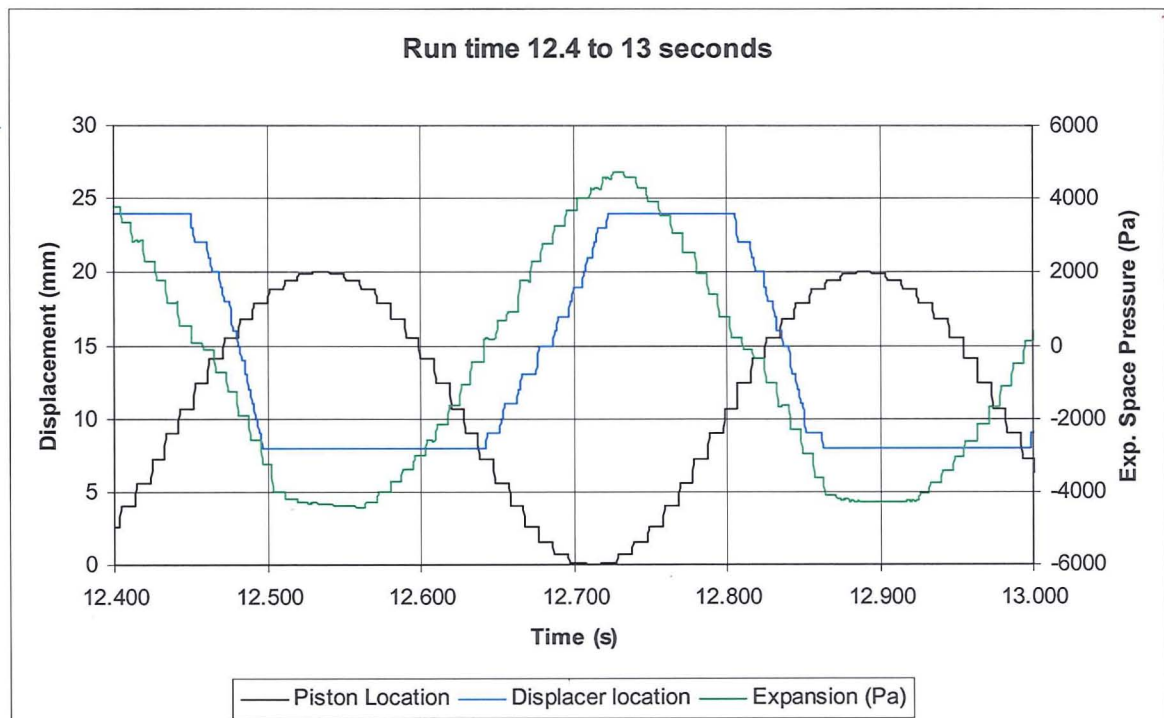


Figure 4.25 Piston and Displacer referred to P_e (12.4 to 13s)

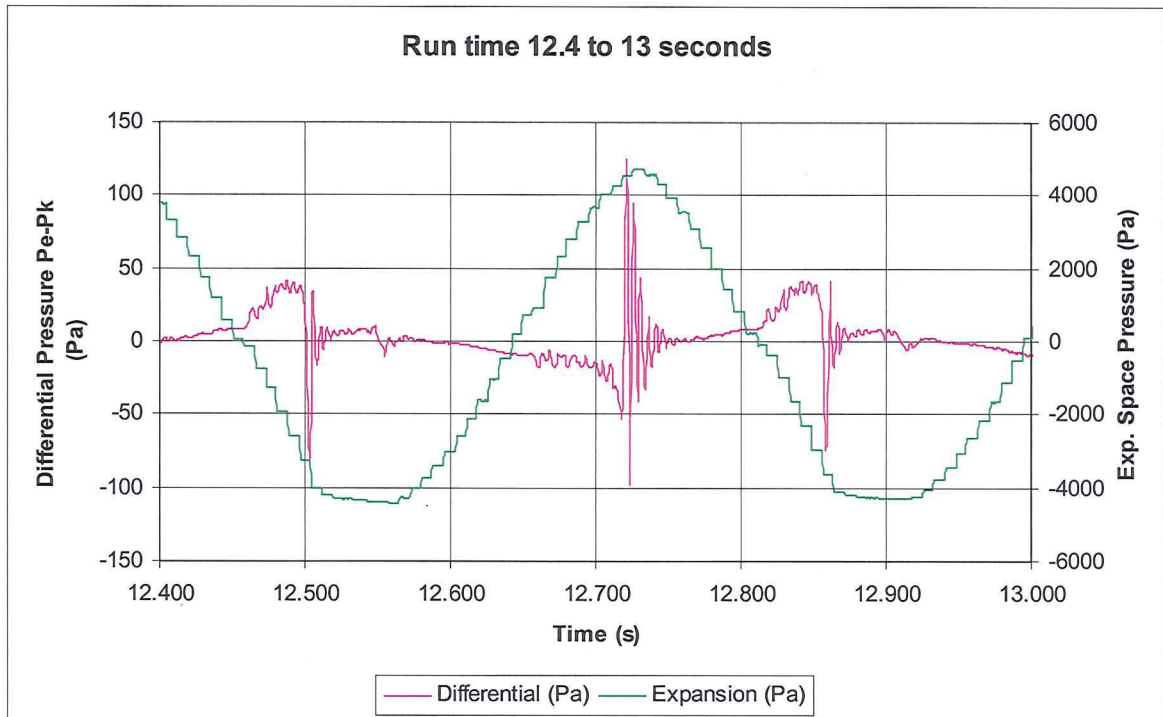


Figure 4.26 Differential Pressure referred to Pe (12.4 to 13s)

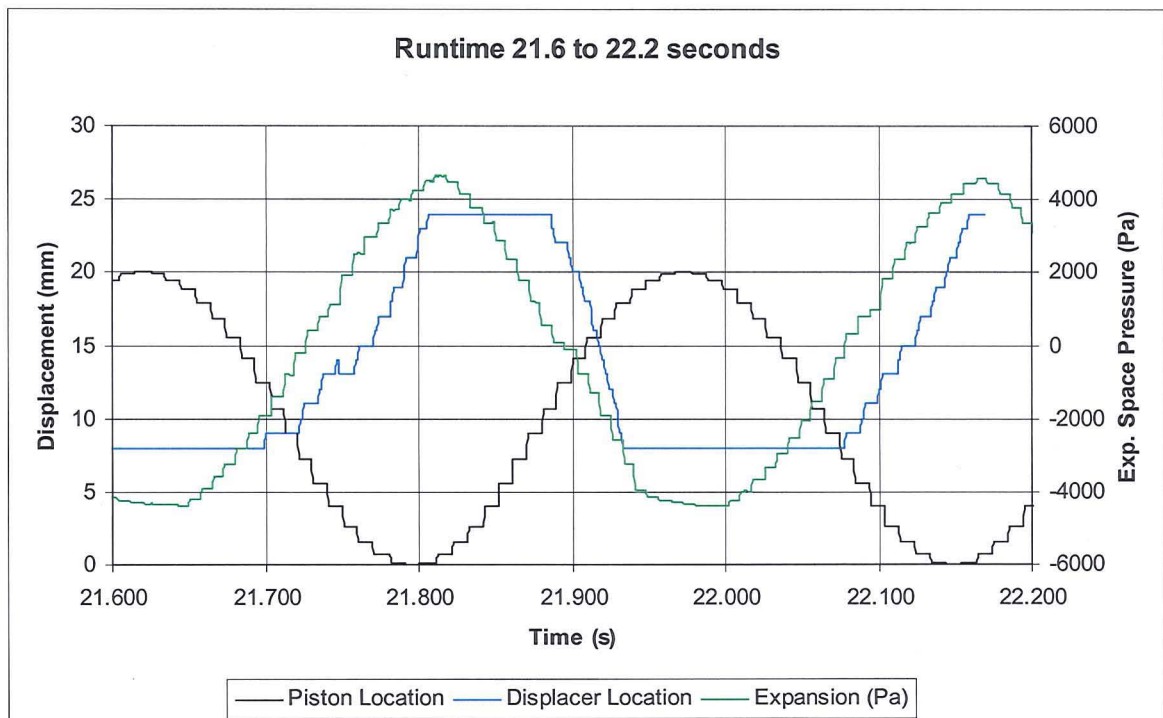


Figure 4.27 Piston and Displacer Location referred to Pe (21.6 to 22.2s)

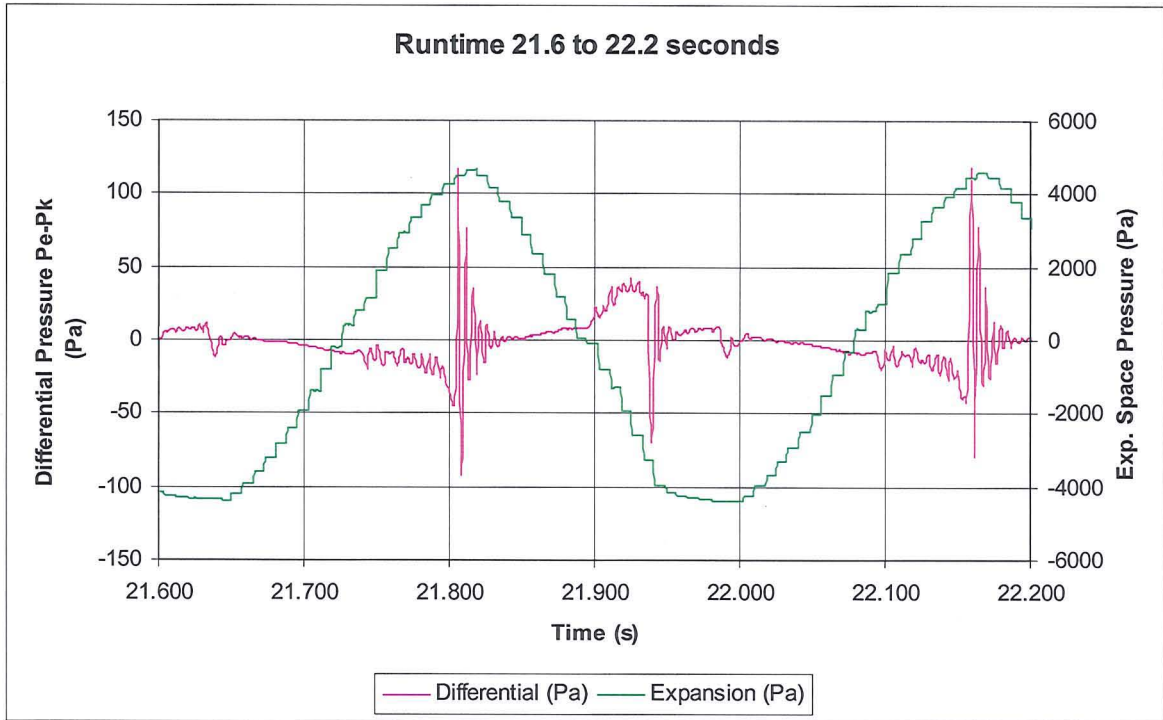


Figure 4.28 Differential Pressure referred to Pe (21.6 to 22.2s)

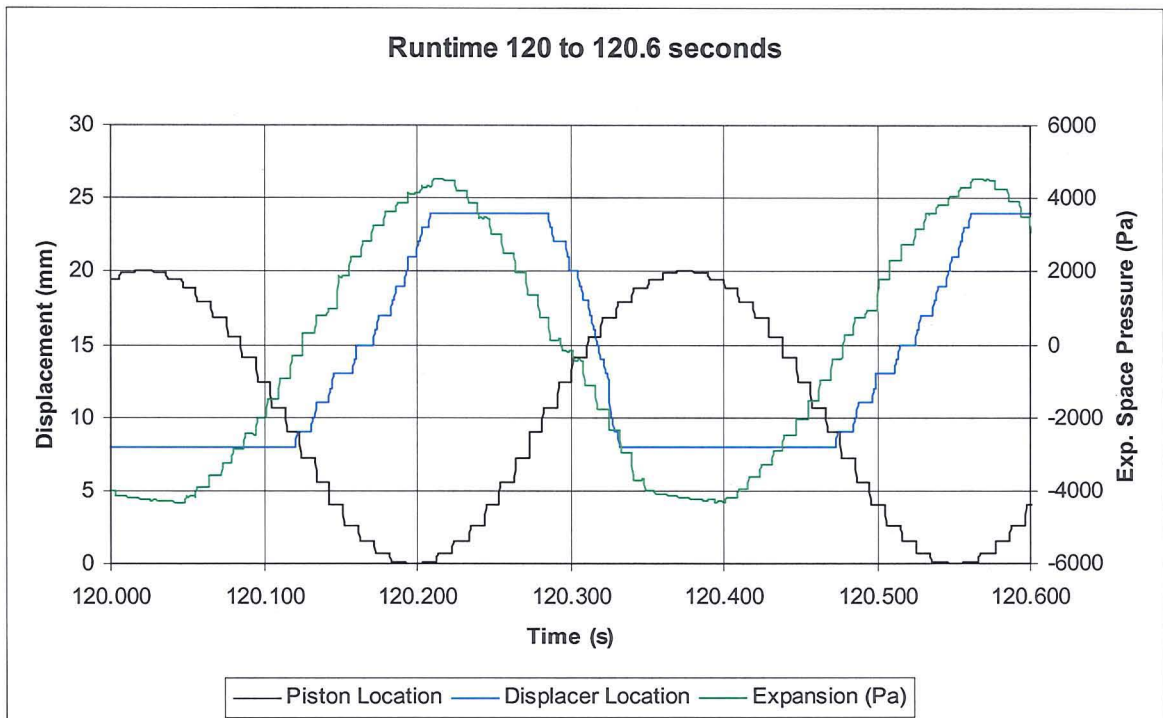


Figure 4.29 Piston and Displacer Location referred to Pe (120 to 120.6s)

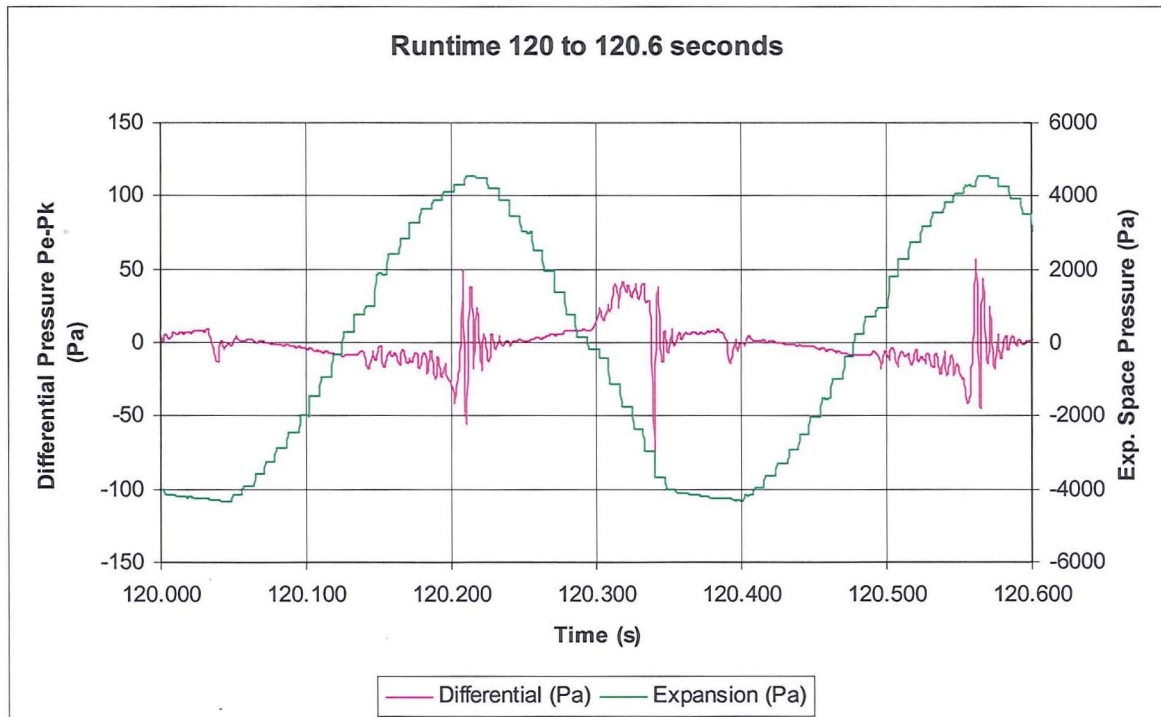


Figure 4.30 Differential Pressure referred to P_e (120 to 120.6s)

4.7 Qualitative results

Through the experimental phase the data for many tens of engine runs are collected and analysed. The above graphs have been taken from one such run and are considered representative of the body of data as a whole. Future work may consider further statistical analysis of the data sets.

Figures 4.21 to 4.30 are given as a representative set of results for the first 120 second of engine runtime. After this period the engine may be considered to have achieved stable running, with further changes in operation due to the decaying temperature differential.

Table 4.1 shows that in the first twelve seconds the temperature differential drops by 7°C ; from figures 4.16 to 4.18 inclusive it can be seen that this drop is almost totally due to the source temperature changing.

From $t = 12$ to $t = 120$ the drop is only 3°C

Figure 4.21 shows the variations of the positions of the piston and displacer and the relative expansion pressure at start up. The relative expansion pressure is about 180° anti-phase, lagging the piston slightly. When the pressure is at a maximum the piston is just after bottom dead centre on the upstroke. The movement of the displacer shows the expansion space pressure required to rise above a 'lifting' pressure in order to overcome gravity acting upon the displacer assembly mass. It can be seen that as soon as the pressure changes the displacer begins to drop, the drop gradient being noticeably sharper than the rise gradient. The flywheel is rotating at 150 rpm.

Figure 4.22 shows the variations of the differential pressure across the displacer, measured from tapings shown in figure 4.14 at start up. The first spike coincides with the drop of the displacer, with 'ringing' at the point where the displacer contacts the expansion space spring and expansion space low pressure. The second spike coincides with the displacer rising and contacting with the compression space spring at compression space maximum pressure.

Figures 4.23 and 4.24 show the variations for run time 3.4 to 4 seconds. The flywheel speed is now 176.7 rpm. The spikes in the differential pressure, coinciding with the displacer contacting the stub springs, have increased for the displacer drop, and decreased for the displacer rise. The relative pressure for the expansion space has dropped by 2000 Pa for the high pressure part of the cycle. The low pressure part remains the same.

Figures 4.25 and 4.26 show the variations for run time 12.4 to 13 seconds. The flywheel speed remains at 176.7 rpm. A noticeable lag between the displacer and pressure variations is now developing. The spikes observed in the differential pressure are increasing in the negative direction.

Figures 4.27 and 4.28 show the variations for run time 21.6 to 22.2 seconds. The flywheel speed is now 166.7 rpm. There appears to be no change in phase between displacer location and expansion space pressure. Differential pressure variations appear to be in steady state.

Figures 4.29 and 4.30 show the variations for run time 120 to 120.6 seconds, also considered to be steady state running for the engine. The flywheel speed is 166.7 rpm, which is not too unexpected as the temperature differential from 22 seconds to 120 seconds has only dropped by 3°C. The phase difference between the displacer and expansion space pressure has remained the same. Only the differential pressure trace has become more pronounced.

5 Theoretical Analysis and Numerical Techniques

This chapter reproduces a full third order analysis of the low temperature differential Ringbom - Stirling engine, using conservation laws and the ideal gas law.

5.1 The Ringbom Stirling engine and third order analysis

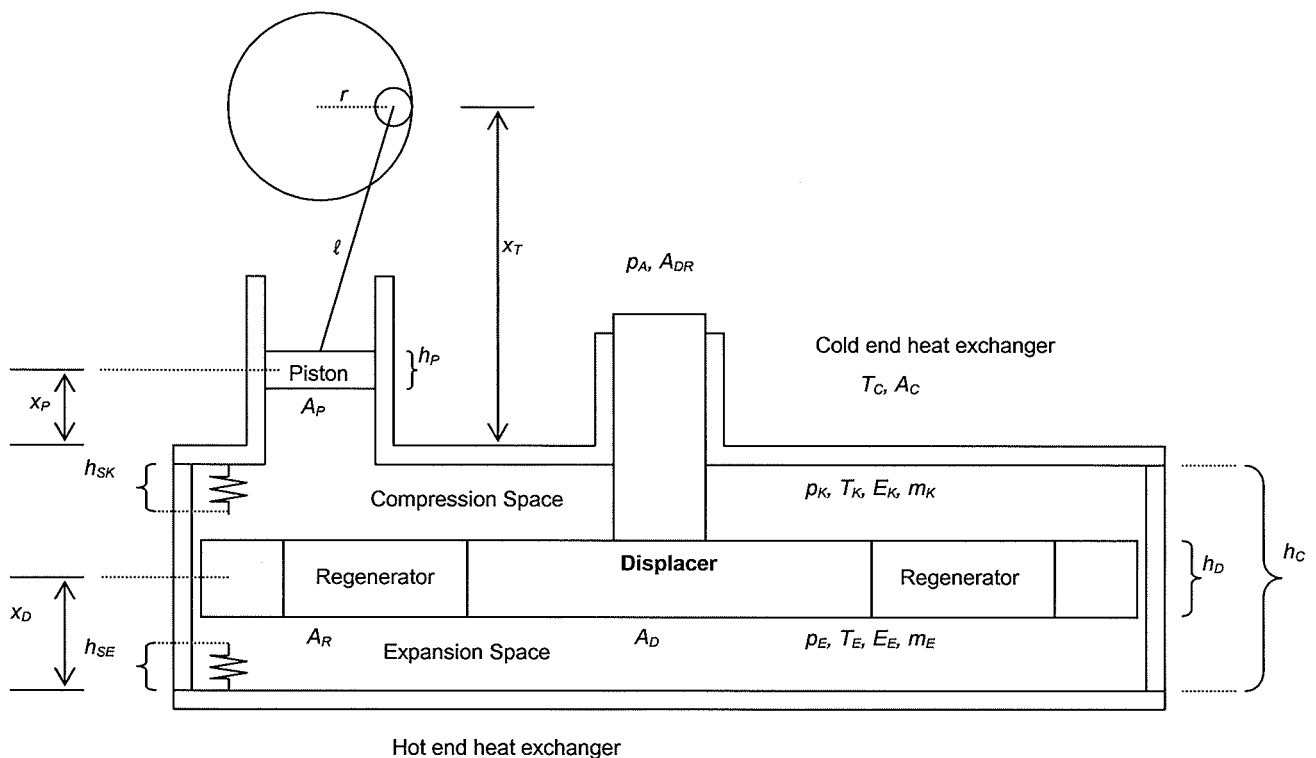


Figure 5.1 Schematic of Ringbom Stirling engine

The analysis requires that each of the nodes, spaces and elements are identified. Figure 5.1 shows a schematic of a Ringbom Stirling engine with relevant points indicated.

To simplify the governing equations, several assumptions are necessarily made, these being:

- The engine alignment is vertical
- Pressures in all spaces are uniform
- Temperatures in all spaces are uniform

- The working fluid is air which behaves as a perfect gas
- No flow through the annular gap formed by the displacer and chamber wall
- The mass of working fluid in the regenerator is constant
- The flow through the regenerator can be modelled as flow through pipes
- Heat transfer within the matrix is solely between the matrix material and the working fluid, i.e. no alternative thermal pathways such as axial conduction
- Temperatures of hot and cold plates are constant throughout the process
- No frictional pressure drop losses in the regenerator
- Adiabatic chamber walls and regenerator screen
- Mechanical losses and windage may be accounted for in one term
- Connecting rod has no mass

The following conventions are used:

- Work done on the system is negative
- Thermal energy into the system is positive

5.2 Analysis of the expansion space

All mass flow to and from the expansion space is considered to traverse the regenerator, driven by the pressure difference either side of the regenerative matrix. Initially flow through the annular gap and consequent heat transfer to the chamber wall is included in the regenerator terms. A constant (K_{MR}) can be formed, which accounts for the flow properties of the fluid through the regenerator.

Hence an equation describing the mass flow may be written as:

$$\dot{m}_R = K_{MR} (P_E - P_K) \quad \text{Equation 5.1}$$

Where flow out of the expansion space is considered as positive, and inward flow as negative.

If $P_E > P_K$ then \dot{m} is positive [$\dot{m}_R > 0$]

else

If $P_E < P_K$ then \dot{m} is negative [$\dot{m}_R < 0$]

Equation 5.2

The mass conservation in the expansion space per unit time (rate of change in mass) may be expressed as:

$$\Delta m_E = -\dot{m}_R \Delta t$$

$$\frac{dm_E}{dt} = -\dot{m}_R$$

Equation 5.3

The energy balance in the expansion space may be considered as the energy entering the space from the source (hot plate), minus the energy leaving the space due to mass flow (or plus the energy entering the expansion space on the conjugate cycle where flow enters the expansion space from the regenerator), and minus the energy required to perform work upon the displacer, which may be written as:

$$\Delta E_E = (E_{Source} - E_{Flow} - W_{displacer}) \Delta t$$

Equation 5.4

Where

$$E_E = C_v \cdot m_E \cdot T_E$$

Equation 5.5

And E_{Source} is heat flow from the hot end heat exchanger which can be expressed as:

$$\dot{Q} = K_{HH} (T_H - T_E) \Delta t$$

Equation 5.6

Where K_{HH} is the constant of convective heat transfer for the source surface, T_H is the source surface temperature, T_E is the expansion space temperature and Δt is the time step for the rate of heat exchange.

Where E_{Flow} is an expression for the energy in the mass exiting or entering the expansion space:

If $\dot{m}_R > 0$ then

$$E_{Flow} = C_p T_E \dot{m}_R \Delta t$$

else

If $\dot{m}_R < 0$ then

$$E_{Flow} = C_p T_{RE} \dot{m}_R \Delta t$$

Equation 5.7

Where T_{RE} is the temperature of the working fluid entering the expansion space from the regenerator.

Where $W_{displacer}$ is the work done to lift the displacer against external pressure. The pressure in the expansion space acts upon the available surface area of the displacer and will move the displacer a distance Δx_D , this may be written as:

$$W_{Displacer} = P_E \cdot A_D \cdot \Delta x_D$$

Equation 5.8

Hence the energy balance equation may be written as:

If $P_E \geq P_K$ then

$$\Delta(C_v m_E T_E) = K_{HH} (T_H - T_E) \Delta t - C_p \dot{m}_R T_E \Delta t - P_E A_D \Delta x_D$$

else

If $P_E \leq P_K$ then

$$\Delta(C_v m_E T_E) = K_{HH} (T_H - T_E) \Delta t - C_p \dot{m}_R T_{RE} \Delta t - P_E A_D \Delta x_D$$

Equation 5.9

Equation 5.9 may be rewritten as:

$$\Delta(C_v m_E T_E) = K_{HH} (T_H - T_E) \Delta t - C_p \dot{m}_R T_1^* \Delta t - P_E A_D \Delta x_D$$

where

If $\dot{m}_R > 0$ then $T_1^* = T_E$

If $\dot{m}_R < 0$ then $T_1^* = T_{RE}$

Equation 5.10

Rewriting in terms of the rate of change (time domain) results in:

$$\left(\frac{dE_E}{dt}\right) = K_{HH}(T_H - T_E) - C_p \dot{m}_R T_1^* - P_E A_D \frac{dx_D}{dt} \quad \text{Equation 5.11}$$

Inspecting $E_E = C_V m_E T_E$ and differentiating with respect to time, where C_V is a constant, the following result can be obtained:

$$\frac{dE_E}{dt} = C_V \frac{dm_E}{dt} T_E + C_V m_E \frac{dT_E}{dt} \quad \text{Equation 5.12}$$

Noting that

$$\frac{dm_E}{dt} = -\dot{m}_R \quad \text{Equation 5.13}$$

Equation 5.12 can be written as

$$\frac{dE_E}{dt} = -C_V \dot{m}_R T_E + C_V m_E \frac{dT_E}{dt} \quad \text{Equation 5.14}$$

Rewriting the expansion space inequality expression to include the modified left hand side gives:

$$C_V m_E \frac{dT_E}{dt} - C_V \dot{m}_R T_E = K_{HH}(T_H - T_E) - C_p T_1^* \dot{m}_R - P_E A_D \frac{dx_D}{dt} \quad \text{Equation 5.15}$$

which may be rewritten as:

$$C_V m_E \frac{dT_E}{dt} = K_{HH}(T_H - T_E) - P_E A_D \frac{dx_D}{dt} + C_V \dot{m}_R T_E - C_p T_1^* \dot{m}_R \quad \text{Equation 5.16}$$

The term containing the specific heat at constant pressure may be re written with C_p being expressed as $C_V + R$, where R is the gas constant for the working fluid.

$$C_V m_E \frac{dT_E}{dt} = K_{HH} (T_H - T_E) - P_E A_D \frac{dx_D}{dt} + C_V \dot{m}_R T_E - (C_V + R) \dot{m}_R T_1^* \quad \text{Equation 5.17}$$

Rearranging this new term yields equation 5.18

$$C_V m_E \frac{dT_E}{dt} = K_{HH} (T_H - T_E) - P_E A_D \frac{dx_D}{dt} + C_V \dot{m}_R (T_E - T_1^*) - R \dot{m}_R T_1^* \quad \text{Equation 5.18}$$

The pressure in the expansion space may be calculated using the ideal gas law

$$PV = mRT \quad \text{Equation 5.19}$$

Which may be expressed as:

$$P_E = \frac{m_E R T_E}{V_E} \quad \text{Equation 5.20}$$

Where V_E is the instantaneous volume of the expansion space.

Equation 5.20 may then be rewritten as:

$$P_E = \frac{m_E R T_E}{A_D (x_D - 0.5h_D)} \quad \text{Equation 5.21}$$

5.3 Analysis of the compression space

The compression space analysis follows a similar method to that employed for the expansion space. The mass flow term is modified to include mass ingress and egress due to imperfect sealing of the piston and displacer in their respective linings.

Following the reasoning as expanded for the expansion space then

$$\dot{m}_R = K_{MR}(P_E - P_K) \quad \text{Equation 5.22}$$

And

$$\dot{m}_A = K_{MA}(P_A - P_K) \quad \text{Equation 5.23}$$

$$\frac{dm_K}{dt} = \dot{m}_R + \dot{m}_A \quad (\text{positive as mass is entering}) \quad \text{Equation 5.24}$$

But

\dot{m}_A consists of two components \dot{m}_{MP} and \dot{m}_{MD}

hence

$$\frac{dm_K}{dt} = \dot{m}_R + \dot{m}_{MP} + \dot{m}_{MD} \quad \text{Equation 5.25}$$

The energy balance for the compression space is made up of five terms.

- Heat removed via the cold plate
- Heat coming in from the regenerator
- Heat removed due to leakage to the atmosphere
- Work done by the displacer
- Work done on the piston

Which may be written as:

$$\Delta E_K = (-E_{Sink} + E_{Regen} + E_{Leakage} + W_{Displacer} - W_{Piston}) \Delta t \quad \text{Equation 5.26}$$

This is developed in a similar way to the expansion space above, therefore only the key steps will be given.

Defining T_2^* and T_3^* as

$$P_E > P_K \text{ then } \dot{m}_R > 0 \text{ and } T_2^* = T_{RK}$$

$$P_E < P_K \text{ then } \dot{m}_R < 0 \text{ and } T_2^* = T_K$$

$$P_A < P_K \text{ then } \dot{m}_A < 0 \text{ and } T_3^* = T_K$$

$$P_A > P_K \text{ then } \dot{m}_A > 0 \text{ and } T_3^* = T_A$$

Equation 5.27

The first expansion of the energy equation gives

$$\Delta E_K = -K_{HC}(T_K - T_C)\Delta t + P_K(A_D - A_{DR})\Delta x_D - P_K A_P \Delta x_P + C_p \dot{m}_R T_2^* \Delta t + C_p \dot{m}_A T_3^* \Delta t$$

Equation 5.28

Inspecting $E_K = C_V m_K T_K$ and differentiating with respect to time where C_V is a constant; using the product rule, the following result can be obtained:

$$\frac{dE_K}{dt} = C_V \frac{dm_K}{dt} T_K + C_V m_K \frac{dT_K}{dt}$$

Equation 5.29

Using a similar expansion to the equations for the expansion space, and remembering that the flow term is now positive, the equation for the compression space may be formed:

$$C_V T_K (\dot{m}_R + \dot{m}_A) + C_V m_K \frac{dT_K}{dt} = -K_{HC}(T_K - T_C) + C_p T_2^* \dot{m}_R + C_p T_3^* \dot{m}_A + P_K (A_D - A_{DR}) \frac{dx_D}{dt} - P_K A_P \frac{dx_P}{dt}$$

Equation 5.30

Transposing equation 5.30

$$C_V m_K \frac{dT_K}{dt} = -K_{HC}(T_K - T_C) + P_K (A_D - A_{DR}) \frac{dx_D}{dt} - P_K A_P \frac{dx_P}{dt} - C_V \dot{m}_R T_K + (C_V + R) \dot{m}_R T_2^* - C_V \dot{m}_A T_K + (C_V + R) \dot{m}_A T_3^*$$

Equation 5.31

Rearranging equation 5.31

$$\begin{aligned}
 C_V m_K \frac{dT_K}{dt} = & -K_{HC}(T_K - T_C) + P_K(A_D - A_{DR}) \frac{dx_D}{dt} - P_K A_P \frac{dx_P}{dt} \\
 & - C_V \dot{m}_R T_K + (C_V + R) \dot{m}_R T_2^* - C_V \dot{m}_A T_K + (C_V + R) \dot{m}_A T_3^*
 \end{aligned}
 \tag{Equation 5.32}$$

Combining like terms

$$\begin{aligned}
 C_V m_K \frac{dT_K}{dt} = & -K_{HC}(T_K - T_C) + P_K(A_D - A_{DR}) \frac{dx_D}{dt} - P_K A_P \frac{dx_P}{dt} \\
 & + C_V \dot{m}_R (T_2^* - T_K) + R \dot{m}_R T_2^* + C_V \dot{m}_A (T_3^* - T_K) + R \dot{m}_A T_3^*
 \end{aligned}
 \tag{Equation 5.33}$$

To develop equation 5.33 further, the piston velocity may be written in terms of the flywheel angle theta. Equation 5.35 is the equation for piston velocity. We may now substitute for x_p by θ . This is derived from piston geometry as shown in figure 5-7, which is defined by equation 5.34.

$$x_p = x_T - (\ell^2 - r^2 \sin^2 \theta)^{0.5} - r \cos \theta
 \tag{Equation 5.34}$$

$$\dot{x}_p = \left[\frac{r^2 \sin \theta \cos \theta}{(\ell^2 - (r \sin \theta)^2)^{0.5}} + r \sin \theta \right] \cdot \frac{d\theta}{dt}
 \tag{Equation 5.35}$$

Gives:

$$\begin{aligned}
 C_V m_K \frac{dT_K}{dt} = & -K_{HC}(T_K - T_C) + P_K(A_D - A_{DR}) \frac{dx_D}{dt} \\
 & - P_K A_P \left[\frac{r^2 \sin \theta \cos \theta}{(\ell^2 - r^2 (\sin \theta)^2)^{0.5}} + r \sin \theta \right] \cdot \frac{d\theta}{dt} \\
 & + C_V \dot{m}_R (T_2^* - T_K) + R \dot{m}_R T_2^* + C_V \dot{m}_A (T_3^* - T_K) + R \dot{m}_A T_3^*
 \end{aligned}
 \tag{Equation 5.36}$$

The pressure in the compression space is calculated using the ideal gas law, as before, resulting in:

$$P_K = \frac{m_k RT_K}{(A_D - A_{DR})(h_C - 0.5h_D - x_D) + A_P(x_P - 0.5h_P)} \quad \text{Equation 5.37}$$

5.4 Analysis of the displacer

The displacer motion is caused by a pressure difference between the internal space and the atmosphere.

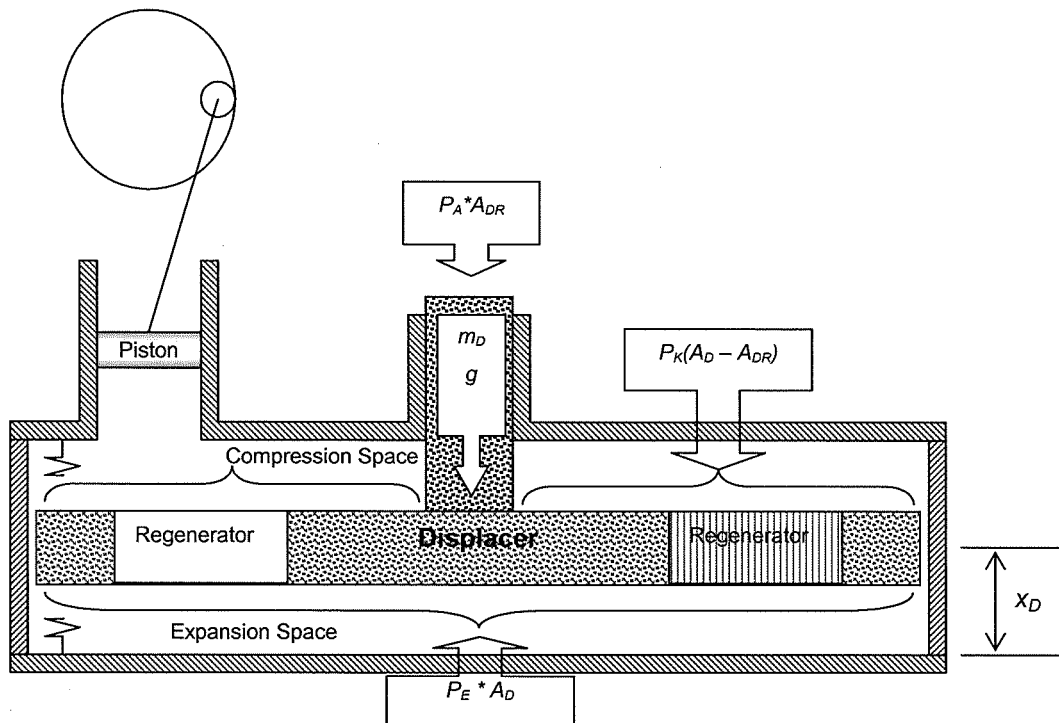


Figure 5.2 Forces acting upon the displacer

In the region of unconstrained displacer travel, the line of action for the mid point of the displacer (centre of mass) x_D will always be in the space bounded by the stub spring length and \pm half the displacer height. Two inequalities may be set up to describe this region.

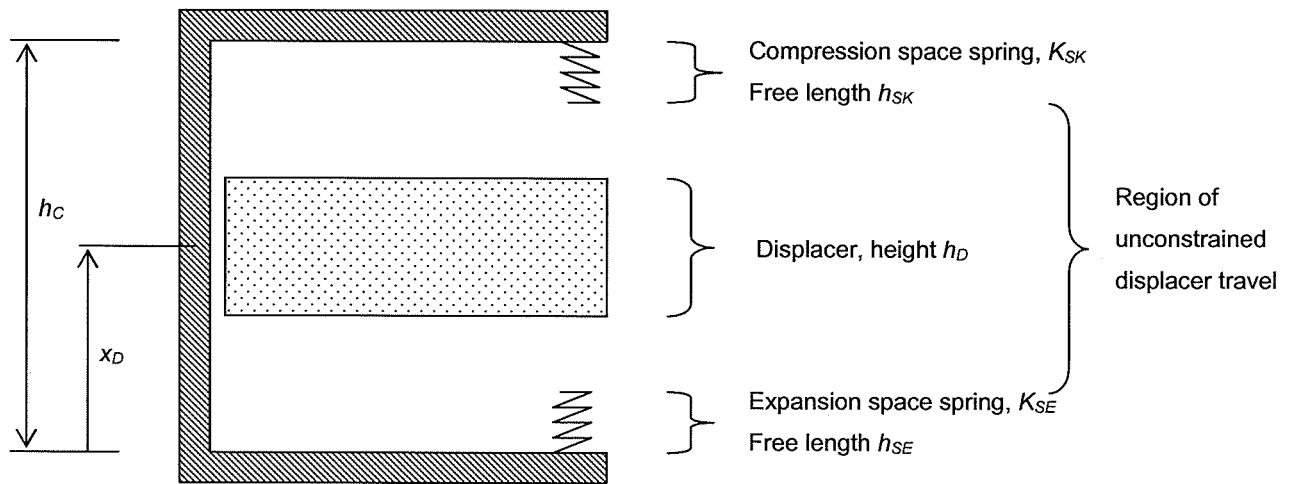


Figure 5.3 Detail section of stub springs and displacer

Consider the arrangement shown in figure 5.2 and 5.3

For the expansion space spring

$$x_D > h_{SE} + 0.5h_D \tag{Equation 5.38}$$

For the compression space spring

$$x_D < h_C - h_{SK} - 0.5h_D \tag{Equation 5.39}$$

Thus the equation for motion not constrained by the action of either of the stub springs becomes:

$$m_D \ddot{x}_D = P_E A_D - m_D g - P_K (A_D - A_{DR}) - P_A A_{DR} \tag{Equation 5.40}$$

It should be remembered that there are two caveat conditions, one where the length of the compressed springs should not be greater than the void which they fill, and one where the extreme surfaces of the displacer are not allowed to travel beyond the physical boundaries set by the inner surfaces of the hot and cold plates, which can be written as:

$$\begin{aligned} x_D &> 0.5h_D \\ x_D &< h_C - 0.5h_D \end{aligned}$$

Equation 5.41

Only in the regions controlled by the stub springs will equation 5.40 require modification by the addition of forces representing the spring.

For the expansion space controlled by the spring of length h_{SE} , the additional force is

$$F_{DE} = K_{SE}(h_{SE} + 0.5h_D - x_D)$$

Equation 5.42

For the compression space controlled by the spring of length h_{SK} the additional force is

$$F_{DK} = K_{SK}(h_C - h_{SK} - 0.5h_D - x_D)$$

Equation 5.43

Introducing parameter F_{DA} the three conditions of upper restraint, no restraint and lower restraint may be described using one equation. The operator is set by the inequality below:

$$\begin{aligned} \text{for } 0.5h_D < x_D < h_{SE} + 0.5h_D & \quad \text{then } F_{DA} = F_{DE} = K_{SE}(h_{SE} + 0.5h_D - x_D) \\ \text{for } h_{SE} + 0.5h_D \leq x_D \leq h_C - h_{SK} - 0.5h_D & \quad \text{then } F_{DA} = 0 \\ \text{for } h_C - h_{SK} - 0.5h_D < x_D < h_C - 0.5h_D & \quad \text{then } F_{DA} = F_{DK} = K_{SK}(h_C - h_{SK} - 0.5h_D - x_D) \end{aligned}$$

Equation 5.44

And the governing equation for the displacer becomes:

$$m_D \ddot{x}_D = P_E A_D - m_D g - P_K (A_D - A_{DR}) - P_A A_{DR} + F_{DA}$$

Equation 5.45

Which may be rewritten as:

$$m_D \ddot{x}_D = A_D(P_E - P_K) - m_D g + A_{DR}(P_K - P_A) + F_{DA}$$

Equation 5.46

5.5 Analysis of the piston / flywheel assembly

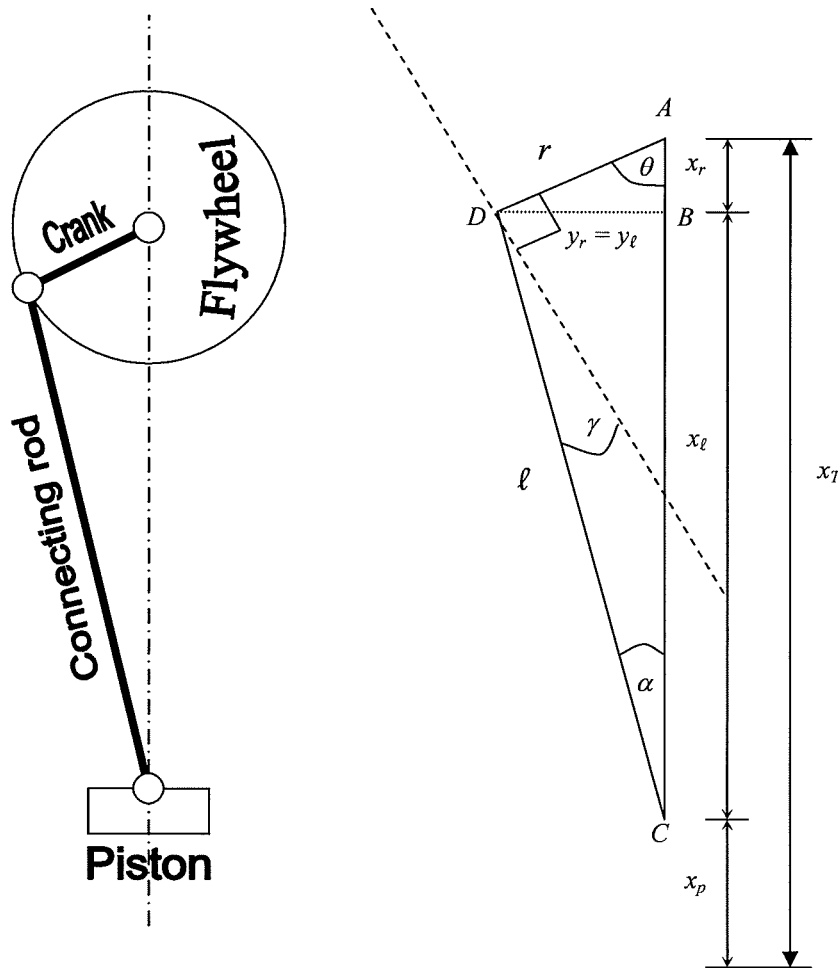


Figure 5.4 Piston and flywheel assembly

Figure 5.4, shows the piston flywheel assembly, the position of the crank pin, the length of the crank r and the angle theta, from a given datum. Similarly the connecting rod end point can be calculated from length ℓ and pivot angle alpha. Alternatively by considering the geometry in Cartesian coordinates the location of the crank pin may be described by two dimensions (x and y).

As an analytical tool it is useful to describe either alpha in terms of theta or theta in terms of alpha. This means that only one angle is required, with the other being

automatically evaluated. From the geometrical construction above it may be seen that each triangle has one side in common (the length y_r subtending θ and y_ℓ , subtending α); it is this communality which will allow one angle to be written in terms of the other.

From the above construct the components of the triangles may be written as:

$$x_r = r \cos \theta \quad \text{Equation 5.47}$$

$$y_r = r \sin \theta \quad \text{Equation 5.48}$$

$$x_\ell = \ell \cos \alpha \quad \text{Equation 5.49}$$

$$y_\ell = \ell \sin \alpha \quad \text{Equation 5.50}$$

As stated above and by inspection it can be seen that

$$y_r = y_\ell \quad \text{Equation 5.51}$$

Hence

$$r \sin \theta = \ell \sin \alpha \quad \text{Equation 5.52}$$

And, transposing for $\sin \alpha$

$$\sin \alpha = \frac{r}{\ell} \sin \theta \quad \text{Equation 5.53}$$

since

$$\cos \alpha = \pm \left(1 - \sin^2 \alpha\right)^{\frac{1}{2}} \quad \text{Equation 5.54}$$

and inserting the above identity for $\sin \alpha$

$$\cos \alpha = \pm \left(1 - \left(\frac{r}{\ell}\right)^2 \sin^2 \theta\right)^{\frac{1}{2}} \quad \text{Equation 5.55}$$

The positive root is taken for the upward stroke, and the change in quadrant accounts for the negative root so the \pm operator may be omitted.

As

$$x_{\ell} = \ell \cos \alpha \quad \text{Equation 5.56}$$

Then

$$x_{\ell} = \ell \left(1 - \left(\frac{r}{\ell}\right)^2 \sin^2 \theta\right)^{\frac{1}{2}} \quad \text{Equation 5.57}$$

From inspection

$$x_p = x_T - x_{\ell} - x_r \quad \text{Equation 5.58}$$

And

$$x_T = \ell + r + 0.5h_p + \delta_s \quad \text{Equation 5.59}$$

Rewriting

$$x_p = x_T - \ell \left(1 - \left(\frac{r}{\ell} \right)^2 \sin^2 \theta \right)^{\frac{1}{2}} - r \cos \theta$$

Equation 5.60

Or

$$x_p = x_T - \left(\ell^2 - r^2 \sin^2 \theta \right)^{\frac{1}{2}} - r \cos \theta$$

Equation 5.61

5.5.1 Piston

With reference to figure 5.5, the forces acting upon the piston may be written as:

$$m_p \ddot{x}_p = A_p (P_k - P_A) - m_p \cdot g - F_p \cos \alpha$$

Equation 5.62

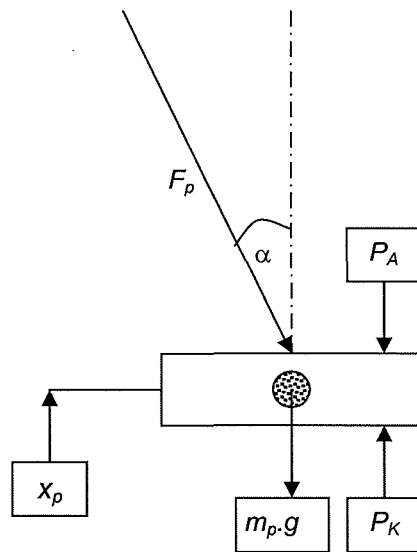


Figure 5.5 Piston forces

5.5.2 The flywheel

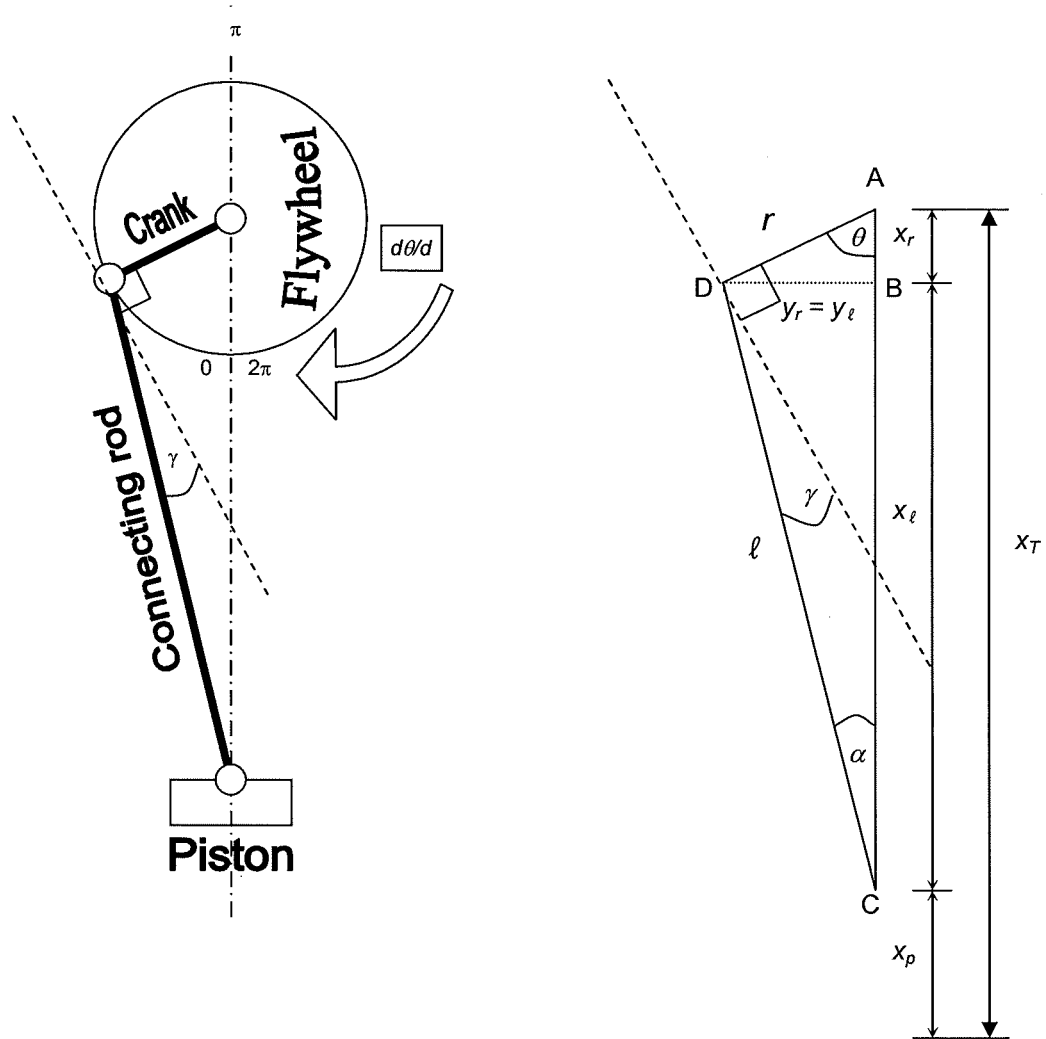


Figure 5.6 Piston-flywheel dynamics

Similarly, the balance of the flywheel in the region

$$0 < \theta < \pi$$

Shows that

$$I_F \ddot{\theta} = T_F - loss_F \tag{Equation 5.63}$$

Where the loss function is assumed to be represented by

$$I_{oss_F} = K_{DF} \frac{d\theta}{dt} \quad \text{Equation 5.64}$$

And T_F , the torque acting upon the flywheel, equals to the force multiplied by the perpendicular distance to axis of rotation, or to be precise, the component of force transmitted via the connecting rod, acting tangentially to the flywheel multiplied by the axis to crankpin length.

Rewriting

$$T_F = F_p \cdot \cos \gamma \cdot r \quad \text{Equation 5.65}$$

Hence

$$I_F \ddot{\theta} = F_p \cos \gamma \cdot r - K_{DF} \dot{\theta} \quad \text{Equation 5.66}$$

Angle ADC is calculated from the sum of angles inside a triangle equal to π , so

$$\angle ADC = \pi - (\theta + \alpha) \quad \text{Equation 5.67}$$

And γ is the angle formed by the tangential force and the connecting rod. Thus it is deduced that part of the angle ADC will always have a component of value π .

Hence

$$\gamma = \frac{\pi}{2} - (\theta + \alpha) \quad \text{Equation 5.68}$$

By applying the double angle formula to equation 5.68 it may be rewritten as

$$\cos \gamma = \sin(\alpha + \theta) \quad \text{Equation 5.69}$$

The above derivations result in two equations which describe the system of forces acting upon the piston and flywheel arrangement, re written as equations 5.70 and 5.71 below.

$$m_p \ddot{x}_p = A_p (P_k - P_A) - m_p \cdot g - F_p \cos \alpha \quad \text{Equation 5.70}$$

$$I_F \ddot{\theta} = F_p \cos \gamma \cdot r - K_{DF} \dot{\theta} \quad \text{Equation 5.71}$$

By multiplying equation 5.70 by $r \cos \gamma$

And multiplying equation 5.71 by $\cos \alpha$

We get

$$m_p r \cos \gamma \ddot{x}_p = A_p (P_k - P_A) r \cos \gamma - m_p \cdot g \cdot r \cos \gamma - F_p \cos \alpha \cdot r \cos \gamma \quad \text{Equation 5.72}$$

And

$$I_F \cos \alpha \ddot{\theta} = F_p \cos \gamma \cdot \cos \alpha \cdot r - K_{DF} \dot{\theta} \cdot \cos \alpha \quad \text{Equation 5.73}$$

Rewriting equation 5.73 for $F_p \cos \gamma \cdot \cos \alpha \cdot r$

$$F_p \cos \gamma \cdot \cos \alpha \cdot r = I_F \ddot{\theta} (\cos \alpha) + K_{DF} \dot{\theta} \cdot \cos \alpha \quad \text{Equation 5.74}$$

Substitute equation 5.74 into equation 5.72

$$m_p \ddot{x}_p (r \cos \gamma) = A_p (P_k - P_A) (r \cos \gamma) - m_p g (r \cos \gamma) - I_F \ddot{\theta} \cos \alpha - K_{DF} \dot{\theta} \cos \alpha \quad \text{Equation 5.75}$$

Moving the acceleration terms to the left hand side gives

$$m_p \ddot{x}_p (r \cos \gamma) + I_F \ddot{\theta} \cos \alpha = A_p (P_k - P_A) (r \cos \gamma) - m_p \cdot g (r \cos \gamma) - K_{DF} \dot{\theta} \cos \alpha$$

Equation 5.76

For the downward stroke from top dead centre (tdc) to bottom dead centre (bdc), where $\pi < \theta < 2\pi$. Changes in polarity that account for the force direction change during the downward stroke are accounted for by trigonometric relationships.

From equation 5.61 the displacement of the piston (x_p) can be calculated for any angle θ . The first and second derivatives (w.r.t. time) will yield equations for velocity and acceleration of the piston.

Thus the equation 5.61 for displacement of the piston can be used to find velocity and acceleration respectively.

$$x_p = x_T - (\ell^2 - r^2 \sin^2 \theta)^{0.5} - r \cos \theta \quad \text{(Copy of equation 5.61)}$$

$$\dot{x}_p = \left[\frac{r^2 \sin \theta \cos \theta}{(\ell^2 - r^2 (\sin \theta)^2)^{0.5}} + r \sin \theta \right] \cdot \frac{d\theta}{dt} \quad \text{Equation 5.77}$$

$$\begin{aligned} \ddot{x}_p = & \left[\frac{r^4 (\sin \theta)^2 (\cos \theta)^2}{(\ell^2 - r^2 (\sin \theta)^2)^{1.5}} \right] \cdot \left(\frac{d\theta}{dt} \right)^2 + \left[\frac{r^2 (\cos \theta)^2}{(\ell^2 - r^2 (\sin \theta)^2)^{0.5}} \right] \cdot \left(\frac{d\theta}{dt} \right)^2 \\ & - \left[\frac{r^2 (\sin \theta)^2}{(\ell^2 - r^2 (\sin \theta)^2)^{0.5}} \right] \cdot \left(\frac{d\theta}{dt} \right)^2 + \left[\frac{r^2 (\sin \theta) (\cos \theta)}{(\ell^2 - r^2 (\sin \theta)^2)^{0.5}} \right] \cdot \left(\frac{d^2 \theta}{dt^2} \right) \\ & + r \sin \theta \left(\frac{d^2 \theta}{dt^2} \right) + r \cos \theta \left(\frac{d\theta}{dt} \right)^2 \end{aligned} \quad \text{Equation 5.78}$$

Equations 5.61 and 5.77 are my own derivations, which were checked using Math Cad software. Equation 5.78 was generated using Math Cad.

Putting the identity from equation 5.78 into 5.76 the force balance may be rewritten as

$$\begin{aligned}
 & m_p r \cos \gamma \left\{ \frac{r^4 (\sin \theta)^2 (\cos \theta)^2}{(\ell^2 - (r \sin \theta)^2)^{1.5}} - \frac{r^2 (\sin \theta)^2}{(\ell^2 - (r \sin \theta)^2)^{0.5}} + \frac{r^2 (\cos \theta)^2}{(\ell^2 - (r \sin \theta)^2)^{0.5}} + r \cos \theta \right\} \left(\frac{d\theta}{dt} \right)^2 + \\
 & m_p r \cos \gamma \left\{ \frac{r^2 (\sin \theta) (\cos \theta)}{(\ell^2 - (r \sin \theta)^2)^{0.5}} + r \sin \theta \right\} \left(\frac{d^2 \theta}{dt^2} \right) + I_F \cos \alpha \left(\frac{d^2 \theta}{dt^2} \right) \\
 & = A_p (P_k - P_A) r \cos \gamma - m_p \cdot g \cdot r \cos \gamma - K_{DF} \frac{d\theta}{dt} \cos \alpha
 \end{aligned}$$

Equation 5.79

Rearranging equation 5.79 into separate terms in acceleration

$$\begin{aligned}
 & \left\{ m_p r \cos \gamma \left[\frac{r^2 (\sin \theta) (\cos \theta)}{(\ell^2 - (r \sin \theta)^2)^{0.5}} + r \sin \theta \right] + I_F \cos \alpha \right\} \left(\frac{d^2 \theta}{dt^2} \right) = \\
 & A_p (P_k - P_A) r \cos \gamma - m_p \cdot g \cdot r \cos \gamma - K_{DF} \frac{d\theta}{dt} \cos \alpha \\
 & - m_p r \cos \gamma \left\{ \frac{r^4 (\sin \theta)^2 (\cos \theta)^2}{(\ell^2 - (r \sin \theta)^2)^{1.5}} + \frac{r^2 ((\cos \theta)^2 - (\sin \theta)^2)}{(\ell^2 - (r \sin \theta)^2)^{0.5}} + r \cos \theta \right\} \left(\frac{d\theta}{dt} \right)^2
 \end{aligned}$$

Equation 5.80

Rewriting equation 5.80 gives

$$\begin{aligned}
 & \left\{ m_p r^3 \cos \gamma \frac{(\sin \theta) (\cos \theta)}{(\ell^2 - (r \sin \theta)^2)^{0.5}} + r^2 m_p \cos \gamma \sin \theta + I_F \cos \alpha \right\} \left(\frac{d^2 \theta}{dt^2} \right) = \\
 & - m_p r \cos \gamma \left\{ \frac{r^4 (\sin \theta)^2 (\cos \theta)^2}{(\ell^2 - (r \sin \theta)^2)^{1.5}} + \frac{r^2 ((\cos \theta)^2 - (\sin \theta)^2)}{(\ell^2 - (r \sin \theta)^2)^{0.5}} + r \cos \theta \right\} \left(\frac{d\theta}{dt} \right)^2 \\
 & + A_p (P_k - P_A) r \cos \gamma - m_p \cdot g \cdot r \cos \gamma - K_{DF} \cos \alpha \frac{d\theta}{dt}
 \end{aligned}$$

Equation 5.81

5.6 Analysis of the regenerator

The regenerator is arguably the major contribution to science that the Rev. Stirling [Stirling 1816] introduced. It defied analysis for many years, and now, even with advanced computational fluid dynamics (with programs such as FLUENT [NASA 2004]) the internal workings of the regenerator are still indeterminate. As such the regenerator is often treated as a 'black box' with many simplifying assumptions over the aerodynamic effects and screen orientation made.

The regenerator is complex, and the final design is a compromise of four conflicting requirements.

- To minimise temperature fluctuations within the matrix (thermal instability and loss of efficiency), the ratio of the heat capacity of the matrix to that of the working fluid should be minimised, suggesting a large low porosity matrix
- To reduce the pressure drop as the fluid passes through the matrix (pumping loss), fluid friction should be minimised, suggesting a small highly porous matrix
- The dead space within the matrix reduces the compression ratio (and by implication cycle power), suggesting a small dense matrix
- To improve heat transfer performance at low temperature differentials, the heat transfer area must be maximised, suggesting a large finely divided matrix

5.6.1 Simple regenerator

The regenerator is usually a series of mesh screens stacked one on top of the other. For the first analysis a single screen is employed as shown in figure 5.7 below. This screen forms a cell that completely fills the void length with the free flow cross sectional area defined by mesh geometry. Several simplifying assumptions made for the first model are detailed in the bullet points below.

- Each screen is thermally isolated from adjacent screens thus eliminating axial heat transfer by conduction
- The regenerator walls are perfect insulators
- Specific heat capacity of materials and fluid are constant across the operating range
- Inlet and outlet temperatures are uniform over the screen
- Material properties remain constant throughout the operating range

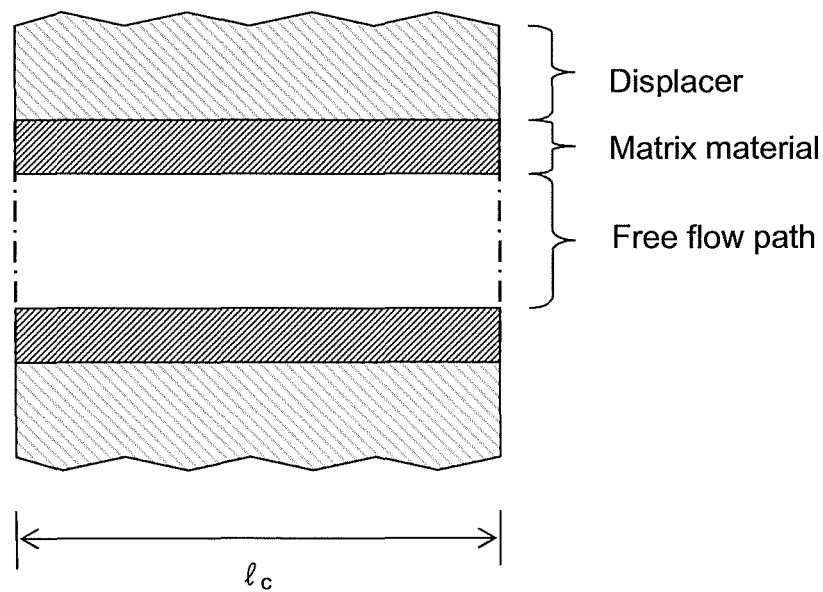


Figure 5.7 Simple one cell regenerator

For the flow through the cell

$$\Delta E_R = E_{IN} - E_{OUT} - E_{MATRIX} \quad \text{Equation 5.82}$$

$$E_R = C_V m_R \Delta T \quad \text{Equation 5.83}$$

Where, as before it was considered that

$$\frac{dE_R}{dt} = C_V \frac{dm_R}{dt} T_R + C_V m_R \frac{dT_R}{dt} \quad \text{Equation 5.84}$$

It should be remembered that, as the mass flow entering the regenerative space is equal to the mass flow leaving the regenerative space (conservation of mass and definition of a control volume), then the mass within the control volume will remain constant, nullifying the mass flow term of equation 5.84.

Hence

$$\frac{dE_R}{dt} = C_V m_R \frac{dT_R}{dt} \quad \text{Equation 5.85}$$

And, for the fluid

$$C_V m_R \frac{dT_R}{dt} = \dot{m}_R C_p (T_E - T_R) - K_{HR} (T_R - T_M) \quad \text{Equation 5.86}$$

For the matrix material

$$E_M = K_{HR} (T_R - T_M) \quad \text{Equation 5.87}$$

Which, when a similar process as above is applied and using an inequality statement as before, the conjugate action of the flow may be accounted for

$$\begin{aligned} & \text{for } P_E \geq P_K, \quad T_3 = (T_E - T_R) \\ & \text{else} \\ & \text{for } P_E < P_K, \quad T_3 = (T_R - T_K) \end{aligned} \quad \text{Equation 5.88}$$

Resulting in, for the flow

$$C_V m_R \frac{dT_R}{dt} = \dot{m}_R C_p (T_3) - K_{HR} (T_R - T_M) \quad \text{Equation 5.89}$$

And for the matrix

$$C_M m_M \frac{dT_m}{dt} = K_{HR} (T_R - T_M) \quad \text{Equation 5.90}$$

5.6.2 Multi cell regenerator

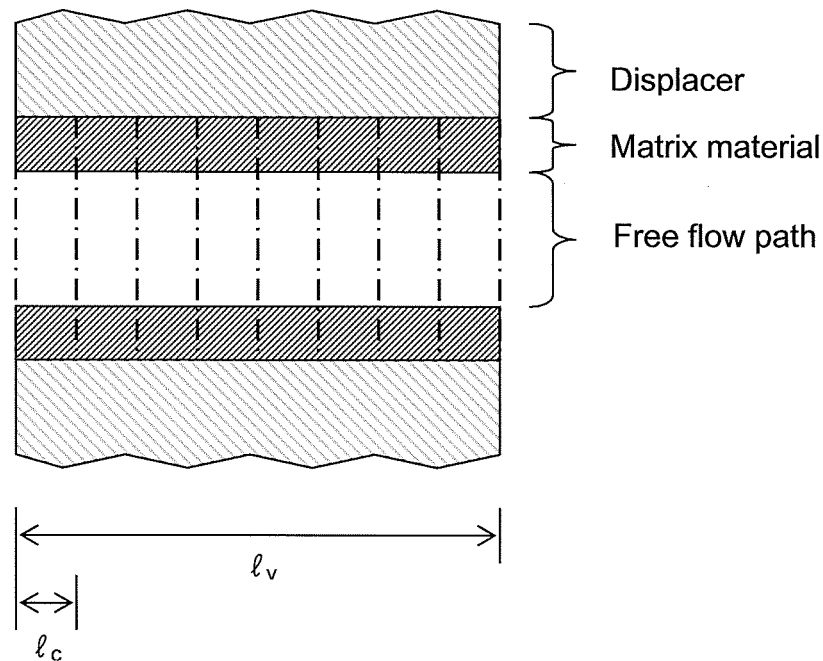


Figure 5.8 The multi cell regenerator

The analysis of the multi cell regenerator is similar to that of the single cell, with the inclusion of one more term in the flow equation.

This extra term accounts for the fact that the entry temperature for any cell is no longer the source (or sink on return blow) temperature, but the preceding cell exit temperature.

Special cases are the outer cells, which are in contact with the source (or sink). Following the same steps as outlined in section above two equations are formed, as given below.

The general case for a regenerator made of N cells (screens)

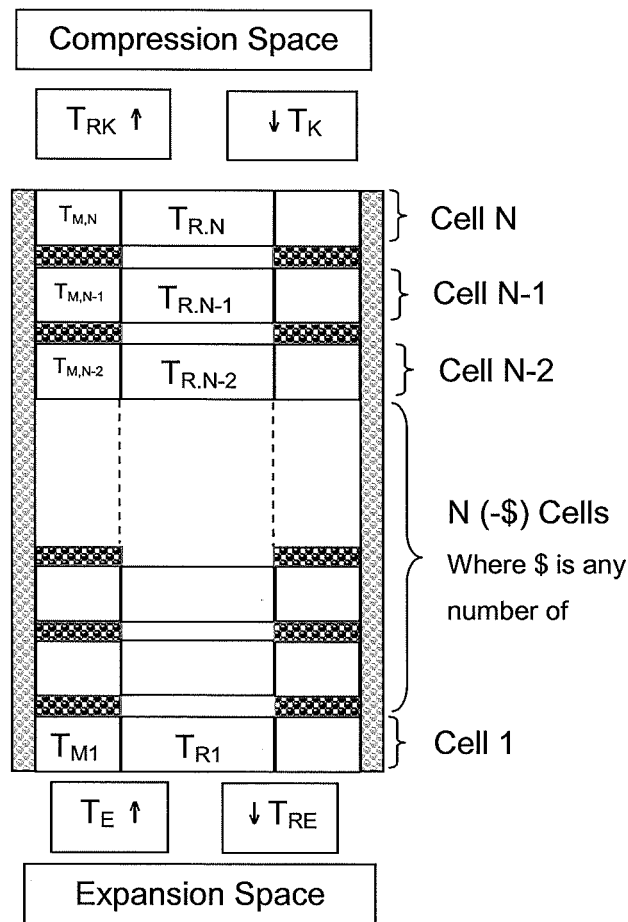


Figure 5.9 Regenerator of N cells

For $P_E \geq P_K$

Cell 1, next to the expansion space

$$\frac{dT_{R1}}{dt} = \frac{C_p \dot{m}_R}{C_v m_{RC}} (T_E - T_{R1}) - \frac{K_{HRM}}{C_v m_{RC}} (T_{R1} - T_{M1}) \tag{Equation 5.91}$$

$$\frac{T_{M1}}{dt} = \frac{K_{HRM}}{C_M m_{MC}} (T_{R1} - T_{M1}) \tag{Equation 5.92}$$

For cells 2 to N, where N is the total number of cells, and $l = 2$ to N, then the generic form may be written as

$$\frac{dT_{R,I}}{dt} = \frac{C_p \dot{m}_R}{C_v m_{RC}} (T_{R,I-1} - T_{R,I}) - \frac{K_{HRM}}{C_v m_{RC}} (T_{R,I} - T_{M,I})$$

Equation 5.93

$$\frac{T_{M,I}}{dt} = \frac{K_{HRM}}{C_M m_{MC}} (T_{R,I} - T_{M,I})$$

Equation 5.94

And for the last cell which bounds the compression space, $I=N$,

$$\frac{dT_{R,N}}{dt} = \frac{C_p \dot{m}_R}{C_v m_{RC}} (T_{R,N-1} - T_{R,N}) - \frac{K_{HRM}}{C_v m_{RC}} (T_{R,N} - T_{M,N})$$

Equation 5.95

$$\frac{T_{M,N}}{dt} = \frac{K_{HRM}}{C_M m_{MC}} (T_{R,N} - T_{M,N})$$

Equation 5.96

Remember that the temperature of the air in the last cell is also the temperature T_{RK} . Hence the last cell may be rewritten as:

$$\frac{dT_{RK}}{dt} = \frac{C_p \dot{m}_R}{C_v m_{RC}} (T_{R,N-1} - T_{RK}) - \frac{K_{HRM}}{C_v m_{RC}} (T_{R,N} - T_{M,N})$$

Equation 5.97

$$\frac{T_{M,N}}{dt} = \frac{K_{HRM}}{C_M m_{MC}} (T_{R,N} - T_{M,N})$$

Equation 5.98

For $P_E < P_K$, using a similar method to the one above

Cell 1 (adjacent to expansion chamber) where $T_{R1} = T_{RE}$

$$\frac{dT_{RE}}{dt} = \frac{C_p \dot{m}_R}{C_v m_{RC}} (T_{RE} - T_{R2}) - \frac{K_{HRM}}{C_v m_{RC}} (T_{RE} - T_{M1})$$

Equation 5.99

$$\frac{T_{M1}}{dt} = \frac{K_{HRM}}{C_M m_{MC}} (T_{RE} - T_{M1})$$

Equation 5.100

The general term becomes

$$\frac{dT_{R,I}}{dt} = \frac{C_p \dot{m}_R}{C_v m_{RC}} (T_{R,I} - T_{R,I+1}) - \frac{K_{HRM}}{C_v m_{RC}} (T_{R,I} - T_{M,I})$$

Equation 5.101

$$\frac{T_{M,I}}{dt} = \frac{K_{HRM}}{C_M m_{MC}} (T_{R,I} - T_{M,I})$$

Equation 5.102

Cell N becomes

$$\frac{dT_{R,N}}{dt} = \frac{C_p \dot{m}_R}{C_v m_{RC}} (T_{R,N} - T_K) - \frac{K_{HRM}}{C_v m_{RC}} (T_{R,N} - T_{M,N})$$

Equation 5.103

$$\frac{T_{M,N}}{dt} = \frac{K_{HRM}}{C_M m_{MC}} (T_{R,N} - T_{M,N})$$

Equation 5.104

5.7 Summary of governing equations

Expansion space

$$\dot{m}_R = K_{MR} (P_E - P_K)$$

(copy of equation 5.1)

$$\frac{dm_E}{dt} = -\dot{m}_R$$

(copy of equation 5.3)

$$C_v m_E \frac{dT_E}{dt} = K_{HH} (T_H - T_E) - P_E A_D \frac{dx_D}{dt} + C_v \dot{m}_R (T_E - T_1^*) - R \dot{m}_R T_1^*$$

(copy of equation 5.18)

$$P_E = \frac{m_E R T_E}{A_D (x_D - 0.5h_D)} \quad (\text{copy of equation 5.21})$$

Compression space

$$\dot{m}_A = K_{MA} (P_A - P_K) \quad (\text{copy of equation 5.23})$$

$$\frac{dm_K}{dt} = \dot{m}_R + \dot{m}_A \quad (\text{positive as mass is entering}) \quad (\text{copy of equation 5.24})$$

$$\begin{aligned} C_V m_K \frac{dT_K}{dt} = & -K_{HC} (T_K - T_C) + P_K (A_D - A_{DR}) \frac{dx_D}{dt} \\ & - P_K A_P \left[\frac{r^2 \sin \theta \cos \theta}{(\ell^2 - r^2 (\sin \theta)^2)^{0.5}} + r \sin \theta \right] \cdot \frac{d\theta}{dt} \\ & + C_V \dot{m}_R (T_2^* - T_K) + R \dot{m}_R T_2^* + C_V \dot{m}_A (T_3^* - T_K) + R \dot{m}_A T_3^* \end{aligned} \quad (\text{copy of equation 5.36})$$

$$P_K = \frac{m_k R T_K}{(A_D - A_{DR})(h_C - 0.5h_D - x_D) + A_P (x_P - 0.5h_P)} \quad (\text{copy of equation 5.37})$$

Displacer

$$m_D \ddot{x}_D = A_D (P_E - P_K) - m_D g + A_{DR} (P_K - P_A) + F_{DA} \quad (\text{copy of equation 5.46})$$

$$\begin{aligned} \text{for } 0.5h_D < x_D < h_{SE} + 0.5h_D & \quad \text{then } F_{DA} = F_{DE} = K_{SE} (h_{SE} + 0.5h_D - x_D) \\ \text{for } h_{SE} + 0.5h_D \leq x_D \leq h_C - h_{SK} - 0.5h_D & \quad \text{then } F_{DA} = 0 \\ \text{for } h_C - h_{SK} - 0.5h_D < x_D < h_C - 0.5h_D & \quad \text{then } F_{DA} = F_{DK} = K_{SK} (h_C - h_{SK} - 0.5h_D - x_D) \end{aligned} \quad (\text{copy of equation 5.44})$$

Piston / flywheel assembly

$$\sin \alpha = \frac{r}{\ell} \sin \theta \quad (\text{copy of equation 5.53})$$

$$\cos \gamma = \sin(\alpha + \theta) \quad (\text{copy of equation 5.69})$$

$$x_p = x_T - \ell \left(1 - \left(\frac{r}{\ell} \right)^2 \sin^2 \theta \right)^{\frac{1}{2}} - r \cos \theta \quad (\text{copy of equation 5.60})$$

$$m_p \ddot{x}_p = A_p (P_k - P_A) - m_p \cdot g - F_p \cos \alpha \quad (\text{copy of equation 5.62})$$

$$\begin{aligned} & \left\{ m_p r^3 \cos \gamma \frac{(\sin \theta)(\cos \theta)}{(\ell^2 - (r \sin \theta)^2)^{0.5}} + r^2 m_p \cos \gamma \sin \theta + I_F \cos \alpha \right\} \left(\frac{d^2 \theta}{dt^2} \right) = \\ & - m_p r \cos \gamma \left\{ \frac{r^4 (\sin \theta)^2 (\cos \theta)^2}{(\ell^2 - (r \sin \theta)^2)^{1.5}} + \frac{r^2 ((\cos \theta)^2 - (\sin \theta)^2)}{(\ell^2 - (r \sin \theta)^2)^{0.5}} + r \cos \theta \right\} \left(\frac{d\theta}{dt} \right)^2 \\ & + A_p (P_k - P_A) r \cos \gamma - m_p \cdot g \cdot r \cos \gamma - K_{DF} \cos \alpha \frac{d\theta}{dt} \end{aligned} \quad (\text{copy of equation 5.81})$$

Regenerator

$$C_V m_R \frac{dT_R}{dt} = \dot{m}_R C_p (T_3) - K_{HR} (T_R - T_M) \quad (\text{copy of equation 5.89})$$

$$C_M m_M \frac{dT_M}{dt} = K_{HR} (T_R - T_M) \quad (\text{copy of equation 5.90})$$

5.8 Numerical techniques

In the previous section the equations required to describe the engine processes were developed.

These equations are discretised using the following approximations.

$$\frac{dx}{dt} = \frac{x_{t+\Delta t} - x_t}{\Delta t} \quad \text{Equation 5.105}$$

And

$$\frac{d^2x}{dt^2} = \frac{x_{t+2\Delta t} - 2x_{t+\Delta t} + x_t}{\Delta t^2} \quad \text{Equation 5.106}$$

5.8.1 Flywheel location

Auxiliary angles

$$\sin \alpha = \frac{r}{\ell} \sin \theta \quad \text{Equation 5.107}$$

$$\alpha = \arcsin\left(\frac{r}{\ell} \sin \theta\right) \quad \text{Equation 5.108}$$

$$\cos \gamma = \sin(\alpha + \theta) \quad \text{Equation 5.109}$$

$$\gamma = \arccos(\sin(\alpha + \theta)) \quad \text{Equation 5.110}$$

$$\begin{aligned} & \left\{ m_p r^3 \cos \gamma \frac{(\sin \theta)(\cos \theta)}{(\ell^2 - (r \sin \theta)^2)^{0.5}} + r^2 m_p \cos \gamma \sin \theta + I_F \cos \alpha \right\} \left(\frac{d^2 \theta}{dt^2} \right) = \\ & - m_p r \cos \gamma \left\{ \frac{r^4 (\sin \theta)^2 (\cos \theta)^2}{(\ell^2 - (r \sin \theta)^2)^{1.5}} + \frac{r^2 ((\cos \theta)^2 - (\sin \theta)^2)}{(\ell^2 - (r \sin \theta)^2)^{0.5}} + r \cos \theta \right\} \left(\frac{d\theta}{dt} \right)^2 \\ & - K_{DF} \cos \alpha \frac{d\theta}{dt} + A_p (P_k - P_A) r \cos \gamma - m_p \cdot g \cdot r \cos \gamma \end{aligned} \quad \text{Equation 5.111}$$

Let

$$A = m_p r^3 \cos \gamma \frac{(\sin \theta)(\cos \theta)}{(\ell^2 - (r \sin \theta)^2)^{0.5}} + r^2 m_p \cos \gamma \sin \theta + I_F \cos \alpha \quad \text{Equation 5.112}$$

$$B = -m_p r \cos \gamma \left\{ \frac{r^4 (\sin \theta)^2 (\cos \theta)^2}{(\ell^2 - (r \sin \theta)^2)^{1.5}} + \frac{r^2 ((\cos \theta)^2 - (\sin \theta)^2)}{(\ell^2 - (r \sin \theta)^2)^{0.5}} + r \cos \theta \right\} \quad \text{Equation 5.113}$$

$$C = -K_{DF} \cos \alpha \quad \text{Equation 5.114}$$

$$D = +A_p (P_k - P_A) r \cos \gamma - m_p \cdot g \cdot r \cos \gamma \quad \text{Equation 5.115}$$

Simplifying the expression to

$$A \frac{d^2 \theta}{dt^2} = B \left(\frac{d\theta}{dt} \right)^2 + C \frac{d\theta}{dt} + D \quad \text{Equation 5.116}$$

Expanding the differential terms for small changes

$$\frac{\theta_{(t+2\Delta t)} - 2\theta_{(t+\Delta t)} + \theta_{(t)}}{\Delta t^2} A = \left(\frac{\theta_{(t+\Delta t)} + \theta_{(t)}}{\Delta t} \right)^2 B + \frac{\theta_{(t+\Delta t)} + \theta_{(t)}}{\Delta t} C + D \quad \text{Equation 5.117}$$

And dividing through by A

$$\frac{\theta_{(t+2\Delta t)} - 2\theta_{(t+\Delta t)} + \theta_{(t)}}{\Delta t^2} = \left(\frac{\theta_{(t+\Delta t)} + \theta_{(t)}}{\Delta t} \right)^2 \frac{B}{A} + \frac{\theta_{(t+\Delta t)} + \theta_{(t)}}{\Delta t} \frac{C}{A} + \frac{D}{A} \quad \text{Equation 5.118}$$

Multiplying by Δt^2

$$\theta_{(t+2\Delta t)} - 2\theta_{(t+\Delta t)} + \theta_{(t)} = (\theta_{(t+\Delta t)} + \theta_{(t)})^2 \frac{B}{A} + (\theta_{(t+\Delta t)} + \theta_{(t)})\Delta t \frac{C}{A} + \frac{D}{A} \Delta t^2$$

Equation 5.119

 Making $\theta_{t+2\Delta t}$ the subject

$$\theta_{(t+2\Delta t)} = 2\theta_{(t+\Delta t)} - \theta_{(t)} + (\theta_{(t+\Delta t)} + \theta_{(t)})^2 \frac{B}{A} + (\theta_{(t+\Delta t)} + \theta_{(t)})\Delta t \frac{C}{A} + \frac{D}{A} \Delta t^2$$

Equation 5.120

Rewriting with identities inserted

$$\theta_{(t+2\Delta t)} = 2\theta_{(t+\Delta t)} - \theta_{(t)}$$

$$\begin{aligned} & - \left[\frac{m_p r \cos \gamma \left\{ \frac{r^4 (\sin \theta)^2 (\cos \theta)^2}{(\ell^2 - (r \sin \theta)^2)^{1.5}} + \frac{r^2 ((\cos \theta)^2 - (\sin \theta)^2)}{(\ell^2 - (r \sin \theta)^2)^{0.5}} + r \cos \theta \right\}}{m_p r^3 \cos \gamma \frac{(\sin \theta)(\cos \theta)}{(\ell^2 - (r \sin \theta)^2)^{0.5}} + r^2 m_p \cos \gamma \sin \theta + I_F \cos \alpha} \right] (\theta_{(t+\Delta t)} + \theta_{(t)})^2 \\ & - \left[\frac{K_{DF} \cos \alpha \frac{d\theta}{dt}}{m_p r^3 \cos \gamma \frac{(\sin \theta)(\cos \theta)}{(\ell^2 - (r \sin \theta)^2)^{0.5}} + r^2 m_p \cos \gamma \sin \theta + I_F \cos \alpha} \right] (\theta_{(t+\Delta t)} + \theta_{(t)}) \Delta t \\ & + \left[\frac{A_p (P_k - P_A) r \cos \gamma - m_p \cdot g \cdot r \cos \gamma}{m_p r^3 \cos \gamma \frac{(\sin \theta)(\cos \theta)}{(\ell^2 - (r \sin \theta)^2)^{0.5}} + r^2 m_p \cos \gamma \sin \theta + I_F \cos \alpha} \right] \Delta t^2 \end{aligned}$$

Equation 5.121

5.8.2 Piston location

$$x_p = x_T - (\ell^2 - r^2 \sin^2 \theta)^{0.5} - r \cos \theta \quad \text{Equation 5.122}$$

5.8.3 Displacer location

$$m_D \ddot{x}_D = A_D (P_E - P_K) - m_D g + A_{DR} (P_K - P_A) + F_{DA} \quad \text{Equation 5.123}$$

$$\frac{d^2 x_D}{dt^2} = \frac{1}{m_D} (A_D (P_E - P_K) - m_D g + A_{DR} (P_K - P_A) + F_{DA}) \quad \text{Equation 5.124}$$

$$\frac{x_{D,(t+2\Delta t)} - 2x_{D,(t+\Delta t)} + x_{D,(t)}}{\Delta t} = \frac{1}{m_D} [A_D (P_E - P_K) - m_D g + A_{DR} (P_K - P_A) + F_{DA}] \quad \text{Equation 5.125}$$

$$x_{D,(t+2\Delta t)} = 2x_{D,(t+\Delta t)} - x_{D,(t)} + \frac{\Delta t}{m_D} [A_D (P_E - P_K) - m_D g + A_{DR} (P_K - P_A) + F_{DA}] \quad \text{Equation 5.126}$$

Where the inequality for the spring forces may be declared by

$$\begin{aligned} \text{for } 0.5h_D < x_D < h_{SE} + 0.5h_D & \quad \text{then } F_{DA} = F_{DE} = K_{SE} (h_{SE} + 0.5h_D - x_D) \\ \text{for } h_{SE} + 0.5h_D \leq x_D \leq h_C - h_{SK} - 0.5h_D & \quad \text{then } F_{DA} = 0 \\ \text{for } h_C - h_{SK} - 0.5h_D < x_D < h_C - 0.5h_D & \quad \text{then } F_{DA} = F_{DK} = K_{SK} (h_C - h_{SK} - 0.5h_D - x_D) \end{aligned}$$

$$\quad \text{Equation 5.127}$$

And bounded by upper and lower limits of

$$h_C - 0.5h_D \geq x_D \geq 0.5h_D \quad \text{Equation 5.128}$$

5.8.4 Compression space temperature

$$\begin{aligned}
 C_V m_K \frac{dT_K}{dt} = & -K_{HC}(T_K - T_C) + P_K(A_D - A_{DR}) \frac{dx_D}{dt} \\
 & - P_K A_P \left[\frac{r^2 \sin \theta \cos \theta}{(\ell^2 - r^2 (\sin \theta)^2)^{0.5}} + r \sin \theta \right] \cdot \frac{d\theta}{dt} \\
 & + C_V \dot{m}_R (T_2^* - T_K) + R \dot{m}_R T_2^* + C_V \dot{m}_A (T_3^* - T_K) + R \dot{m}_A T_3^*
 \end{aligned}$$

Equation 5.129

$$\begin{aligned}
 \frac{dT_K}{dt} = & -\frac{K_{HC}}{C_V m_K} (T_K - T_C) + \frac{P_K}{C_V m_K} (A_D - A_{DR}) \frac{dx_D}{dt} \\
 & - \frac{P_K A_P}{C_V m_K} \left[\frac{r^2 \sin \theta \cos \theta}{(\ell^2 - (r \sin \theta)^2)^{0.5}} + r \sin \theta \right] \cdot \frac{d\theta}{dt} \\
 & + \frac{C_V \dot{m}_R}{C_V m_K} (T_2^* - T_K) + \frac{R \dot{m}_R}{C_V m_K} T_2^* + \frac{C_V \dot{m}_A}{C_V m_K} (T_3^* - T_K) + \frac{R \dot{m}_A}{C_V m_K} T_3^*
 \end{aligned}$$

Equation 5.130

$$\begin{aligned}
 \frac{dT_K}{dt} = & -\frac{K_{HC}}{C_V m_K} (T_K - T_C) + \frac{P_K}{C_V m_K} (A_D - A_{DR}) \frac{dx_D}{dt} \\
 & - \frac{P_K A_P}{C_V m_K} \left[\frac{r^2 \sin \theta \cos \theta}{(\ell^2 - (r \sin \theta)^2)^{0.5}} + r \sin \theta \right] \cdot \frac{d\theta}{dt} \\
 & + \frac{C_V \dot{m}_R}{C_V m_K} (T_2^* - T_K) + \frac{R \dot{m}_R}{C_V m_K} T_2^* + \frac{C_V \dot{m}_A}{C_V m_K} (T_3^* - T_K) + \frac{R \dot{m}_A}{C_V m_K} T_3^*
 \end{aligned}$$

Equation 5.131

$$\begin{aligned}
 \frac{T_{K,(t+\Delta t)} - T_{K,(t)}}{\Delta t} = & -\frac{K_{HC}}{C_V m_K} (T_K - T_C) + \frac{P_K}{C_V m_K} (A_D - A_{DR}) \frac{(x_{D,(t+\Delta t)} - x_{D,(t)})}{\Delta t} \\
 & - \frac{P_K A_P}{C_V m_K} \left[\frac{r^2 \sin \theta \cos \theta}{(\ell^2 - (r \sin \theta)^2)^{0.5}} + r \sin \theta \right] \frac{(\theta_{(t+\Delta t)} - \theta_{(t)})}{\Delta t} \\
 & + \frac{C_V \dot{m}_R}{C_V m_K} (T_2^* - T_K) + \frac{R \dot{m}_R}{C_V m_K} T_2^* + \frac{C_V \dot{m}_A}{C_V m_K} (T_3^* - T_K) + \frac{R \dot{m}_A}{C_V m_K} T_3^*
 \end{aligned}$$

Equation 5.132

$$\begin{aligned}
 T_{K,(t+\Delta t)} = & T_{K,(t)} - \frac{K_{HC} \Delta t}{C_V m_K} (T_K - T_C) + \frac{P_K}{C_V m_K} (A_D - A_{DR}) (x_{D,(t+\Delta t)} - x_{D,(t)}) \\
 & - \frac{P_K A_P}{C_V m_K} \left[\frac{r^2 \sin \theta \cos \theta}{(\ell^2 - (r \sin \theta)^2)^{0.5}} + r \sin \theta \right] (\theta_{(t+\Delta t)} - \theta_{(t)}) \\
 & + \frac{\dot{m}_R \Delta t}{m_K} (T_2^* - T_K) + \frac{R \dot{m}_R \Delta t}{C_V m_K} T_2^* + \frac{\dot{m}_A \Delta t}{m_K} (T_3^* - T_K) + \frac{R \dot{m}_A \Delta t}{C_V m_K} T_3^*
 \end{aligned}$$

Equation 5.133

$$\begin{aligned}
 T_{K,(t+\Delta t)} = & T_{K,(t)} \left(1 - \frac{K_{HC} \Delta t}{C_V m_K} - \frac{\dot{m}_R \Delta t}{m_K} - \frac{\dot{m}_A \Delta t}{m_K} \right) + T_C \left(\frac{K_{HC} \Delta t}{C_V m_K} \right) \\
 & + T_2^* \left(\frac{\dot{m}_R \Delta t}{m_K} + \frac{R \dot{m}_R \Delta t}{C_V m_K} \right) + T_3^* \left(\frac{R \dot{m}_A \Delta t}{C_V m_K} - \frac{\dot{m}_A \Delta t}{m_K} \right) \\
 & + \frac{P_K}{C_V m_K} (A_D - A_{DR}) (x_{D,(t+\Delta t)} - x_{D,(t)}) \\
 & - \frac{P_K A_P}{C_V m_K} \left[\frac{r^2 \sin \theta \cos \theta}{(\ell^2 - (r \sin \theta)^2)^{0.5}} + r \sin \theta \right] (\theta_{(t+\Delta t)} - \theta_{(t)})
 \end{aligned}$$

Equation 5.134

Where

$$\dot{m}_A = \dot{m}_{MP} + \dot{m}_{MD}$$

Equation 5.135

and if

$$\begin{aligned}
 P_E > P_K \text{ and } \dot{m}_R > 0 \text{ then } T_2^* &= T_{RK} \\
 P_E < P_K \text{ and } \dot{m}_R < 0 \text{ then } T_2^* &= T_K \\
 P_A < P_K \text{ and } \dot{m}_A < 0 \text{ then } T_3^* &= T_K \\
 P_A > P_K \text{ and } \dot{m}_A > 0 \text{ then } T_3^* &= T_A
 \end{aligned}$$

Equation 5.136

5.8.5 Mass flow for compression space

$$\frac{dm_E}{dt} = -\dot{m}_R \quad \text{Equation 5.137}$$

$$m_{E,(t+\Delta t)} = m_{E(t)} - \dot{m}_R \Delta t \quad \text{Equation 5.138}$$

$$\dot{m}_R = K_{MR}(P_E - P_K) \quad \text{Equation 5.139}$$

5.8.6 Expansion space temperature

$$C_V m_E \frac{dT_E}{dt} = K_{HH}(T_H - T_E) - P_E A_D \frac{dx_D}{dt} + C_V \dot{m}_R (T_E - T_1^*) - R \dot{m}_R T_1^* \quad \text{Equation 5.140}$$

$$\frac{dT_E}{dt} = \frac{1}{C_V m_E} \left[K_{HH}(T_H - T_E) - P_E A_D \frac{dx_D}{dt} + C_V \dot{m}_R (T_E - T_1^*) - R \dot{m}_R T_1^* \right] \quad \text{Equation 5.141}$$

$$\frac{T_{E,(t+\Delta t)} - T_{E,(t)}}{\Delta t} = \frac{1}{C_V m_E} \left[K_{HH}(T_H - T_{E,(t)}) - P_E A_D \frac{x_{D,(t+\Delta t)} - x_{D,(t)}}{\Delta t} + C_V \dot{m}_R (T_{E,(t)} - T_1^*) - R \dot{m}_R T_1^* \right] \quad \text{Equation 5.142}$$

$$T_{E,(t+\Delta t)} = T_{E,(t)} + \frac{\Delta t}{C_V m_E} \left[K_{HH}(T_H - T_{E,(t)}) - P_E A_D \frac{x_{D,(t+\Delta t)} - x_{D,(t)}}{\Delta t} + C_V \dot{m}_R (T_{E,(t)} - T_1^*) - R \dot{m}_R T_1^* \right] \quad \text{Equation 5.143}$$

$$T_{E,(t+\Delta t)} = T_{E,(t)} + \frac{\Delta t K_{HH}}{C_V m_E} (T_H - T_{E,(t)}) - \frac{P_E A_D}{C_V m_E} (x_{D,(t+\Delta t)} - x_{D,(t)}) + \frac{\dot{m}_R \Delta t}{m_E} (T_{E,(t)} - T_1^*) - \frac{R \dot{m}_R \Delta t}{C_V m_E} T_1^*$$

Equation 5.144

$$T_{E,(t+\Delta t)} = T_{E,(t)} \left(1 - \frac{\Delta t K_{HH}}{C_V m_E} + \frac{\dot{m}_R \Delta t}{m_E} \right) + T_H \frac{\Delta t K_{HH}}{C_V m_E} - T_1^* \left(\frac{\dot{m}_R \Delta t}{m_E} + \frac{R \dot{m}_R \Delta t}{C_V m_E} \right) - \frac{P_E A_D}{C_V m_E} (x_{D,(t+\Delta t)} - x_{D,(t)})$$

Equation 5.145

Where

$$\text{If } P_E > P_K \text{ then } T_1^* = T_E$$

$$\text{If } P_E < P_K \text{ then } T_1^* = T_{RE}$$

Equation 5.146

5.8.7 Mass flow for expansion space

$$\frac{dm_K}{dt} = \dot{m}_R + \dot{m}_A$$

Equation 5.147

$$\frac{m_{K,(t+\Delta t)} - m_{K,(t)}}{\Delta t} = \dot{m}_R + \dot{m}_A$$

Equation 5.148

$$m_{K,(t+\Delta t)} = m_{K,(t)} + (\dot{m}_R + \dot{m}_A) \Delta t$$

Equation 5.149

$$\dot{m}_A = K_{MA} (P_A - P_K)$$

Equation 5.150

5.8.8 Compression space pressure

$$P_K = \frac{m_k RT_K}{(A_D - A_{DR})(h_C - 0.5h_D - x_D) + A_P(x_P - 0.5h_P)}$$

Equation 5.151

5.8.9 Compression space mass

$$m_k = \frac{P_K (A_D - A_{DR})(h_C - 0.5h_D - x_D) + A_P(x_P - 0.5h_P)}{RT_K}$$

Equation 5.152

5.8.10 Expansion space pressure

$$P_E = \frac{m_E RT_E}{A_D(x_D - 0.5h_D)}$$

Equation 5.153

5.8.11 Expansion space mass

$$m_E = \frac{P_E A_D (x_D - 0.5h_D)}{RT_E}$$

Equation 5.154

5.8.12 Regenerator

For $P_E > P_K$

Cell 1, fluid in regenerator

$$\frac{dT_{R1}}{dt} = \frac{C_p \dot{m}_R}{C_v m_{RC}} (T_E - T_{R1}) - \frac{K_{HRM}}{C_v m_{RC}} (T_{R1} - T_{M1})$$

Equation 5.155

$$\frac{T_{R1(t+\Delta t)} - T_{R1(t)}}{\Delta t} = \frac{C_p \dot{m}_R}{C_v m_{RC}} (T_{E(t)} - T_{R1(t)}) - \frac{K_{HRM}}{C_v m_{RC}} (T_{R1(t)} - T_{M1(t)})$$

Equation 5.156

$$T_{R1(t+\Delta t)} = T_{R1(t)} + \frac{C_p \dot{m}_R \Delta t}{C_v m_{RC}} (T_{E(t)} - T_{R1(t)}) - \frac{K_{HRM} \Delta t}{C_v m_{RC}} (T_{R1(t)} - T_{M1(t)})$$

Equation 5.157

$$T_{R1(t+\Delta t)} = T_{R1(t)} \left(1 - \frac{C_p \dot{m}_R \Delta t}{C_v m_{RC}} - \frac{K_{HRM} \Delta t}{C_v m_{RC}} \right) + T_{E(t)} \frac{C_p \dot{m}_R \Delta t}{C_v m_{RC}} + T_{M1(t)} \frac{K_{HRM} \Delta t}{C_v m_{RC}}$$

Equation 5.158

$$T_{R1(t+\Delta t)} = T_{R1(t)} \left(1 - \frac{(C_v + R) \dot{m}_R \Delta t}{C_v m_{RC}} - \frac{K_{HRM} \Delta t}{C_v m_{RC}} \right) + T_{E(t)} \frac{(C_v + R) \dot{m}_R \Delta t}{C_v m_{RC}} + T_{M1(t)} \frac{K_{HRM} \Delta t}{C_v m_{RC}}$$

Equation 5.159

Cell 1, matrix material

$$\frac{dT_{M1}}{dt} = \frac{K_{HRM}}{C_M m_{MC}} (T_{R1} - T_{M1})$$

Equation 5.160

$$\frac{T_{M1(t+\Delta t)} - T_{M1(t)}}{\Delta t} = \frac{K_{HRM}}{C_M m_{MC}} (T_{R1} - T_{M1})$$

Equation 5.161

$$T_{M1(t+\Delta t)} = T_{M1(t)} + \frac{K_{HRM} \Delta t}{C_M m_{MC}} (T_{R1(t)} - T_{M1(t)})$$

Equation 5.162

$$T_{M1(t+\Delta t)} = T_{M1(t)} \left(1 - \frac{K_{HRM} \Delta t}{C_M m_{MC}} \right) + T_{R1(t)} \frac{K_{HRM} \Delta t}{C_M m_{MC}}$$

Equation 5.163

General term for cells J to N, where J = 2 to N

$$\frac{dT_{R,J}}{dt} = \frac{C_p \dot{m}_R}{C_v m_{RC}} (T_{R,J-1} - T_{R,J}) - \frac{K_{HRM}}{C_v m_{RC}} (T_{R,J} - T_{M,J})$$

Equation 5.164

$$\frac{T_{R,J(t+\Delta t)} - T_{R,J(t)}}{\Delta t} = \frac{C_p \dot{m}_R}{C_v m_{RC}} (T_{R,J-1} - T_{R,J}) - \frac{K_{HRM}}{C_v m_{RC}} (T_{R,J} - T_{M,J})$$

Equation 5.165

$$T_{R,J(t+\Delta t)} = T_{R,J(t)} + \frac{C_p \dot{m}_R \Delta t}{C_v m_{RC}} (T_{R,J-1} - T_{R,J}) - \frac{K_{HRM} \Delta t}{C_v m_{RC}} (T_{R,J} - T_{M,J})$$

Equation 5.166

$$T_{R,J(t+\Delta t)} = T_{R,J(t)} \left(1 - \frac{(C_v + R) \dot{m}_R \Delta t}{C_v m_{RC}} - \frac{K_{HRM} \Delta t}{C_v m_{RC}} \right) + T_{R,J-1(t)} \frac{(C_v + R) \dot{m}_R \Delta t}{C_v m_{RC}} - T_{M,J(t)} \frac{K_{HRM} \Delta t}{C_v m_{RC}}$$

Equation 5.167

General term for matrices J to N, where J = 2 to N

$$\frac{dT_{M,J}}{dt} = \frac{K_{HRM}}{C_M m_{MC}} (T_{R,J} - T_{M,J})$$

Equation 5.168

$$T_{M,J(t+\Delta t)} = T_{M,J(t)} \left(1 - \frac{K_{HRM} \Delta t}{C_M m_{MC}} \right) + T_{R,J(t)} \frac{K_{HRM} \Delta t}{C_M m_{MC}}$$

Equation 5.169

For $P_E < P_K$ (conjugate flow)

Fluid now enters from the compression space into the first (also the Nth cell) at T_K , the temperature of the fluid in the cell and the matrix have been calculated previously (on first blow set to $T_{ambient}$)

Cell N, fluid in regenerator

$$\frac{dT_{RN}}{dt} = \frac{C_p \dot{m}_R}{C_v m_{RC}} (T_K - T_{R,N(t)}) - \frac{K_{HRM}}{C_v m_{RC}} (T_{R,N(t)} - T_{M,N(t)})$$

Equation 5.170

$$\frac{T_{R,N(t+\Delta t)} - T_{R,N(t)}}{\Delta t} = \frac{C_p \dot{m}_R}{C_v m_{RC}} (T_{K(t)} - T_{R,N(t)}) - \frac{K_{HRM}}{C_v m_{RC}} (T_{R,N(t)} - T_{M,N(t)})$$

Equation 5.171

$$T_{R,N(t+\Delta t)} = T_{R,N(t)} \frac{C_p \dot{m}_R \Delta t}{C_v m_{RC}} (T_{K(t)} - T_{R,N(t)}) - \frac{K_{HRM} \Delta t}{C_v m_{RC}} (T_{R,N(t)} - T_{M,N(t)})$$

Equation 5.172

$$T_{R,N(t+\Delta t)} = T_{R,N(t)} \left(1 - \frac{(C_v + R) \dot{m}_R \Delta t}{C_v m_{RC}} - \frac{K_{HRM} \Delta t}{C_v m_{RC}} \right) + T_{K(t)} \frac{(C_v + R) \dot{m}_R \Delta t}{C_v m_{RC}} + T_{M,N(t)} \frac{K_{HRM} \Delta t}{C_v m_{RC}}$$

Equation 5.173

More generally for cells N-1 to 1, for J=N-1 to 1

$$\frac{dT_{R,J}}{dt} = \frac{C_p \dot{m}_R}{C_v m_{RC}} (T_{R,J+1} - T_{R,J}) - \frac{K_{HRM}}{C_v m_{RC}} (T_{R,J} - T_{M,J})$$

Equation 5.174

$$\frac{T_{R,J(t+\Delta t)} - T_{R,J(t)}}{\Delta t} = \frac{C_p \dot{m}_R}{C_v m_{RC}} (T_{R,J+1(t)} - T_{R,J(t)}) - \frac{K_{HRM}}{C_v m_{RC}} (T_{R,J(t)} - T_{M,J(t)})$$

Equation 5.175

$$T_{R,J(t+\Delta t)} = T_{R,J(t)} + \frac{C_p \dot{m}_R \Delta t}{C_v m_{RC}} (T_{R,J+1} - T_{R,J}) - \frac{K_{HRM} \Delta t}{C_v m_{RC}} (T_{R,J} - T_{M,J})$$

Equation 5.176

$$T_{R,J(t+\Delta t)} = T_{R,J(t)} \left(1 - \frac{C_p \dot{m}_R \Delta t}{C_v m_{RC}} - \frac{K_{HRM} \Delta t}{C_v m_{RC}} \right) + T_{R,J+1(t)} \frac{C_p \dot{m}_R \Delta t}{C_v m_{RC}} - T_{M,J(t)} \frac{K_{HRM} \Delta t}{C_v m_{RC}}$$

Equation 5.177

$$T_{R,J(t+\Delta t)} = T_{R,J(t)} \left(1 - \frac{(C_v + R)\dot{m}_R \Delta t}{C_v m_{RC}} - \frac{K_{HRM} \Delta t}{C_v m_{RC}} \right) + T_{R,J+1(t)} \frac{(C_v + R)\dot{m}_R \Delta t}{C_v m_{RC}} - T_{M,J(t)} \frac{K_{HRM} \Delta t}{C_v m_{RC}}$$

Equation 5.178

Cell N, matrix material

$$\frac{T_{M,N}}{dt} = \frac{K_{HRM}}{C_M m_{MC}} (T_{R,N} - T_{M,N})$$

Equation 5.179

$$\frac{T_{M,N(t+\Delta t)} - T_{M,N(t)}}{\Delta t} = \frac{K_{HRM}}{C_M m_{MC}} (T_{R,N} - T_{M,N})$$

Equation 5.180

$$T_{M,N(t+\Delta t)} = T_{M,N(t)} + \frac{K_{HRM} \Delta t}{C_M m_{MC}} (T_{R,N(t)} - T_{M,N(t)})$$

Equation 5.181

$$T_{M,N(t+\Delta t)} = T_{M,N(t)} \left(1 - \frac{K_{HRM} \Delta t}{C_M m_{MC}} \right) + T_{R,N(t)} \frac{K_{HRM} \Delta t}{C_M m_{MC}}$$

Equation 5.182

General term for matrices N-1 to 1, where J = N-1 to 1

$$\frac{T_{M,J}}{dt} = \frac{K_{HRM}}{C_M m_{MC}} (T_{R,J} - T_{M,J})$$

Equation 5.183

$$T_{M,J(t+\Delta t)} = T_{M,J(t)} \left(1 - \frac{K_{HRM} \Delta t}{C_M m_{MC}} \right) + T_{R,J(t)} \frac{K_{HRM} \Delta t}{C_M m_{MC}}$$

Equation 5.184

5.9 Preparation of data for the program

Thus far a third order analysis has been applied to the Ringbom Stirling engine. The use of numerical techniques has produced a series of equations ready for encoding. The order in which these equations are applied will now be discussed.

The program is divided into six discrete parts, but has been written as one program rather than subroutines or modules. These parts are:

- Declaring variable names with kind parameters
- Initialise variables by allocating values
- Initial calculations for engine geometry and start up values ($t = 0$)
- Calculations for the first time step ($t = \Delta t$)
- Calculations for the second time step ($t = t + \Delta t$)
- Third and subsequent time step calculations

The programming language chosen has changed as the complexity and amount of data generated has increased. The final program is written in FORTRAN in preference to Microsoft VBA or Excel. The time step requires that 1 million sets of calculations are performed for one second of predicted engine run time. Each set is performed upon the governing equations as expanded in section 5.8 and given in appendix B, thus for one second of predicted run time over one hundred million calculations are performed. VBA and Excel are limited in their application as they are high level languages, residing five levels above machine code. This severely reduces run speed when compared to FORTRAN which resides just one level above machine code. Issues with errors due to translation tables and rounding are also eliminated.

5.9.1 Order of calculations

In deciding upon the order of calculation, the way in which the engine operates must be considered. Although some Stirling engines, such as the free piston variants are self starting, this particular design is not. Therefore to start the engine an impetus is applied to the flywheel.

The starting angle (theta) of the flywheel is important as the location of the piston is calculated using theta. This has a direct implication with respect to engine starting, as the location of the piston with the engine cold in effect controls the

quantity of working fluid (mass) contained within the engine. The relevance of this should be clear from chapter 2. Suffice to say that if the piston starts at bottom dead centre then there will not be enough fluid within the engine to sustain operation, and if the piston starts too high in its cylinder then there will be too much expanded fluid within the engine to allow the piston to complete its cycle.

For the initial condition calculation, the piston location is required when calculating the volume of the compression and expansion spaces. This in turn is used to calculate the mass of air contained in the compression space. Other initial conditions are set as given in tables 5.1, 5.4, 5.5 and 5.6.

At start-up, an impetus is applied to the flywheel; hence the first calculation is for the new flywheel angle. The piston, being directly connected to the flywheel, is the next element to be addressed. Next the displacer location is calculated. Knowing the displacer location allows expansion and compression space pressures to be calculated. This pressure differential is the driving gradient for mass flow through the regenerator; hence the mass balance can be calculated. This now means that fluid temperatures for the regenerator, expansion space and compression space can be calculated.

The expressions for flywheel angle and displacer location are discretised from second order differential equations. This means that the first and second time step calculations for any run must have specific conditions applied. The third and subsequent calculations will be able to use previous time step values. Hence the order of calculation is:

1. Flywheel angle θ
2. Piston location
3. Displacer location
4. Expansion space and compression space pressures
5. Mass flow and mass balance
6. Matrix temperatures
7. Expansion and compression space temperatures

5.10 Testing the program

The program has undergone several stages of development and refinement resulting in code for one cell, two cell and multiple cell regenerators. Before any data generated by the programs was considered to be 'predictive', the operation of the program had to be confirmed by testing.

Initially the program was tested for stability, with the internal temperatures and pressures for all nodes throughout the engine set to equal the ambient conditions. The flywheel angle at start-up was set to $\pi/4$, this was to approximate correct amount of working fluid within the engine. This is taken from the description of operation of the Ringbom – Stirling engine variant as modified by Senft [Senft 2000]. The positive direction of rotation is taken as anti-clockwise (as viewed toward the engine), hence the piston is rising.

For the Ringbom engine to operate correctly the working fluid must be fully expanded within the engine at a point in the cycle when the piston is just below top dead centre. The energy stored within the flywheel (and the piston itself) will cause the piston to continue on its path upwards. As this happens the increased volume causes the fully expanded gas to create a vacuum with relation to the surrounding pressure, taken as atmospheric. It is this vacuum which initiates the return stroke of the displacer to begin. This implies that for a fully sealed engine the working temperature differential must be critical. If in the above scenario the internal mass occupies a greater volume when expanded (say by an increase in heat), then the internal pressure cannot fall below that of the surrounding fluid (air), and the displacer will never fall.

All leakages and losses are set to zero, and an impetus equal to the starting velocity of 25 radians per second is applied to the flywheel. Due to the complex and fast initial transients, the time interval required for convergence has to be 1E-7 of a second or less. The implication of this is that simulations require long run times, with 120 seconds of simulated run requiring one hour of computer run time.

It is seen that with the initial conditions set as given in the text, the simulation will run continuously at the given start impetus, which is expected.

It was considered that 120 seconds of engine run time was sufficient for the simulation to be representative of steady state operation.

For the first runs of the simulation, the values for the variables that define the engine are set as closely as possible to those known for the physical engine. As more realistic values for the engine variables became available, they were incorporated into the program.

The reason for this is to investigate how closely the simulation will predict stable engine operation when compared to a known working engine. As such, this will assist in the verification of the program.

5.10.1 Parameters of the model

The characteristics of the various components, such as their dimensions and masses for the virtual engine, are given in table 5.1. These were taken directly from the second test engine built at Napier University, the engineering drawings being given in Appendix A.

The standard physical constants used in the modelling are given in Table 5.5.

The remaining parameters, which are given in Table 5.6, were determined by a combination of analytical and experimental considerations, described below.

The regenerator is made from coils of steel wool packed into the regenerator void. As indicated in the literature review, the flow path through the regenerator may be modelled as axial flow through tubes. The equations used to simulate the engine use several constants, these are defined below.

Table 5.1 Physical characteristics of the test engine

Component	Mass	Unit
Base	2170	g
Cylinder	3129	g
Head	1703	g
Piston and connecting rod assembly	35.8	g
Displacer and regenerator assembly	33.56	g
Component	Length	Unit
Base	46	mm
Cylinder	70	mm
Head	70	mm
Piston	20	mm
Connecting rod	65.0	mm
Displacer and regenerator assy	10	mm
Displacer chamber	29	mm
Stub spring	5	mm
Crank arm	11	mm
Component	Diameter	Unit
Base	152	mm
Cylinder	152	mm
Head	152	mm
Piston	34	mm
Displacer	115	mm
Displacer chamber	116	mm
Effective heat transfer surface	116	mm
Displacer rod	14	mm
Regenerator diameter	25	mm

5.10.2 Inertia of the flywheel

The value for the inertia of the flywheel was approached in two ways. The first was to take the value generated by a commercially available computer aided design package. The second was to make a hand calculation.

The inertia value for the flywheel is taken directly from AutoCAD Inventor 10. This is calculated by the program for any model drawing

$$I_{yy} = 534 \text{ kg mm}^2$$

This value has some error due to the density value used by Inventor in its computations

For the hand calculation the density of the flywheel material is calculated from the mass and volume of the actual part. From this the actual density of 2270 kg/m^3 was calculated, almost double that of the Inventor 10 value. This has led to the use of the hand calculation value being used, as detailed below.

This approach broke the flywheel into two disks, one taking the flywheel as a whole solid. The other disk represents the amount of mass cut out of the flywheel, using the standard formula

$$I_{FW} = \frac{1}{2} mr^2 \quad \text{Equation 5.185}$$

Considering the physical form of the flywheel as shown in appendix A, this gives a value for the inertia as

$$I_{FW} = 0.00068616 \text{ kg m}^2$$

5.10.3 Spring constant

The stub springs were cut from the same length of coiled steel; hence it was assumed that the expansion space spring and compression space spring can be rated equally.

The spring rate was calculated empirically, with a given deflection per unit force being used. The spring constant is calculated from transposition shown in equation 5.186.

$$F = K_s \cdot x$$

$$\text{where } F = m \cdot g$$

$$\text{hence } K_s = \frac{m \cdot g}{x}$$

Equation 5.186

The mass and deflection being:

Spring compression mass	0.55	kg
Spring compression	0.005	m

Gives the spring rate as:

$$K_{SE} = 1079.1 \text{ N/m}$$

$$K_{SK} = 1079.1 \text{ N/m}$$

5.10.4 Flow leakage constants

Philosophy: A cylinder, sealed at one end, has a piston inserted in the open end. The piston is allowed to fall under the control of gravity. As the piston falls, fluid is displaced due to the reduction of volume. By timing the fall over a known distance the mass flow may be calculated. Knowing the mass flow rate the flow constant may be calculated.

Pressure due to piston under gravity

$$F_p \downarrow = m \cdot g \quad \text{Equation 5.187}$$

hence

$$P_p \downarrow = \frac{m_p \cdot g}{A_p} \quad \text{Equation 5.188}$$

If the system is perfectly sealed, then the downward force will be atmospheric pressure plus the piston pressure, setting up an equal and opposite reactive force. As the system is not perfectly sealed then this downward pressure causes a mass flow out of the system.

$$m_{air} = \frac{(p_{atm} \cdot V_p)}{(R \cdot T)} \quad \text{Equation 5.189}$$

where

$$V_p = \pi \cdot D_{pl}^2 \cdot 0.25 \cdot h_{drop} \quad \text{Equation 5.190}$$

And

$$\dot{m}_A = K_{MP} (p_{cylinder} - p_{atmos}) \quad \text{Equation 5.191}$$

But

$$\dot{m} = \frac{mass}{unit\ time} \quad \text{Equation 5.192}$$

therefore

$$K_{MP} = \frac{\left(\frac{m_{air}}{t} \right)}{\left(p_{cylinder} - p_{atmos} \right)} \quad \text{remember } P_{cylinder} = P_{atmos} + P_{due\ to\ mass}$$

Equation 5.193

Table 5.2 Experimental data for mass flow constant

Piston drop height	0.017	m
Displacer rod drop height	0.04	m
Displacer drop height	0.015	m
Piston drop time	145	s
Displacer rod drop time	70	s
Displacer drop time	0.3	s

Table 5.3 Intermediate values

Mass of air piston moved	1.87903E-05	Kg
Mass of air displacer guide moved	7.49623E-06	Kg
Mass of air displacer chamber moved	0.00019299	kg
MFR piston	1.29588E-07	kg/s
MFR displacer guide	1.07089E-07	kg/s
MFR regenerator	0.000643299	kg/s
Pressure due to piston	321.9864204	N/m ²
Pressure due to displacer rod	637.2693844	N/m ²
Pressure due to displacer	23.20615327	N/m ²

Table 5.4 Mass flow constants

$K_{MP} =$	4.0246E-10
$K_{MD} =$	1.6804E-10
$K_{MR} =$	2.7721E-05

5.10.5 Flywheel loss parameters

The flywheel loss parameter was determined directly by measuring the deceleration of the flywheel/piston assembly. The test engine was split so that the bottom and the top of the piston were open to atmosphere. Thus ensuring that the pressures above and below the piston were identical. The engine orientation was maintained as vertical. The piston movement within its containing cylinder was included, since it allowed a comprehensive modelling of the whole flywheel assembly. It was estimated that the friction between the piston and its containing cylinder accounted for about 60% of all losses.

Assuming that the losses are proportional to the angular velocity, ω the instantaneous velocity is given as

$$\omega = \omega_0 e^{-\frac{k_{DF}}{I_F} t} \quad \text{Equation 5.194}$$

where all symbols have their usual meaning.

From the measured position of the flywheel, as a function of time, the instantaneous angular velocity was determined, also as a function of time. A typical example is shown in Figure 5.10.

An exponential trend line was then applied, which showed that the overall loss coefficient is about $0.00003 \text{ kg m}^2 \text{ s}^{-1}$. Hence k_{DF} , which accounts for about 40% is approximately $10^{-5} \text{ kg m}^2 \text{ s}^{-1}$. This value is used, but the sensitivity of the results to this choice was also investigated.

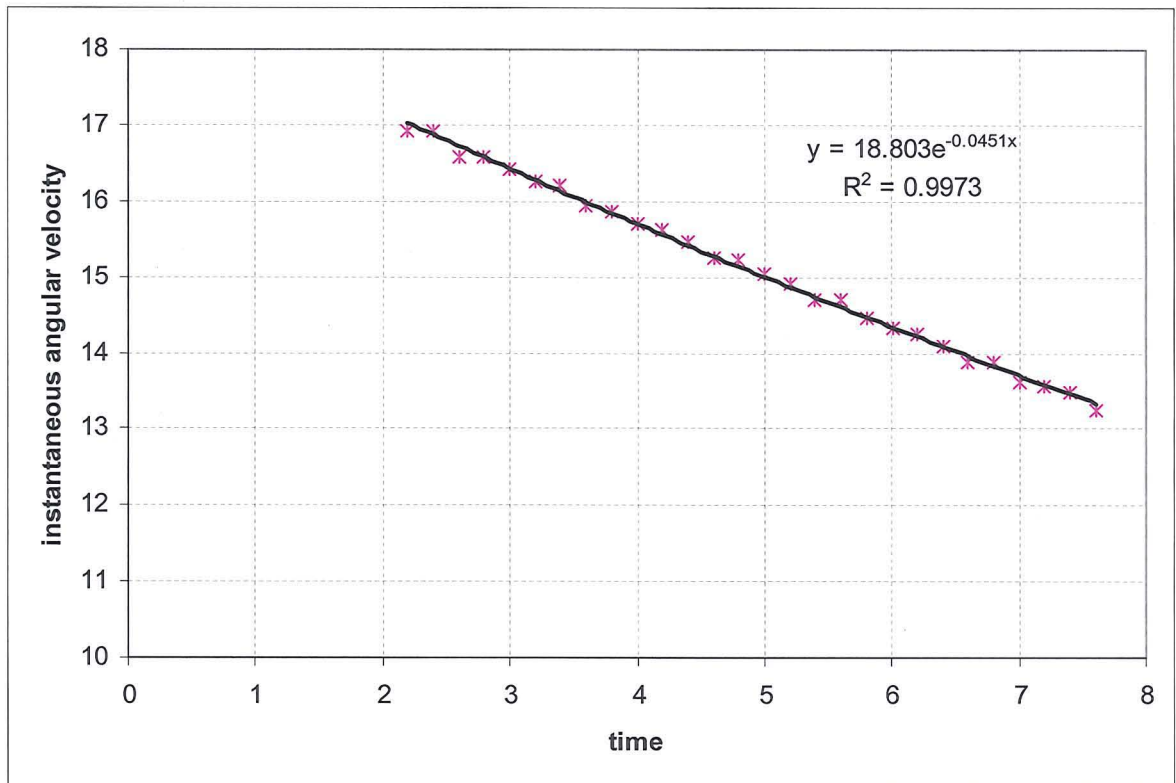


Figure 5.10 Graph of change in angular velocity with respect to time

5.10.6 Heat transfer parameter for internal surfaces

5.10.6.1 Heat transfer from hot reservoir

The analysis of heat transfer from the source and sink to and from the working fluid is a difficult problem. This is due to the flow in the expansion and compression spaces being complex. Hence, only an estimate will be made.

The estimate is based upon the flow of fluid past the surface of the source and sink.

The typical movement of the displacer taken from the prediction program data is shown in figure 5.11 below.

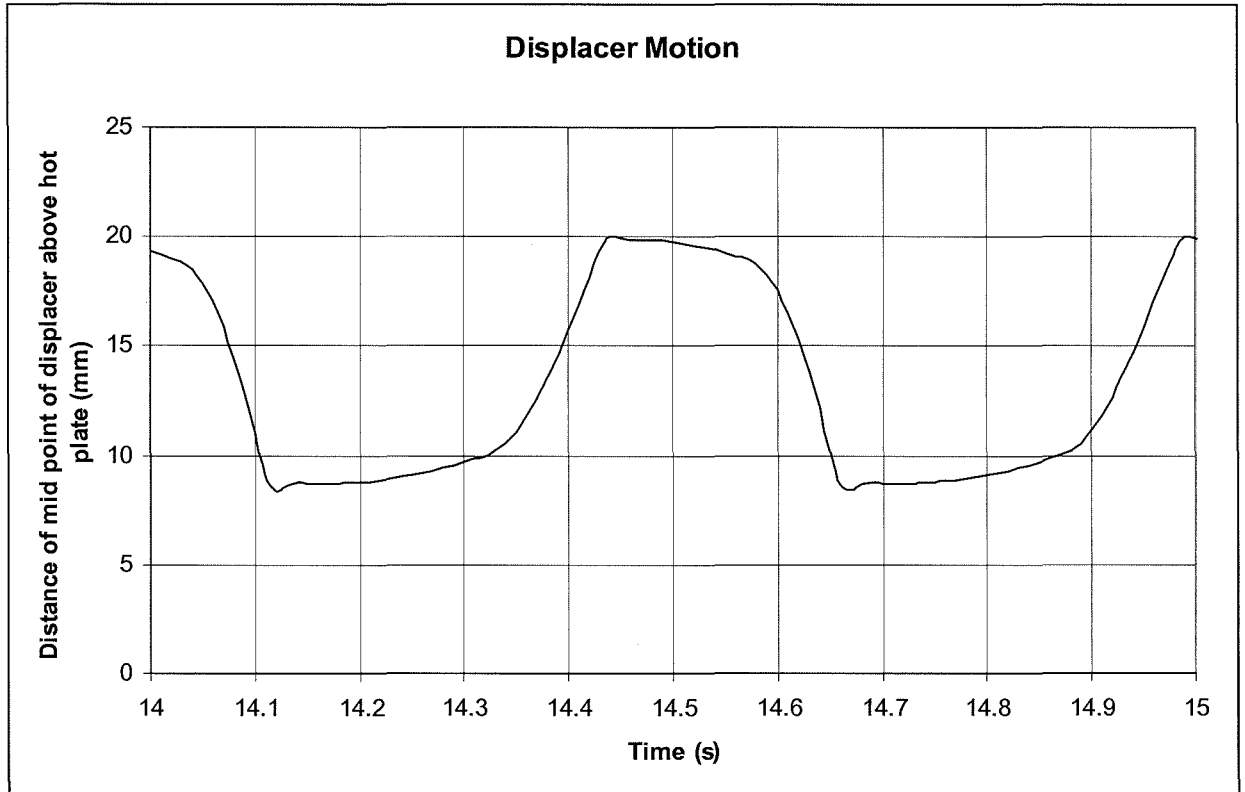


Figure 5.11 Displacer motion

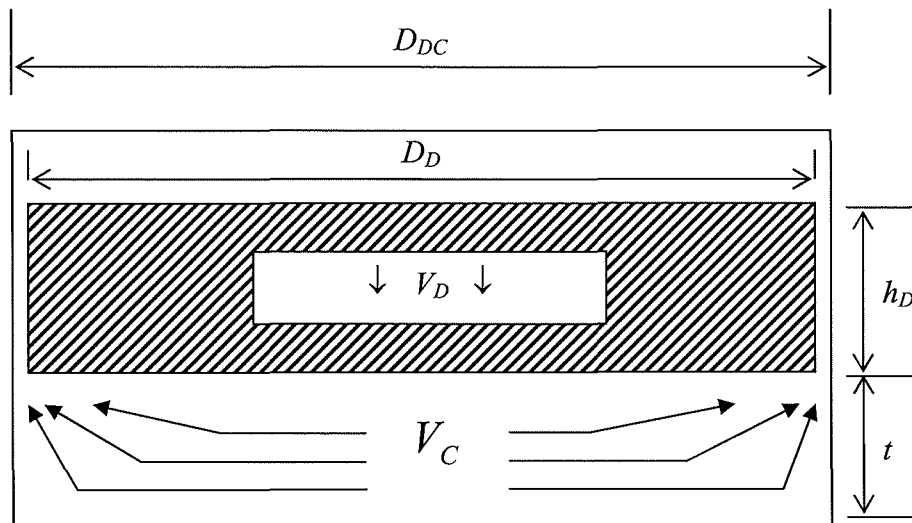


Figure 5.12 Displacer within the displacer chamber

The displacer descends in about 15% of the duration of each cycle, or more generally, fraction τ of the cycle. The total stroke of the displacer is about 16mm, hence the average velocity of the displacer during this period is:

$$V_D = \frac{16E^{-3}}{\tau t_c} \quad \text{Equation 5.195}$$

Where t_c is the period of each cycle, defined by convention as

$$t_c = \frac{1}{f} \quad \text{Equation 5.196}$$

therefore

$$V_D = \frac{16E^{-3}}{\tau} f \quad \text{Equation 5.197}$$

If one was to assume further that the typical position of the displacer was half way down. The thickness or the gap between the bottom of the displacer and the heat transfer surface is 10mm,

Hence the area of the cylinder on the outside of the displacer through which all the fluid will pass is

$$\pi D_D t \quad \text{Equation 5.198}$$

Since the frontal area of the displacer is

$$\pi \left(\frac{D_D}{2} \right)^2 \quad \text{Equation 5.199}$$

The velocity of the fluid across the surface of the cylinder, V_c is

$$V_c = V_D \frac{D_D}{4t} \quad \text{Equation 5.200}$$

It is next assumed that we can approximate with flow over a flat plate, hence from Incropera [Incropera 2002].

$$\bar{Nu} = 0.66 \text{Re}^{\frac{1}{2}} \text{Pr}^{\frac{1}{3}} \quad \text{Equation 5.201}$$

And

$$\bar{Nu} = \frac{\bar{h} \frac{D_D}{2}}{k} \quad \text{Equation 5.202}$$

Rearranging

$$\bar{h} = \frac{\bar{Nu} k}{\frac{D_D}{2}} \quad \text{Equation 5.203}$$

Inserting values

$$\bar{h} \approx 15$$

And

$$Q = \bar{h} A_S \Delta T \quad \text{Equation 5.204}$$

But, earlier we defined

$$Q = K_{HH} \Delta T \quad \text{Equation 5.205}$$

Hence

$$K_{HH} = \bar{h} A_S \quad \text{Equation 5.206}$$

Therefore $K_{HH} = 0.15$

However it must be considered that the flow is highly turbulent and must include the characteristics of an impinging jet. It will be assumed that:

$$K_{HH} \approx 0.3$$

If it is further assumed that $K_{HC} = K_{HH}$

A sensitivity analysis was performed by using different values for $K_{HC} = K_{HH}$

5.10.6.2 Porosity of regenerator matrix

The porosity is a measure of how densely the regenerator is packed and is defined as the proportion of non solid volume to the total volume of material.

To find the non solid volume of the wire wool regenerator the mass and density of which are known, is straightforward, and may be calculated using the relationship volume = mass divided by density.

The volume which the regenerator will occupy is again easily calculated from the diameter and depth of the void.

By subtracting the solid volume from the total volume the non solid volume can be found.

Thus for the dimensions and materials used the regenerator has a porosity of 95%

5.10.6.3 Structure of regenerator cells

The regenerator is defined by two elements, one being the mass of working fluid occupying the free flow volume. The other element is the regenerator matrix itself, considering its geometry and mass.

The matrix in this case is wire wool, the total mass of which is known, as well as the nominal diameter. From this information the total volume occupied by the regenerator may be calculated. As previously stated the porosity is 95%, so the volume occupied by the mass within the regenerator must be 5% of the total volume, leaving 95% of the total volume to be occupied by the working fluid mass. Knowing this volume and the density of air means that the total mass of air may be calculated.

The masses were modified by being divided by the number of cells to yield the mass of matrix material and mass of air per cell.

5.10.6.4 Heat transfer within the regenerator matrix

Pressure drop in the annular space between the displacer and displacer chamber:

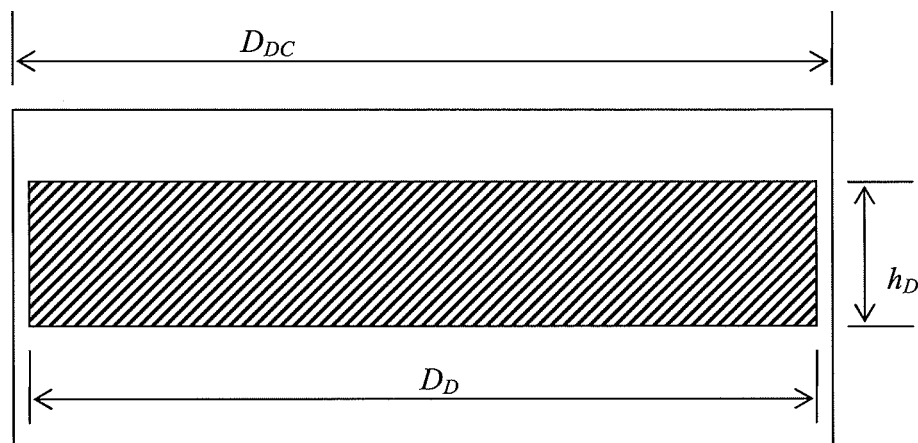


Figure 5.13 Displacer inside the displacer chamber showing annular gap

The thickness of the annular gap may be found from the difference of the two diameters. It is assumed that the gap is uniform, and that the displacer is uni-axial with the displacer chamber.

Hence

$$t_a = \frac{D_{DC} - D_D}{2} \quad \text{Equation 5.207}$$

The result of which, using the above parameters is 5E-4.

If we now assume that the annulus can be unravelled, the space may now be approximated as the gap between two parallel plates. The flow regime for parallel plates is well studied and the following expansions may be applied.

Mass flow rate per unit width for laminar flow.

$$\dot{m}_{uw} = \rho \frac{2 \left(\frac{t_G}{2}\right)^3 \Delta p}{3 \mu \ell} \quad \text{Equation 5.208}$$

Therefore

$$\dot{m}_{uw} = \frac{t_G^3}{12 \nu \ell} \Delta p \quad \text{Equation 5.209}$$

Total flow becomes

$$\dot{m}_A = \dot{m}_{uw} \pi D_D \quad \text{Equation 5.210}$$

Inserting identities becomes

$$\dot{m}_A = \frac{t_G^3 \pi D_D}{12 \nu \ell} \Delta p \quad \text{Equation 5.211}$$

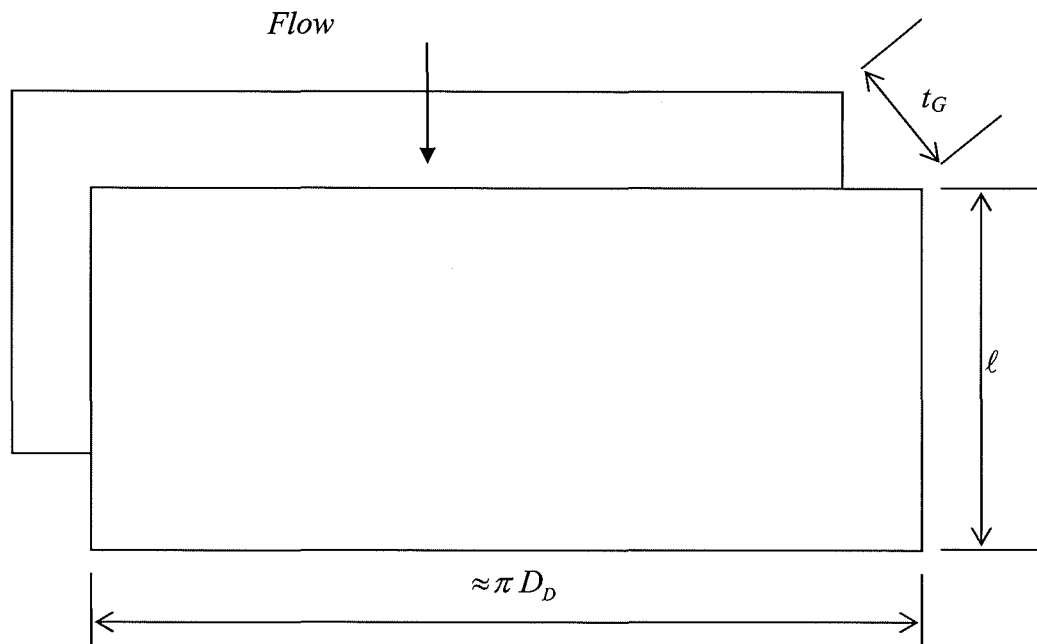


Figure 5.14 Equivalent annular gap shown as two plates

But from previous work we know that

$$\dot{m}_A = K_A \Delta p \quad \text{Equation 5.212}$$

So

$$K_A = \frac{t_G^3 \pi D_D}{12\nu l} \quad \text{Equation 5.213}$$

Using this equation K_A is calculated as 2.2E-5. The experimental value is 2.1E-5 indicating that the majority of the flow is via the annular gap formed between the displacer and displacer chamber wall.

To find the heat transfer rate into the two walls from the fluid we may use

$$Q = h A \Delta T \quad \text{Equation 5.214}$$

And the surface area is

$$A_s = \pi D_D \ell \quad \text{Equation 5.215}$$

Then for two surfaces, with different heat transfer coefficients we have

$$Q = (h_{disp} + h_{dc}) \pi D_D \ell \Delta T \quad \text{Equation 5.216}$$

If it is assumed that $h_{disp} \approx h_{dc}$ then

$$Q = h 2\pi D_D \ell \Delta T \quad \text{Equation 5.217}$$

For this type of flow regime $Nu \approx 8$ [Incropera and De Witt]

Where

$$Nu = \frac{h D_{eq}}{k} \quad \text{Equation 5.218}$$

And equivalent diameter D_{eq} is defined as

$$D_{eq} = \frac{4A}{P} \quad \text{Equation 5.219}$$

When inserting identities becomes

$$D_{eq} = 2t_G \quad \text{Equation 5.220}$$

Rewriting equation 5.216 gives

$$h = \frac{Nu k}{2t_G} \quad \text{Equation 5.221}$$

Inserting this identity into equation 5.215 gives

$$Q = \frac{Nu k}{2t_G} \cdot \frac{2\pi D_D \ell}{1} \Delta T \quad \text{Equation 5.222}$$

Rewriting yields

$$Q = \frac{Nu k \pi D_D \ell}{t_G} \Delta T \quad \text{Equation 5.223}$$

Previously we defined Q as

$$Q = K_{HRM} \Delta T \quad \text{Equation 5.224}$$

So now an equation describing K_{HRM} may be written

$$K_{HRM} = \frac{Nu k \pi D_D \ell}{t_G} \quad \text{Equation 5.225}$$

The calculations indicate a value of approximately 1.5 W/K; however some flow does go through the regenerator, so a reasonable assumption for the value of K_{HRM} is:

$$K_{HRM} \approx 2 / ns$$

Where ns is the number of matrix screens making up the regenerator and is used in table 5.6. This value is used, and its sensitivity was investigated.

5.10.6.5 Parameters for engine

Table 5.5 Physical constants used for the engine

Description	Value	Unit
Acceleration due to gravity	9.80665	m/s ²
Ambient temperature	280	K
Atmospheric pressure	101325	Pa
Cold plate temperature	280	K
Density for stainless steel	7850	kg/m ³
Density of air	1.2	Kg/m ³
Gas constant for air	287	J/kg K
Hot plate temperature	355	K
C_p constant pressure for air @ 300K	1005	J/kg K
C_v constant volume for air @ 300K	718	J/kg K
C_p matrix iron	448	J/kg K

Table 5.6 Geometry and constants calculated by the prediction program

Description	Value	Unit
Area of cold plate internal transfer via compression space	0.010568318	m ²
Area of displacer chamber	0.010568318	m ²
Area of displacer effective	0.010568318	m ²
Area of displacer rod (CSA)	0.000153938	m ²
Area of displacer solid	0.010386891	m ²
Area of hot plate heat transfer surface	0.010568318	m ²
Area of piston	0.00090792	m ²
Combined flywheel / piston losses	1E-5	kg m ² s ⁻¹
Constant for mass flow past displacer rod	1.1209E-10	m ² s
Constant for mass flow past piston	4.02465E-10	m ² s
Constant for mass flow through regenerator	2.05646E-05	m ² s
Convective heat transfer for cold plate	0.3	W/K

Convective heat transfer for hot plate	0.3	W/K
Heat transfer constant for matrix	$2/ns^*$	W/K
Initial flywheel angular velocity	25	Radian/s
Mass of regenerator material in regenerator cell	$0.00753/ns^*$	Kg
Mass of working fluid in regenerator cell	$0.000022/ns^*$	Kg
Moment of inertia	0.00068616	kg m ²
Number of cells	2	
Number of regenerators	4	
Regenerator porosity	95	%
Spring rate constant for compression space spring	1000	kg/m
Spring rate constant for expansion space spring	1000	kg/m
Time step in seconds	0.0000001	s
Total length of crank arm and connecting rod	0.076	m
Total mass of matrix material	0.00753	kg

* Where ns is the number of screens in the matrix (cells)

5.11 Theoretical results

5.11.1 Quantitative results

The development and testing of the computer program involved many runs, collecting very large amounts of data. Each data set varies with the change in variable value and in some cases such as regenerator definition, calculation philosophy.

To standardise a series of runs for comparison purposes was a necessity. As detailed above, the values for constants and geometry are taken from the engine. In this way the physical engine is replicated as closely as possible by the computer program.

Time windows used in the physical engine are:

0 to 0.6 seconds

3.4 to 4.0 seconds

12.4 to 13 seconds

21.6 to 22.2 seconds

119.4 to 120.0 seconds

It can be seen that each interval time slot lasts for a period of 0.6 of a second, this is due to the limitations of the data logging system.

The time windows used for the computational model are:

12 to 14 seconds

21 to 23 seconds

118 to 120 seconds

These time slots were chosen to mirror those for the test engine data, but also neglecting start up behaviour at this point and concentrating on steady state operation.

The temperature differential is worked slightly differently to that of the real engine. In the case of the computer model the hot and cold ends are isothermal, where for the real engine the temperatures can be seen to decay.

A temperature differential of 75K has been taken as representative of the starting differential of the test engine.

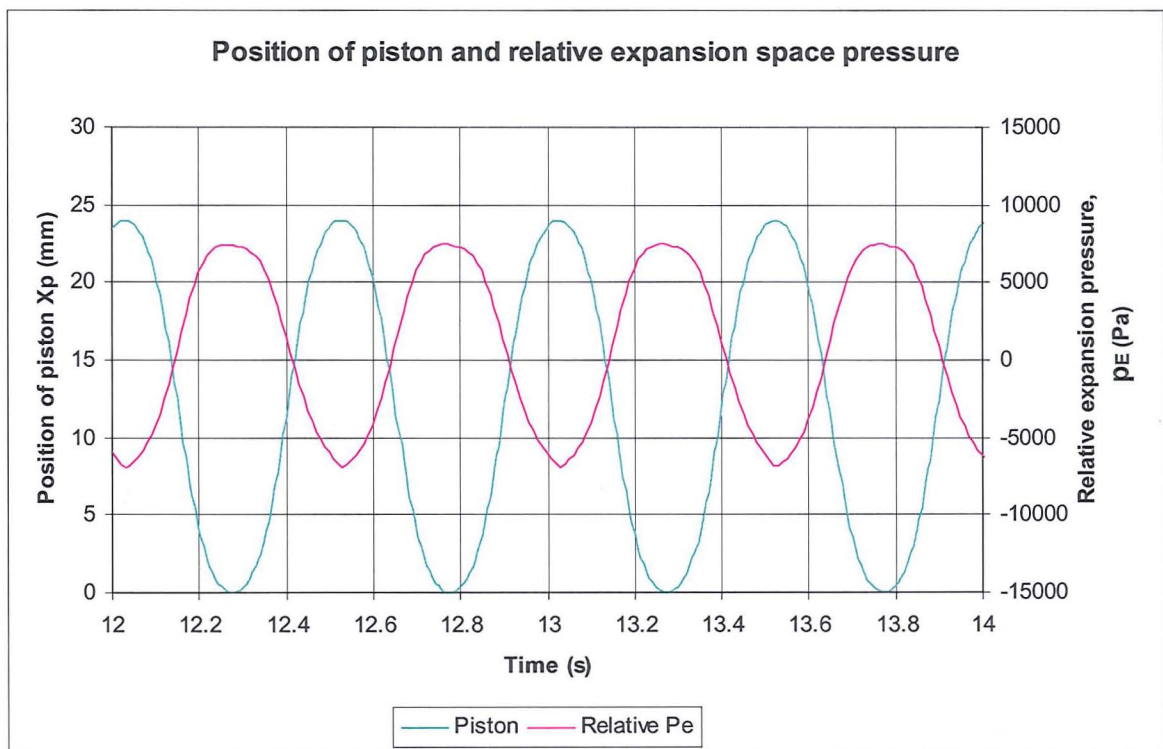


Figure 5.15 Piston and relative expansion pressure 12 to 14 seconds

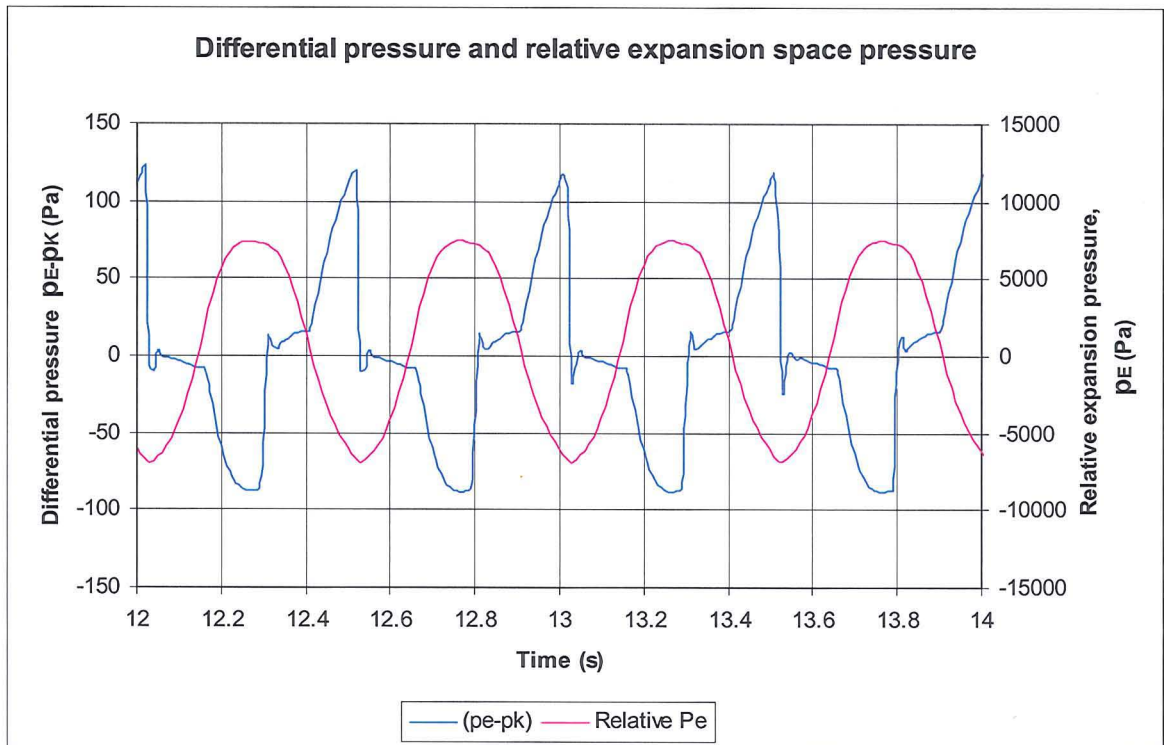


Figure 5.16 Differential and relative expansion pressures, 12 to 14 seconds

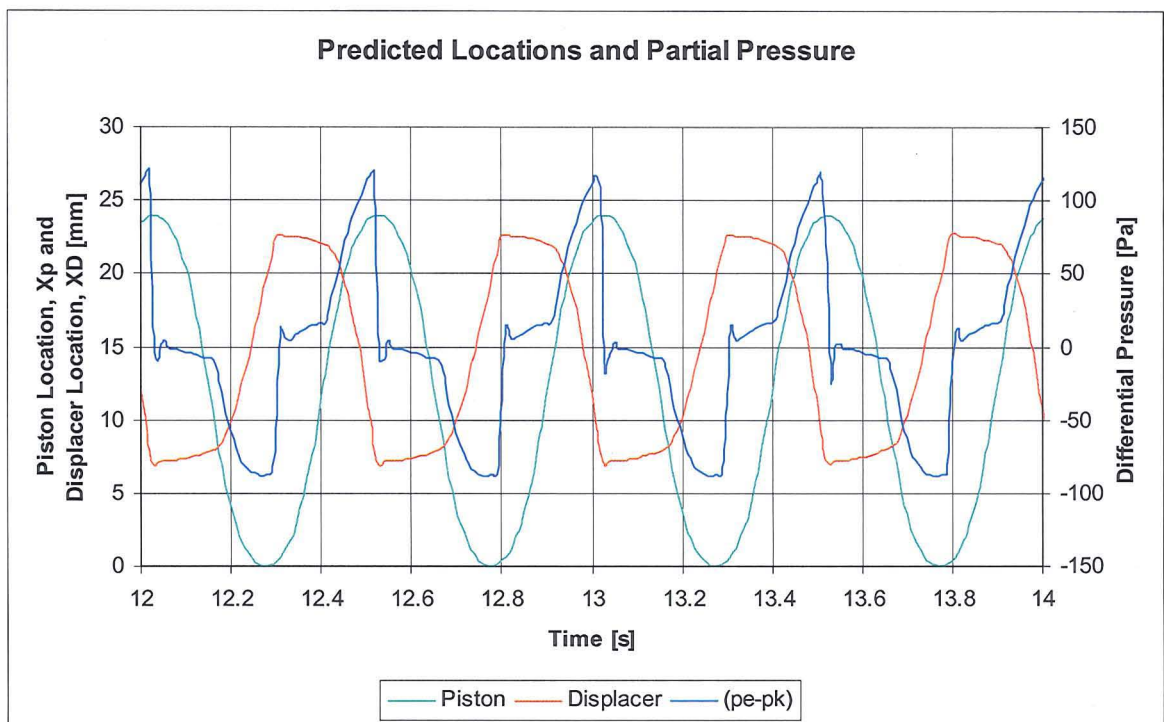


Figure 5.17 Piston and Displace position with reference to differential pressure

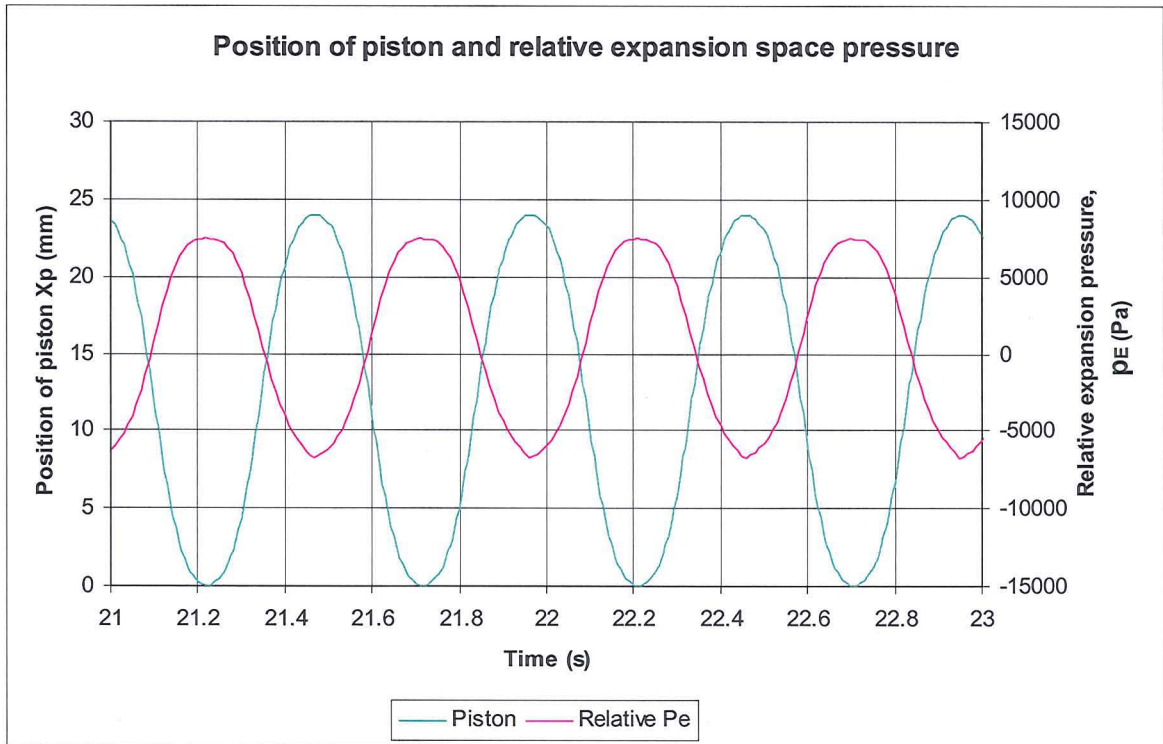


Figure 5.18 Piston and relative expansion pressure 21 to 23 seconds

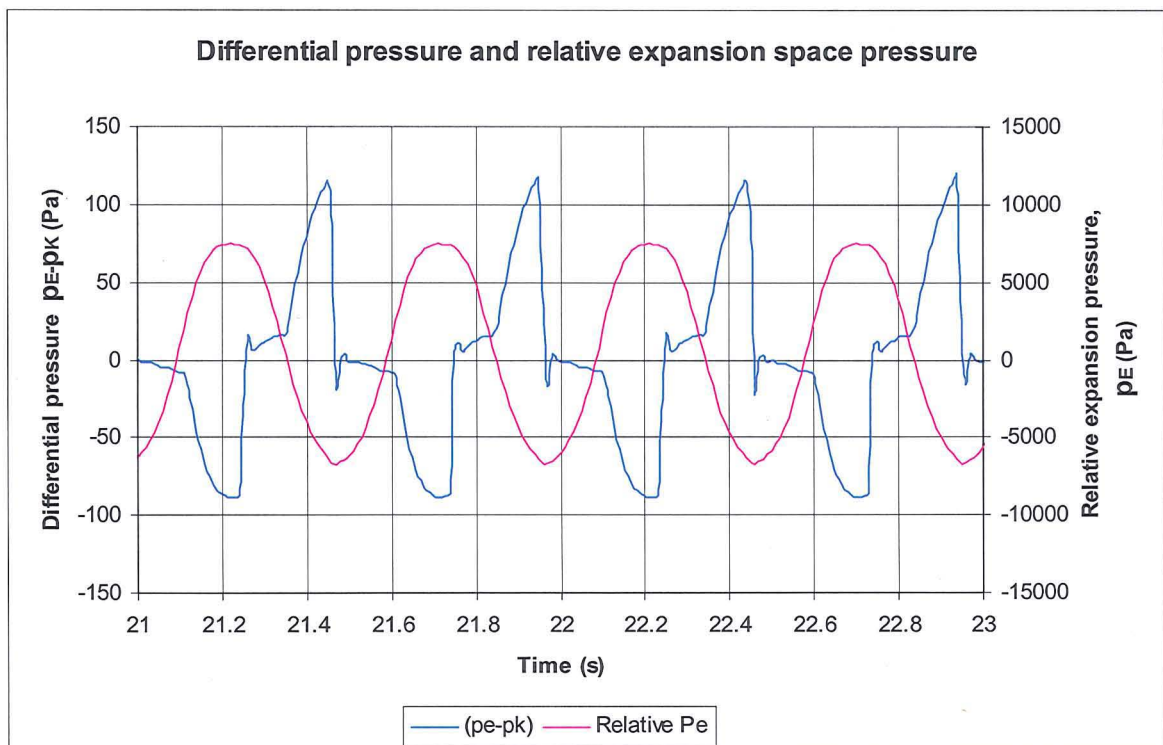


Figure 5.19 Differential and relative expansion pressures, 21 to 23 seconds

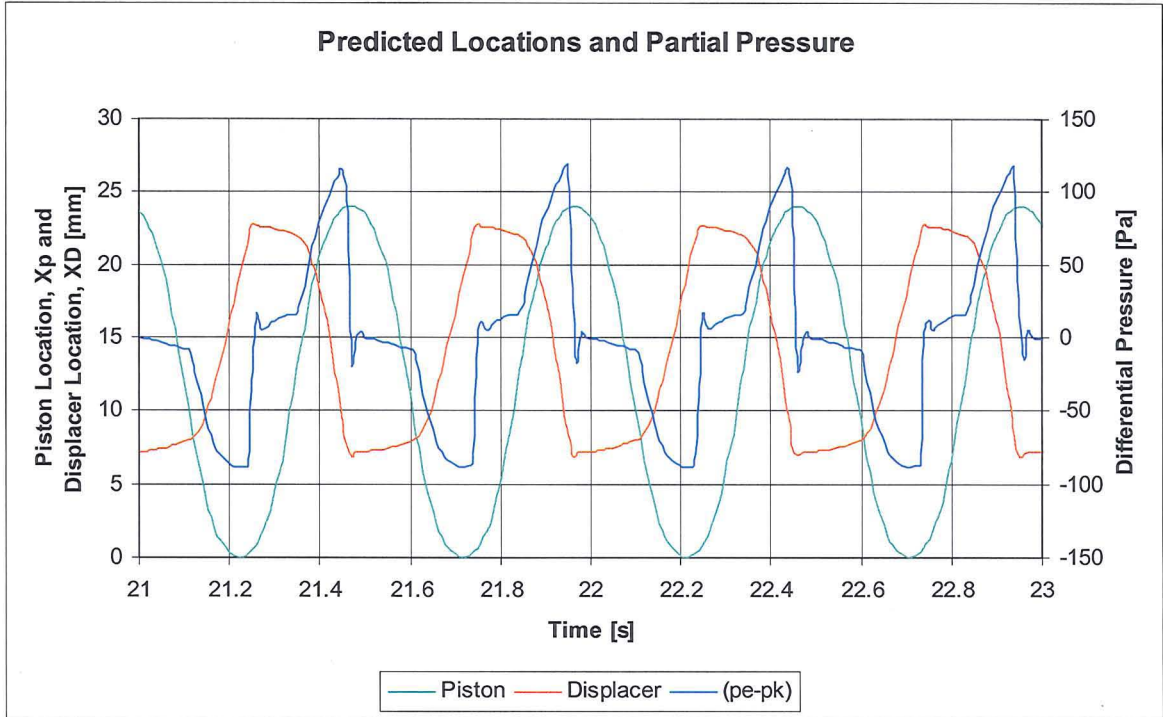


Figure 5.20 Piston and Displace position with reference to differential pressure

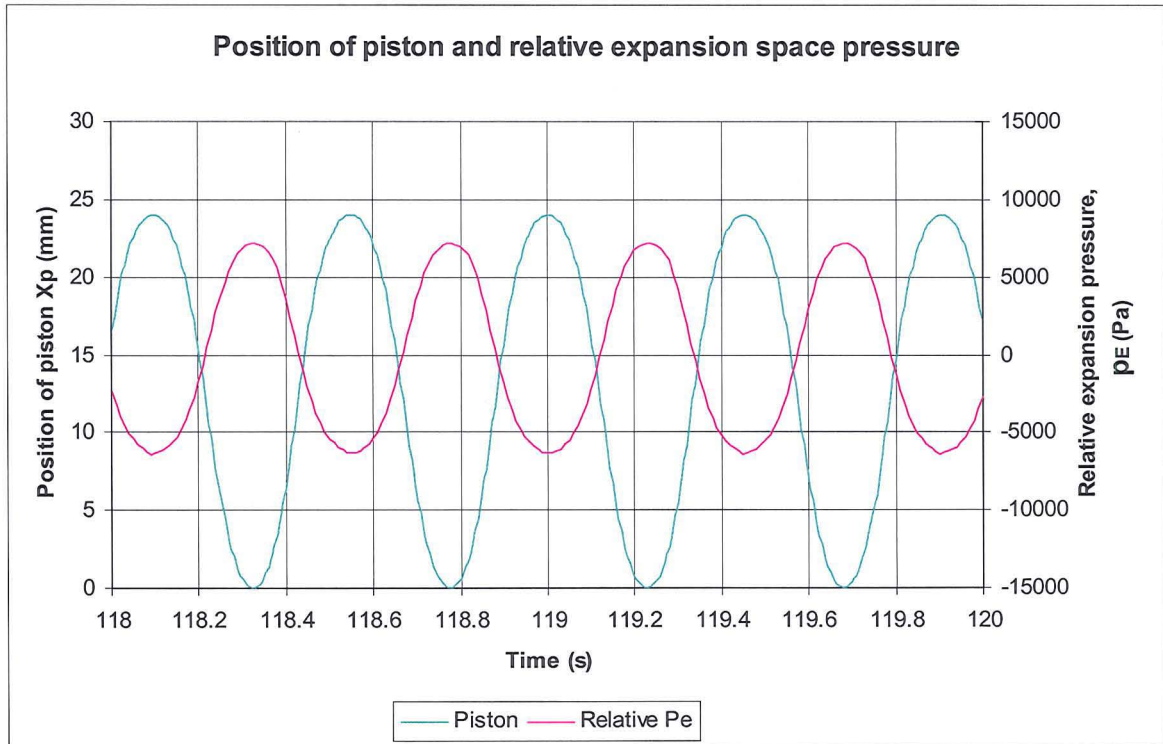


Figure 5.21 Piston and relative expansion pressure 118 to 120 seconds

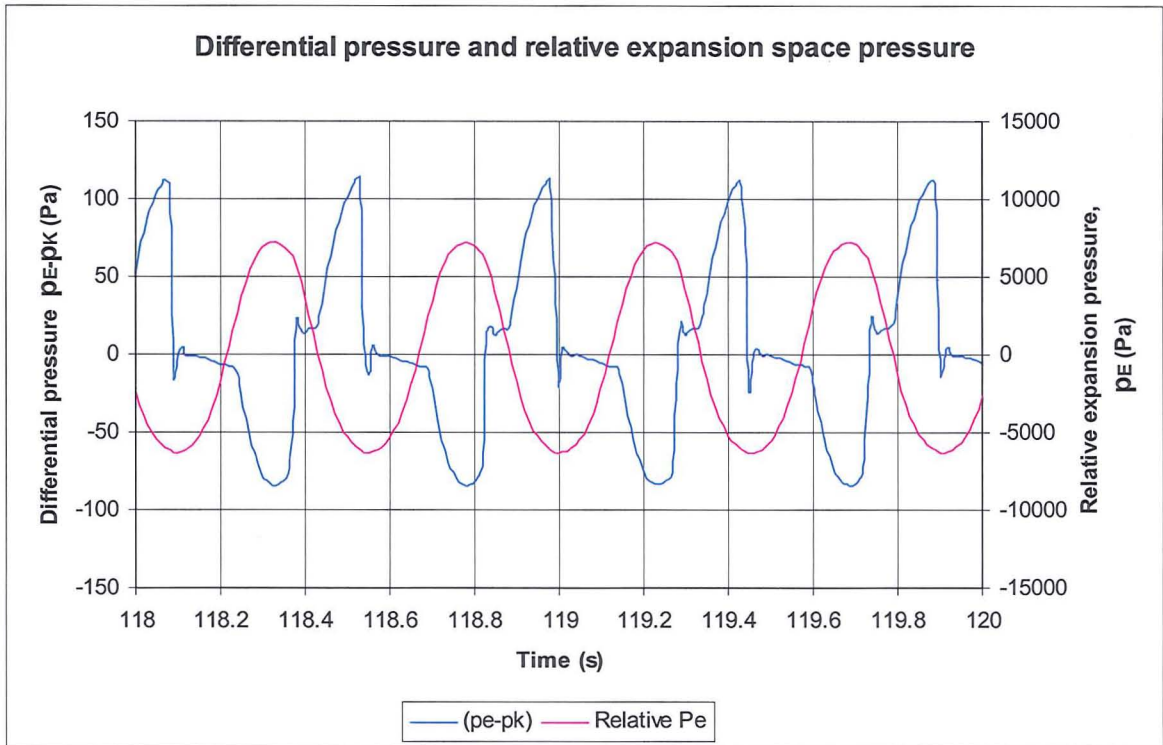


Figure 5.22 Differential and relative expansion pressures, 118 to 120 seconds

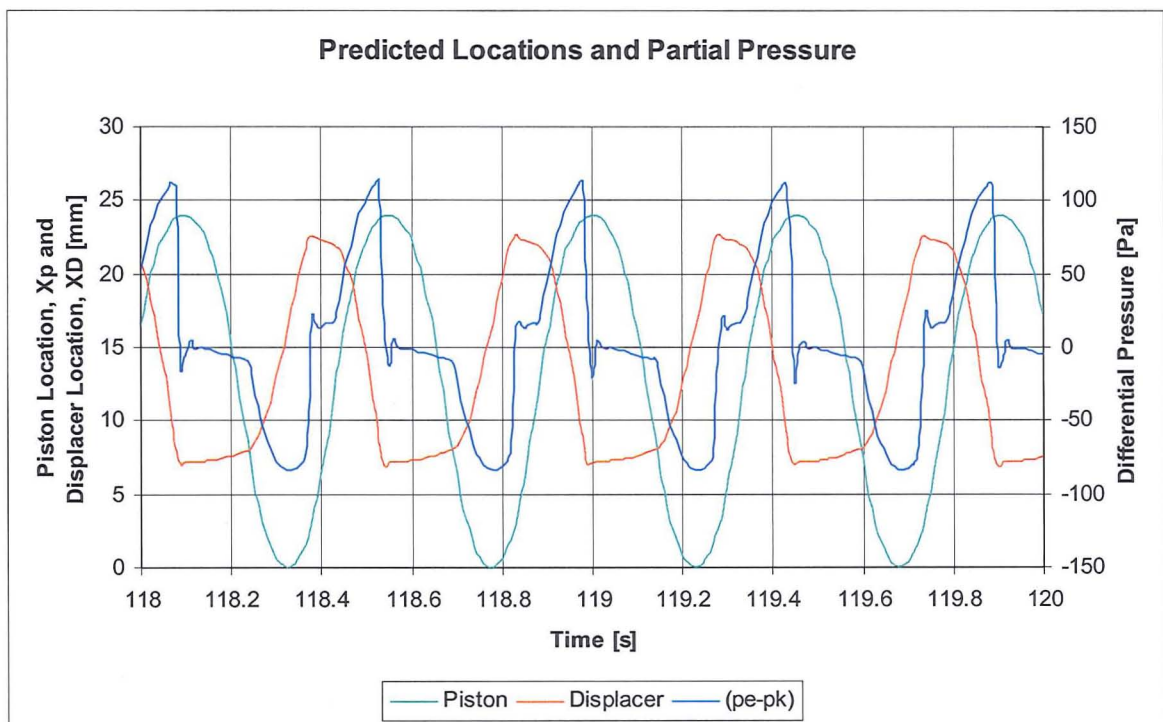


Figure 5.23 Piston and Displace position with reference to differential pressure

5.11.2 Qualitative analysis

The engine simulation program has been written in three forms, these having relevance as to the construction of the regenerator. The programs have been written to simulate a one cell 'black box' regenerator, a two cell regenerator and a multi cell regenerator. The one cell and multi cell regenerators were put aside in favour of a two cell regenerator. The one cell was found to be over simplistic, and could not show trends through the regenerator, taking the whole as one. The multi cell required noticeably longer run times and generated much larger data files. Regenerative matrices and their flow and thermal characteristics could easily occupy a research thesis by themselves. Therefore it was decided that a two cell matrix would be sufficient to show trends within the regenerator without over complication.

It was decided that the data for a series of runs would be taken. These runs were designed to simulate the engine with differing flywheel angles and with different temperature differentials. The order for these runs is given in table 5.8. Runs 5, 11 and 17 were given special attention as the temperature differential is the same as that for the real engine for start up and sustained motion.

Table 5.7 Verification runs

Run	Start angle	Displacer mass	Ambient temperature	Hot plate temperature	Differential temperature	File name
1	" $\pi/4$ "	25g	280	320	40	01_tc01
2	" $\pi/4$ "	25g	280	330	50	01_tc02
3	" $\pi/4$ "	25g	280	340	60	01_tc03
4	" $\pi/4$ "	25g	280	350	70	01_tc04
5	" $\pi/4$ "	25g	280	360	80	01_tc05
6	" $\pi/4$ "	25g	280	370	90	01_tc06
7	" $\pi/5$ "	25g	280	320	40	01_tc07
8	" $\pi/5$ "	25g	280	330	50	01_tc08
9	" $\pi/5$ "	25g	280	340	60	01_tc09

10	" $\pi/5$ "	25g	280	350	70	01_tc10
11	" $\pi/5$ "	25g	280	360	80	01_tc11
12	" $\pi/5$ "	25g	280	370	90	01_tc12
13	" $\pi/6$ "	25g	280	320	40	01_tc13
14	" $\pi/6$ "	25g	280	330	50	01_tc14
15	" $\pi/6$ "	25g	280	340	60	01_tc15
16	" $\pi/6$ "	25g	280	350	70	01_tc16
17	" $\pi/6$ "	25g	280	360	80	01_tc17
18	" $\pi/6$ "	25g	280	370	90	01_tc18

A brief description of the runs will now be given in table 5.8.

Table 5.8 Run description

Run	Differential temperature	Comment
1	40	The flywheel rotates several times before starting to rock
2	50	The flywheel rotates several times before starting to rock
3	60	Sustained motion from input of impetus, although reversal of direction of motion, 1050 rad in 120 seconds
4	70	Initial rotation turns quickly to rocking/stall for short time, then sustained motion to 1320 rad in 120 seconds
5	80	Initial rotation turns to stall which lasts slightly longer then sustained motion, 1584 rad in 120 seconds
6	90	Initial rotation turns to stall which lasts slightly longer then sustained motion, 1855 rad in 120 seconds
7	40	The flywheel rotates several times before starting to rock
8	50	The flywheel rotates several times before starting to rock
9	60	Sustained motion from input of impetus, although motion reverses, 1046 rad in 120 seconds
10	70	Initial acceleration decreases, sustained motion to 1395 rad in 120 seconds

11	80	Initial rotation turns to stall then sustained motion, 1594 rad in 120 seconds
12	90	Initial rotation turns to stall which lasts slightly longer then sustained motion, 1851 rad in 120 seconds
13	40	The flywheel rotates several times before starting to rock
14	50	The flywheel rotates several times before starting to rock
15	60	Initial rotation turns to oscillating for short time then sustained motion to 1108 rad in 120 seconds
16	70	Initial acceleration decreases, sustained motion to 1403 rad in 120 seconds
17	80	Initial rotation turns to stall then sustained motion, 1557 rad in 120 seconds
18	90	Initial rotation turns to stall which lasts slightly longer, then sustained motion, 1838 rad in 120 seconds

The lowest temperature differential applied to the engine is 40K, it was seen that the flywheel rotates for 1.2 seconds before initial stall, and then rocks with decreasing amplitude. After 12 seconds the motion had almost ceased, with the engine components becoming stationary by 22 seconds. This series showed the inertia of the flywheel assembly driving the piston, and so driving the pressure variations within the engine, hence displacer location.

The next temperature differential applied is 50K. It was deduced that the flywheel turns in the same direction for 6.24 seconds. After this time the flywheel stops momentarily and then commences small oscillations. At the 27 second point these oscillations suddenly triple in magnitude, and then very slowly increase; even with very long runs simulating ten minutes of engine run time, these oscillations do not become large enough to complete one revolution of the flywheel. The time between 6.24 seconds and 27 seconds may be the warm-up time for the regenerator.

This series begins with the flywheel inertia driving the piston, causing the fluid motion within the engine. What can be seen after 6.24 seconds is the start of the

engine working as a heat engine. The sustained oscillations of the flywheel indicate that there must be a thermodynamic and fluid cycle occurring, but without sufficient energy density to complete the kinematic cycle.

With a temperature differential of 60K and 70K the data showed the engine sustaining motion. The piston is leading the displacer and pressure is also leading the displacer. Maximum pressure is at bottom dead centre, or just before bottom dead centre for the piston. It can be seen that a bulk pressure is building up, so the displacer movement is not complete. This shows transition from being motored to motoring. This can also be a gas cycle being initiated. There are pressure spikes on differential pressure trace, which coincide with displacer contact of compression space spring.

Higher temperature differentials showed the pressure drop and cycle initiation after the internal pressure has stalled the engine with the piston held at top dead centre. This pressure drop is due to the mass leaving the engine. Higher temperatures also indicated an increased angular velocity.

This shows the engine with an increased internal temperature differential. There is a slight increase in phase shift with the displacer with respect to the expansion space pressure. The simulation reproduces many of the motions seen on the test engine, such as rocking of the flywheel, and piston lock at top dead centre if the temperature or fluid mass is too great for the initial conditions for sustained motion.

The runs described above are taken as representative of the type of testing the simulation has gone through, and only represent a very small amount of the simulated data gathered.

For the final runs of the prediction program the values for the engine constants were all checked to be the latest, and the parameters of the engine all checked to be the correct value.

A representative starting differential of 75K was applied to the initial conditions and the simulation run for 125 seconds. A printout of the final program is given in appendix B.

The chosen parameters show the engine starting immediately with no rocking or piston lock evident.

Figure 5.15 shows the data for piston position and relative expansion space pressure for 12 to 14 seconds. At this point the engine is settling into steady state operation with a running speed of 114 rpm. The graph indicates that maximum expansion space pressure occurs at the same time as piston bottom dead centre. From the description of engine operation this is expected. It is noteworthy, that the pressure differential is not symmetrical about the zero pressure point. There is a range of +8KPa when the piston is at bdc to -6KPa when the piston is at tdc.

Figure 5.16 shows the differential pressure in comparison to the relative expansion pressure. When the differential pressure is positive, then it is indicative that p_E is greater than p_K , and when the differential pressure is negative, then p_E is less than p_K . It is interesting to see the differential pressure in antiphase to the relative pressure.

By inspecting figure 5.17 the shape of the differential pressure line can begin to be explained. As the displacer dwells at bottom dead centre the piston descends using the energy stored by the flywheel on the upward stroke. Heat is still being rejected from the chamber to the cold plate, so the compression space pressure is still falling slightly. Eventually the point is reached where the compressed fluid can be compressed no more for the given conditions, and the pressure rises rapidly due to the piston downward movement. This increasing pressure begins to lift the displacer and mass flows from the compression space to the expansion space. The expansion space pressure begins to rise due to expansion of the working fluid. The expansion space pressure continues to increase and the displacer accelerates under the increasing pressure. At the point where the displacer contacts the compression space spring, there is a small bounce on the spring, which can also be seen in the differential pressure line. As the displacer dwells in

the top of the engine the differential pressure becomes positive, and the expansion space pressure becomes greater than the compression space pressure; this is not surprising as the displacer is sitting in the compression space and the majority of fluid is in the expansion space. The expansion space pressure increases to a point just before top dead centre. It is at this point, if the literature is to be believed, that the displacer would begin its journey downwards. It is evident from the trace that the displacer has begun its journey downward at least two tenths of a second before this. This departure from the expected behaviour will be in some part due to the mass of the displacer under gravity, and in some part to the imperfect sealing of the engine. As the displacer falls, the working fluid will be passed through the regenerator and into the compression space. The almost instantaneous drop in expansion space pressure will be due in some part to the piston causing a vacuum to be formed as it continues towards top dead centre, and in some part to the cooling of the working fluid. A transient spike can be seen as the displacer contacts the expansion space spring and bounces slightly. There is then a gradual reduction in pressure to a point where the compression space pressure becomes greater than the expansion space pressure and the cycle continues.

It should be noted that the displacer is leading the piston by approximately 180° .

Figures 5.18 to 5.20 show the same graphs but for the time slot 21 to 23 seconds. The velocity is now 109 radians per second and the phase difference between the displacer and piston remains at about 180° .

Figures 5.21 to 5.23 show the graphs for the time slot 118 to 120 seconds. The velocity is now 126 radians per second and the phase difference between the displacer and piston remains the same.

6 Discussion

In this work the author has realised one main point about the Stirling engine and the Ringbom variant: very little is known about how the internal processes interact. In this thesis a third order method of investigating these processes for a Low Temperature Differential Ringbom – Stirling engine is presented.

To illustrate the lack of understanding that exists, the author and the supervisory team, at the start of the analytical work, each came up with a brief description of how the engine operates. Each description was different, and in the final account the author would say that each member brought a different aspect to the table, so in some ways we were right, and in other ways the work has provided enlightenment.

The work is divided into two distinct parts, firstly the computer model and secondly the test engine. The computer model, although following third order methodology, has been developed independently of any outside influence. Thus the derivation of the equation sets and application of numerical techniques are original to this work. The same is applicable to the computer program which has been written using the output from the numerical techniques.

The test engine is based on a design by Senft, which in turn has come from the designs of Kolin and Ringbom. Two engines have been manufactured, the first one to the design of Senft, and the second one with modifications to accommodate the instrument package.

As can be seen in the preceding chapters, the instrument package and data logging were designed and built (where required) at Napier University.

This means that every aspect of the work, from theory to computer model and from engineering drawing to a fully instrumented engine with data logging, has been undertaken by the author.

This has culminated in the production of two sets of data, one predicting engine operation, and one of the engine itself.

6.1 Comparison of the data sets

The test engine was built to check the validity of the computer program, although it is the variables within the program which are set as close as possible to the test engine. As such, the nominal conditions are taken from the test engine runs.

The theoretical predictions are given in chapter 5 section 10, and refer to figures 5.15 to 5.23 inclusive. Experimental data is given in chapter 4 section 5, and refers to figures 4.21 to 4.30 inclusive.

It can be seen that for similar conditions for the theoretical and experimental results, the variation of the differential expansion pressure ($p_E - p_A$) is approximately π radian out of phase with the variation of the position of the power piston, x_p . This shows that the prediction of operation of the engine is correct and the theory behind the prediction is sound. To begin to test the accuracy of prediction, the amplitudes of the two results can be compared. It can be seen that the theoretical amplitude of the pressure variation is in the region of 6700Pa, whereas the variation for the experimental data is 4500Pa, a difference of about 30%. There could be several possible reasons for this error, the most likely being the mass flow round the displacer rod and piston. The loss parameter is calculated from experimental data using the mass of the element under gravity to cause the flow. With the higher dynamic pressures encountered whilst the engine is running the flow loss parameter will be larger. There could also be additional quenching effects of the ingress mass; although this is considered in the theoretical work the degree of quenching upon the cycle as a whole may operate slightly differently. It is assumed in the model that all mass flow within the engine goes through the regenerator, and the annular gap formed between the displacer and chamber wall is included in this term. In reality we have seen that this is not the case, although the flow through the gap in some ways approximates the flow through the regenerator when considering heat transfer from the moving medium

and regenerative exchange. The porosity of the gap must be less than that of the regenerator, so the pressure difference can equalise at a greater rate experimentally than theoretically.

In both the theoretical and experimental results, the phase relationship between the variations in piston, x_P , and displacer, x_D , location are in the region of π rad. Although there is the expected offset to allow the change in pressure difference to initiate displacer strokes. The variation in position of the piston is approximately sinusoidal, as would be expected in the flywheel conrod system utilised in the engine and program. It is the motion of the displacer which is interesting, and which both the theoretical prediction and experimental results indicate would occur. The variation in location for the displacer is discontinuous in nature, with dwell points in the bottom and top of the displacer cylinder. Both sets of data indicate that the displacer will dwell in the bottom for a longer period than at the top of the displacer cylinder. This may be explained by the fact that the displacer has to be raised against gravity so; the lifting force has to overcome gravity acting upon the mass of the displacer before motion can begin. On the downward stroke the force of gravity upon the mass of the displacer is already trying to initiate the downward movement of the displacer, so the pressure differential does not need to be reversed to such an extent to initiate the downward displacement stroke. This effect of gravity upon the displacer may also be seen in the slow rise time and fast drop time for the displacer. It should also be noted that the contact and bounce with the stub springs is predicted and seen experimentally. The bounce is also indicated by rapid reversals in the differential pressure.

The predicted and experimental variations of the pressure differential, $p_E - p_K$, indicate a good correlation, although the predicted value is yet again higher than the experimental value. Once again this is probably due to the dynamic loss value being greater than the experimentally derived one.

It is interesting to note that the test engine would stop at a temperature differential of around 54K, whereas the prediction suggested a temperature differential of 60K.

The engine speed increases with temperature differential, which once again shows a good correlation, with the predicted engine speed being slightly lower than that of the test engine.

Different initial flywheel angles were tested; it may not be obvious at first glance, but the mass of the working fluid contained within the engine is a direct function of initial flywheel angle. This will have a critical bearing upon the working temperature differential for a well-sealed engine. Senft alluded to this when discussing the running in of a new engine, but did not give the critical reason, that in a well-sealed engine the amount of working fluid is fixed. In a Ringbom engine this is critical as the working fluid has to be expanded to its maximum extent, before the power piston reaches top dead centre or bottom dead centre, in order to initiate the displacement stroke. If the temperature is too great, then the pressure differential will never take place, hence the engine can never run. So in this engine it is the very fact that there are leaks that allows the engine to attain a working mass of fluid; this means that the engine is self regulating to a point. If the flow of mass to the atmosphere was to be reduced, the engine would run at lower temperature differentials, but not over such a wide range of differentials.

7 Conclusions and further work

In this work, third order analysis methods have been applied to a Low Temperature Differential Ringbom – Stirling Engine (LTDRSE). A set of equations has been presented which describe the mechanical, thermal and fluid processes occurring for each element of the engine. A numerical program has been written to analyse the behaviour of the engine. A test engine has been built and the data from both compared. The theoretical prediction gives an excellent correlation for the variation in element location and pressures, the values of which have an error of between 25% and 30%.

Phenomena which have been predicted were also observed on the test engine data, for example:

- If the initial temperature differential falls below the required differential, the flywheel turns but does not complete one revolution, rather it is observed to 'rock' back and forth. In chapter 4 the starting temperature for sustained engine operation was found to be 54K. Smaller temperature differentials would result in either rocking as described above or a natural decay of engine revolutions as the differential became much closer. This differential was noted to be in the order of 65K for the prediction program from chapter 5. Thus the engine requires a 17% lower temperature differential than the prediction program to run in a sustained manner. This indicates that there is a minimum temperature differential required for sustained engine operation, with a strong correlation between predicted and actual operation. The difference may be explained by the way in which the constants for engine losses were calculated, given in chapter 5 section 10, and covered in the discussion, chapter 6.
- The major theoretical advantage of the LTDRSE is the discontinuous motion of the displacer. As covered in the literature review, this type of motion brings the cycle process paths closer to the ideal set out as the Stirling cycle. In the results generated from the prediction program this is

evident, even to the degree of longer dwell times at bottom stroke to top stroke, where the rise of the displacer is slower than the fall of the displacer.

- In the theoretical operation of the LTDRSE given in chapter 2 section 5, the piston is either just before top dead centre or just before bottom dead centre when displacer motion is initiated; from the figures giving test engine operation in chapter 4 and the predicted engine operation in chapter 5, this point of initiation can be seen.
- The magnitude of the temperature differential has a direct effect upon the angular velocity of the flywheel. As the temperature differential is increased so does the angular velocity of the rotating elements. The prediction program under predicts engine running speed by 25%, as is discussed in chapter 6.
- A sensitivity analysis has shown that the steady state operation is independent of the initial conditions, and appears to be mainly a function of temperature differential.

The arena for this work is complex and there are many differing opinions as to how the LTDRSE operates and how an analysis should be applied. The author has tried to follow a unique path, being aware of, but not blindly following the work of others. As such the author believes that this is a credible attempt to produce a prediction program for a Low Temperature Differential Ringbom – Stirling Engine.

The prediction program produces results which correlate well with the results from the test engine. Further work will need to be undertaken to improve the accuracy of prediction program by investigating the loss coefficients for the dynamic situation. Other areas will have to address the simplifying assumptions in more detail, as well as the regenerator model and other heat loss paths such as the displacer chamber wall.

7.1 Further work

Further work to improve the accuracy of prediction will need to cover the regenerator in more depth. The heat and mass transfer parameters throughout the cycle need to be addressed more fully. Many simplifying assumptions were applied to the theoretical model, these will need to be addressed and where possible reduced or removed.

The theoretical model needs to be modified to take into account the large masses of the hot and cold reservoirs; this way the quantity of heat energy being transferred from the source and rejected to the sink may be quantified, and infers that the gross heat energy converted by the engine to perform work during operation may also be quantified

Improvements to the design of the LTDRSE, considered as a result of this work are as follows:

- The orifice which leads to the piston / cylinder assembly should be connected directly to the expansion space. With the present design the expanding air within the engine is required to enter the compression space to exert any force upon the piston face. This calls for an additional traverse of the regenerator and the annular gap between the displacer and displacer chamber wall, and unnecessary contact with the cold plate thus, removing energy from the expansion process.
- The hot and cold plates should have extended heat transfer surfaces to improve the heat flow in and out of the engine.
- The regenerative matrix should be removed from the displacer, thus reducing displacer mass, and placed in the annular gap. This will reduce the amount of work required to move the displacer.

References

- ALTMAN, A. 2003. SNAPpro Stirling Numerical Analysis Program. *Proceedings of the 11th International Stirling Engine Conference, Rome. 19th – 21st November 2003 pp166 -172.*
- ATKINSON, L. HARLEY, P. and HUDSON, J. 1989. *Numerical Methods with Fortran 77: A practical introduction.* Addison Wesley: Wokingham.
- BACON, D. and STEPHENS, R. 1998. *Mechanical Technology.* Third Edition. Butterworth-Heinemann: Oxford
- BEAL, W. 1980. Paper in *Energy for Rural Development.* US national Academy of sciences.
- BERCHOWITZ, D,M 1988. *Operational Characteristics of Free-Piston Stirling Engines.* 23rd Inter Society Energy Conversion Engineering Conference Volume 1.
- BISHOP, R.H. 2004. *Learning With LabVIEW 7 Express.* Pearson Education Inc: New Jersey
- BIN LI. 2005. Development of a Solar Dish Stirling Power System in China. *Proceedings of the 12th International Stirling Engine Conference, Durham. 7th – 9th September 2005. pp 90-95.*
- BLOCH, S. 2003. *Excel for Engineers and Scientists.* Second Edition. John Wiley and Sons Inc: New York
- BONNET, S. 2003. Thermodynamic Solar Energy Conversion: Reflections on the Optimal Solar Concentration Ratio. *Proceedings of the 11th International Stirling Engine Conference, Rome. 19th – 21st November 2003 pp263 -271.*
- BOSTOCK, L. and CHANDLER, S. 1991. *Mathematics Mechanics and Probability.* Sixth Reprint. ST(P): Cheltenham

- BRITISH PETROLEUM. June 2002. *BP Statistical Review*, (s.l.): (s.n.)
- BRITISH PETROLEUM. June 2006. *BP Statistical Review*, (s.l.): (s.n.)
- CASSEDY, E.S. and GROSSMAN, P.Z. 1998. *Introduction to Energy: Resources, Technology and Society*. Second edition. Cambridge University Press: Cambridge
- CENGEL, Y. BOLES, M. 1994. *Thermodynamics: An Engineering Approach*. Second Edition. McGraw-Hill: New York
- CHAPMAN, S. 1998. *Introduction to Fortran 90/95: Basic Engineering Series and Tools*. McGraw-Hill: Boston MA.
- CHEN, N. C. J. and GRIFFIN, F. P. 1983. A review of Stirling Engine Mathematical Models. Oak Ridge National Laboratory. ORNL/CON-135
- DEPARTMENT OF TRADE AND INDUSTRY. 2006. *Digest of UK Energy Statistics. (DUKES)*. (s.l.) (s.n.)
- DHAR, M. 1999. *Stirling Space engine program. Vol1 and 2*. National Aeronautics and Space Administration (NASA): NASA/CR 1999-209164/VOL1 and VOL2
- DOUGLAS, J. GASIOREK, J. and SWAFFIELD, J. 2001 *Fluid Mechanics*. Fourth Edition. Prentice Hall: Harlow
- EON UK. Powergen micro CHP. CHPA Members' Briefing 5th July 2005
- EASTOP, T. and McCONKEY, A. 1993. *Applied Thermodynamics for Engineering Technologists*. Fifth edition. Pearson Education: Harlow
- FIELD, A. and HOLE, G. 2003. *How to Design and Report Experiments*. Sage: London

FINKLESTEIN, T. 1961. Generalised Thermodynamic analysis of Stirling Engines. Society of Automotive Engineers, Winter Annual Meeting, January 11 – 15 Detroit Michigan, Paper 118B

FINKLESTEIN, T. ORGAN, A. 2001. *Air Engines*. Professional Engineering Publishing: London

GEDEON, D.R. 1978. Optimisation of Stirling Cycle Machines. *In: 13th Annual Intersociety Energy Conversion Engineering Conference*. The American Society of Mechanical Engineers.

HANN, B. 1998. *Fortran 90 for Scientists and Engineers*. Arrowsmith Ltd: London

HARGREAVES C.M. 1991. *The Phillips Stirling Engine*. Elsevier: Amsterdam

HOLMAN, J. 1992. *Heat Transfer: in SI Units*. Seventh Edition. McGraw-Hill: London

HOLMAN, J.P. 2001 *Experimental Methods for Engineers*. Seventh Edition. McGraw-Hill: Boston

GOSWAMI, D.Y. ed. *23rd Intersociety Energy Conversion Engineering Conference*. The American Society of Mechanical Engineers.

INCROPERA, F. DEWITT, D. 2002. *Fundamentals of Heat and Mass Transfer*. Fifth Edition. John Wiley and Sons: New York

INTERNATIONAL ENERGY AGENCY. 2001. *Key World Energy Statistics*. (s.l.) (s.n.)

INTERNATIONAL ENERGY AGENCY. 2006. *Key World Energy Statistics*. (s.l.) (s.n.)

ISEC. *Proceedings of the 11th International Stirling Engine Conference*. (2003)

ISEC. *Proceedings of the 12th International Stirling Engine Conference*. (2005)

ISEC. *Proceedings of the 9th International Stirling Engine Conference*. (1999)

KAYS, W. and LONDON, A. 1998. *Compact Heat Exchangers*. Third Edition
Reprinted with Corrections. Krieger Publishing: Florida

KIRKLEY, D.W. 1962 Determination for the Optimum Configuration for a Stirling Engine. *Journal of Mechanical Engineering Science*, Volume 4 Number 3 pp 204 – 212.

KNOLES, T.R. 1997. Composite Matrix Regenerator for Stirling Engines. National Aeronautics and Space Agency: NAS3-26294.

KOLIN, I. et al. 2000. Geothermal Electricity Production by Means of the Low Temperature Difference Stirling Engine. *Proceedings of the World Geothermal Congress 2000*, Kyushu-Tohoku, Japan. May 28th – June 10th 2000.

KOLIN, I. Recent developments of the flat plate Stirling engine, *Proceedings of the 21st Intersociety Energy Conversion Engineering Conference*, Paper 869113, San Diego, California, 25 - 29 August (1986).

LANNEY, G. 2000. Update on the NASA GRC Stirling Technology Development Project. National Aeronautics and Space Administration. NASA/TM 2000-210592.

LANNEY, G. et al. 2002. *Stirling Technology Development at NASA GRC*. National Aeronautics and Space Agency. NASA/TM 2001-211315/REV1.

MARTINI, W.R., *Stirling Engine Design Manual*. 2004 reprint of 1983 edition, University Press of the Pacific: Honolulu

National Maritime Research Institute, Japan. 1995 to present.
www.nmri.go.jp/index_e.html

MENDOZA, P et al. 2003. Stirling Engines in Peru: An opportunity for Regional Development. *Proceedings of the 11th International Stirling Engine Conference, Rome. 19th – 21st November 2003 pp280 -284*

METCALF, M. and REID, J. 2003. *Fortran 90/95 Explained*. Second Edition. Oxford University Press: Oxford

MICROGEN ENERGY LTD. 2003. Smart power: smart design: smart living. Brochure Microgen Energy Ltd. Reading. www.microgen.com

MIDDLEMAN, S. 1997. *An Introduction to Mass and Heat Transfer: Principles of Analysis and Design*. John Wiley and Sons: New York

MIDDLEMAN, S. 1998. *An Introduction to Fluid Dynamics: Principles of Analysis and Design*. John Wiley and Sons: New York

MUNEER, T. KUBIE, J and GRASSIE, T. 2003. *Heat Transfer: A Problem Solving Approach*. Taylor and Francis: London

NORTON, R. 1999. *Design of Machinery: An Introduction to the Synthesis and Analysis of Mechanisms and Machines*. Second Edition. McGraw-Hill: New York

ORGAN, A.J. 1992. *Thermodynamics and gas Dynamics of the Stirling Cycle Machine*. Cambridge university press: Cambridge

ORGAN, A.J. 1997. *The Regenerator and the Stirling Engine*. Mechanical Engineering Publications Ltd.: London

ORGAN, A.J. 2000a. Two Centuries of the Thermal Regenerator. *Proceedings of the Institution of Mechanical Engineers*, vol.214 part C, pp 269 – 288.

- ORGAN, A.J. 2000b. Stirling's Air Engine – A Thermodynamic Appreciation. *Proceedings of the Institution of Mechanical Engineers*, vol.214 part C, pp 511 – 536.
- ORGAN, A.J. 2000c. Regenerator Thermal Design in a Nutshell. *Proceedings of the Institution of Mechanical Engineers*, vol.214 Part C.
- OSTROWSKY, O. 2003. *Engineering Drawing With CAD Applications*. Butterworth-Heinemann: Amsterdam
- RAO, S.S. 1995. *Mechanical Vibrations*. Third Edition. Addison Wesley: Reading MA.
- READER, G.T and HOOPER, C. 1983. *Stirling Engines*. E & F. N. Spon: Cambridge
- REDLICH, R.W. and BERCHOWITZ, D.M. 1985. Linear Dynamics of Free-Piston Stirling Engines. *Procedures of the Institution of Mechanical Engineers*. Volume1 Number A3
- RINGBOM, O. US Patent Number 856 (1907).
- RIZZO, G. 1999. *The Stirling Engine Manual Volume 2*. Camden Miniature Steam Services: Bath
- RIZZO, G. 2000. *The Stirling Engine Manual Volume1*. Third edition. Camden Miniature Steam Services: Bath
- ROGDAKIS, E.D., BORMPILAS, N.A. and KONIAKOS, I.K. 2003. A Thermodynamic Study for the Optimisation of Stable Operation of Free Piston Stirling Engines. *Energy Conversion and management*. Article in press.
- ROGERS, G. and MAYHEW, Y. 1995. *Thermodynamic and Transport Properties of fluids: in SI Units*. Fifth Edition. Blackwell Publishing: Oxford

- ROMAN, S. 2002. *Writing Excel Macros with VBA*. Second Edition. O'Reilly and Associates: (s.l.)
- SCHMIDT, G. Theory of Lehmans Heat Engine, 1871. *Journal of the German Engineers Union*. Vol. XV, No.1 pp.1-12; No. 2, pp 98-112.
- SENF, J. R. A mathematical model for Ringbom engine operation, *Trans ASME – J. Eng Gas Turbines and Power* 107, 590-595 (1985).
- SENF, J.R. 1993. *Ringbom Stirling Engines*. Oxford University Press: New York
- SENF, J.R. 2000a. *An Introduction to Stirling Engines*. Moriya Press: New York
- SENF, J.R. 2000b. *Miniature Ringbom Engines*. Fifth Reprint. Moriya Press: New York
- SENF, J.R. 2000c. *Low Temperature Differential Stirling Engines*. Fourth Reprint. Moriya Press: New York
- SHERWIN, K. and HORSLEY, M. 1996. *Thermofluids*. Chapman and Hall: (s.l.)
- SIER, R. 1999. *Hot air Caloric and Stirling Engines*. L.A. Mair: Chelmsford
- SIMMONS, C. and MAGUIRE, D. 2004. *Manual of Engineering Drawing: to British and International Standards*. Second Edition. Elsevier Newnes: Amsterdam
- STIRLING, R. UK Patent Number 4081 (1816).
- STROUD, K. 1993. *Engineering Mathematics*. Third Edition. Macmillan Press: (s.l.)
- THE INTERNATIONAL ENERGY AGENCY. 2001. *Key World Energy Statistics*. 2001. STEDI Media: France

THE INTERNATIONAL ENERGY AGENCY. 2006. *Key World Energy Statistics*. 2006. STEDI Media: France

THE MONEY PROGRAMME. TV, BBC 2. 2003 Wednesday 26th March 19:30hrs

THIEME, L.G. and SCHREIBER, J.G. 2000. Update on the NASA GRC Stirling Technology Development Project. NASA/TM-2000-210592, December, 2000.

THIEME, L.G., and SCHREIBER, J.G., and MASON, L.S. 2002. Stirling Technology Development at NASA GRC. NASA/TM-2001-211315/REV1, January, 2002.

THOMAS, B. and WYNDORPS, A. Experimental Examination of Micro-CHP's: Stirling vs. IC Engines. *Proceedings of the 12th International Stirling Engine Conference, Durham. 7th – 9th September 2005. pp123-131*

URIELI, I. and BERCHOWITZ, D.M. 1984. *Stirling Cycle Engine Analysis*. Adam Hilger: (s.l.)

WALKER, G. 1962. An Optimisation of the Principal Design Parameters of Stirling Cycle Machines. *Journal of Mechanical Engineering Science*, vol.4 No. 3, pp 226 - 240.

WALKER, G. 1980. *Stirling Engines*. Oxford University Press: Oxford

WALKER, G. et al. 1994. *The Stirling Alternative Power Systems, Refrigerants and Heat Pumps*. Gordon and Breach Science Publishers: Yverdon

WALKER, G. SENFT, J. 1984. *Free Piston Stirling Engine*. Springer Verlag: Berlin

WELTY, J. et al. 2000. *Fundamentals of Momentum, Heat and Mass Transfer*. Forth Edition. (s.l.): John Wiley and Sons, New York.

WHITE, F. 1994. *Fluid Mechanics*. Third Edition. (s.l.): McGraw-Hill. USA.

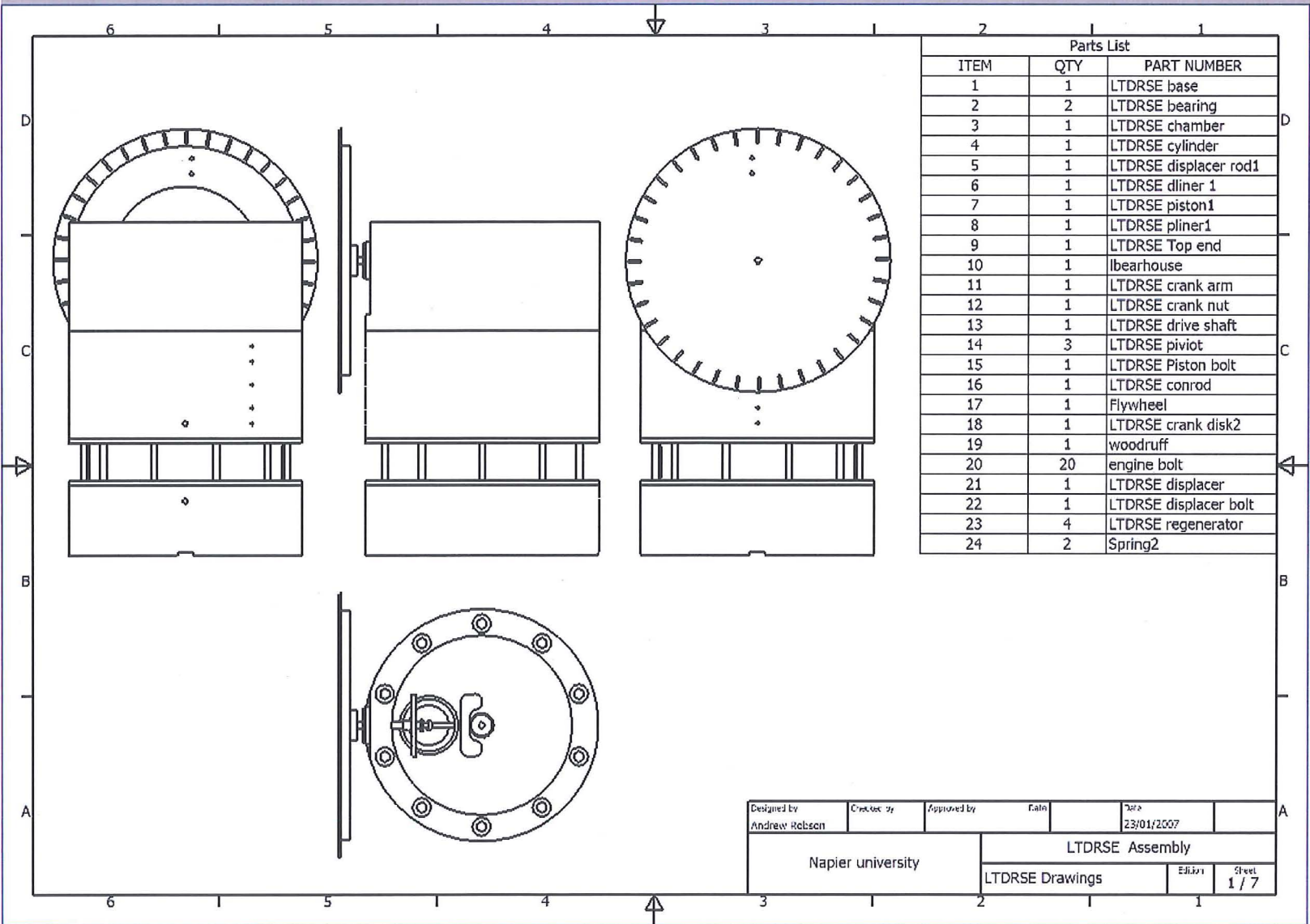
Papers Published

Robson, A. and Grassie, T. Development of a computer model to simulate a low temperature differential Ringbom Stirling engine, *Proceedings of the 12th International Stirling Engine Conference*, Durham, UK, 7 – 9 September (2005).

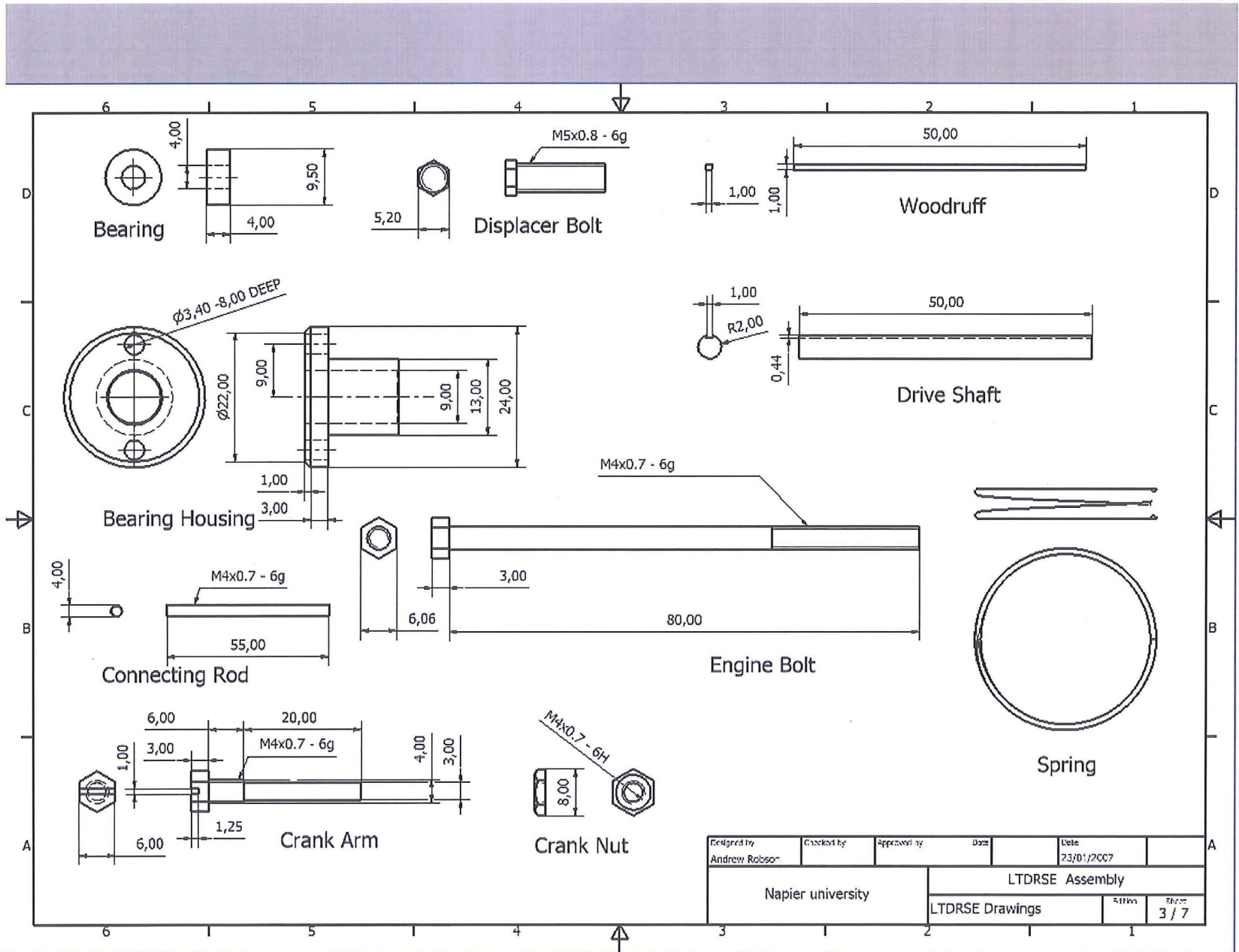
Robson, A. Grassie, T. and Kubie, J. Modelling of a Low Temperature Differential Stirling Engine. *Proceedings of the Institution of Mechanical Engineers, Part C, Journal of Mechanical Engineering Science*. In Print 01-05-2007

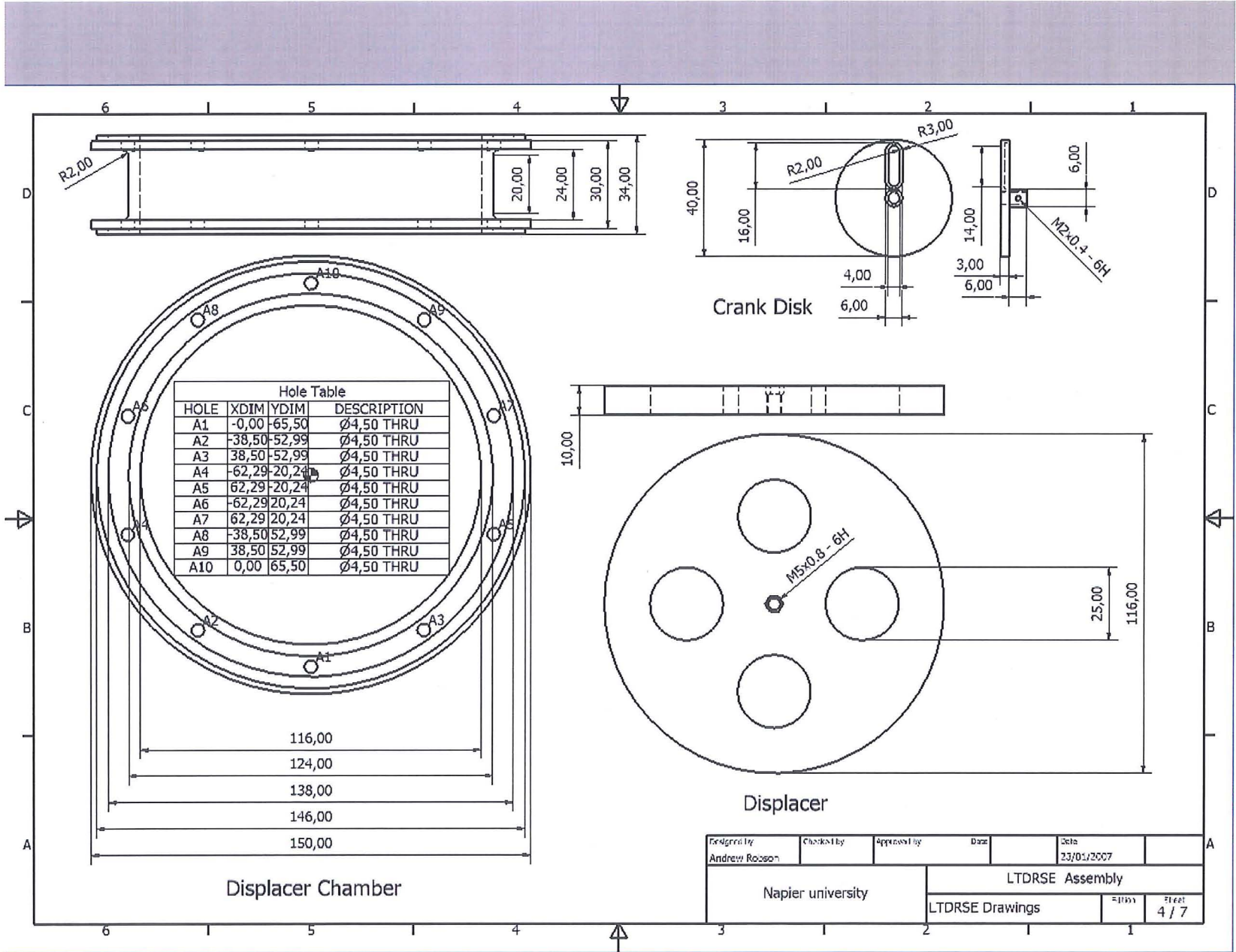
Appendix A Engineering Drawings

A.

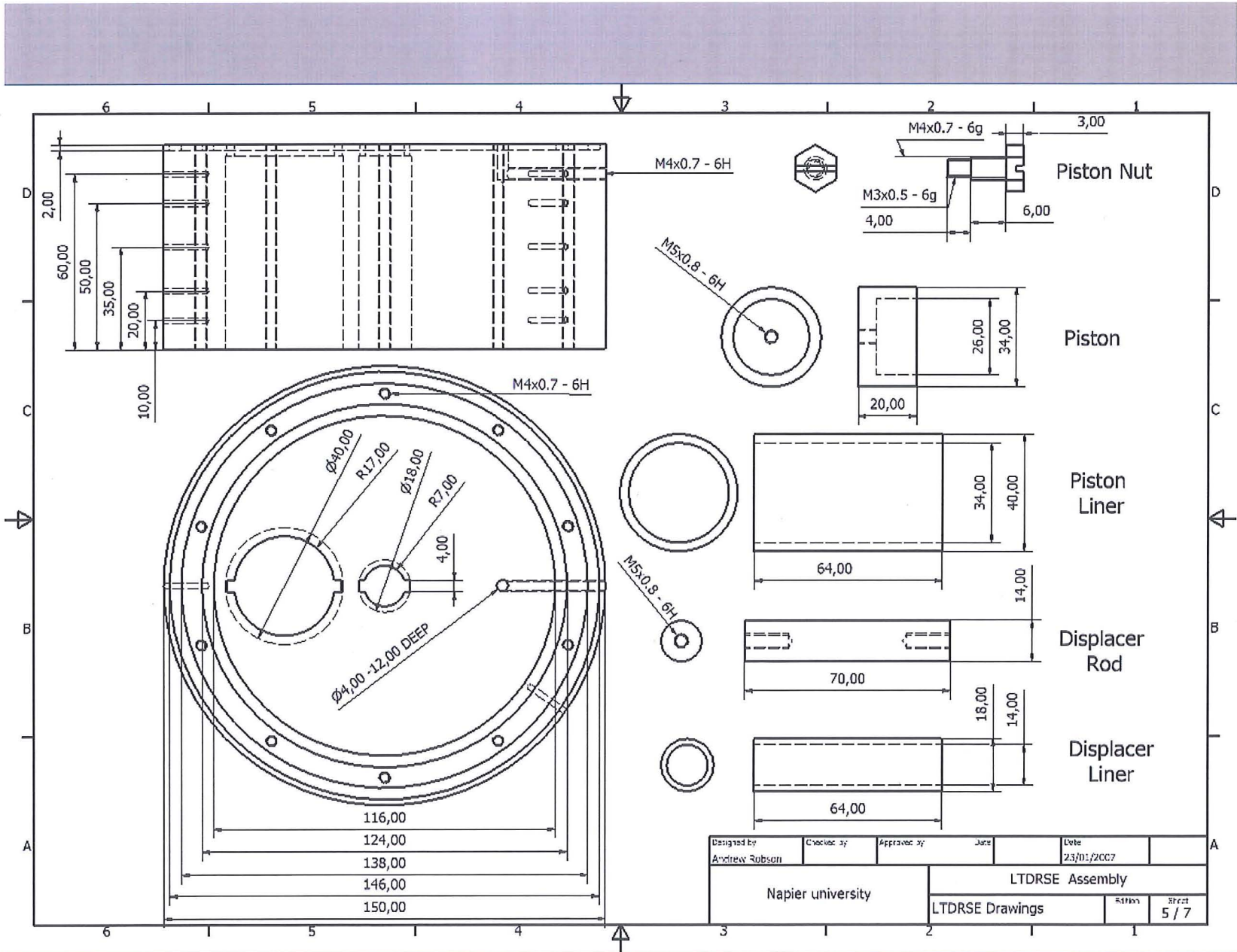


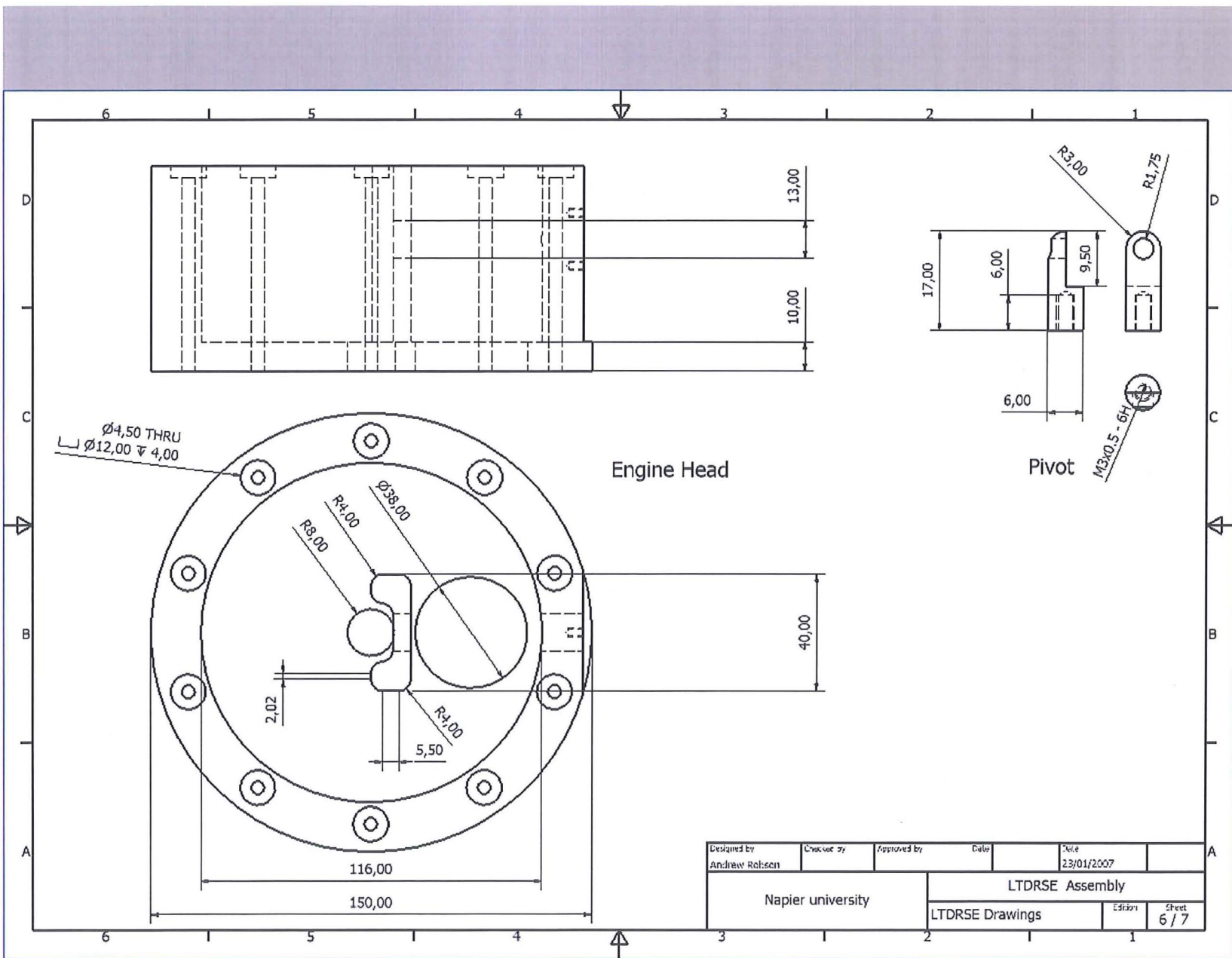
A. 1

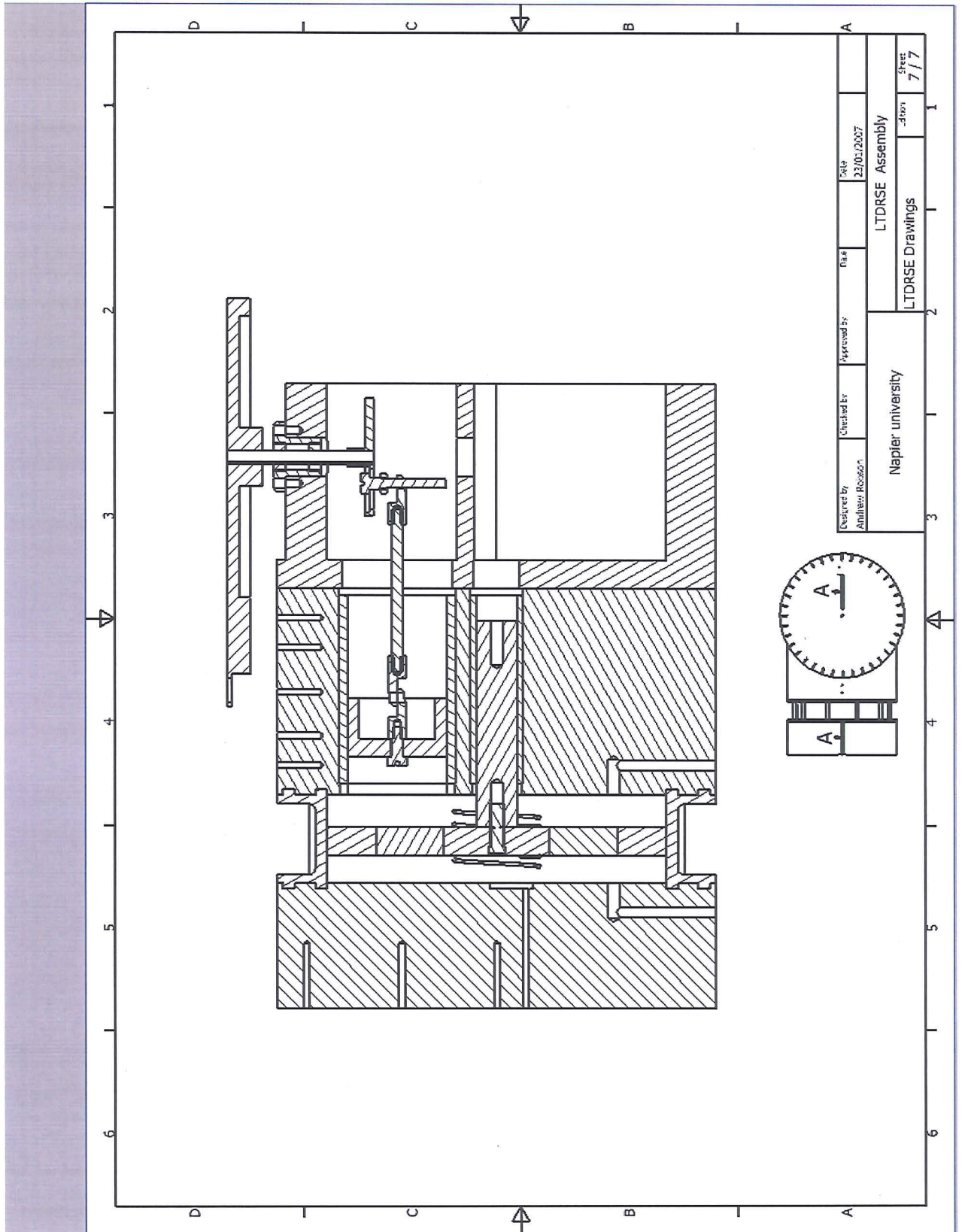




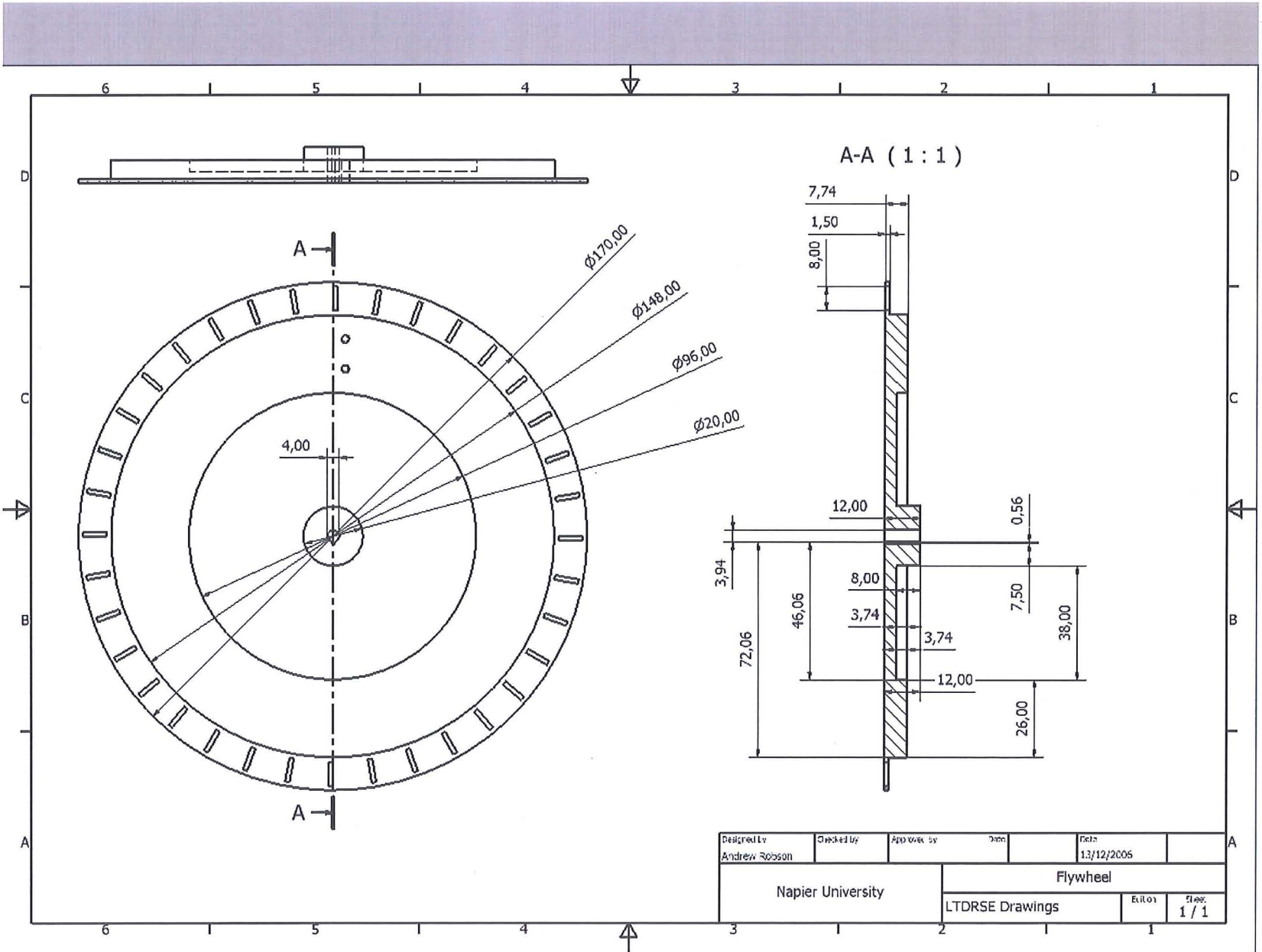
Designed by Andrew Rossion	Checked by	Approved by	Date 23/01/2007
Napier university		LTD RSE Assembly	
LTD RSE Drawings		Sheet 4 / 7	

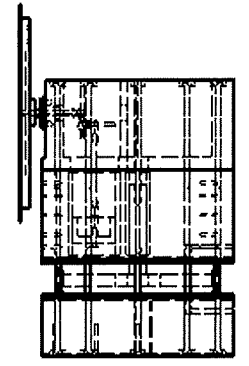
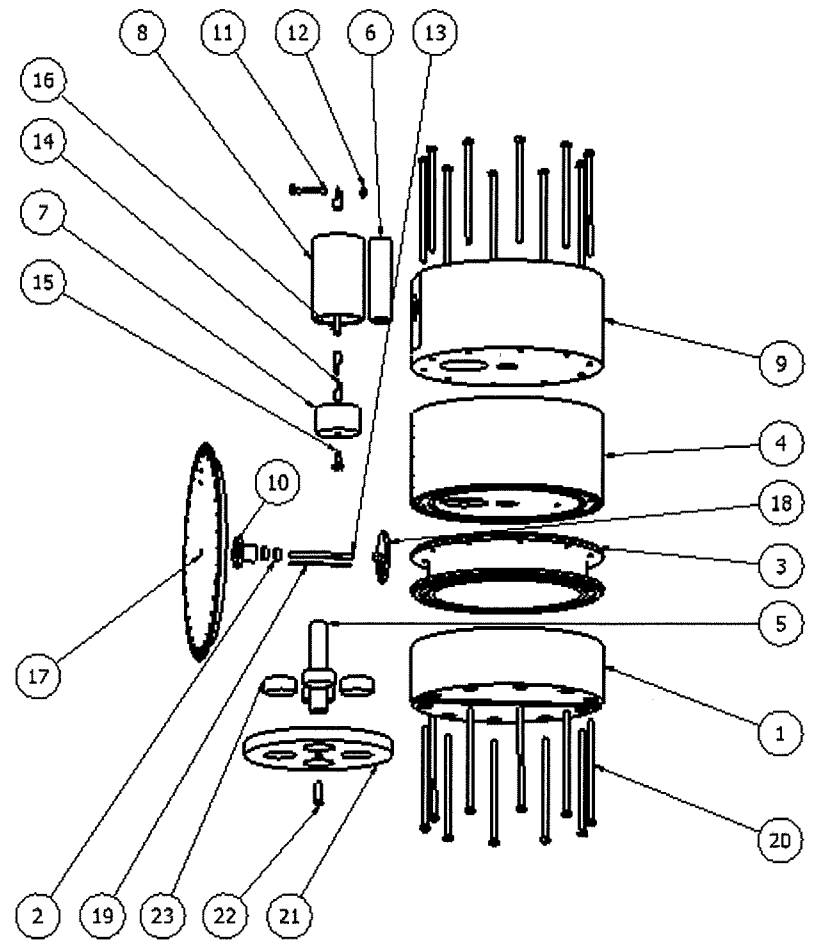






Drawn by Andrew Rossignol	Checked by Napier university	Approved by	Date 23/01/2007	File # LTDRSE Drawings	Sheet # 7/17
Napier university			LTDRSE Assembly		





Parts List			
ITEM	QTY	PART NUMBER	DESCRIPTION
1	1	LTDRSE base	
2	2	LTDRSE bearing	
3	1	LTDRSE chamber	
4	1	LTDRSE cylinder	
5	1	LTDRSE displacer rod1	
6	1	LTDRSE dliner 1	
7	1	LTDRSE piston1	
8	1	LTDRSE pliner1	
9	1	LTDRSE Top end	
10	1	lbearhouse	
11	1	LTDRSE crank arm	
12	1	LTDRSE crank nut	
13	1	LTDRSE drive shaft	
14	3	LTDRSE pivot	
15	1	LTDRSE Piston bolt	
16	1	LTDRSE conrod	
17	1	Flywheel	
18	1	LTDRSE crank disk2	
19	1	woodruff	
20	20	engine bolt	
21	1	LTDRSE displacer	
22	1	LTDRSE displacer bolt	
23	4	LTDRSE regenerator	

Designed by Andrew Robson	Checked by	Approved by	Date	Date 02/05/2006
Napier University			Engine 2	
			Ringassy5	Sheet 1 / 1

Parts List			
ITEM	QTY	PART NUMBER	DESCRIPTION
1	1	lhot plate	
2	1	lchamber	
3	1	lcoldend	
4	1	ldisp guide	
5	1	lpcylinder	
6	1	lcylinder Base	
7	1	lbearhouse	
8	1	lbearplate	
9	1	lconrod	
10	1	lcrank disk	
11	2	lcrankbear	
12	1	lcrank Pin	
13	1	lcrankshaft	
14	1	lflywheel	
15	1	lflywheel hub	
16	1	lpistn Yoke	
17	1	lpiston	
18	1	ldisp rod	
19	1	ldisplacer	
20	5	lregenerator	
21	11	ISO 7092 4.50	Washer ISO 7092 - 4
22	10	ISO 4762 M4x30	Bolt M4x30 ISO 4762

Designed by Andrew Robson	Checked by	Approved by	Date	Scale 29/04/2006
Napier University			Engine 1 Exploded Assembly	
			LTDRSE	Sheet 1 / 1

Appendix B Engine Simulation Program

```
!*****  
!  
! PROGRAM: Twocell_V9  
!  
!*****
```

program Twocell_V9

! Version 9.0

! Author Andrew Robson

! Napier University, Edinburgh

! Date 31 january 2007

! A program to simulate a Low Temperature Differential Ringbom Stirling Engine

! With the following simplifying assumptions:

! 1 Engine alignment vertical

! 2 Only working fluid loss via piston and displacer rod gaps

! 3 Temperatures and pressures are uniform in each space

! 4 All windage and friction losses can be accounted for by one term

! 5 Flow to/from compression and expansion spaces is through the regenerator

! 6 Heat transfer path is via the hot and cold plates, adiabatic otherwise

! 7 Mass of working fluid in the regenerator is constant

! 8 Heat transfer within the regenerator is purely between the fluid and matrix

! 9 There is no axial or radial conduction within the matrix

! 10 Regenerator wire section is square

! 11 Rotating parts are balanced

! 12 Heat transfer and conduction for regenerator wire is axi-symmetric

! 13 All bearing / sliding surfaces are frictionless

! 14 All regenerator cells enclose identical volumes

! 15 Working fluid adheres to the ideal gas law

! In naming variables the quantity (primary {Length, Mass, Time} or secondary)

! prefixes the variable name

! Disable FORTRAN's implicit function

IMPLICIT none

! Assign names to variables

! Geometry

! Lengths (Base Dimension length)

REAL, PARAMETER :: hc = 0.070	! Height of cold plate
REAL, PARAMETER :: hd = 0.0100	! Height of displacer
REAL, PARAMETER :: hdc = 0.029	! Height of displacer chamber
REAL, PARAMETER :: hh = 0.046	! Height of hot plate
REAL, PARAMETER :: hp = 0.020	! Height of piston
REAL, PARAMETER :: hse = 0.005	! Natural length of expansion space spring
REAL, PARAMETER :: hsk = 0.005	! Natural length of compression space spring
REAL, PARAMETER :: l = 0.065	! Length of connecting rod
REAL, PARAMETER :: lr = 0.020	! Length of regenerator side if square
REAL, PARAMETER :: r = 0.011	! Length of crank arm
REAL, PARAMETER :: offset = 0.0 !0.0345	! Height of centre of piston above chamber at bdc
REAL(8) :: cell	! Length of regenerator cell, wire dia plus gap
REAL(8) :: tnh	! Total number of holes
REAL,PARAMETER :: halfp = 0.010	! Half piston height
REAL,PARAMETER :: halfd = 0.005	! Half displacer height
REAL(8) :: hadp	! Height of piston face above datum at bdc
REAL(8) :: lgap	! Length of gap in mesh
REAL(8) :: xds	! Height of mid point of displacer static (t=-1)
REAL(8) :: xd (t=0)	! Height of mid point of displacer above datum
REAL(8) :: xd1 (t=1)	! Height of mid point of displacer above datum
REAL(8) :: xd2 (t=2)	! Height of mid point of displacer above datum
REAL(8) :: xps	! Height of mid point of piston static (t=-1)
REAL(8) :: xp	! Height of mid point of piston above datum (t=0)
REAL(8) :: xp1	! Height of mid point of piston above datum (t=1)
REAL(8) :: xp2	! Height of mid point of piston above datum (t=2)
REAL(8) :: xt	! Total length of crank arm and connecting rod

! Diameters

REAL, PARAMETER :: dc = 0.152 ! Diameter of cold plate
 REAL, PARAMETER :: dd = 0.115 ! Diameter of displacer
 REAL, PARAMETER :: ddc = 0.116 ! Diameter of displacer chamber
 REAL, PARAMETER :: ddr = 0.0140 ! Diameter of displacer rod
 REAL, PARAMETER :: dh = 0.152 ! Diameter of hot plate
 REAL, PARAMETER :: dp = 0.0340 ! Diameter of piston
 REAL, PARAMETER :: dr = 0.025 ! Diameter of regenerator void (if circular)
 REAL, PARAMETER :: drw = 0.00010 ! Diameter of regenerator wire

REAL(8) :: lrx = 0.0220
 REAL(8) :: lry = 0.0220
 REAL(8) :: aperture
 REAL(8) :: epsilon2
 REAL(8) :: mrw
 REAL(8) :: vrt
 REAL(8) :: mdis = 0.020
 REAL(8) :: mair
 REAL(8) :: mair2
 REAL(8) :: mms
 REAL, PARAMETER :: rohair = 1.2
 REAL(8) :: Tair0
 REAL(8) :: Tair1
 REAL(8) :: Tair2
 REAL(8) :: Tms0
 REAL(8) :: Tms1
 REAL(8) :: Tms2

! Areas (Base Dimension length squared)

REAL(8) :: aa ! Area of annular gap (displacer and chamber wall)
 REAL(8) :: ac ! Area of cold plate
 REAL(8) :: ad ! Area of displacer
 REAL(8) :: adc ! Area of displacer chamber
 REAL(8) :: ade ! Area of displacer effective
 REAL(8) :: adr ! Area of displacer rod (CSA)

Appendix B Engine Simulation Program

REAL(8) :: afr ! Area of free flow front surface of regenerator
(holes)

REAL(8) :: ah ! Area of hot plate

REAL(8) :: ap ! Area of piston

REAL(8) :: ar ! Area of regenerator (solid plus holes, ie
combined)

REAL(8) :: are ! Effective frontal area of regenerator

REAL(8) :: agap ! Area of one cell flow face

! Volumes (Base Dimension length cubed)

REAL(8) :: vc ! Volume of cold plate

REAL(8) :: vd ! Volume of displacer

REAL(8) :: vdc ! Volume of displacer chamber

REAL(8) :: vh ! Volume of hot plate

REAL(8) :: vpc ! Volume of piston cylinder

REAL(8) :: ve ! Volume of expansion space (instantaneous)

REAL(8) :: ves ! Expansion space volume

REAL(8) :: vks ! Compression space volume

REAL(8) :: vpd ! Piston dead volume

REAL(8) :: vps ! Piston swept volume on startup

REAL(8) :: vr ! Free flow volume for displacer

REAL(8) :: vcell ! Volume of one regenerator cell

REAL(8) :: vdwc ! Volume of matrix material bounding one cell

REAL(8) :: vmms ! Volume occupied by total mass of matrix screens

REAL(8) :: vspace ! Volume of space occupied by air (total)

REAL(8) :: vair ! Volume of air in regenerator (total)

REAL(8) :: vair2 ! Volume of air in regenerator (total) second calc

! Masses

REAL(8) :: me ! Mass of working fluid in expansion space (t0)

REAL(8) :: me1 ! Mass of working fluid in expansion space (t1)

REAL(8) :: me2 ! Mass of working fluid in expansion space (t2)

REAL(8) :: mk ! Mass of working fluid in compression space (t0)

REAL(8) :: mk1 ! Mass of working fluid in compression space (t1)

REAL(8) :: mk2 ! Mass of working fluid in compression space (t2)

REAL(8) :: mm ! Mass of matrix

REAL(8) :: mmc ! Mass of regenerator material in cell

REAL(8) :: mr ! Mass of working fluid in regenerator

Appendix B Engine Simulation Program

REAL(8) :: mrt	! Mass of working fluid in regenerator (total)
REAL(8) :: mrc	! Mass of working fluid in regenerator cell
REAL(8) :: mddot	! Mass flow via displacer rod/guide
REAL(8) :: mpdot	! Mass flow via piston wall
REAL(8) :: mrdot	! Mass flow through the regenerator
REAL(8) :: mrcell	! Mass flow one cell
REAL(8) :: modmrdot	! Modified mass flow
REAL(8) :: mpd	! Mass of working fluid in cylinder dead space
REAL, PARAMETER :: mc = 3.129	! Mass of cold plate (kg)
REAL, PARAMETER :: mh = 2.170	! Mass of hot plate (kg)
REAL, PARAMETER :: mp = 0.0358	! Mass of piston (kg)
REAL, PARAMETER :: mda = 0.03356	! Mass of displacer assembly (kg)

! Temperatures

REAL, PARAMETER :: Ta = 280	! Ambient temperature in kelvin
REAL(8) :: Tc	! Cold plate temperature
REAL(8) :: Th	! Hot plate temperature
REAL(8) :: Te0	! Expansion space temperature (t0)
REAL(8) :: Te1	! Expansion space temperature (t1)
REAL(8) :: Te2	! Expansion space temperature (t2)
REAL(8) :: Tk0	! Compression space temperature (t0)
REAL(8) :: Tk1	! Compression space temperature (t1)
REAL(8) :: Tk2	! Compression space temperature (t2)
REAL(8) :: Tfluid0c1 = Ta	! Fluid temp, time 0, cell1
REAL(8) :: Tfluid1c1 = Ta	! Fluid temp, time dt, cell1
REAL(8) :: Tfluid2c1 = Ta	! Fluid temp, time t+dt, cell1
REAL(8) :: Tfluid0c2 = Ta	! Fluid temp, time 0, cell2
REAL(8) :: Tfluid1c2 = Ta	! Fluid temp, time dt, cell2
REAL(8) :: Tfluid2c2 = Ta	! Fluid temp, time t+dt, cell2
REAL(8) :: Tmat0c1 = Ta	! Matrix temp, time 0, cell1
REAL(8) :: Tmat1c1 = Ta	! Matrix temp, time dt, cell1
REAL(8) :: Tmat2c1 = Ta	! Matrix temp, time t+dt, cell1
REAL(8) :: Tmat0c2 = Ta	! Matrix temp, time 0, cell2
REAL(8) :: Tmat1c2 = Ta	! Matrix temp, time dt, cell2
REAL(8) :: Tmat2c2 = Ta	! Matrix temp, time t+dt, cell2
REAL(8) :: Ti	! Inlet temperature for simple regenerator
REAL(8) :: Tinc1	
REAL(8) :: Tinc2	

REAL(8) :: Trk

REAL(8) :: Tre

REAL(8) :: carnot

! Properties declared as parameters

REAL, PARAMETER :: g = 9.80665

! Acceleration due to gravity

REAL, PARAMETER :: ra = 287

! Gas constant for air (J/kg K)

REAL, PARAMETER :: cc = 900

! SHC cold plate aluminium (J/kg K)

REAL, PARAMETER :: ch = 900

! SHC hot plate aluminium (J/kg K)

REAL, PARAMETER :: cm = 448

! SHC matrix iron (J/kg K)

REAL, PARAMETER :: cp = 1005

! SHC, constant pressure for air @ 300K (J/kg K)

REAL, PARAMETER :: cv = 718

! SHC, constant volume for air @ 300K (J/kg K)

REAL, PARAMETER :: ifw = 6.86E-4

! Moment of inertia (kg m²)

REAL, PARAMETER :: rohrw = 7850

!kg/m³ density for stainless steel

REAL, PARAMETER :: pi = 3.14159265358979324

! Numerical constant

REAL, PARAMETER :: pix2 = pi * 2

! Pi multiplied by 2

! Miscellaneous

REAL(8) :: epsilon

! Regenerator surface porosity

INTEGER :: nr = 4

! Number of regenerators

INTEGER, PARAMETER :: ns = 2

! Number of screens

REAL(8) :: mn = 40

! Mesh number for regenerator screen

REAL(8) :: f1

! Displacer spring force inequality operator

REAL(8) :: wn

! Number of wires which would stack into

regenerator

! Initialise regenerator arrays, length equal to number of screens (ns)

REAL, dimension(ns) :: Tm0, Tm1, Tm2, Tr0, Tr1, Tr2

! Construct regenerator array, initialise all values to ambient temperature

DATA Tm0 / ns*ta /

DATA Tm1 / ns*ta /

DATA Tm2 / ns*ta /

DATA Tr0 / ns*ta /

DATA Tr1 / ns*ta /

DATA Tr2 / ns*ta /

! Declare operator for mass flow temperature

REAL(8) :: T1

REAL(8) :: T2

REAL(8) :: T3

REAL(8) :: T4

! Pressures

REAL, PARAMETER :: pa = 101325

! Atmospheric pressure (Pa)

REAL(8) :: pe

! Expansion space pressure (t0)

REAL(8) :: pe1

! Expansion space pressure (t1)

REAL(8) :: pe2

! Expansion space pressure (t2)

REAL(8) :: pk

! Compression space pressure (t0)

REAL(8) :: pk1

! Compression space pressure (t1)

REAL(8) :: pk2

! Compression space pressure (t2)

REAL(8) :: pdiff = 0

! Pe - Pk

! Angles

REAL(8) :: alpha

REAL(8) :: alpha1

REAL(8) :: gamma

REAL(8) :: gamma1

REAL(8) :: theta

REAL(8) :: theta1

REAL(8) :: theta2

REAL(8) :: thetas

! Intermediate

!Displacer location intermediate calculations

REAL(8) :: dv1

! halfd

REAL(8) :: dv2

! hse+halfd

Appendix B Engine Simulation Program

```
REAL(8) :: dv3           ! hdc-hsk-halfd
REAL(8) :: dv4           ! hdc-halfd
```

! Flywheel angle intermediate calculations

```
REAL(8) :: pl1          ! Piston location
REAL(8) :: pl2          ! Piston location
```

! Expansion space temperature intermediate calculations

```
REAL(8) :: est1        ! Equation 1 for expansion space
REAL(8) :: est2        ! Equation 2 for expansion space
REAL(8) :: est3        ! Equation 3 for expansion space
REAL(8) :: est4        ! Equation 4 for expansion space
REAL(8) :: est5        ! Equation 5 for expansion space
```

! Compression space temperature intermediate calculations

```
REAL(8) :: cst1        ! Equation 1 for compression space
REAL(8) :: cst2        ! Equation 2 for compression space
REAL(8) :: cst3        ! Equation 3 for compression space
REAL(8) :: cst4        ! Equation 4 for compression space
REAL(8) :: cst5        ! Equation 5 for compression space
REAL(8) :: cst6        ! Equation 6 for compression space
REAL(8) :: cst7        ! Equation 7 for compression space
REAL(8) :: cst8        ! Equation 8 for compression space
```

! Flywheel angle theta intermediate calculations

```
REAL(8) :: efw1        ! Equation 1 for flywheel
REAL(8) :: efw2        ! Equation 2 for flywheel
REAL(8) :: efw3        ! Equation 3 for flywheel
REAL(8) :: efw4        ! Equation 4 for flywheel
```

! Regenerator intermediate calculations

```
REAL(8) :: regen1      ! regenerator flow constant
REAL(8) :: regen2      ! regenerator flow constant
REAL(8) :: regen3      ! regenerator flow constant
```

Appendix B Engine Simulation Program

! Counters

```
REAL(8) :: count1 = 0.000000000    ! First counter
INTEGER(8) :: count2 = 0.000000000 ! Second counter
INTEGER(8) :: count3 = 0.000000000 ! Third counter
INTEGER(8) :: count4 = 0.000000000 ! Fourth counter
INTEGER(8) :: count5 = 0.000000000 ! Fifth counter
INTEGER(8) :: count6 = 0.000000000 ! sixth counter
INTEGER(8) :: count8 = 0.000000000 ! eighth counter
INTEGER(8) :: writeat              ! Write interval for output
INTEGER tvl                        ! Test variable integer
REAL tvr                           ! Test variable real
```

! Efficiency

```
REAL(8) :: thclock = 7.0000000
REAL(8) :: thspace = 1.0000000
REAL(8) :: thstart = 0
REAL(8) :: thstop = 100
LOGICAL :: startsum = .false.
LOGICAL :: stopsum = .false.
REAL(8) :: worksum = 0
REAL(8) :: heatsum = 0
REAL(8) :: thermeff = 0
REAL(8) :: thsign = 1
```

```
REAL, PARAMETER:: omega = 25      ! Flywheel angular velocity
```

! Time

```
REAL, PARAMETER :: delta = 1d-7    ! Time step in seconds
REAL, PARAMETER :: rtime = 30      ! Run time in seconds
REAL(8) :: eclock = 0.000000000    ! Engine clock
REAL(8) :: progr                   ! Number of repetitions for calculations
REAL(8) :: time1, time2
REAL(8) :: date1
INTEGER(8) :: timemf = 0
INTEGER(8) :: timemfc = 0
```

! Constants

Appendix B Engine Simulation Program

```
REAL, PARAMETER :: kdf = 1E-4 ! Combined flywheel-piston losses, assumption
REAL, PARAMETER :: khc = 0.3 ! Convective heat transfer for cold plate 0.309
WILL RUN AFTER 20 SECS
REAL, PARAMETER :: khh = 0.3 ! Convective heat transfer for hot plate 0.309
REAL, PARAMETER :: khrm = 1.5 ! Heat transfer constant for matrix (ns = 2)(equiv
1/ns)
REAL, PARAMETER :: kmr = 2.05646E-5 ! Constant for mass flow through regenerator
REAL, PARAMETER :: kmp = 4.02465E-10 ! Constant for mass flow past piston
REAL, PARAMETER :: kmd = 1.12029E-10 ! Constant for mass flow past displacer rod
REAL, PARAMETER :: kse = 1000 ! Spring rate constant for expansion space spring
(1000)
REAL, PARAMETER :: ksk = 1000 ! Spring rate constant for compression space
spring (1000)
```

! Date and time stamp

```
CHARACTER (len=12) date, time ! date and time from cpu
```

```
call date_and_time(date)
```

```
call cpu_time(time1)
```

```
progr = rtime/delta
```

```
writeat = 99999
```

! Open file storage

!open file for data storage Fujitsu laptop

```
open (1, file = "C:\documents and settings\andy\my documents\my data
sources\20070112\kdf1emin4_3dns_khc0.3D")
```

!open file storage for variable checking Fujitsu laptop

```
open (3, file = "C:\documents and settings\andy\my documents\my data
sources\20070112\kdf1emin4_3divns_khc0.3V")
```

!open file storage for efficiency Fujitsu laptop

```
open (5, file = "C:\documents and settings\andy\my documents\my data
sources\20070112\kdf1emin4_3divns_khc0.3E")
```

!open file storage for regenerator Fujitsu laptop

Appendix B Engine Simulation Program

```
open (7, file = "C:\documents and settings\andy\my documents\my data sources\20070112\kdf1emin4_3divns_khc0.3P")
```

```
!open file storage for regenerator Fujitsu laptop
```

```
open (9, file = "C:\documents and settings\andy\my documents\my data sources\20070112\kdf1emin4_3divns_khc0.3M")
```

```
! Assign initial values to temperatures ( in Kelvin)
```

```
Tc = 280                                ! Cold plate temperature
Th = 355                                ! Hot plate temperature
Te0 = Ta                                ! Expansion space temperature (t0)
Tk0 = Ta                                ! Compression space temperature (t0)
T1 = Ta
T2 = Ta
T3 = Ta
T4 = Ta
Te1 = Ta
Tk1 = Ta
Te2 = Ta
Tk2 = Ta
Ti = Ta
Trk = Ta
Tre = Ta
Tair0 = Tc
Tms0 = Tc
Tair1 = Tc
Tms1 = Tc
Tair2 = Tc
Tms2 = Tc
```

```
! Assign initial pressures ( in Pascal)
```

```
pe = pa                                ! Expansion space pressure (t0)
pk = pa                                ! Compression space pressure (t0)
pe1 = pa                                ! Expansion space pressure (t1)
pk1 = pa                                ! Compression space pressure (t1)
pe2 = pa                                ! Expansion space pressure (t2)
pk2 = pa                                ! Compression space pressure (t2)
```

Appendix B Engine Simulation Program

! Calculations for engine geometry

```

xt = l + r                                ! Total length of crank arm and connecting rod
lgap = (25.4E-3 / mn) - drw                ! Length of gap
cell = 25.4E-3 / mn                       ! Length of cell
wn = ((hd)/(drw))                         ! Number of wires in regenerator
!print*, 'cell = ', cell
!print*, 'lgap = ', lgap
!print*, 'wn = ', wn

!epsilon = (lgap**2)/(lgap + drw)**2       ! Ratio of areas or porosity
!print*, 'epsilon = ', epsilon
epsilon = 0.95

aa = pi* 0.25*(ddc**2 - dd**2)            ! Area of displacer/chamber wall annulus
ac = pi*ddc**2*0.25                       ! Area of cold plate
ad = pi*dd**2*0.25                         ! Area of displacer
ar = pi*dr**2*0.25                        ! Frontal area of one regenerator
adr = pi*ddr**2*0.25                     ! Area of displacer rod face (CSA)
ah = pi*ddc**2*0.25                      ! Area of hot plate
ap = pi*dp**2*0.25                       ! Area of piston face (CSA)
adc = pi*ddc**2*0.25                     ! Area of the displacer chamber
agap= lgap**2                             ! Area of flow face for one cell,
are = ar * (1-epsilon)                   ! Area of regenerator effective
ade = ad - (nr*are) -aa                  ! Area of displacer effective

!print*, ac, ad, adc, adr, ah, ap

!vc = ac*hc                               ! Volume of cold plate
!vd = (ad - (nr*ar))*hd                   ! Volume of displacer
!vdc = adc * hdc                          ! Volume of displacer chamber
!vh = ah*hh                               ! Volume of hot plate
!vpc = ap * 0.0325                        ! Volume of piston cylinder dead space
!vdwc = pi * drw**2 *0.25 * (cell + lgap)
!vcell=(lgap**3)+(((lgap**2)-(pi*drw**2*0.25))*(lgap+cell))

!mrc = (pa*vcell)/(ra*ta)                 ! Mass of fluid in one cell
!mmc = rohrw * vdwc                       ! Mass of matrix material in one cell

aperture = (0.0254/mn)-drw

```

```

epsilon2 = aperture**2/(aperture+drw)**2
mrw = rohrw*pi*drw**2*0.25*(lrx*(lry/(aperture+drw))+lry*(lrx/(aperture+drw)))*nr*wn
!print*, 'epsilon2 = ', epsilon2
!print*, 'mrw = ', mrw

```

```
!Regenerator Calculations
```

```

mms = 0.00753
mmc = 0.003765
vmms = mms/rohrw
vspace = vmms / (1-epsilon)
vair = vspace*epsilon
vair2 = (nr*ar*epsilon*hd)
mrt = vair*rohair
mair = vair*rohair/ns
mair2 = vair2*rohair/ns
mmc = mms/ns
mrc = mrt/ns

```

```

!print*, 'Vmms = ', vmms, 'Vspace = ', vspace
!print*, 'Vair = ', vair
!print*, 'Vair2 = ', vair2
!print*, 'mair = ', mair
!print*, 'mair2 = ', mair2
!print*, 'mms = ', mms, 'mmc = ', mmc
!print*, 'mrc = ', mrc

```

```

carnot = (th-tc)/th
timemf = 1/delta
timemfc = timemf

```

```
write (5,*) 'Carnot efficiency = ', carnot*100
```

```
! Check matrix is within limits
```

```

if (drw >= cell) then
  print*, 'solid matrix, reduce wire dia', cell
else if (lgap >= cell) then
  print*, 'wire non existant, increase dia'

```

```

end if

dv1    = halfd
dv2    = hse+halfd
dv3    = hdc-hsk-halfd
dv4    = hdc-halfd

! Find the mass of working fluid at start

!The engine volume is made up from the sum of the following volumes
!The expansion space is the volume below the displacer expansion space face at rest upon the
stub spring,
! = (hse - (mda * g / kse))*adc
!The regenerator free volume for n regenerators
! =(nr * (ar *epsilon)*hd)
!The compression space inclusive of the cylinder dead volume. Volume at rest is dependent upon
flywheel angle.
!WRITE CODE LATER TO ACCOUNT FOR FLYWHEEL ANGLE....FOR NOW TAKE BDC =
32.5mm FOR FACE OF PISTON ABOVE CHAMBER
! = (hc-(hd+(hse - (mda * g / kse))))*(adc-adr)

! For mass use ideal gas law m=pv/RT

ves = (hse - (mda * g / kse))*adc
vr = (nr * (ar *epsilon)*hd)
vks = (hdc - hd - (hse - (mda * g / kse)))*(adc-adr)

! time = 0

thetas = pi/5
theta = thetas                                ! Initial flywheel angle (in radians)

!Flywheel angles

alpha = asin( (r/l) * sin(theta))

gamma = acos(sin(theta + alpha))

xp = (xt - ((l**2 - (r * sin(theta))**2)**0.5) - (r * cos(theta))) + offset !location of piston above datum
including offset

```

! Displacer location

$xd = hse + halfD - (mda * g / kse)$

!Initial position of the displacer

!tests for displacer location

if ($xd < dv1$) **then**

!displacer fouling hot plate

Print*, 'displacer on hot plate'

stop

else if ($xd > dv1$.and. $xd < dv2$) **then**

!displacer under influence of expansion space

spring

$f1 = kse * (hse + halfD - xd)$

else if ($xd > dv2$.and. $xd < dv3$) **then**

!displacer unconstrained

$f1 = 0$

else if ($xd > dv3$.and. $xd \leq dv4$) **then**

!displacer under influence of compression space

spring

$f1 = ksk * (hdc - hsk - halfD - xd)$

else if ($xd > dv4$) **then**

!displacer fouling cold plate

Print*, 'displacer on cold plate'

stop

end if

$hadp = xp + halfp$

! Piston face above datum for any theta

$me = (pe * ves) / (ra * Te0)$

! Mass of fluid in expansion space

$mr = (pe * vr) / (ra * Te0)$

Engine at ambient hence temperature of regenerator is in equilibrium with expansion space

$!mpd = pk * (hadp * pi * dp^{**2} * 0.25) / (ra * Tk0)$

$mpd = pk * (xp * pi * dp^{**2} * 0.25) / (ra * Tk0)$

$mk = (pk * vks) / (ra * Tk0) + mpd$

! Mass of fluid in compression space

$ve = (xd - halfD) * adc$

$vpc = ap * xp$

!write (1,100)

!write (*,100)

write (1,600)

write (*,600)

write (7,300)

**!write (1,200) eclock, theta, (xp-0.0345)*1000, xd*1000, Te0, Tk0, pe, pk, &
!(pe-pk), me*1000000, mk*1000000, Tair0, Tms0**

**!write (*,200) eclock, theta, (xp-0.0345)*1000, xd*1000, Te0, Tk0, pe, pk, &
!(pe-pk), me*1000000, mk*1000000, Tair0, Tms0**

!write (1,700) eclock, Te0, Tk0, (pe-pk), Tair0, Tms0

!write (*,700) eclock, Te0, Tk0, (pe-pk), Tair0, Tms0

**write (1,700) eclock, Te0, Tfluid0c1, Tfluid0c2, Tk0, Tmat0c1, Tmat0c2, xp*1000, xd*1000, theta,
(pe-pk), (me+mk)*1000000**

**write (*,700) eclock, Te0, Tfluid0c1, Tfluid0c2, Tk0, Tmat0c1, Tmat0c2, xp*1000, xd*1000, theta,
(pe-pk), (me+mk)*1000000**

write (7,400) eclock, vpc*1000000, pk

**!write (1,700) eclock, Te0, Tair0, Tk0, Tms0, xp*1000, xd*1000, theta, (pe-pk), (me+mk)*1000000,
vpc*1000000**

!write (1,700) eclock, Te0, Tk0, (pe-pk), Tair0, Tms0

!write (*,700) eclock, Te0, Tk0, (pe-pk), Tair0, Tms0

!write (3,*) 'mesh number = ', mn

!write (3,*) 'No of screens = ', ns

!write (3,*) 'Omega = ', omega

!write (3,*) 'Flywheel start angle = ', thetas

!write (3,*)

! Piston location

$$xp1 = xt - ((l^{**2} - (r * \sin(\theta_1))^{**2})^{**0.5}) - (r * \cos(\theta_1)) + \text{offset}$$

! Displacer location

$$xd1 = xd$$

! Expansion space pressure

$$pe1 = (me * ra * Te0) / (adc * (xd1 - \text{halfd}))$$

! Compression space pressure

$$pk1 = (mk * ra * Tk0) / (((adc - adr) * (hdc - \text{halfd} - xd1)) + (ap * (xp1 - \text{halfp})))$$

! Mass flow rates

$$\text{mrdot} = \text{kmr} * (pe1 - pk1) \quad \text{! Mass flow through the regenerator}$$

$$\text{mddot} = \text{kmd} * (pa - pk1) \quad \text{! Mass flow past the displacer rod}$$

$$\text{mpdot} = \text{kmp} * (pa - pk1) \quad \text{! Mass flow past the piston}$$

$$\text{mrcell} = \text{mrdot} / \text{tnh}$$

! Masses

$$me1 = me - (\delta * \text{mrdot})$$

$$mk1 = mk + (\delta * (\text{mrdot} + \text{mddot} + \text{mpdot}))$$

! Regenerator intermediate variables

$$\text{lregen1} = ((cv+ra)*\text{mrdot}*\delta)/(cv*\text{mair}/ns)$$

$$\text{lregen2} = ((\text{khrm}*\delta)/(cv*\text{mair}/ns))$$

$$\text{lregen3} = ((\text{khrm}*\delta)/(cm*\text{mms}/ns))$$

$$\text{regen1} = ((cv+ra)*\text{mrdot}*\delta)/(cv*\text{mair})$$

```
regen2 = ((khrm*delta)/(cv*mair))
regen3 = ((khrm*delta)/(cm*mms))
```

```
!print*, regen1, regen2, regen3
```

```
! Simple Regenerator
```

```
if (pe2>=pk2) then
```

```
Tinc1 = Te0 - Tfluid0c1
```

```
Tinc2 = Tfluid0c1-Tfluid0c2
```

```
else if (pe2<pk2) then
```

```
Tinc1 = Tfluid0c2 - Tk0
```

```
Tinc2 = Tfluid0c1 - Tfluid0c2
```

```
end if
```

```
Tfluid1c1 = Tfluid0c1+Tinc1*regen1+Tmat0c1*regen2-Tfluid0c1*regen2
```

```
Tfluid1c2 = Tfluid0c2+Tinc2*regen1+Tmat0c2*regen2-Tfluid0c2*regen2
```

```
Tmat1c1 = Tmat0c1+Tfluid0c1*regen3-Tmat0c1*regen3
```

```
Tmat1c2 = Tmat0c2+Tfluid0c2*regen3-Tmat0c2*regen3
```

```
!if (pe1>=pk1) then
```

```
!Ti = Te0-Tair0
```

```
!else if (pe<pk1) then
```

```
!Ti = Tair0-Tk0
```

```
!end if
```

```
!Tair1 = Tair0+Ti*regen1+Tms0*regen2-Tair0*regen2
```

```
!Tms1 = Tms0+Tair0*regen3-Tms0*regen3
```

```
! Expansion space temperature (use values from previous step)
```

```
if (pe1 >= pk1) then
```

```
T1 = Te0
```

```
else if (pe1 < pk1) then
```

```

T1 = Tfluid1c1
end if

est1 = Te0
est2 = (Th - Te0)*(khh * delta / (cv * me1))
est3 = (xd1 - xd)*(pe1 * ad / (cv * me1))
est4 = (Te0 - T1)*(mrdot*delta/me1)
est5 = T1 * (ra*mrdot*delta)/(cv*me1)

Te1 = est1 + est2 - est3 + est4 - est5

! Compression space temperature

if (pe1 >= pk1) then
  T2 = Tfluid1c2
else if (pe1 < pk1) then
  T2 = Tk0
end if

if (pa >= pk1) then
  T3 = Ta
else if (pa < pk1) then
  T3 = Tk0
end if

cst1 = Tk0
cst2 = (Tk0 - Tc)*(khc*delta/(cv*mk1))
cst3 = (xd1 - xd)*(pk1*(ad-adr)/(cv*mk1))
cst4 = (theta1 - theta)*((pk1*ap)/(cv*mk1))*(((r**2 * sin(theta1) * cos(theta1)) / (l**2 - (r *
sin(theta1))**2)**0.5) + &
(r * sin(theta1)))
cst5 = (T2 - Tk0)*(mrdot*delta/mk1)
cst6 = T2*(ra*mrdot*delta/(cv*mk1))
cst7 = (T3 - Tk0)*((mpdot+mddot)*delta/mk1)
cst8 = T3*(ra*(mpdot+mddot)*delta/(cv*mk1))

Tk1 = cst1 - cst2 + cst3 - cst4 + cst5 + cst6 + cst7 + cst8

!!!!!!!!!!!!!!!!!!!!!!!!!!!!!!          !!!!!!!!!!!!!!!!!!!!!!!!!!!!!!!

```

! Second step, time = 2 x delta

! Engine run time

eclock = eclock + delta

count8 = count8 + 1

! Flywheel angle theta for second timestep

!calculations of THETA2

```
EFW1=(R**3)*MP*cos(GAMMA1)*sin(THETA1)*cos(THETA1)/((L**2-(R*sin(THETA1))**2)**0.5)+&
(R**2)*MP*cos(GAMMA1)*sin(THETA1)+IFW*cos(ALPHA1)
EFW2=-R*MP*G*cos(GAMMA1)+R*(PK2-PA)*AP*cos(GAMMA1)
EFW3=-KDF*cos(ALPHA1)
EFW4=-R*MP*cos(GAMMA1)*((((R**2)*sin(THETA1)*cos(THETA1))**2)/((L**2-
(R*sin(THETA1))**2)**1.5))+&
(R**2)*((cos(THETA1))**2-(sin(THETA1))**2)/(((L**2)-(R*sin(THETA1))**2)**0.5)+R*cos(THETA1))
THETA2=2*THETA1-THETA+(DELTA**2)*EFW2/EFW1+DELTA*(THETA1-
THETA)*EFW3/EFW1+&
((THETA1-THETA)**2)*EFW4/EFW1
```

! Flywheel sub angles

alpha1 = asin((r/l) * sin(theta2))

gamma1 = acos(sin(theta2 + alpha1))

! Piston location

xp2 = xt - ((l**2 - (r * sin(theta2))**2)**0.5) - (r * cos(theta2)) + offset

! Displacer location

! Find value for additional force

if (xd < dv1) **then**

!displacer fouling hot plate

Print*, 'displacer on hot plate'

stop

Appendix B Engine Simulation Program

```
else if (xd > dv1 .and. xd < dv2) then           !displacer under influence of expansion
space spring
f1 = kse * (hse + halfD - xd)
else if (xd > dv2 .and. xd < dv3) then           !displacer unconstrained
f1 = 0
else if (xd > dv3 .and. xd < dv4) then           !displacer under influence of compression
space spring
f1 = ksk * (hdc - hsk - halfD - xd)
else if (xd >= dv4 ) then
Print*, 'displacer on cold plate'                 !displacer fouling cold plate
stop
end if

xd2 = (2*xd1) - xd + (delta**2/mda)*((ad * (pe1 - pk1))+(adr * (pk1 - pa))-(mda * g)+f1)

! Expansion space pressure

pe2 = (me1 * ra * Te1) / (adc * (xd2 - halfd))

! Compression space pressure

pk2 = (mk1 * ra * Tk1) / (((adc - adr) * (hdc - halfd - xd2)) + (ap * (xp2 - halfp)))

! Mass flow rates

mrdot = kmr*(pe2 - pk2)

mddot = kmd * (pa - pk2)

mpdot = kmp * (pa - pk2)

mrcell = mrdot/tnh

! Masses

me2 = me1 - (delta * mrdot)

mk2 = mk1 + (delta * (mrdot + mddot + mpdot))
```

```
! Regenerator
```

```
regen1 = ((cv+ra)*mrdot*delta)/(cv*mair)
```

```
regen2 = ((khrm*delta)/(cv*mair))
```

```
regen3 = ((khrm*delta)/(cm*mms))
```

```
!print*, regen1, regen2, regen3
```

```
! pe>pk
```

```
! Time 2, Cell 1
```

```
! Simple Regenerator
```

```
! Regenerator
```

```
!regen1 = ((cv+ra)*mrdot*delta)/(cv*mair/ns)
```

```
!regen2 = ((khrm*delta)/(cv*mair/ns))
```

```
!regen3 = ((khrm*delta)/(cm*mms/ns))
```

```
! pe>pk
```

```
! Time 2, Cell 1
```

```
! Simple Regenerator
```

```
!if (pe2>=pk2) then
```

```
!Ti = Te1-Tair1
```

```
!else if (pe2<pk2) then
```

```
!Ti = Tair1-Tk1
```

```
!end if
```

```
if (pe2>=pk2) then
```

```
Tinc1 = Te1 - Tfluid1c1
```

```
Tinc2 = Tfluid1c1-Tfluid1c2
```

```
else if (pe2<pk2) then
```

```
Tinc2 = Tfluid1c2 - Tk1
```

$$Tinc1 = Tfluid1c1 - Tfluid1c2$$

end if

$$Tfluid2c1 = Tfluid1c1 + Tinc1 * regen1 + Tmat1c1 * regen2 - Tfluid1c1 * regen2$$

$$Tfluid2c2 = Tfluid1c2 + Tinc2 * regen1 + Tmat1c2 * regen2 - Tfluid1c2 * regen2$$

$$Tmat2c1 = Tmat1c1 + Tfluid1c1 * regen3 - Tmat1c1 * regen3$$

$$Tmat2c2 = Tmat1c2 + Tfluid1c2 * regen3 - Tmat1c2 * regen3$$

!if (pe2 >= pk2) then

$$!Ti = Te1 - Tair1$$

!else if (pe2 < pk2) then

$$!Ti = Tair1 - Tk1$$

!end if

$$!Tair2 = Tair1 + Ti * regen1 + Tms1 * regen2 - Tair1 * regen2$$

$$!Tms2 = Tms1 + Tair1 * regen3 - Tms1 * regen3$$

! Expansion space temperature (use values from previous step)

!if (pe2 >= pk2) then

$$!T1 = Te1$$

!else if (pe2 < pk2) then

$$!T1 = Tair2$$

!end if

if (pe2 >= pk2) then

$$T1 = Te1$$

else if (pe2 < pk2) then

$$T1 = Tfluid2c1$$

end if

$$est1 = Te1$$

$$est2 = (Th - Te1) * (khh * delta / (cv * me2))$$

$$est3 = (xd2 - xd1) * (pe2 * ad / (cv * me2))$$

$$est4 = (Te1 - T1) * (mrdot * delta / me2)$$

$$est5 = T1 * (ra * mrdot * delta) / (cv * me2)$$

Te2 = est1 + est2 - est3 + est4 - est5

! Compression space temperature

!if (pe2 >= pk2) then

!T2 = Tair2

!else if (pe2 < pk2) then

!T2 = Tk1

!end if

!if (pa >= pk2) then

!T3 = Ta

!else if (pa < pk2) then

!T3 = Tk1

!end if

if (pe2 >= pk2) then

T2 = Tfluid2c2

else if (pe2 < pk2) then

T2 = Tk1

end if

if (pa >= pk2) then

T3 = Ta

else if (pa < pk2) then

T3 = Tk1

end if

cst1 = Tk1

cst2 = (Tk1 - Tc)*(khc*delta/(cv*mk2))

cst3 = (xd2 - xd1)*(pk2*(ad-adr))/(cv*mk2)

cst4 = (theta2 - theta1)*((pk2*ap)/(cv*mk2))*(((r**2 * sin(theta2) * cos(theta2)) / (l**2 - (r * sin(theta2))**2)**0.5) + &

(r * sin(theta2)))

cst5 = (T2 - Tk1)*(mrdot*delta/mk2)

cst6 = T2*(ra*mrdot*delta/(cv*mk2))

cst7 = (T3 - Tk1)*((mpdot+mddot)*delta/mk2)

cst8 = T3*(ra*(mpdot+mddot)*delta/(cv*mk2))

Appendix B Engine Simulation Program

$Tk2 = cst1 - cst2 + cst3 - cst4 + cst5 + cst6 + cst7 + cst8$

!!!!!!!!!!!!!! !!!!!!!!!!!!!!!!!!! !!!!!!!!!!!!!!!

!Third and remaining calculations

count1 = 0

!Setup loop

do count3 = 1, progr

!Engine clock

eclock = eclock + delta

!thclock = eclock

count1 = count1 + delta

count8 = count8+1

! Reassign values

theta = theta1

theta1 = theta2

xd = xd1

xd1 = xd2

Te1 = Te2

Tk1 = Tk2

me1 = me2

mk1 = mk2

!Tair1 = Tair2

!Tms1 = Tms2

Tmat1c1 = Tmat2c1

Tmat1c2 = Tmat2c2

Tfluid1c1 = Tfluid2c1

Tfluid1c2 = Tfluid2c2

do count2=1,ns

Tm0(count2)=Tm1(count2)

Tm1(count2)=Tm2(count2)

!Tm2(count2)=0

Tr0(count2)=Tr1(count2)

Tr1(count2)=Tr2(count2)

!Tr2(count2)=0

end do

! Flywheel angle theta for subsequent timesteps

!calculations of subsequent THETA2

EFW1=(R**3)*MP*cos(GAMMA1)*sin(THETA1)*cos(THETA1)/((L**2-(R*sin(THETA1))**2)**0.5)+&

(R**2)*MP*cos(GAMMA1)*sin(THETA1)+IFW*cos(ALPHA1)

EFW2=-R*MP*G*cos(GAMMA1)+R*(PK2-PA)*AP*cos(GAMMA1)

EFW3=-KDF*cos(ALPHA1)

EFW4=-R*MP*cos(GAMMA1)*(((R**2)*sin(THETA1)*cos(THETA1))**2)/((L**2-

(R*sin(THETA1))**2)**1.5))+&

(R**2)*((cos(THETA1))**2-(sin(THETA1))**2)/((L**2)-(R*sin(THETA1))**2)**0.5)+R*cos(THETA1))

THETA2=2*THETA1-THETA+(DELTA**2)*EFW2/EFW1+DELTA*(THETA1-

THETA)*EFW3/EFW1+&

((THETA1-THETA)**2)*EFW4/EFW1

! Flywheel sub angles

alpha1 = asin((r/l) * sin(theta2))

gamma1 = acos(sin(theta2 + alpha1))

! Piston location

xp2 = xt - ((l**2 - (r * sin(theta2))**2)**0.5) - (r * cos(theta2)) + offset

! Displacer location

! Find value for additional force

```

if (xd < dv1) then                                     !displacer fouling hot plate
Print*, 'displacer on hot plate'
stop
else if (xd > dv1 .and. xd < dv2) then                 !displacer under influence of expansion
space spring
f1 = kse * (hse + halfD - xd)
else if (xd > dv2 .and. xd < dv3) then                 !displacer unconstrained
f1 = 0
else if (xd > dv3 .and. xd < dv4) then                 !displacer under influence of compression
space spring
f1 = ksk * (hdc - hsk - halfD - xd)
else if (xd >= dv4 ) then
Print*, 'displacer on cold plate'                       !displacer fouling cold plate
stop
end if

```

$$xd2 = (2*xd1) - xd + (\text{delta}^{**2}/\text{mda})*((\text{ad} * (\text{pe2} - \text{pk2})) + (\text{adr} * (\text{pk2} - \text{pa})) - (\text{mda} * \text{g}) + \text{f1})$$

! Expansion space pressure

$$\text{pe2} = (\text{me1} * \text{ra} * \text{Te1}) / (\text{adc} * (\text{xd2} - \text{halfd}))$$

! Compression space pressure

$$\text{pk2} = (\text{mk1} * \text{ra} * \text{Tk1}) / (((\text{adc} - \text{adr}) * (\text{hdc} - \text{halfd} - \text{xd2})) + (\text{ap} * (\text{xp2} - \text{halfp})))$$

! Mass flow rates

$$\text{mrdot} = \text{kmr} * (\text{pe2} - \text{pk2})$$

$$\text{mddot} = \text{kmd} * (\text{pa} - \text{pk2})$$

$$\text{mpdot} = \text{kmp} * (\text{pa} - \text{pk2})$$

$$\text{mrcell} = \text{mrdot}/\text{tnh}$$

! Masses

me2 = me1 - (delta * mrdot)

mk2 = mk1 + (delta * (mrdot + mddot + mpdot))

ve = (xd2-halfD)*adc

vpc = ap * xp2

! Regenerator

!print*, cv+ra, mrdot

!regen1 = ((cv+ra)*mrdot*delta)/(cv*mair/ns)

!regen2 = ((khrm*delta)/(cv*mair/ns))

!regen3 = ((khrm*delta)/(cm*mms/ns))

regen1 = ((cv+ra)*mrdot*delta)/(cv*mair)

regen2 = ((khrm*delta)/(cv*mair))

regen3 = ((khrm*delta)/(cm*mms))

!print*, regen1, regen2, regen3

!print*,regen1,regen2,regen3

! pe>pk

! Time 2, Cell 1

! Simple Regenerator

!if (pe2>=pk2) then

!Ti = Te1-Tair1

!else if (pe2<pk2) then

!Ti = Tair1-Tk1

!end if

if (pe2>=pk2) then

Tinc1 = Te1 - Tfluid1c1

Tinc2 = Tfluid1c1-Tfluid1c2

else if (pe2 < pk2) then

$$T_{inc2} = T_{fluid1c2} - T_{k1}$$

$$T_{inc1} = T_{fluid1c1} - T_{fluid1c2}$$

end if

$$T_{fluid2c1} = T_{fluid1c1} + T_{inc1} * regen1 + T_{mat1c1} * regen2 - T_{fluid1c1} * regen2$$

$$T_{fluid2c2} = T_{fluid1c2} + T_{inc2} * regen1 + T_{mat1c2} * regen2 - T_{fluid1c2} * regen2$$

$$T_{mat2c1} = T_{mat1c1} + T_{fluid1c1} * regen3 - T_{mat1c1} * regen3$$

$$T_{mat2c2} = T_{mat1c2} + T_{fluid1c2} * regen3 - T_{mat1c2} * regen3$$

! Expansion space temperature (use values from previous step)

if (pe2 >= pk2) then

$$T1 = T_{e1}$$

else if (pe2 < pk2) then

$$T1 = T_{fluid2c1}$$

end if

$$est1 = T_{e1}$$

$$est2 = (T_h - T_{e1}) * (k_{hh} * \delta / (c_v * m_{e2}))$$

$$est3 = (x_{d2} - x_{d1}) * (p_{e2} * a_d / (c_v * m_{e2}))$$

$$est4 = (T_{e1} - T1) * (m_{rdot} * \delta / m_{e2})$$

$$est5 = T1 * (r_a * m_{rdot} * \delta) / (c_v * m_{e2})$$

$$T_{e2} = est1 + est2 - est3 + est4 - est5$$

! Compression space temperature

if (pe2 >= pk2) then

$$T2 = T_{fluid2c2}$$

else if (pe2 < pk2) then

$$T2 = T_{k1}$$

end if

if (pa >= pk2) then

```

T3 = Ta
else if (pa < pk2) then
  T3 = Tk1

end if

cst1 = Tk1
cst2 = (Tk1 - Tc)*(khc*delta/(cv*mk2))
cst3 = (xd2 - xd1)*(pk2*(ad-adr))/(cv*mk2)
cst4 = (theta2 - theta1)*((pk2*ap)/(cv*mk2))*(((r**2 * sin(theta2) * cos(theta2)) / (l**2 - (r *
sin(theta2))**2)**0.5) + &
(r * sin(theta2)))
cst5 = (T2 - Tk1)*(mrdot*delta/mk2)
cst6 = T2*(ra*mrdot*delta/(cv*mk2))
cst7 = (T3 - Tk1)*((mpdot+mddot)*delta/mk2)
cst8 = T3*(ra*(mpdot+mddot)*delta/(cv*mk2))

      Tk2 = cst1 - cst2 + cst3 - cst4 + cst5 + cst6 + cst7 + cst8

if (thclock <= eclock) then
  startsum = .true.
  thstart = theta2
  !thstop = theta2 + pi/2
  thclock = thclock + thspace

      if (theta2 <= 0) then
        thstop = theta2 - pix2
        thsign = -1
      else if (theta2 > 0) then
        thstop = theta2 + pix2
        thsign = 1
      end if
end if

if (startsum == .true.) then
  worksum = worksum + (((theta2-theta1)/delta)**2)
  heatsum = heatsum + (Th - Te2)

```

```

if (thstop*thsign <= sqrt(theta2**2)) then
  thermeff = (kdf*worksum)/(khh*heatsum)
  worksum = 0
  heatsum = 0
  write (5,*) 'thermal efficiency = ', thermeff*100
  startsum = .false.
end if

```

```

end if

```

```

if (count4 >= writeat) then

```

```

  write (1,700) eclock, Te2, Tfluid2c1, Tfluid2c2, Tk2, Tmat2c1, Tmat2c2, xp2*1000, xd2*1000,
  theta2, (pe2-pk2), (me2+mk2)*1000000
  write (*,700) eclock, Te2, Tfluid2c1, Tfluid2c2, Tk2, Tmat2c1, Tmat2c2, xp2*1000, xd2*1000,
  theta2, (pe2-pk2), (me2+mk2)*1000000
  write (7,400) eclock, vpc*1000000, pk2, pe2, pe2-pa

```

```

  !write (1,200) count1, theta2, (xp2-0.0345)*1000, xd2*1000, Te2, Tk2, pe2, pk2, &
  !(pe2-pk2), me2*1000000, mk2*1000000, Tair2, Tms2

```

```

  !write (*,200) count1, theta2, (xp2-0.0345)*1000, xd2*1000, Te2, Tk2, pe2, pk2, &
  !(pe2-pk2), me2*1000000, mk2*1000000, Tair2, Tms2

```

```

    count4 = 0

```

```

  else if (count4 < writeat) then

```

```

    count4 = count4 +1

```

```

  end if

```

```

!if (count8 == timemf) then
!write (1,700) eclock, Te2, Tk2, (pe2-pk2), Tair2, Tms2
!write (*,700) eclock, Te2, Tk2, (pe2-pk2), Tair2, Tms2
!elseif (count8 == timemf+1) then

```

```

!write (1,700) eclock, Te2, Tk2, (pe2-pk2), Tair2, Tms2
!write (*,700) eclock, Te2, Tk2, (pe2-pk2), Tair2, Tms2
!elseif (count8 == timemf+2) then
!write (1,700) eclock, Te2, Tk2, (pe2-pk2), Tair2, Tms2
!write (*,700) eclock, Te2, Tk2, (pe2-pk2), Tair2, Tms2
!timemf = timemf+timemfc
!end if

```

end do

```

call cpu_time(time2)

```

```

write (3,*) 'Time taken = ', (time2 - time1)/60, ' mins'
write (3,*) 'No of calcs = ', progr
write (3,*) 'mesh number = ', mn
write (3,*) 'No of screens = ', ns
write (3,*) 'Omega = ', omega
write (3,*) 'Flywheel start angle = ', thetas

```

```

write (3,*) 'kdf = ', kdf           ! Combined flywheel-piston losses, assumption
write (3,*) 'khc = ', khc         ! Convective heat transfer for cold plate
write (3,*) 'khh = ', khh         ! Convective heat transfer for hot plate
write (3,*) 'khrm = ', khrm       ! Heat transfer constant for matrix
write (3,*) 'kmr = ', kmr         ! Constant for mass flow through regenerator
write (3,*) 'kmp = ', kmp         ! Constant for mass flow past piston
write (3,*) 'kmd = ', kmd         ! Constant for mass flow past displacer rod
write (3,*) 'kse = ', kse         ! Spring rate constant for expansion space spring
write (3,*) 'ksk = ', ksk         ! Spring rate constant for compressio

```

```

write (3,*) 'Ta = ', Ta
write (3,*) 'Tc = ', Tc
write (3,*) 'Th = ', Th
write (3,*) 'dp = ', dp
write (3,*) 'ddr = ', ddr

```

```

write (3,*) 'Stamp ', date, time1, time2

```

```

!format statements

```

Appendix B Engine Simulation Program

```
100 format(' time', t12, 'theta', t23, 'xp', t33, 'xd', t42, 'Te', t53, 'Tk', t63, ' pe', t75, ' pk', &  
t90, 'pe-pk', t100, 'me', t110, 'mk', t123, 'Tair', t133, 'Tmat')
```

```
200 format (f7.3, t8, f12.6, t22, f7.4, t32, f7.4, t42, f9.5, t52, f10.5, t64, f9.2, t76, f9.2, &  
t87, f9.4, t99, f9.5, t110, f9.5, t123, f7.3, t133, f7.3)
```

```
300 format ( '    Time', t14, 'Piston Vol', t28, 'PK', t42, 'Pe', t56, 'Pe-Pa)
```

```
400 format (6(f11.3,' '))
```

```
600 format ( '    eclock', t16, 'Te', t28, 'Tf,cell1', t40, 'Tf,cell2', t52 'Tk', t64, 'Tm,cell1', t76,  
'Tm,cell2', &  
t88, 'Piston', t100, 'Displacer', t112, 'theta', t124, '(pe-pk)', t136, 'Mass' )
```

```
!600 format ( '    eclock', t16, 'Te', t28, 'Tair', t40, 'Tk', t52, 'Tms', t64, 'Piston', t76, &  
!'Displacer', t88, 'theta', t100, 'pe-pk', t112, 'Mass')  
!eclock, Te0, Tfluid0c1, Tfluid0c2, Tk0, Tmat0c1, Tmat0c2, xp*1000, xd*1000, theta, (pe-pk),  
(me+mk)*1000000
```

```
700 format (12(f11.5,' '))
```

```
end program Twocell_V9
```

Appendix D Pressure Sensor Data

All ASDX...D44D

Characteristics	Min.	Typ.	Max.	Units	
Zero pressure offset	2.42	2.50	2.58	V	
Full scale span (FSS) ²		4.00			
Output					
	at max. specified pressure	4.42	4.50	4.58	
	at min. specified pressure	0.42	0.50	0.58	
Total accuracy (0 to 85°C) ³			±2.0	%FSS	
Sample rate	100			Hz	
Response delay ⁴	2.73		14.11	ms	
Quantization step ⁵		3		mV	
Current consumption		6		mA	

110L...-PCB / 430L...-PCB Series

Signal conditioned precision pressure transducers

PERFORMANCE CHARACTERISTICS

1...6 V output version (unless otherwise noted $V_s = 15\text{ V}$, $R_L > 100\text{ k}\Omega$, $t_{\text{amb}} = 25^\circ\text{C}$)

Characteristics			Min.	Typ.	Max.	Proof pressure ²	Common mode pressure	Unit	
Operating pressure ³	differential devices	112LP02D-PCB	0		2	200	300	mbar	
		112LP05D-PCB	0		5	200	300		
		112LP10D-PCB	0		10	200	300		
		112LP25D-PCB	0		25	300	600		
		112LP50D-PCB	0		50	300	600		
	pressure/vacuum devices ³	113LP01D-PCB	-1		1	200	300		
		113LP02D-PCB	-2		2	200	300		
		113LP05D-PCB	-5		5	200	300		
		113LP10D-PCB	-10		10	200	300		
		113LP25D-PCB	-25		25	300	600		
		113LP50D-PCB	-50		50	300	600		
	differential devices	112LU01D-PCB	0		1	80	160		"H ₂ O
		112LU02D-PCB	0		2	120	240		
		112LU05D-PCB	0		5	120	240		
112LU10D-PCB		0		10	240	360			
112LU20D-PCB		0		20	240	360			
112LU30D-PCB		0		30	240	360			
pressure/vacuum devices ³	113LU01D-PCB	-1		1	80	160			
	113LU02D-PCB	-2		2	120	240			
	113LU05D-PCB	-5		5	120	240			
	113LU10D-PCB	-10		10	240	360			
	113LU20D-PCB	-20		20	240	360			
	113LU30D-PCB	-30		30	240	360			
Zero pressure offset ⁴	112L...-PCB	0.95	1.0	1.05			V		
	113L...-PCB	3.4	3.5	3.6					
Full scale span ⁵	112L...-PCB	4.9	5.0	5.1					
	113L...-PCB	2.4	2.5	2.6					
Full scale output			6.0						
Output at lowest specified pressure	113L...-PCB		1.0						
Thermal effects (0 to 50°C) ⁶	Offset	113LP01D-PCB		±0.08	±0.20			%FSO/°C	
		11...LP02D-PCB		±0.04	±0.10				
		11...LU01D-PCB		±0.04	±0.10				
		all other devices		±0.02	±0.05				
	Span	113LP01D-PCB		±0.08	±0.20				
		11...LP02D-PCB		±0.04	±0.10				
Non-linearity and hysteresis (BSL) ⁷			±0.1	±0.25			%FSO		
				±0.5					
Long term stability ⁸									
Response time (10 to 90 %)				1			ms		
Position sensitivity	all 1 and 2 mbar devices			0.5			%FSO/g		
	all other devices			0.1					
Current consumption				4.2			mA		
Power supply rejection	Offset			0.05			%FSO/V		
	Span			0.05					